

QUENCH DYNAMICS OF ONE DIMENSIONAL  
MULTI-COMPONENT QUANTUM GASES

BY

HUIJIE GUAN

A dissertation submitted to the  
School of Graduate Studies  
Rutgers, The State University of New Jersey  
in partial fulfillment of the requirements  
for the degree of  
Doctor of Philosophy  
Graduate Program in Physics and Astronomy

Written under the direction of

Natan Andrei

and approved by

---

---

---

---

---

New Brunswick, New Jersey

May, 2018

## ABSTRACT OF THE DISSERTATION

# Quench Dynamics of One Dimensional Multi-component Quantum Gases

by Huijie Guan

Dissertation Director: Natan Andrei

This thesis studies the quench dynamics of strongly correlated quantum systems described by one dimensional integrable Hamiltonians. We develop the Yudson approach for such systems in terms of contour integrals allowing the expansion of arbitrary states in terms of the Bethe Ansatz eigenstates which in turn provides the means to calculate the time evolution of such observables as densities or noise correlations from any initial states.

As a motivation to the present work, I present the state of art ultracold atom techniques and fundamental questions related to the quench dynamics. Then various Bethe ansatz solutions are discussed. This is followed by an introduction to the Yudson approach where advantages and difficulties are listed. As applications of the Yudson approach, I studied the nonequilibrium dynamics of the Lieb-Liniger model, (bosonic) Gaudin-Yang model, quenched from a Mott state with a superfluid Hamiltonian. Integration contours are specified for various models and different interactions. It is shown that the Yudson approach incorporates all free states and bound states into the contour, separating them apart sheds light on the validity of the String hypothesis. The result is affirmative for Lieb-Liniger model, but not for the Gaudin-Yang model. Our calculations for the density and correlation shows that for interacting system, if the pre-quench state has negligible overlap among the particles, the system retains this feature after the quench. Particularly, normalized noise function  $c(z, -z)$  at the origin shows different stages. Shortly after the quench, the sign are different for attractive and repulsive interaction. Then they both quickly approaches the value where possibility to find both particles equals zero. Then the value increases gradually for attractive models, while  $c(0, 0)$  remains small for repulsive systems.

## Acknowledgements

It is still a vivid memory when I first arrived at the U.S, sitting on a bus, being unsure about everything, ranging from what to eat for dinner to how to survive in a foreign country and how to start a research with so little knowledge about advance techniques. Here I am, about to graduate. It turns out to be such an exciting journey. There are so many people that I am indebted to. Without them, I would never be the same.

First, I would like to thank my adviser, professor Natan Andrei. I am so used to thinking as a student rather than a scientist, it is Natan who urges me to step out of my comfort zone to explore the unknown area. His solid knowledge, strong enthusiasm and sharp physics intuition inspires me to be a better physicist. I appreciate the collaboration with professor Lea Santos, who brings me to the fascinating world of numeric calculations. She is so patient to teach and willing to learn.

I would also like to thank the professors who taught me in and outside classes. I am grateful to professor Joel Shapiro. I have taken three courses with him. He is always able to present complicated and abstract material in a clear fashion. His courses equips me with necessary skills for my research. I enjoyed those courses. I am also indebted to Professor Piers Coleman. After taking his many-body courses twice, I still audit his course occasionally. His many-body book is the classic to me. I also want to thank professor Emil Yuzbashyan for his advanced topics in condensed matter. It opens my eyes to exciting fields in modern physics. I must also say thank you to professor Weida Wu, who provides suggestions in choosing a research field in my first year here.

I would like to say thank you to my group members. First to Deepak Iyer, who starts up my research experience. He is so patient in teaching me the techniques and is also open to different ideas. I will remember his support and suggestion in my hard phases. He also shows me how to balance between research and life. Second to Wenshuo Liu, the only Chinese follow in the group. I am grateful to have him in my group. I have the most discussion with him from academic to everyday life. I would also like to thank Garry Goldstein for being a role model as a great scientist full of smart ideas. I also want to thank Chris Munson. His warm personality enlightens my research life. I am also obliged to my office mate, Roshan Tourani and other

group member Adrian Culver, Colin Rylands, Vaibhav Dwivedi and Caitlin Carpenter.

Outside of the research life, I also got a lot of help from my friends. In those days when I do not have a car, it is Yanan and Qin who took me to grocery stores every week for more than a year. It is also with them that I went to the outlet, went skiing, dined out, went cruising and to the cinema. How boring life would be without them. I am also grateful for their continuous help while I am preparing for a job. I would also like to thank my Chinese colleagues that give me a sense of belonging and offered me help when in need. I would also like to thank Eliav Edrey who answered lots of questions in the early days of my graduate life. I am indebted to Zhizhong and Wei. Even today when I need help, I think of them first and they are always there to help, in cases of sickness, moving etc. I also want to thank my friends in the church. The meeting every Friday are the highlights to my graduate life. I want to thank Kaiyan for those refreshing hours in the gym.

Most importantly, I am grateful to my family. Thanks to my son Anthony for joining the family. Thanks to my parents. Without them, it is impossible for an inexperienced mother to make through those busy days. Thanks to my husband, Jianpeng, for being there with me, sharing every little thing, in hard days and happy day.

## Dedication

*To my family, Xin Wang, Hongbo Guan and Jianpeng Liu*

# Table of Contents

<b>Abstract</b> . . . . .	ii
<b>Acknowledgements</b> . . . . .	iii
<b>Dedication</b> . . . . .	v
<b>List of Figures</b> . . . . .	viii
<b>1. Introduction</b> . . . . .	1
1.1. Ultracold Atom Experiment . . . . .	1
1.1.1. Optical Lattice . . . . .	1
1.1.2. Feshbach Resonance . . . . .	3
1.1.3. Measurement . . . . .	5
1.2. Nonequilibrium Dynamics . . . . .	7
1.3. Outline of the Thesis . . . . .	10
<b>2. Bethe Ansatz</b> . . . . .	12
2.1. Coordinate Bethe Ansatz . . . . .	13
2.1.1. Lieb-Liniger Model . . . . .	13
2.2. Algebraic Bethe Ansatz . . . . .	19
2.2.1. XXZ Model . . . . .	22
2.3. Nested Bethe Ansatz . . . . .	32
2.3.1. Gaudin-Yang Model . . . . .	32
<b>3. Yudson Approach</b> . . . . .	41
3.1. Bethe Ansatz as Complete Basis . . . . .	41
3.2. Yudson Contour Integral Representation . . . . .	42
3.3. Advantages and Disadvantages . . . . .	44
<b>4. Quench Dynamics of Lieb-Liniger Gas</b> . . . . .	48
4.1. Central Theorem . . . . .	49

4.1.1. Repulsive Case . . . . .	50
4.1.2. Attractive Case . . . . .	51
4.2. Two particle Dynamics . . . . .	55
4.3. Multiparticle Dynamics in Asymptotic Limit . . . . .	70
4.3.1. Wavefunction Approach . . . . .	71
4.3.2. Form Factor Approach . . . . .	81
<b>5. Quench Dynamics of Gaudin-Yang Gas . . . . .</b>	<b>84</b>
5.1. Central Theorem . . . . .	88
5.1.1. One Impurity Case . . . . .	88
5.1.2. Multi-impurity Case . . . . .	92
5.2. Physical Interpretation in terms of Bound states . . . . .	96
5.3. Two Distinguishable Particle Case . . . . .	104
5.4. One Impurity in Multi-particle Bath . . . . .	110
5.5. Moving Impurity in Multi-particle Bath . . . . .	116
<b>6. Quench Dynamics of Bosonic Gaudin-Yang model . . . . .</b>	<b>121</b>
6.1. Bethe Ansatz solution . . . . .	121
6.2. Yudson Representation . . . . .	123
6.3. Central Theorem . . . . .	124
6.4. Bound states . . . . .	124
6.5. Time evolution . . . . .	125
<b>7. Conclusion and Outlook . . . . .</b>	<b>128</b>
7.1. Conclusion . . . . .	128
7.2. Future Work . . . . .	129
<b>Bibliography . . . . .</b>	<b>131</b>

## List of Figures

1.1.	Illustration of 2D (a) and 3D (b) optical lattice created by sets of contour-propagating waves. Figure from [?] . . . . .	3
1.2.	(1.2a) Mechanism of a Fashbach resonance in a two-channel model. (1.2b) Scattering length $a$ and bound state energy $E$ near Feshbach resonance. Figure from [?] . . . . .	6
4.1.	Integration contour for the Lieb-Liniger model with attractive or repulsive interaction. . . . .	49
4.2.	Pole positions for various $k$ integrations in the repulsive case. Integrated variables are marked on the upper-left corner of the graph . . . . .	52
4.3.	Pole positions for various $k$ integrations in the attractive case. Integrated variables are marked on the upper-left corner of the graph . . . . .	54
4.4.	Example of a saddle point. Figure from Wikimedia . . . . .	60
4.5.	Density evolution for systems with two particles. Figure 4.5a describes repulsive case and Figure 4.5b describes attractive case. Figure 4.5c compares the density at the origin between $c = 5$ and $c = -5$ cases. Figure 4.5d shows the relative density difference. . . . .	62
4.6.	Normalized noise correlation for a two-particle system at $t = 0.02$ (a), $0.1$ (b), $0.5$ (c) and $2$ (d) respectively. Blue line is for repulsive case. Orange line is for attractive case. Green line depicts the free model. . . . .	67
4.7.	Density evolution for two particles moving towards each other. Figure4.7a is for repulsive case. Figure 4.7b is for attractive case. Figure 4.7c compares the density at the origin between $c = 5$ and $c = -5$ cases. Figure 4.7d shows the relative density difference at the origin. . . . .	69
4.8.	Normalized noise correlation for a system with two particles moving towards each other with $k_0 = \pm 10$ . Various figures show results for different times, $t = 0.02$ (a), $0.1$ (b), $0.5$ (c) and $2$ (d) respectively. Blue line is for repulsive case. Orange line is for attractive case. Green line works for free model. . . . .	70

4.9. Normalised noise correlation function in the large time limit. Figure 4.9a describes a system with 3 particles. Figure 4.9b describes a 5-particle system. . . .	77
4.10. Illustration of shifting contours across a pole . . . . .	78
4.11. Illustration of shifting integration contours in a 3-particle system . Figure 4.11a represents the original integral. Contours in Figure 4.11b go through the saddle points. The rest corresponds to pole contributions related to different string configurations. . . . .	79
4.12. Normalised noise correlation function in the large time limit for a system with 3 particles. . . . .	81
5.1. Example integration contours in the Yudson representation for a system with $N - 2$ majority fermions and two impurities. In this example, the $m$ th and $n$ th particles are the impurities counting from the left to right. Figure 5.1a is for repulsive case and Figure 5.1b is for attractive case. . . . .	87
5.2. Pole structure of the integrand of the $\mu$ integration. Both plots apply to systems with $N - 1$ majority fermions and one impurity fermion which is the $m$ th particle counting from the left. Figure 5.2a is for systems with repulsive interaction. Figure 5.2b is for systems with attractive interaction. . . . .	89
5.3. Pole structure of the integrand of the $\mu_1$ integration. Crosses represent poles from $k$ 's and dots represent pole form $\mu_2$ . Among the $N$ fermions, the $m$ th and $n$ th are the impurities. Figure 5.3a is for systems with repulsive interaction. Figure 5.3b is for systems with attractive interaction. . . . .	94
5.4. Examples of $k - \mu$ string and $\mu - k$ string whose length is longer than two. . . .	97
5.5. String states separated out as a result of closing $\mu$ contours from above and shifting all $k$ 's to the real axis. See text for detailed explanation of notations . .	100
5.6. Time evolution of density distribution. Figure 5.6a and 5.6b shows Time evolution of down spin (yellow) and up spin (blue) at $t = 0, 0.02, 0.05, 0.1$ for $c = 5$ and $c = -5$ respectively. Figure 5.6c and 5.6d compare the density of the up spin for different interaction. Figure 5.6e compares the density of the up spin at the origin between $c = 5$ and $c = -5$ cases. Figure 5.6f shows the relative density difference of the up spin between $c = 5$ and $c = -5$ at the origin. . . . .	106
5.7. Normalized noise correlation for a two-particle system with one up spin and one down spin. The down spin is initially to the left to the up spin. The figure shows the correlation at $t = 0.02$ (a), $0.1$ (b), $0.5$ (c) and $2$ (d) respectively. . . . .	108

- 5.8. The leading order of the noise function with  $\sigma \ll a$  are plotted here. Both figures are for large time  $t = 10$  with the impurity located at the second site. Figure 5.8a describes a system with 3 particles. Figure 5.8b is for systems with 10 particles. . . . . 115
- 5.9. Time evolution of the down spin(yellow) and the up spin(blue) at  $t = 0, 0.02, 0.05, 0.1$  for a system with one down spin and one up spin. The down spin moves with  $k_0 = 5$  in the initial state. 5.9a is for repulsive case and 5.9b is for attractive case. 117
- 5.10. Leading order of the noise function with  $\sigma \ll a$ . Both figures are for large time  $t = 10$  with the impurity initially located at the second site and moving with momentum  $k_0 = 5$ . Figure 5.10a describes a system with 3 particles. Figure 5.10b is for systems with 10 particles. . . . . 120

# Chapter 1

## Introduction

### 1.1 Ultracold Atom Experiment

Ultracold atom systems consist of atoms that are cold, dilute and usually neutral. The temperature can be as low as nanokelvin, even picokelvin [? ]. At such low temperature, thermal fluctuation is suppressed and quantum effects dominates. Thus, coherent, macroscopic matter waves exist in the system and Bose-Einstein condensation and Fermi degeneracy are achieved. The typical size of the system ranges from a few to  $10^7$  atoms. And the density is from  $10^{12}$  to  $10^{15}$  particles per  $\text{cm}^3$  to avoid the formation of molecules. This spare us any not well understood interaction. Since the atoms are usually electrically neutral, the whole interaction is well controlled by the Feshbach resonance. Thus both Bose-Einstein condensate and strongly interacting systems can be realized. With large sets of methods to isolate, manipulate and probe the state, the ultracold atom system can be used to simulate quantum states in solid state physics. Moreover, since the constitutes are heavier and colder than the electrons, the time scale of the dynamics are longer compared to that in a solid state system. Therefore, no ultrafast equipment is needed in the experiment. At the same time, as the systems are well isolated from the environment and defect free, the coherent time is very long, this enables one to observe long-lived coherent quantum dynamics. The ultracold atom systems benefit greatly from the ability to control the configuration of the system, to tune the interaction and to measure with great precision, which will be discussed here.

#### 1.1.1 Optical Lattice

Optical lattice, which consists of hundreds of thousands of microtraps, is formed by the interference of counter-propagating laser beams. This artificial crystal of light traps neutral atoms by optical dipole force, an effect called the AC Stark Shift. When light illuminates the atoms, it induces a dipole moment in the atom, which in turn interacts with the light. This modifies the internal energy of the atoms. As the electric field from the laser varies periodically in space, the optical dipole interaction appears as a spatially dependent potential, with

$V = -E \cdot d \propto \alpha |E(r)|^2$ , where  $\alpha$  is the polarizability of the atom, and  $|E(r)|$  is the spatially averaged electric field. When two counter-propagating laser beams are superimposed, one gets a standing wave of the form  $V = V_0 |\sin(kx)|^2$  with  $k = \frac{2\pi}{\lambda}$ , whose period is  $a = \frac{\lambda}{2}$ .

One important advantage of the optical lattice is its tunability of many parameters. First, the dimensionality of the lattice can be varied from 3D to 1D, depending on the configuration of the standing wave imposed. As shown in ??, two sets of perpendicular laser beams create a 2D optical lattice that confines the atoms in an 1D tube. Or three such sets of beams create a cubic array of potential. If the confinement in one direction is much weaker than the other two, one gets back to a 2D array of optical tubes. To make even more complex systems, one can change the relative angle of the standing wave to get triangular lattices [? ], honeycomb lattices [? ] or kagome lattices [? ]. Second, one can change the separation between adjacent sites by varying the wavelength of the light. The depth of the potential can also be controlled by the intensity of the beam. This will affect the hopping among different sites as well as on-site interaction. Lastly, by tuning the laser frequency  $\omega_L$  around the atomic resonance  $\omega_o = (\epsilon_e - \epsilon_g)/\hbar$  ( $\epsilon_e$  being excited energy level and  $\epsilon_g$  being ground state energy), the potential can be attractive or repulsive. When  $\omega_L < \omega_o$ , the potential is attractive, the atoms stay at the high intensity spots. When  $\omega_L > \omega_o$ , the potential is repulsive and the atoms are low field seeking.

Thanks to these features, together with the Feshbach resonance, cold atoms in optical lattice become a valuable model system to study physical situations described by simple Hamiltonians, say Lieb-Liniger model [? ], Gaudin-Yang model [? ? ? ], Hubbard model [? ], Bose-Hubbard model [? ] or Ising model [? ]. For the continuum models, i.e. the Lieb-Liniger model and Gaudin-Yang model, the Hamiltonian is characterized by the contact interaction strength, determined by the Feshbach resonance. For lattice models such as the Hubbard model and Bose-Hubbard model, the Hamiltonian is characterized by the hopping parameter ( $J$ ) and the on-site interaction ( $U$ ). The connection between these parameters and the lattice potential is discussed in [? ]. As shown in [? ],  $J$  and  $U$  can be expressed in terms of the Wannier function, which can be readily calculated numerically from the bandstructure calculation. As to the spin model, the corresponding Hamiltonian can be derived by the Jordan-Wigner transformation from the Hubbard model. To summarize, the optical lattice makes it possible to simulate simple Hamiltonians which used to be a simplification of real complex systems.

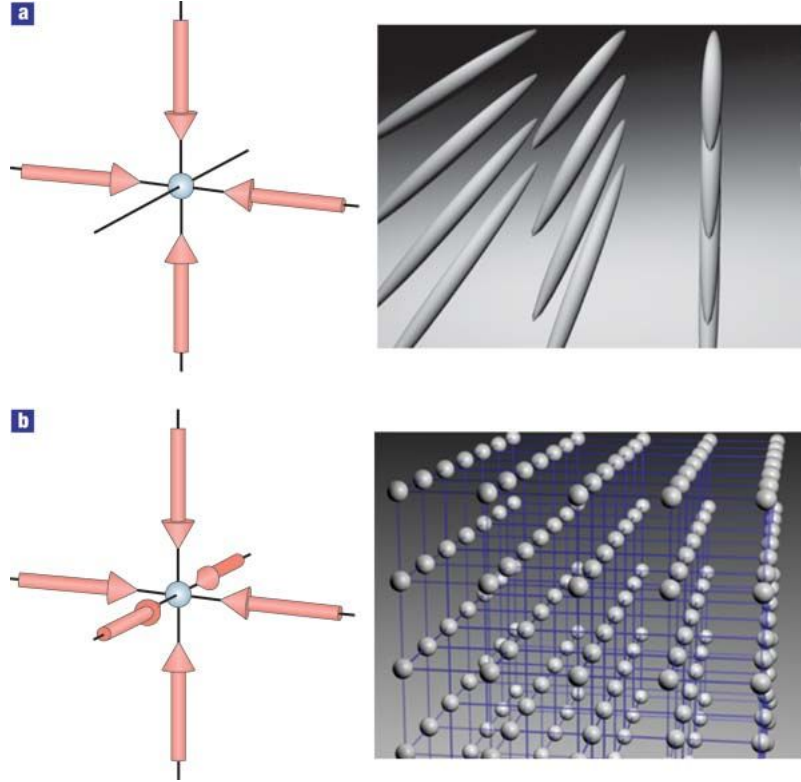


Figure 1.1: Illustration of 2D (a) and 3D (b) optical lattice created by sets of counter-propagating waves. Figure from [? ]

### 1.1.2 Feshbach Resonance

For cold atom experiment, the Feshbach resonance is a unique tool that provides easy control over the effective interaction among particles. The effective interaction is characterized by the scattering phase shift  $\delta_l$  and scattering length  $a_l$ , with  $l$  relates to the angular momentum. In the context of cold atoms, where the kinetic energy is small, the centrifugal cost for  $l \neq 0$  is too much. Thus one only needs to consider the s-wave scattering, i.e.  $a_0$  and  $\delta_0$ . By tuning the system through the Feshbach resonance with magnetic field,  $a_0$  can vary over an enormous range, including positive infinity and negative infinity, see Figure ?? .

Feshbach resonance can be elastic or inelastic. Elastic Feshbach resonance may happen in systems like Cesium  $|F = 4, M_F = 3\rangle$  ( $F$  being the quantum number for the total spin). To understand this resonance, consider the example of two-particle scatterings . The relative motion can be studied as a single-particle scattering problem from a quantum well. To make our life easier consider a square quantum well  $V_0 < 0$  from 0 to  $R$ . Then the wavefunction in

the radial direction equals

$$u(r) = \begin{cases} A \sin(k'r) & r < R \\ B \sin(kr + \delta) & r > R \end{cases} \quad (1.1)$$

with  $k = \frac{\sqrt{2mE}}{\hbar}$  and  $k' = \frac{\sqrt{2m(E+V)}}{\hbar}$ . The boundary condition leads to

$$k' \cot(k'R) = k \cot(kr + \delta_0)$$

whose solution equals

$$\tan(\delta_0) = \frac{k \tan(k'R) - k \tan(kR)}{k' + k \tan(kR) \tan(k'R)}$$

$$\xrightarrow{kR \ll 1} -kR \left( \frac{\tan(k'R)}{k'R} - 1 \right)$$

$a_0$  is fixed by the condition that  $u(a_0) = 0$  as seen from outside the well.<sup>1</sup> From equation ??, one get

$$a_0 \xrightarrow{kR \ll 1} \frac{\tan(\delta_0)}{k}$$

$$\xrightarrow{kR \ll 1} -R \left( \frac{\tan(k'R)}{k'R} - 1 \right)$$

Thus, we can see that for  $k'R < \pi/2$ ,  $a_0$  is negative. As one increases  $V$ , the scattering length oscillates between positive and negative values, sweeping through positive infinity and negative infinity. This corresponds to the Feshbach resonance. At these values ( $k'R = \frac{(2n-1)\pi}{2}$ ), the well is just enough to hold  $n$  bound states, and one of them has zero bounding energy. As the cross section for  $l = 0$  equals  $\sigma = 4\pi a_0^2$ , it also diverges in the Feshbach resonance.

For inelastic Feshbach resonance, multiple atomic states are involved. For example, in sodium gas, atoms in the state  $|m_s = -1/2, m_I = 3/2\rangle$  which correlate into  $|F = 1, m_F = 1\rangle$  ( $S, I, F$  are quantum number for electronic, nuclear, and total spin) may collide and result in the Feshbach resonance [? ]. This results from the coupling with a quasibound state  $|S = 1, m_s = 1, I = 3, m_I = 1\rangle$ . The former is called an open channel and the latter is called a closed channel. When the energy of one of the bound states in the closed channel approaches the energy of two free particles, the scattering gets enhanced and the Feshbach resonance occurs. What happens is that the two free particles transform into the quasibound state, stay together and return to the free state [? ].

As the two states have different spin configuration, the relative energy between them can be varied by external magnetic field. Thus, the bound state can be tuned into resonance with

---

<sup>1</sup>This explains why some scattering length is negative, which is a result of tracing the wavefunction backwards

the continuum state. Near the Feshbach resonance, the scattering length  $a_0$  varies with the magnetic field as

$$a = a_{bg} \left( 1 - \frac{\Delta}{B - B_0} \right)$$

with  $a_{bg}$  being the background scattering length of the open channel, which is as short ranged as the van der Waals force.  $B_0$  and  $\Delta$  define the location and width of the resonance. In the vicinity of the Feshbach resonance, the scattering length blows up to positive or negative infinity.

When  $a_0$  is positive which corresponds to repulsive interaction, the energy of the contributing bound state is lower than the free state energy. This leads to a real bound state and bosonic molecules are formed. The BEC state is obtained. When  $a$  is negative which leads to an effective attraction, the relevant bound state energy is higher than the initial state. This makes the molecule unstable. Atoms bind loosely and BCS state emerges. Thus, the Feshbach resonance leads to the crossover between the BEC and BCS states.

Besides the aforementioned crossover, cold atom systems have also realize other strongly-correlated quantum phases, say Tonk-Girardeau Gas [? ? ] and phase transition from superfluid side to Mott insulator side [? ? ]. Experiments with these systems not only improve our previous understanding of them, but also provide a platform to study systems that are beyond what can be calculated. Such approach is also referred to as quantum simulation.

To sum up, the Feshbach resonance provides the flexibility to tune the effective interaction by external magnetic field. This happens when a quasibound state couples to a free state and their energy are the same. Sweeping the magnetic field across the resonance, the scattering length varies from positive infinity to negative infinity. Different phase of the system are probed. For more information, see Ref. [? ? ? ? ],

### 1.1.3 Measurement

Measurements on the atomic gases are made from optical observation of a probe laser shone on the cloud. The detection exploits three kinds of processes in the atom-light interaction: emission, absorption and phase shift. This corresponds to three imaging techniques, fluorescence imaging, absorption imaging and phase contrast imaging [? ].

Fluorescence imaging is most convenient. A laser beam near the atomic resonance is shone on the atoms, gets absorbed and re-emitted. The scattered light is then collected to form an image. Absorption imaging is the most common method. It collects the unscattered light and images the shadow created by the atomic absorption. This method yields stronger signal than

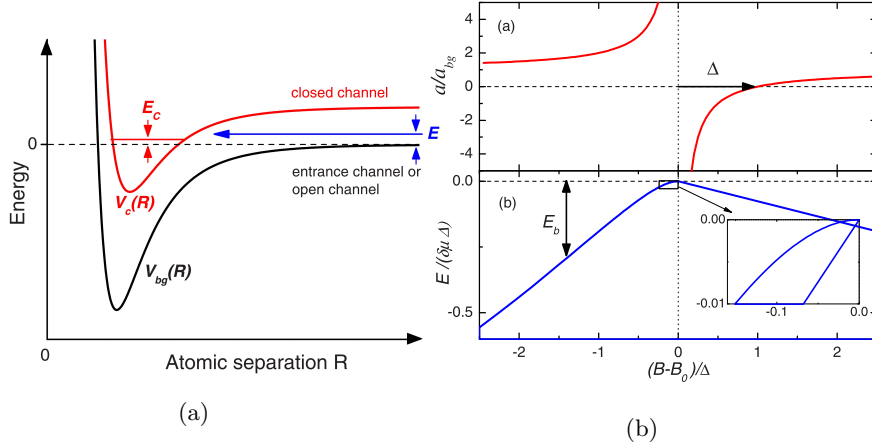


Figure 1.2: (??) Mechanism of a Feshbach resonance in a two-channel model. (??) Scattering length  $a$  and bound state energy  $E$  near Feshbach resonance. Figure from [? ]

the previous one, since light is scattered into all directions in the fluorescence imaging. Both methods are destructive and one need repeated preparation of the same initial state to obtain information about time evolution. Phase contrast imaging is less invasive. An off-resonance light propagates through the atomic gas and gets a phase shift when scattered. Meanwhile, a phase shifter is placed at the focal point that adds a phase of  $\pi/2$  ( $-\pi/2$ ) only to the unscattered light. This configuration enhances the signal and enables one to take a measure on the clouds without affecting it.

An primary measurement that experimentalists made with these techniques is the time-of-flight measurement[? ]. In order to probe a certain state  $|\Psi(T)\rangle$ , one removes the trapping potential and lets the atoms expand ballistically for another period of time  $t$  and then detects the density distribution of the state  $|\Psi(T+t)\rangle$ . Neglecting the initial size in the cloud, this reveals information about the momentum distribution in the state  $|\Psi(T)\rangle$ [? ? ]. That is to say  $\langle n(x, t+T) \rangle_{TOF} = \langle n(k, T) \rangle_{trap}$ . However, each experimental image record a single realization of the density with a lot of spikes. To obtain the density distribution, one need to average over an ensemble of images. In the meanwhile, these fluctuations contain information about higher order correlation, which is important to characterize strongly correlated systems [? ? ]. As discussed in [? ], there are periodic peaks or dips in the density-density correlation functions measured in a time-of-flight experiments. The origin of these peaks and dips is from quantum statistics of the bosonic and fermionic gas. The behaviour away from these locations depends on the many-body state.

Note, in a typical image, each pixel record a substantial number  $N$  of particles, which greatly

suppress the fluctuation by the order  $\frac{1}{\sqrt{N}}$  [? ]. In order to better measure the correlation function and obtain real space density distribution, experimentalists need more local detection. In [? ], single site resolved imaging is realized, but they have not reached the single-atom sensitivity. The difficulty lies in the low signal-to-noise ratio. This obstacle is overcome recently [? ] via high-resolution fluorescence imaging. Such in-situ imaging with single-atom sensibility provides direct information about the density and correlation and enables one to visualize transition from the Bose-Einstein condensate to the Mott insulator state [? ? ].

Aside from the aforementioned momentum distribution, correlation and density distribution function, there are other observables that experimentalists measure to characterize the states of the system [? ]. For example, momentum resolved excitation spectrum are studied in [? ? ] using two-photon Bragg scattering. In [? ? ], transport coefficient relating to the atomic mass flow are studied and Bloch observables are observed. Moreover, quasi-momentum distribution are obtained by band mapping techniques [? ? ] and fraction of doubly occupied sites are measured [? ].

To sum up, the ultracold atom systems provide unique and valuable opportunities for the study of a diverse range of quantum phenomena with easily accessible time scale, long coherent length and high tunability. Its development re-ignited other fields which would be quite challenging to study in the context of condensed matter, one of the fields is the nonequilibrium dynamics.

## 1.2 Nonequilibrium Dynamics

In the previous part, we have talked about systems of ultracold atoms in an optical lattice, which are well isolated from the environment, with convenient timescale and rich toolbox for manipulation and measurement. With these features, the ultracold gases make a unique contribution to the area of nonequilibrium dynamics, spurring questions about whether steady states emerge, how do observables equilibrate and validity of thermodynamic ensembles in describing the equilibrium states in large isolated systems.

A simple setup to study the nonequilibrium process is by quantum quench, i.e. changing one of the system parameters, which can be carried out fast or slow, globally or locally, and see how the state evolves. After the quench, the initial state which is usually the ground state of the initial Hamiltonian become superposition of a vast span of eigenstates of the new Hamiltonian

$H$  and will evolve unitarily as

$$|\Psi(t)\rangle = e^{-iHt}|\Psi(0)\rangle = \sum_n C_n e^{-i\epsilon_n t} |\phi_n\rangle \quad (1.2)$$

with  $|\Psi(t)\rangle$  describes the state of the system at time  $t$ ,  $|\phi_n\rangle$  relates to the eigenstate of  $H$  with eigenenergy  $\epsilon_n$ .

This expression contradicts with ergodicity, which plays a fundamental role in statistical mechanics. The ergodicity says that all states within some energy window are equally important and the system will visit all the corresponding points in phase space. It justifies the notion of ensemble. And calculation of any observable for a time evolved state at large time is equivalent to that averaged over states in the ensemble with some proper weight factor. Thus, the observable only depends on macroscopic quantities which are universal to the ensemble, not on the microscopic state that the system initially is. Thus, we say the state reaches thermal equilibrium.

Classically, the equilibration is made possible by chaos. However, this mechanism does not work in quantum system. As shown in equation ??, the system evolves unitarily under the influence of the Hamiltonian after quench and remembers everything about the initial state. Thus, a pure state will not evolve into a thermal state, though the latter works very well for most observables (which are local) in most systems (which are not integrable or many-body localized).

In an attempt to explain the apparent thermalization, Deutsch and Srednicki proposed the Eigenstate Thermalization Hypothesis (ETH) [? ?]. Instead of focusing on the asymptotic state, the ETH examines the properties of matrix elements of local observables  $\langle \Psi(t)|A|\Psi(t)\rangle$ . Based on equation ??, one has

$$\begin{aligned} \langle \Psi(t)|A|\Psi(t)\rangle &= \sum_{m,n} c_m^* c_n e^{-i(\epsilon_n - \epsilon_m)t} \langle \phi_m|A|\phi_n\rangle \\ &\stackrel{t > t_{th}}{\approx} \sum_n |c_n|^2 \langle \phi_n|A|\phi_n\rangle \end{aligned}$$

In the second line, off-diagonal terms are dropped after some thermalization time  $t_{th}$  when these terms lose coherence [?]. What ETH states is that for those operators that thermalize, their matrix elements are thermal in a sense that  $\langle \phi_n|A|\phi_n\rangle = A(\epsilon_n)$ , i.e. the observable is a smooth function of the energy. Then, one has

$$\langle \Psi(t)|A|\Psi(t)\rangle \stackrel{t > t_{th}}{\approx} A(\epsilon_n)$$

Since the choice of state  $|\Psi(0)\rangle$  is arbitrary, the above expression indicates that any state, either be eigenstate or a superposition of them, thermalize. With this relation, it is straightforward

to see that expectation value of  $A$  of any state will evolve into the prediction of microcanonical ensemble[? ]

$$\langle \Psi(t)|A|\Psi(t) \rangle \stackrel{t > t_{th}}{\approx} \frac{1}{N_{\epsilon_n, \Delta\epsilon_n}} \sum_{|\epsilon_\alpha - \epsilon_n| < \Delta\epsilon_n} \langle \alpha|A|\alpha \rangle$$

As pointed out in [? ], it is also possible to rewrite the above relation with canonical ensemble, as the latter is equivalent to the microcanonical ensemble in the thermodynamics limit

$$\langle \Psi(t)|A|\Psi(t) \rangle \stackrel{t > t_{th}}{\approx} \frac{1}{Z} \sum_{\alpha} e^{-\beta\epsilon_\alpha} \langle \alpha|A|\alpha \rangle$$

where the inverse temperature is fixed by the initial state  $\langle \Psi(0)|H|\Psi(0) \rangle = 1/Z \sum_{\alpha} e^{-\beta\epsilon_\alpha} \epsilon_\alpha$ .

In short, we have seen how the ETH results in thermal behavior in some observables. A necessary condition on the observable to thermalize is locality. That is the observable should have support on a relative small number of particles compare to the whole system. Physically, that means though the whole system evolves unitarily, the subsystem thermalizes, with the rest of the system serves as a heat bath [? ].

There are also situations where ETH does not hold, thus the system does not relax to thermalization for a long time. One of them happens in integrable models, which are the main topic of this thesis. In [? ] the authors calculated two local observables via diagonal ensemble, microcanonical ensemble and for two specific eigenstates. The results are very different for integrable system, while for non-integrable model, results by various approaches agree with each other. Experimentally, systems that are close to integrable also shows non-thermal behaviours. In the quantum Newton's cradle experiment, two pulses of opposite momentum are sent into a 1-D boson system in a harmonic trap, it is observed that the system retains oscillation after thousands of period [? ].

Due to the presence of large number of conserved quantities in integrable systems, the dynamics is much constrained, thus does not thermalize easily. However, these systems do approach a quasi-stationary state called pre-thermalized state. Such state cannot be described by the usual thermodynamic ensemble with fixed number of total energy and particle number. Effect of all integral of motion needs to be properly incorporated. Thus it is natural to consider a generalized Gibbs ensemble (GGE), which says that the density matrix equals

$$\rho_{GGE} = \frac{1}{Z_{GGE}} \exp\left(-\sum_m \lambda_m I_m\right)$$

with  $I_m$  being the conserved quantities. For the Lieb linger model characterized by quasi-momentum  $ks$ , these conserved charges take the simple form  $I_m|k\rangle = \sum_i k_i^m |k\rangle$ .  $\lambda_m$  is the Langrange multipliers fixed by the initial condition.  $Z_{GGE}$  is the partition function. Just as

how maximum-entropy principle leads to the Gibbs ensemble, the same principle also results in GGE with all constraint considered. Similarly, the eigenstate thermalization hypothesis should also be modified to include all conserved quantities [? ]. Such generalization is confirmed experimentally. The authors in [? ] show that it is impossible to use a single temperature, as in Gibbs ensemble, to explain the interference pattern they obtained after coherently splitting one boson gas into two. Instead, they need 10 temperature-like parameters to properly fit the results. This reflects the complex behaviour of an integrable system which can be described by GGE with some appropriate Langrange multipliers. Thus, when valid, the GGE description save one from following the evolution of the integrable system to a stationary state, i.e.

$$\langle \Theta(t \rightarrow \infty) \rangle = \text{Tr}[\rho_{GGE}\Theta]$$

However, in strongly correlated systems, it is still very hard, if possible, to explicitly carry out the trace. Recently, it was shown that generalized Gibbs ensemble is equivalent to an appropriately chosen eigenstate in the infinite system [? ? ]. i.e.

$$\text{Tr}[\rho_{GGE}\Theta] = \langle k_0 | \Theta | k_0 \rangle$$

In [? ], the authors obtained the quasimomentum distribution for the state, thus fix  $|k_0\rangle$  explicitly. This enables them to calculate the two-body and three-body correlation functions.

Although the idea of GGE has been widely accepted and proved to be correct in systems that are equivalent to free fermions [? ? ], there are still doubts on its validity in general systems. As shown in [? ], the GGE prediction for late-time correlation in XXZ model deviates from first principle calculation. The authors in [? ] argue that the failure of GGE is due to the presence of bound states, where the conserved charges cannot uniquely determines the quasimomentum distribution. This is further confirmed by [? ] where it is found that the local charges only depend on the distribution of real quasimomentum, while the correlation function depends on distribution of all complex parameters. Thus, a complete understanding of the asymptotic behavior of a non-equilibrium system is still eluded.

### 1.3 Outline of the Thesis

The remainder of the thesis is organized as follows

In chapter 2, I provide a detailed review on various Bethe Ansatz methods, which are the building blocks for solving quench dynamics. In chapter 2.1, I discuss the coordinate Bethe Ansatz and its application to the Lieb-Liniger model. This solution will be used in chapter 4 to study quench dynamics of a one-dimensional boson gas. In chapter 2.2, algebraic Bethe

Ansatz is used to solve the XXZ model. Based on these two methods, we talked about nested Bethe Ansatz and how it solves the Gaudin-Yang model. Its solution will be the cornerstone for studying the non-equilibrium dynamics in a 1-D fermion system with two species.

In chapter 3, I introduce the main approach used in this thesis, called Yudson Approach. The Yudson presentation provides an efficient way to expand any state in terms of Bethe Ansatz solutions in an infinite system. In chapter 3.1, I discussed the obstacle encountered if one directly uses the Bethe Ansatz solution for the expansion. In chapter 3.2, the Yudson representation is obtained as a simple modification of the usual resolution of the identity  $\mathbb{1} = |k\rangle\langle k|$ . Then in chapter 3.3, I discussed its advantages and disadvantages.

In chapter 4, I apply the Yudson formalism to the study of quench dynamics of Lieb-Liniger model. Chapter 4.1 is devoted to the Central theorem. The integral contours of the representation are specified for attractive and repulsive cases. Proof of the Yudson expansion as an identity resolution is provided. In chapter 4.2, the exact solution for the two-particle scenario is obtained. Density and correlation as a function of time or in the asymptotic limit are plotted and analyzed. In chapter 4.3, I discussed the multiparticle dynamics in the large time limit. Local observables are calculated from the time evolved wavefunction via the Yudson approach. I also talked about the possibility of incorporating the well-studied form factor results into the Yudson approach.

In chapter 5, I studied the time evolution of a two component fermion system described by the Gaudin-Yang model. In chapter 5.1, central theorem is proved for the single impurity case first, where only one fermion is different from the rest of the gases. Then the proof is generalized to systems with multiple impurities. In chapter 5.2, I discuss the physical interpretation of the Yudson representation in terms of bound states. There I will show how bound states emerge dynamically. In chapter 5.3, quench dynamics of two distinguishable particles are studied. Compared with the result in chapter 4.2, the role of quantum statistic becomes clear. In chapter 5.4 and 5.5, I discuss the non-equilibrium dynamics in a system consisting of single impurity and a multi-particle bath, with the impurity being static or kinetic in the initial state.

Chapter 6 is devoted to the time evolution of a two component boson system described by the bosonic Gaudin-Yang model. Bethe ansatz is derived in section 6.1. Yudson representation with interaction specific contour is given in section 6.2. In section 6.3, I discussed the proof of central theorem focusing on the unique aspects of this model compared to the fermionic counterpart. In section 6.4, different types of bound states that exists in the system is listed. The time evolution of local observables are calculated and compared with the fermionic equivalent in section 6.5.

In chapter 7, I make the conclusion and discuss possible future directions that are promising

with the current technique.

## Chapter 2

### Bethe Ansatz

The Bethe Ansatz was first proposed by H. Bethe in 1931 [?] while studying the Heisenberg ferromagnetic problem. It was later used to solve various models like Kondo problem [? ], Hubbard model [? ], Lieb-Liniger model [? ? ], Gaudin-Yang model [? ? ], Anderson model [? ], etc. These Bethe Ansatz solvable models are not free in a sense that the many-body problem cannot be reduced into a single particle one. However, the Bethe Ansatz generalizes this idea so that the many-body dynamics can be factorized into a series of two particle scattering processes. These two particle scattering processes are characterized by scattering matrices. Let's say that  $S_{12}$  describes the process that particle 1 which is initially to the left of particle 2 jumps to the right. Since the problem can be factorized, the sequence of these two particle scattering processes does not matter. This imposes three constraints on the scattering matrices. They are  $S_{ij}S_{ji} = \mathbb{1}$ ,  $S_{jk}S_{ik}S_{ij} = S_{ij}S_{ik}S_{jk}$  and  $S_{ij}S_{mn} = S_{mn}S_{ij}$ . They are known as the Yang-Baxter Equations. As the scattering matrices usually consist of permutation operators which act on the spin space, they do not commute in general. These relations define a class of systems which are Bethe Ansatz solvable. These are also called integrable models. The relation reveals the fact that these systems have more conservation laws, as is the case for classical systems. Actually, the number of integrals of motion for quantum integrable models is infinite. This is the reason why factorization is valid in these systems. One cannot tell if a model is integrable or not from the Hamiltonian. One needs to solve the two particle problem and get the scattering matrix. Only if the scattering matrix satisfies the Yang-Baxter equation can we say the model is integrable. Sometimes, a model can be non-integrable except for a special set of parameters. One example is the two-impurity Anderson model.

The Bethe Ansatz can be further categorized into several forms. The one initially proposed for the Heisenberg model is called Coordinate Bethe Ansatz, as the solution of the problem is expressed in terms of wavefunction in the coordinate space. Algebraic Bethe Ansatz is another form which describes states by raising and lowering operators acting on a reference state. Different models have different commutation relations among these operators, which is why the method gets the adjective algebraic. Nested Bethe Ansatz is a generalization of the Coordinate

Bethe Ansatz applied to systems with internal degrees of freedom. Like the Coordinate Bethe Ansatz, Nested Bethe Ansatz also focuses on the wavefunction. One difference is that besides the momentum which is related to the charge motion, there is also spin rapidity that characterizes spin wave. One can combine the previous two methods to obtain the wavefunctions of the Nested Bethe Ansatz. To do that, one writes down the spacial part of the wavefunction in terms of Coordinate Bethe Ansatz and expresses the spin part using Algebraic Bethe Ansatz. As an illustration, we are going to solve Lieb-Liniger model via Coordinate Bethe Ansatz, XXZ model using Algebraic Bethe Ansatz, then discuss the Nested Bethe Ansatz solution for Gaudin-Yang model. The solution of Lieb-Liniger Model and Gaudin-Yang model will also play an important role for later chapters when we talk about Yudson's Approach for time evolution of a quenched system.

## 2.1 Coordinate Bethe Ansatz

### 2.1.1 Lieb-Liniger Model

As an example of the Coordinate Bethe Ansatz, we will study spinless bosons in a continuous one-dimensional system where particles interact via contact interactions. The model is called the Lieb-Liniger model, defined by the following Hamiltonian

$$H = \int_x \partial_x \Psi^\dagger(x) \partial_x \Psi(x) + c \Psi^\dagger(x) \Psi^\dagger(x) \Psi(x) \Psi(x)$$

where  $\Psi^\dagger(x)$  ( $\Psi(x)$ ) is the creation (annihilation) operator of spinless boson at the point  $x$ . The operator satisfies the canonical commutation relation  $[\Psi^\dagger(x), \Psi(x')] = \delta(x - x')$ .  $c$  parametrizes the strength of the interaction. An eigenstate is defined as follows, with  $|0\rangle$  being the Fock vacuum state.

$$|\Psi\rangle = \int_x f(x_1, x_2, \dots, x_N) \Psi^\dagger(x_1) \Psi^\dagger(x_2) \dots \Psi^\dagger(x_N) |0\rangle$$

Here  $f(x_1, x_2, \dots, x_N) = f(\vec{x})$  is the wavefunction which is symmetric in terms of its argument. The integration is defined on an infinite line, i.e.  $\int_x = \int_{-\infty}^{\infty} dx_1 \int_{-\infty}^{\infty} dx_2 \dots \int_{-\infty}^{\infty} dx_N$ . Then from the relation  $H|\Psi\rangle = E|\Psi\rangle$ , we obtain the first-quantized Hamiltonian which acts on the wavefunction directly

$$h = - \sum_i^N \partial_{x_i}^2 + 2c \sum_{i < j}^N \delta(x_i - x_j)$$

An important feature of this Hamiltonian is that particles do not see each other unless they collide. Therefore, for each ordered region where none of the  $x$ 's are the same, the particles can be treated as free and we can write down the wavefunction as product over plane waves

characterized by quasi-momentum  $k_1, k_2, \dots, k_N$ . The final solution should be a superposition of plane waves with the same total energy ( $\sum k_i^2$ ) and total momentum ( $\sum k_i$ ). For a two particle system, this would simply mean a combination of  $e^{ik_1x_1+ik_2x_2}$  and  $e^{ik_2x_1+ik_1x_2}$ . However, for a generic many-body problem, there are much more  $\{k\}$ 's that satisfy this constraint. And we should include all of them, which makes the solution intractable. However, for integrable models, where all interactions can be factorized into a series of two particle scattering processes which preserve the quasi-momentum set  $\{k\}$ , the Hamiltonian is diagonal in the basis of  $\{k\}$  and we need to include only  $k_i$  that belongs to the same set with all possible permutations among themselves. Mathematically, it means, for each sector  $Q$  with the ordering  $\theta(x_{Q1} < x_{Q2} < \dots < x_{QN})$ , the wavefunction can be written as

$$f_Q(x) = \sum_P e^{i \sum_i k_{p_i} x_i} A_Q(P) \theta(x_{Q1} < x_{Q2} < \dots < x_{QN})$$

Moreover, as the wavefunction is symmetric in  $x$ 's,  $A_Q(P)$  is related to  $A_{Q'}(P)$  as we are going to show in detail in the following. Therefore, wavefunction of different sectors are dependent on each other, and we only need one sector to characterize the state, which is usually chosen to be the sector  $\theta(x_1 < x_2 < \dots < x_N)$ .

Before the discussion of the relation among  $A$ 's for different  $Q$ 's, we want to deviate a little bit and talk about the designations of permutations that we are going to use a lot, which can be confusing sometimes.

## Permutations

The permutation group of  $N$  objects are denoted as  $S_N$ . There are  $N!$  elements in this group. To specify an element, we introduce the following notation

$$P_{123} = \begin{pmatrix} 1 & 2 & 3 \\ 2 & 3 & 1 \end{pmatrix}$$

with the meaning that 1 is replaced by 2, 2 is replaced by 3, 3 is replaced by 1. However, it becomes less clear if the starting state is not ordered increasingly. In general, there are two conventions which we will call 'by element' and 'by position'. Permutation by element designates a permutation by the elements that get switched, e.g.  $P_{123} = \begin{pmatrix} 2 & 1 & 3 \\ 3 & 2 & 1 \end{pmatrix}$ . Permutation by position defines a permutation by the positions of element that get changed. e.g.  $P_{123} = \begin{pmatrix} 2 & 1 & 3 \\ 1 & 3 & 2 \end{pmatrix}$ . Both conventions have been widely used, but the mixture of these conventions can lead to problems. To illustrate their differences, we use letter  $P$  for permutation by

element and letter  $Q$  for permutation by position. It's easy to check that  $P_{23}P_{12} = Q_{12}Q_{23} = \begin{pmatrix} 1 & 2 & 3 \\ 3 & 1 & 2 \end{pmatrix}$ . Also, given  $P_1 = Q_1 = \begin{pmatrix} 1 & 2 & 3 \\ 1 & 3 & 2 \end{pmatrix}$ ,  $P_2 = Q_2 = \begin{pmatrix} 1 & 2 & 3 \\ 3 & 2 & 1 \end{pmatrix}$ , we have  $(k_1, k_3, k_2) \cdot (y_1, y_2, y_3)^T = \sum k_{P_1 i} y_i = \sum k_{P_1 P_2 i} y_{P_2 i} = \sum k_{Q_1 i} y_i = \sum k_{Q_2 Q_1 i} y_{Q_2 i}$ , i.e. consecutive permutations act to the right of previous operator for  $P$  and act to the left for  $Q$ . This difference becomes clear with the matrix representation of the permutation. Define

$$\mathbf{k} = (k_1, k_2, \dots, k_N)^T$$

$$(P_{ij})_{mn} = (Q_{ij})_{mn} = \begin{cases} 1, & \{i, j\} = \{m, n\}, \text{ or } i = j \notin \{m, n\} \\ 0, & \text{otherwise} \end{cases}$$

Then

$$(k_{P_1}, k_{P_2}, \dots, k_{P_N}) = (k_1, k_2, \dots, k_N)P$$

$$(k_{Q_1}, k_{Q_2}, \dots, k_{Q_N}) = (k_1, k_2, \dots, k_N)Q^{-1}$$

Therefore, it's not hard to understand the aforementioned difference as

$$\sum_i k_{P_1 i} y_i = \mathbf{k}^T \cdot P_1 \cdot \mathbf{y} = \mathbf{k}^T \cdot P_1 \cdot P_2 \cdot P_2^{-1} \mathbf{y} = \sum_i k_{P_1 P_2 i} y_{P_2 i}$$

$$\sum_i k_{Q_i} y_i = \mathbf{k}^T \cdot Q_1^{-1} \cdot \mathbf{y} = \mathbf{k}^T \cdot Q_1^{-1} \cdot Q_2^{-1} \cdot Q_2 \cdot \mathbf{y} = \sum_i k_{Q_2 Q_1 i} y_{Q_2 i}$$

And the relation between them is now clear that is  $P = Q^{-1}$ . One advantage of the permutation by element, however, is that we can simply treat the transform  $\sum k_{P_1 i} y_i = \sum k_{P_1 P_2 i} y_{P_2 i}$  as replacing  $i$  by  $P_2 i$  without going through the matrix manipulation. Therefore, from now on, we will use this convention, i.e.  $k_{P_i} = (P^{-1} \mathbf{k})_i$ .

With the clarification of our permutation notation, we will discuss the relation between  $A$ 's of different order  $Q$ . From the bosonic property of the wavefunction, we have

$$f_Q(x) = \sum_P e^{ik_{P_i} x_i} A_Q(P) \theta(x_{Q_1} < x_{Q_2} < \dots < x_{Q_N})$$

$$f_{Q'}(y) = \sum_{P'} e^{ik_{P'_i} y_i} A_{Q'}(P') \theta(y_{Q'_1} < y_{Q'_2} < \dots < y_{Q'_N})$$

$$f_Q(x) = f_{Q'}(y)$$

From the Heaviside function, we have  $x_{Q_i} = y_{Q'_i}$ , therefore

$$f_{Q'}(y) = \sum_{P'} e^{ik_{P'_i} x_{Q Q'^{-1} i}} A_{Q'}(P') \theta(x_{Q_1} < x_{Q_2} < \dots < x_{Q_N})$$

$$= \sum_{P'} e^{ik_{P' Q' Q^{-1} i} x_i} A_{Q'}(P') \theta(x_{Q_1} < x_{Q_2} < \dots < x_{Q_N})$$

$$= f_Q(x)$$

$$A_{Q'}(P') = A_Q(P) \quad \text{if} \quad P = P'Q'Q^{-1}$$

i.e.

$$A_Q(P) = A_{Q'}(PQQ'^{-1})$$

Again, as we have shown here, the amplitude for sectors of different ordering are dependent on each other. We may focus on one sector and obtain the wavefunction for all sectors by the above relation.

Now, the Bethe Ansatz solution can be written as the following in the sector  $x_1 < x_2 < \dots < x_N$

$$f(x) = \sum_P e^{ik_{P_i}x_i} A(P)\theta(x_1 < x_2 < \dots < x_N)$$

Within this sector, all of the coordinates are different, then Schrodinger Equation yields,

$$hf(x) = \sum_i k_i^2 \sum_P e^{ik_{P_i}x_i} A(P)\theta(x_1 < x_2 < \dots < x_N) = Ef(x)$$

i.e.

$$E = \sum_i k_i^2$$

On the boundary of the sector, say  $x_i = x_j$  with  $i < j$ ,  $hf(x) - Ef(x)$  has some terms with  $\delta(x_i - x_j)$  which need to vanish as well, i.e.

$$i(k_{P_i} - k_{P_j})e^{ik_{P_i}x_i} A(P) + i(k_{P'_i} - k_{P'_j})e^{ik_{P'_i}x_i} A(P') + ce^{ik_{P_i}x_i} A(P) + ce^{ik_{P'_i}x_i} A(P') = 0$$

Here we have picked out  $P' = PP_{ij}$  so that the plane wave part are identical. From this equation, we obtain the following relation

$$\begin{aligned} A(PP_{ij})\theta(j - i) &= \frac{k_{P_i} - k_{P_j} - ic}{k_{P_i} - k_{P_j} + ic} A(P)\theta(j - i) \\ &= A_{k_{P_i}}(P_{ij})A(P)\theta(j - i) \end{aligned}$$

Or alternatively

$$A(P' = PP_{ij})\theta(i < j) = \frac{k_{P'_j} - k_{P'_i} - ic}{k_{P'_j} - k_{P'_i} + ic} A(P)\theta(i < j)$$

For our convenience, we can choose  $A(\mathbf{1}) = 1$ , this corresponds to  $k_1$  pairs with the smallest coordinate,  $k_2$  pairs with the next-smallest coordinate, etc. Then, in general, we can write

$$A(P) = \prod_{\substack{i < j \\ P_i > P_j}} \frac{k_{P_j} - k_{P_i} - ic}{k_{P_j} - k_{P_i} + ic} = \prod_{\substack{i < j \\ P^{-1}i > P^{-1}j}} \frac{k_i - k_j - ic}{k_i - k_j + ic}$$

So far, we have derived the Bethe Ansatz eigenstate of the Lieb-Linger model and showed that wavefunctions with different ordering of the  $x$ 's are dependent on each other. Now, we will show

that permutation on the  $k$ 's will also leave the wavefunction unchanged up to a phase factor that depends on  $k$  and the permutation. As an example, we will show that  $f_{P_{ij}k}(x) = f_k(x)S^*(P_{ij})$  with  $S(P)$  being the scattering matrix related to permutation  $P$ , i.e.  $S(P_{ij}) = \frac{k_i - k_j - ic}{k_i - k_j + ic}$  for  $i < j$ .

$$\begin{aligned}
f_{k'}(x) &= \sum_{P'} e^{ik'_{P'm}x_m} A_{k'}(P') \theta(x_1 < \dots < x_N) \\
&= \sum_{P'} e^{ik_{P'_{ij}m}x_m} A_{P'_{ij}k}(P') \theta(x_1 < \dots < x_N) \\
&= \sum_P e^{ik_{Pm}x_m} A_{P_{ij}k}(P_{ij}P) \theta(x_1 < \dots < x_N) \\
A_{P_{ij}k}(P_{ij}P) &= \prod_{\substack{m < n \\ P^{-1}P_{ij}m > P^{-1}P_{ij}n}} \frac{k_{P_{ij}m} - k_{P_{ij}n} - ic}{k_{P_{ij}m} - k_{P_{ij}n} + ic} \\
&= \prod_{\substack{P_{ij}\alpha < P_{ij}\beta \\ P^{-1}\alpha > P^{-1}\beta}} \frac{k_\alpha - k_\beta - ic}{k_\alpha - k_\beta + ic} \\
&= \prod_{\substack{\alpha < \beta \\ P^{-1}\alpha > P^{-1}\beta}} \frac{k_\alpha - k_\beta - ic}{k_\alpha - k_\beta + ic} S^*(P_{ij}) \\
&= A_k(P) S^*(P_{ij})
\end{aligned}$$

The third line can be understood by comparing the following ration

$$\begin{aligned}
&\prod_{\substack{P_{ij}\alpha < P_{ij}\beta \\ P^{-1}\alpha > P^{-1}\beta}} \frac{k_\alpha - k_\beta - ic}{k_\alpha - k_\beta + ic} \Big/ \prod_{\substack{\alpha < \beta \\ P^{-1}\alpha > P^{-1}\beta}} \frac{k_\alpha - k_\beta - ic}{k_\alpha - k_\beta + ic} \\
&= \prod_{\substack{P_{ij}\alpha < P_{ij}\beta \\ \alpha > \beta \\ P^{-1}\alpha > P^{-1}\beta}} \frac{k_\alpha - k_\beta - ic}{k_\alpha - k_\beta + ic} \Big/ \prod_{\substack{P_{ij}\alpha > P_{ij}\beta \\ \alpha < \beta \\ P^{-1}\alpha > P^{-1}\beta}} \frac{k_\alpha - k_\beta - ic}{k_\alpha - k_\beta + ic} \\
&= \prod_{\substack{P_{ij}\alpha < P_{ij}\beta \\ \alpha > \beta \\ P^{-1}\alpha > P^{-1}\beta}} \frac{k_\alpha - k_\beta - ic}{k_\alpha - k_\beta + ic} \prod_{\substack{P_{ij}\alpha < P_{ij}\beta \\ \alpha > \beta \\ P^{-1}\alpha < P^{-1}\beta}} \frac{k_\alpha - k_\beta - ic}{k_\alpha - k_\beta + ic} \\
&= \prod_{\substack{P_{ij}\alpha < P_{ij}\beta \\ \alpha > \beta}} \frac{k_\alpha - k_\beta - ic}{k_\alpha - k_\beta + ic} \\
&= \frac{k_i - k_j + ic}{k_i - k_j - ic} \\
&= S^*(P_{ij})
\end{aligned}$$

Replacing  $A_{P_{ij}k}(P_{ij}P)$  with  $A_k(P)S(P_{ij})$ , we obtain the relation  $f_{P_{ij}k}(x) = f_k(x)S^*(P_{ij})$  for  $i < j$ . Thus  $|k\rangle$  and  $|Pk\rangle$  are the same state and

$$|Pk\rangle = S_k^*(P)|k\rangle \quad (2.2)$$

One property of the Bethe Ansatz wavefunction that we can get from this relation is that  $\lim_{k_i \rightarrow k_j} f_k(x) = -\lim_{k_i \rightarrow k_j} f_{P_{ij}k}(x)$ , i.e.  $f_k(x)$  vanishes as  $k_i \rightarrow k_j$  for any  $i$  and  $j$ . This means that none of the particle could have the same quasi-momentum even if they are bosons. This is a general property of the Bethe Ansatz solutions.

### Bethe Equation

Typically, the next step after we get the wavefunction is to impose periodic boundary condition, i.e.  $f(x_1, x_2, \dots, x_N) = f(x_1 + L, x_2, \dots, x_N)$ , with  $L$  being the size of the system. Write out the right hand side explicitly

$$f(x_1 + L, x_2, \dots, x_N) = \sum_{P'} e^{ik_{P'_1}x_2 + ik_{P'_2}x_3 \dots ik_{P'_N}(x_1+L)} A(P') \theta(x_2 < x_3 < \dots < (x_N + L))$$

and compare with  $f(x_1, x_2, \dots, x_N)$ , one can see that when  $P' = P \begin{pmatrix} 1 & 2 & \dots & N \\ 2 & 3 & \dots & 1 \end{pmatrix}$ , both sides have exponential  $e^{ik_{P_i}x_i}$  which can be cancelled, and we arrive at the equation

$$e^{-ik_{P_1}L} = A(P')/A(P) = \prod_{i \neq 1} \frac{k_{P_1} - k_{P_i} - ic}{k_{P_1} - k_{P_i} + ic}$$

i.e.

$$e^{-ik_iL} = \prod_{j \neq i} \frac{k_i - k_j - ic}{k_i - k_j + ic}, \quad i = 1, \dots, N$$

These equations are the *Bethe equations*, a set of  $N$  coupled equations which are usually hard to solve. To get around this problem, people set the system size to infinity while keeping the density of the particle constant, i.e. go to thermodynamic limit. Thus, instead of solving each  $k$  set that satisfies the Bethe equation, they now look for the distribution of these  $k$ 's. This method is called *thermodynamic Bethe Ansatz*, which has successfully solved both ground state and excited state properties of many systems. We will not go in that direction, but only talk about the patterns of these  $k$  solutions that satisfy Bethe equation in this limit. We want to show that for repulsive case, i.e.  $c > 0$ , only real  $k$ 's are allowed, while for attractive case with  $c < 0$ , there are complex  $k$  solutions which correspond to bound states.

Assuming that there are complex  $k$  solutions, and  $k_i$  is the one with greatest positive imaginary part. Then the left hand side of the Bethe equation goes to infinity in the limit  $L \rightarrow \infty$ . This means that one of the denominator on the right hand side must vanish, i.e.  $k_j = k_i + ic$  for some  $j$ . However, this would violate the assumption that the imaginary part of  $k_i$  is greatest, if  $c$  is positive. Similar argument can be made for  $k_i$  with the most negative imaginary part, and we arrive at the conclusion that for repulsive interaction, all  $k$  solutions have to be real. On

the other hand, this would not be a problem for system with attractive interaction. It simply implies that if there is a solution  $k_i$  with positive imaginary part, there must be another  $k_j$  with the same real part but lies below  $k_i$  by distance  $|c|$  in the complex plane. Similarly, a  $k_j$  in the lower-half plane is always accompanied by another one at  $k_i = k_j + i|c|$ <sup>1</sup>. The pattern that satisfies this is a string in the complex plane, i.e.

$$k_i = k - i \frac{n+1-2j}{2} c, \quad j = 1, \dots, n$$

Here  $n$  is the length of the string, and the solution of an attractive system may include several strings of different lengths. A string of length  $n$  is also called an  $n$ -string, it corresponds to a bound state among  $n$  particles. As an example, if  $k_1, k_2$  and  $k_3$  form a 3-string, then

$$\begin{aligned} f(x) &\sim \sum_P e^{ik(x_{P^{-1}1} + x_{P^{-1}2} + x_{P^{-1}3})} e^{c(x_{P^{-1}1} - x_{P^{-1}3})} \theta(P^{-1}1 > P^{-1}2) \theta(P^{-1}2 > P^{-1}3) \theta(x_1 < x_2 < x_3) \\ &= \sum_P e^{ik(x_{P^{-1}1} + x_{P^{-1}2} + x_{P^{-1}3})} e^{-c|x_{P^{-1}1} - x_{P^{-1}2}|/2 - c|x_{P^{-1}2} - x_{P^{-1}3}|/2 - c|x_{P^{-1}1} - x_{P^{-1}3}|/2} \theta(P^{-1}1 > P^{-1}2) \\ &\quad \theta(P^{-1}2 > P^{-1}3) \end{aligned}$$

Here, due to the divergence of  $S_{12}$  and  $S_{23}$ , only the permutations that satisfy the relation  $P^{-1}1 > P^{-1}2$  and  $P^{-1}2 > P^{-1}3$  contribute. This would be more easily understood if we multiply the wavefunction by the phase  $A(P_{13})^* = \frac{k_1 - k_2 + ic}{k_1 - k_2 - ic} \frac{k_2 - k_3 + ic}{k_2 - k_3 - ic} \frac{k_1 - k_3 + ic}{k_1 - k_3 - ic}$ . Then only the terms that satisfy the two Heaviside functions do not vanish. We have used the symmetry property among  $x$ 's to get the second line. From here, it is clear why a 3-string corresponds to a bound state among three particles, as the amplitude of the wavefunction decreases exponentially as the distance between any of them gets greater. This string pattern of the solution is called *String hypothesis*. This has not been proved but it is widely believed that this is true for infinite system. In the later chapter, we are going to confirm the validity of this hypothesis indirectly by showing that the complete basis of Bethe Ansatz solution indeed involves these string solutions.

## 2.2 Algebraic Bethe Ansatz

As a second form of the Bethe solution, *Algebraic Bethe Ansatz* will be the next subject to talk about here. Two very good references on this topic among many others are the one by L.D Faddeev ([? ]) and F. Franchini ([? ]). The Algebraic Bethe Ansatz is also called *Quantum*

---

<sup>1</sup>Note that the existence of  $k_j = k_i + ic$  is only necessary for the right hand side of Bethe equation to vanish. We will not talk about its sufficiency which would involve the ambiguity of  $\frac{0}{0}$ . This pattern is only a hypothesis, we will not rely on it for any calculation in this thesis

*Inverse Scattering* method. It is a quantum version of the *Inverse Scattering* method which has been used to study classical integrable system long before the development of Algebraic Bethe Ansatz. For quantum systems with classical counterpart, the construction of the two methods also shows similarity. Both methods map a non-trivial interacting problem to a simpler one by the introduction of an auxiliary field. This auxiliary degree of freedom decouples the interaction among the physical degrees of freedom such that the latter only interact with the auxiliary field. This interaction is represented by a  $L$ -operator, e.g.  $L_{ia}(\lambda)$  describes the scattering matrix between physical site  $i$  and auxiliary field. The *monodromy matrix* defined as  $\mathcal{T}_a(\lambda) = L_{na}(\lambda) \dots L_{1a}(\lambda) = \begin{pmatrix} A(\lambda) & B(\lambda) \\ C(\lambda) & D(\lambda) \end{pmatrix}$ , expressed in the auxiliary space  $\mathcal{H}^a$ , then encodes the interaction of the auxiliary field with the whole physical system. Here each entry is an operator that acts on the physical space  $\mathcal{H} = \bigoplus_{i=1}^N \mathcal{H}_i$ . To retrieve the *Transfer Matrix*<sup>2</sup> which characterizes the interaction among physical degrees of freedom, one traces over auxiliary field and gets  $T(\lambda) = \text{Tr}_a \mathcal{T}_a(\lambda) = A(\lambda) + D(\lambda)$ . Here  $\lambda$  is a continuous parameter belong to the auxiliary field. This extra parameter gives us more degrees of freedom, as we are going to see that  $[T(\lambda), T(\mu)] = 0$ . Therefore transfer matrix with different parameter share the same eigenvectors. Thus one may solve an easier eigen problem for some  $T(\lambda)$  claiming that they are also the solution of the physical problem.

The construction starts with the following relations, which are examples of Yang-Baxter relation

$$L_{ia}(\lambda)L_{ib}(\mu)R_{ab}(\lambda - \mu) = R_{ab}(\lambda - \mu)L_{ib}(\mu)L_{ia}(\lambda) \quad (2.3)$$

$$\mathcal{T}_a(\lambda)\mathcal{T}_b(\mu)R_{ab}(\lambda - \mu) = R_{ab}(\lambda - \mu)\mathcal{T}_b(\mu)\mathcal{T}_a(\lambda) \quad (2.4)$$

with subscript  $a$  and  $b$  denote two different auxiliary space  $\mathcal{H}^a$  and  $\mathcal{H}^b$ . Note the second relation (2.4) can be derived from the first one easily as  $[L_{ia}, L_{jb}] = 0$  for  $i \neq j$ ,  $a \neq b$  and

$$\begin{aligned} \mathcal{T}_a(\lambda)\mathcal{T}_b(\mu)R_{ab}(\lambda - \mu) &= L_{na}(\lambda) \dots L_{1a}(\lambda)L_{nb}(\mu) \dots L_{1b}(\mu)R_{ab}(\lambda - \mu) \\ &= L_{na}(\lambda)L_{nb}(\mu) \dots L_{1a}(\lambda)L_{1b}(\mu)R_{ab}(\lambda - \mu) \\ &= L_{na}(\lambda)L_{nb}(\mu) \dots R_{ab}(\lambda - \mu)L_{1b}(\mu)L_{1a}(\lambda) \\ &= R_{ab}(\lambda - \mu)L_{nb}(\mu)L_{na}(\lambda) \dots L_{1b}(\mu)L_{1a}(\mu) \\ &= R_{ab}(\lambda - \mu)\mathcal{T}_b(\mu)\mathcal{T}_a(\lambda) \end{aligned}$$

---

<sup>2</sup>Its name originates from solving classical two dimensional models, like six-vertex model. This name has no particular meaning in the context here

Here relation (??) can also be written as

$$(\mathcal{T}(\lambda) \otimes \mathcal{T}(\mu)) R(\lambda - \mu) = R(\lambda - \mu) \Pi (\mathcal{T}(\mu) \otimes \mathcal{T}(\lambda)) \Pi \quad (2.5)$$

with  $\Pi$  being the permutation operator that exchanges the two auxiliary degrees of freedom.

$$\Pi = \begin{pmatrix} 1 & 0 & 0 & 0 \\ 0 & 0 & 1 & 0 \\ 0 & 1 & 0 & 0 \\ 0 & 0 & 0 & 1 \end{pmatrix}_{ab}$$

This relation reveals an important property of the system. Multiply  $R^{-1}(\lambda, \mu)$  from the left on both sides and take the trace over both auxiliary fields. Due to cyclic property of the trace, we get  $T(\lambda)T(\mu) = T(\mu)T(\lambda)$ , i.e  $[T(\lambda), T(\mu)] = 0$ . Expand the transfer matrix in power of its entry, we get an infinite set of charges that commute with each other. One of them, as show later, is the Hamiltonian. This guarantees the integrability of the system.

The construction relies on the relation (??) and (??) which also impose a constraint on the R-matrix as

$$\begin{aligned} & L_{ia}(\lambda)L_{ib}(\mu)L_{ic}(\nu)R_{bc}(\mu - \nu)R_{ac}(\lambda - \nu)R_{ab}(\lambda, \nu) \\ &= R_{bc}(\mu - \nu)L_{ia}(\lambda)L_{ic}(\nu)L_{ib}(\mu)R_{ac}(\lambda - \nu)R_{ab}(\lambda - \mu) \\ &= R_{bc}(\mu, \nu)R_{ac}(\lambda - \nu)L_{ic}(\nu)L_{ia}(\lambda)L_{ib}(\mu)R_{ab}(\lambda, \nu) \\ &= R_{bc}(\mu - \nu)R_{ac}(\lambda - \nu)R_{ab}(\lambda - \mu)L_{ic}(\nu)L_{ib}(\mu)L_{ia}(\lambda) \end{aligned}$$

i.e.

$$\begin{aligned} & L_{ia}(\lambda)L_{ib}(\mu)L_{ic}(\nu) \\ &= R_{bc}(\mu - \nu)R_{ac}(\lambda - \nu)R_{ab}(\lambda - \mu)L_{ic}(\nu)L_{ib}(\mu)L_{ia}(\lambda)R^{-1}_{ab}(\lambda, \mu)R^{-1}_{ac}(\lambda, \nu)R^{-1}_{bc}(\mu, \nu) \end{aligned}$$

Here one has passed  $R_{bc}$  first though the product of  $L$  operator and then pass  $R_{ac}$  and  $R_{ab}$  successively. One can also reverse this process and calculate  $L_{ia}(\lambda)L_{ib}(\mu)L_{ic}(\nu)R_{ab}(\lambda, \nu)R_{ac}(\lambda - \nu)R_{bc}(\mu - \nu)$ , then one can obtain the relations

$$\begin{aligned} & L_{ia}(\lambda)L_{ib}(\mu)L_{ic}(\nu) \\ &= R_{ab}(\lambda - \mu)R_{ac}(\lambda - \nu)R_{bc}(\mu - \nu)L_{ic}(\nu)L_{ib}(\mu)L_{ia}(\lambda)R^{-1}_{bc}(\mu, \nu)R^{-1}_{ac}(\lambda, \nu)R^{-1}_{ab}(\lambda, \mu) \end{aligned}$$

Combining these two relations, one obtains the following relation

$$U_{abc}(\lambda, \mu, \nu)L_{ic}(\nu)L_{ib}(\mu)L_{ia}(\lambda)U^{-1}_{abc}(\lambda, \mu, \nu) = L_{ic}(\nu)L_{ib}(\mu)L_{ia}(\lambda)$$

$$U_{abc}(\lambda, \mu, \nu) = R^{-1}_{ab}(\lambda, \mu)R^{-1}_{ac}(\lambda, \nu)R^{-1}_{bc}(\mu, \nu)R_{ab}(\lambda - \mu)R_{ac}(\lambda - \nu)R_{bc}(\mu - \nu) = \mathbf{1}$$

i.e.

$$R_{ab}(\lambda - \mu)R_{ac}(\lambda - \nu)R_{bc}(\mu - \nu) = R_{bc}(\mu - \nu)R_{ac}(\lambda - \nu)R_{ab}(\lambda - \mu) \quad (2.6)$$

This is another example of the Yang-Baxter relation whose role is similar to the adjoint representation of the Lie algebra. A key step of the quantum Inverse Scattering method is to find a R-matrix that satisfies the Yang-Baxter relation. This R-matrix plays a very important role through relation (??) and (??) as it defines the algebraic structure of the L-operator, transfer matrix and its matrix elements which are operators that act in the full quantum space  $\mathcal{H}$ . There are systems with the same R-matrix but different L-operators. They are closely related and can be compared to different representation of the Lie algebra. Examples of this are XXX model and Lieb-Liniger model, XXZ model and sine-Gordon model.

Although the R-matrix plays an important role in the construction of quantum Inverse Scattering method, in general, it is not possible to write down the R-matrix for a specific system<sup>3</sup>. In practice, one looks for solutions of R-matrix that satisfy the Yang-Baxter relation and use Inverse Scattering machinery to identify the problem.

As an example of the Algebraic Bethe Ansatz, we will solve XXZ model with the assumption that we have already known the R-matrix and will show how one relates this R-matrix with the XXZ Hamiltonian.

### 2.2.1 XXZ Model

The R-matrix of XXZ model is

$$R(\lambda - \mu) = \begin{pmatrix} f(\mu, \lambda) & 0 & 0 & 0 \\ 0 & 1 & g(\mu, \lambda) & 0 \\ 0 & g(\mu, \lambda) & 1 & 0 \\ 0 & 0 & 0 & f(\mu, \lambda) \end{pmatrix}_{ab}$$

with  $f(\lambda, \mu) = \frac{\sinh(\lambda - \mu + \phi)}{\sinh(\lambda - \mu)}$ ,  $g(\lambda, \mu) = \frac{\sinh(\phi)}{\sinh(\lambda - \mu)}$ . One can plug it into equation (??) and test that it satisfies the Yang-Baxter equation. Sometimes, people also call  $\tilde{R}(\lambda - \mu) = R(\lambda - \mu)\Pi$  the R-matrix. Here  $\Pi$  is the permutation operator such that in  $\tilde{R}(\lambda - \mu)$ , matrix element  $g(\lambda, \mu)$  and 1 switch position. With this matrix, one may simplify equation (??) as

$$(\mathcal{T}(\lambda) \otimes \mathcal{T}(\mu))\tilde{R}(\lambda - \mu) = \tilde{R}(\lambda - \mu)(\mathcal{T}(\mu) \otimes \mathcal{T}(\lambda))$$

---

<sup>3</sup>In some cases, one can make use of the result from Coordinate Bethe Ansatz to write down R-matrix and we are going to talk about that in the context of Nested Bethe Ansatz

To avoid confusion, we will call this matrix  $\tilde{R}(\lambda - \mu)$  and without explicit specification, we mean  $R(\lambda - \mu)$  by the name R-matrix.

After one write down the R-matrix, one needs to find a  $L$ -operator that also satisfies the Yang-Baxter equation. The solution is not unique. The simplest construction would simply be using the form of the R-matrix up to an arbitrary constant, i.e.  $L_{ia}(\lambda) = C(\lambda)R_{ia}(-\lambda)$  with  $C$  being a complex function of  $\lambda$ . Models defined by these  $L$ -operators are called *fundamental*, and are usually spin models. Other  $L$ -operator satisfying the Yang-Baxter equation can also be found, say, for sine-Gordon model which has the same R-matrix, the  $L$ -operator is a  $2 \times 2$  matrix that is closely related to its classical counterpart. For XXZ model, we can easily write down the  $L$ -operator as

$$\begin{aligned} L_{ia}(\lambda) &= \frac{1}{\sinh(\lambda + \phi)} \begin{pmatrix} \sinh(\lambda + \phi) & 0 & 0 & 0 \\ 0 & \sinh(\lambda) & \sinh(\phi) & 0 \\ 0 & \sinh(\phi) & \sinh(\lambda) & 0 \\ 0 & 0 & 0 & \sinh(\lambda + \phi) \end{pmatrix}_{ia} \\ &= \frac{1}{\sinh(\lambda + \phi)} \begin{pmatrix} \sinh(\lambda + \frac{1+\sigma_i^z}{2}\phi) & \sinh(\phi)\sigma_i^- \\ \sinh(\phi)\sigma_i^+ & \sinh(\lambda + \frac{1-\sigma_i^z}{2}\phi) \end{pmatrix}_a \end{aligned}$$

In the second line, the  $L$ -operator is written in the basis of the auxiliary field in  $V^a$ . The monodromy matrix  $\mathcal{T}(\lambda)$  can be written in terms of these  $L$ -operators as  $\mathcal{T}(\lambda) = L_{na}(\lambda) \dots L_{1a}(\lambda)$  also expressed in  $V^a$ . It's easy to see that  $L_{na}(0) = \Pi_{na}$  and  $\mathcal{T}(0) = \Pi_{na} \dots \Pi_{1a}$ . The transfer matrix can then be written as  $T(\lambda) = \text{Tr}_a \mathcal{T}_a(\lambda)$ . As we have seen already  $[T(\lambda), T(\mu)] = 0$ ,  $T(\lambda)$  is the generating function of commuting conserved charges, which in general can be written as

$$\begin{aligned} J_{\{c\}} &= \sum_n \sum_j c_{nj} \frac{d^n \ln(T(\lambda))}{d\lambda^n} \Big|_{\lambda=\lambda_j} \\ [J_{\{c\}}, J_{\{c'\}}] &= 0 \end{aligned}$$

Here, we want to show that the Hamiltonian is among these integrals of motion, to be specific, we want to show that  $H = \frac{d \ln T(\lambda)}{d\lambda} \Big|_{\lambda=0} = \frac{dT(\lambda)}{d\lambda} \Big|_{\lambda=0} T^{-1}(0)$ .<sup>4</sup>

Using the property that  $\Pi_{mn} O_{in} \Pi_{mn} = O_{im}$ , i.e.  $\Pi_{mn} O_{in} = O_{im} \Pi_{mn}$ , we have

$$\begin{aligned} T(0) &= \Pi_{na} \dots \Pi_{1a} \\ &= \Pi_{1a} \Pi_{n1} \dots \Pi_{21} \\ &= \Pi_{1a} \Pi_{12} \Pi_{n2} \dots \Pi_{23} \\ &= \Pi_{1a} \Pi_{12} \Pi_{23} \dots \Pi_{(n-1)n} \end{aligned}$$

---

<sup>4</sup>This expression comes as a definition for the Hamiltonian, as it turns out to be local in real space. People then related this to the XXZ model

As

$$\Pi_{ia} = \begin{pmatrix} 1 & 0 & 0 & 0 \\ 0 & 0 & 1 & 0 \\ 0 & 1 & 0 & 0 \\ 0 & 0 & 0 & 1 \end{pmatrix}_{ia} = \begin{pmatrix} \frac{1+\sigma_i^z}{2} & \sigma_i^- \\ \sigma_i^+ & \frac{1-\sigma_i^z}{2} \end{pmatrix}_a = \frac{1 + \vec{\sigma}_i \vec{\sigma}_a}{2}$$

$\text{Tr}_a \Pi_{ia} = 1$  and  $T(0) = \Pi_{12}\Pi_{23}\dots\Pi_{(n-1)n}$  which is related to the process of transferring particle  $n$  from one end to the other, i.e.  $T(0) = e^{i\hat{P}}$ , with  $\hat{P}$  the momentum operator. Similarly, as  $\mathcal{T}'(0) = \sum_i \Pi_{na}\dots L'_{ia}(0)\dots\Pi_{1a} = \sum_i \Pi_{1a}\Pi_{n1}\dots L'_{i1}(0)\dots\Pi_{12}$ ,  $T'(0) = \text{Tr}_a \mathcal{T}'(0) = \Pi_{n1}\dots L'_{i1}(0)\dots\Pi_{21}$ . Thus

$$\begin{aligned} T'(0)T^{-1}(0) &= \sum_i \Pi_{n1}\dots L'_{i1}(0)\Pi_{i1}\dots\Pi_{n1} \\ &= \sum_i \Pi_{(n-1),n}\dots L'_{in}\Pi_{in}\dots\Pi_{(n-1)n} \\ &= \sum_i L'_{i(i+1)}(0)\Pi_{i(i+1)} \end{aligned}$$

With

$$L'_{i(i+1)}(0) = \begin{pmatrix} 0 & 0 & 0 & 0 \\ 0 & \frac{1}{\sinh \phi} & -\frac{\cosh \phi}{\sinh \phi} & 0 \\ 0 & -\frac{\cosh \phi}{\sinh \phi} & \frac{1}{\sinh \phi} & 0 \\ 0 & 0 & 0 & 0 \end{pmatrix}_{i(i+1)}$$

Therefore

$$\begin{aligned} \frac{d \ln T(\lambda)}{\lambda} \Big|_{\lambda=0} &= \sum_i \begin{pmatrix} 0 & 0 & 0 & 0 \\ 0 & -\frac{\cosh \phi}{\sinh \phi} & \frac{1}{\sinh \phi} & 0 \\ 0 & \frac{1}{\sinh \phi} & -\frac{\cosh \phi}{\sinh \phi} & 0 \\ 0 & 0 & 0 & 0 \end{pmatrix}_{i(i+1)} \\ &= \frac{1}{\sinh \phi} \sum_i \left( \cosh \phi \frac{\sigma_i^z \sigma_{i+1}^z}{2} + \sigma_i^+ \sigma_{i+1}^- + \sigma_i^- \sigma_{i+1}^+ \right) \end{aligned}$$

One can identify this as the Hamiltonian of XXZ model with anisotropy  $\Delta = \cosh \phi > 1$  up to a constant. Thus we showed that  $[T(\lambda), H] = 0$ . Therefore, we can transform the problem of solving for eigenstates of the Hamiltonian into an eigen-problem of the transfer matrix  $T(\lambda) = A(\lambda) + D(\lambda)$ .

To start with, we need to define a reference state such that it vanishes when acted by some 'annihilation operator'. The operators that we have on hand are the four matrix elements of the transfer matrix.  $A(\lambda)$  and  $D(\lambda)$  measures the  $\sigma^z$  at each site without flipping the spins.

$B(\lambda)(C(\lambda))$  flips one spin down (up) along the chain. This can be seen from the conservation of total spin in the z-direction in  $\mathcal{H}^a \oplus \mathcal{H}$ . As  $B(\lambda) = {}_a\langle \uparrow | T(\lambda) | \downarrow \rangle_a$ ,  $B(\lambda)$  must flip down one spin in the physical system. Similar argument applies to  $C(\lambda)$ . Therefore, we may choose  $|0\rangle = \bigoplus_{i=1}^N |\uparrow\rangle_i$  as the reference state which can be annihilated by a destruction operator  $C(\lambda)$ . It's easy to check that indeed, this reference state is an eigenstate of  $T(\lambda)$  as  $A(\lambda) + D(\lambda)|0\rangle = [1 + (\sinh \lambda / \sinh(\lambda + \phi))^N]|0\rangle$ . The other states will be accessed by successive application of the B-operator on  $|0\rangle$  with the requirement that  $[A(\lambda) + D(\lambda)] \prod_i B(\mu_i)|0\rangle = \Lambda(\lambda, \vec{\mu}) \prod_i B(\mu_i)|0\rangle$ . Here  $\Lambda(\lambda, \vec{\mu})$  denotes the eigenvalue of the transfer matrix.

Relation (??) defines 16 commutation relations among the four operators, i.e.

$$\begin{aligned} & \begin{pmatrix} A(\lambda)A(\mu) & A(\lambda)B(\mu) & B(\lambda)A(\mu) & B(\lambda)B(\mu) \\ A(\lambda)C(\mu) & A(\lambda)D(\mu) & B(\lambda)C(\mu) & B(\lambda)D(\mu) \\ C(\lambda)A(\mu) & C(\lambda)B(\mu) & D(\lambda)A(\mu) & D(\lambda)B(\mu) \\ C(\lambda)C(\mu) & C(\lambda)D(\mu) & D(\lambda)C(\mu) & D(\lambda)D(\mu) \end{pmatrix} \begin{pmatrix} f(\mu, \lambda) & 0 & 0 & 0 \\ 0 & 1 & g(\mu, \lambda) & 0 \\ 0 & g(\mu, \lambda) & 1 & 0 \\ 0 & 0 & 0 & f(\mu, \lambda) \end{pmatrix} \\ = & \begin{pmatrix} f(\mu, \lambda) & 0 & 0 & 0 \\ 0 & 1 & g(\mu, \lambda) & 0 \\ 0 & g(\mu, \lambda) & 1 & 0 \\ 0 & 0 & 0 & f(\mu, \lambda) \end{pmatrix} \begin{pmatrix} A(\mu)A(\lambda) & B(\mu)A(\lambda) & A(\mu)B(\lambda) & B(\mu)B(\lambda) \\ C(\mu)A(\lambda) & D(\mu)A(\lambda) & C(\mu)B(\lambda) & D(\mu)B(\lambda) \\ A(\mu)C(\lambda) & B(\mu)C(\lambda) & A(\mu)D(\lambda) & B(\mu)D(\lambda) \\ C(\mu)D(\lambda) & D(\mu)C(\lambda) & C(\mu)D(\lambda) & D(\mu)D(\lambda) \end{pmatrix} \end{aligned}$$

Here we list some of the relations that will be used later

$$B(\lambda)B(\mu) = B(\mu)B(\lambda)$$

$$A(\lambda)B(\mu) = f(\mu, \lambda)B(\mu)A(\lambda) - g(\mu, \lambda)B(\lambda)A(\mu) \quad (2.7)$$

$$D(\lambda)B(\mu) = f(\lambda, \mu)B(\mu)D(\lambda) - g(\lambda, \mu)B(\lambda)D(\mu) \quad (2.8)$$

With these relations, we can calculate  $A(\lambda) \prod_i^N B(\mu_i)|0\rangle$  and  $D(\lambda) \prod_i^N B(\mu_i)|0\rangle$  and derive the condition for  $\prod_i^N B(\mu_i)|0\rangle$  to be an eigenstate.

$$\begin{aligned} & A(\lambda) \prod_i^N B(\mu_i)|0\rangle \\ = & f(\mu_1, \lambda)B(\mu_1)A(\lambda) \prod_{i=1}^N B(\mu_i)|0\rangle - g(\mu_1, \lambda)B(\lambda)A(\mu_1) \prod_{i=2}^N B(\mu_i)|0\rangle \\ = & f(\mu_1, \lambda)f(\mu_2, \lambda)B(\mu_1)B(\mu_2)A(\lambda) \prod_{i=3}^N B(\mu_i)|0\rangle - f(\mu_1, \lambda)g(\mu_2, \lambda)B(\mu_1)B(\lambda)A(\mu_2) \prod_{i=3}^N B(\mu_i)|0\rangle \\ & - g(\mu_1, \lambda)f(\mu_2, \mu_1)B(\lambda)B(\mu_2)A(\mu_1) \prod_{i=3}^N B(\mu_i)|0\rangle + g(\mu_1, \lambda)g(\mu_2, \mu_1)B(\lambda)B(\mu_1)A(\mu_2) \prod_{i=3}^N B(\mu_i)|0\rangle \end{aligned}$$

Collect the terms with  $A(\mu_2)$ ,

$$\begin{aligned} g(\mu_1, \lambda)g(\mu_2, \mu_1) - f(\mu_1, \lambda)g(\mu_2, \lambda) &= \frac{\sinh \phi}{\sinh(\mu_1 - \lambda)} \left( \frac{\sinh \phi}{\sinh(\mu_2 - \mu_1)} - \frac{\sinh(\mu_1 - \lambda + \phi)}{\sinh(\mu_2 - \lambda)} \right) \\ &= \frac{\sinh \phi \sinh(\mu_1 - \mu_2 + \phi)}{\sinh(\mu_2 - \lambda) \sinh(\mu_1 - \mu_2)} \\ &= g(\mu_2, \lambda)f(\mu_1, \mu_2) \end{aligned}$$

Therefore

$$\begin{aligned} A(\lambda) \prod_i^N B(\mu_i)|0\rangle &= f(\lambda, \mu_1)f(\mu_2, \lambda)B(\mu_1)B(\mu_2)A(\lambda) \prod_{i=3}^N B(\mu_i)|0\rangle \\ &\quad - g(\mu_1, \lambda)f(\mu_2, \mu_1)B(\lambda)B(\mu_2)A(\mu_1) \prod_{i=3}^N B(\mu_i)|0\rangle \\ &\quad - g(\mu_2, \lambda)f(\mu_1, \mu_2)B(\lambda)B(\mu_1)A(\mu_2) \prod_{i=3}^N B(\mu_i)|0\rangle \end{aligned}$$

Here, we can see that  $\mu_1$  and  $\mu_2$  are symmetric, which is what one should expect as  $B(\mu_1)$  commutes with  $B(\mu_2)$ . Therefore, we can write down the final result using the symmetry among the  $\mu$ 's and

$$A(\lambda) \prod_i^N B(\mu_i)|0\rangle = a(\lambda) \prod_i f(\mu_i, \lambda) \prod_i B(\mu_i)|0\rangle - \sum_j a(\mu_j)g(\mu_j, \lambda) \prod_{i \neq j} f(\mu_i, \mu_j)B(\lambda) \prod_{i \neq j} B(\mu_i)|0\rangle$$

Similarly, one can obtain

$$D(\lambda) \prod_i^N B(\mu_i)|0\rangle = d(\lambda) \prod_i f(\lambda, \mu_i) \prod_i B(\mu_i)|0\rangle - \sum_j d(\mu_j)g(\lambda, \mu_j) \prod_{i \neq j} f(\mu_j, \mu_i)B(\lambda) \prod_{i \neq j} B(\mu_i)|0\rangle$$

Here  $A(\lambda)|0\rangle = a(\lambda)|0\rangle$ ,  $D(\lambda)|0\rangle = d(\lambda)|0\rangle$ . Summing these two expressions, we get

$$\begin{aligned} \Lambda(\lambda, \vec{\mu}) &= a(\lambda) \prod_i f(\mu_i, \lambda) + d(\lambda) \prod_i f(\lambda, \mu_i) \\ \frac{a(\mu_j)}{d(\mu_j)} &= \prod_{i \neq j} \frac{f(\mu_j, \mu_i)}{f(\mu_i, \mu_j)} \end{aligned}$$

Here, we have used the fact that  $g(\lambda, \mu_j) = -g(\mu_j, \lambda)$ . This second equation is the condition for the state  $\prod_i^N B(\mu_i)|0\rangle$  to be an eigenstate of  $T(\lambda)$  and the Hamiltonian. It is the famous *Bethe equation*, that can also be derived from coordinate Bethe Ansatz by imposing periodic boundary condition. Plug in the expression of  $a$ ,  $d$  and  $f$ , it can be written explicitly as

$$\left( \frac{\sinh(\mu_j + \phi)}{\sinh \mu} \right)^N = \prod_{i \neq j} \frac{\sinh(\mu_i - \mu_j - \phi)}{\sinh(\mu_i - \mu_j + \phi)}$$

The more traditional form can be obtained by replacing  $\mu_j$  with  $\mu_j - \phi/2$ . The Bethe equation then becomes

$$\left( \frac{\sinh(\mu_j + \phi/2)}{\sinh(\mu_j - \phi/2)} \right)^N = \prod_{i \neq j} \frac{\sinh(\mu_j - \mu_i + \phi)}{\sinh(\mu_j - \mu_i - \phi)} \quad (2.9)$$

Like in the case of coordinate Bethe Ansatz, one may then use the thermodynamic Bethe Ansatz machinery to study the distribution of  $\mu$  and then calculate the spectrum and other properties of the system. But we are going to skip that part as we are more interested in the dynamics of a system rather than its thermal properties. Before we close the introduction about the algebraic Bethe Ansatz, let's talk about its relation with the coordinate one. Just as we can recover the first quantized wavefunction from the second quantized operator method, we can also obtain the coordinate Bethe Ansatz from the algebraic expression.

### Obtain Wavefunction from Algebraic Bethe Ansatz

In this part, we want to derive the wavefunction related to excited states created by the B-operator, i.e.  $\sum_{\alpha} \phi(\alpha|\mu) \prod_{i=1}^M \sigma_{\alpha_i}^- |0\rangle \equiv \prod_{i=1}^M B(\mu_i)|0\rangle$ . As the wavefunction is symmetric in its argument  $\alpha$ , we may focus on the region where  $\alpha_1 < \dots < \alpha_M$  and all other regions can be obtained easily from it. We will show that

$$\phi(\alpha|\mu)\theta(\alpha_1 < \dots < \alpha_M) = \sum_{R \in S_M} \prod_{i < j} f(\mu_{Rj}, \mu_{Ri}) \theta(\alpha_i < \alpha_j) \prod_{i=1}^M I(\mu_{Ri}, \alpha_i) \quad (2.10)$$

$$I(\mu, \alpha) = \prod_{m > \alpha} a_m(\mu) b_{\alpha}(\mu) \prod_{n < \alpha} d_n(\mu)$$

Here  $a_i(\mu)$ ,  $b_i(\mu)$  and  $d_i(\mu)$  come from the L-operator acting on the vacuum

$$L_{ia}(\mu) | \uparrow \rangle_i = \begin{pmatrix} a_i(\mu) & b_i(\mu) \sigma_i^- \\ 0 & d_i(\mu) \end{pmatrix} \Big|_a \uparrow \rangle$$

We will start with wavefunction with one spin flip. Then talk about that of two excitations. In the end, generalize it to states with more down spins.

The derivation for the state  $B(\mu)|0\rangle$  is quit simple. As  $B(\mu) = \mathcal{T}(\mu)_{12} = (L_{na}(\mu) \dots L_{1a}(\mu))_{12}$  and  $L_{ia}(\mu)_{21} | \uparrow \rangle_i = 0$ , we have

$$\begin{aligned} B(\mu)|0\rangle &= \sum_i L_{na}(\mu)_{11} \dots L_{(i+1)a}(\mu)_{11} L_{ia}(\mu)_{12} L_{(i-1)a}(\mu)_{22} \dots L_{1a}(\mu)_{22} \\ &= \sum_i \prod_{m > i} a_m(\mu) b_i(\mu) \prod_{n < i} d_n(\mu) \sigma_i^- |0\rangle \end{aligned}$$

i.e.

$$\phi(i|\mu) = \prod_{m > i} a_m(\mu) b_i(\mu) \prod_{n < i} d_n(\mu) = I(i, \mu)$$

Going from one excitation to two is not trivial, because  $L_{ia}(\mu)_{21}$  no longer vanished when acting on a state with down spins. Here we describe the method used in ([? ]) to obtain the wavefunction.

First, divide the  $N$  sites in physical space into two part.  $T_1$  contains site 1 to site  $m$ ,  $T_2$  contains the sites from  $m + 1$  to  $N$ . Here  $m$  can be any integer between 1 and  $N$ . Then

$$T(\mu) = T_2(\mu)T_1(\mu)$$

$$B(\mu) = A_2(\mu)B_1(\mu) + B_2(\mu)D_1(\mu)$$

where  $B_1$  and  $D_1$  act on  $T_1 = \bigoplus_{i=1}^M \mathcal{H}_i$  and  $A_2$  and  $B_2$  act on  $T_2 = \bigoplus_{i=m+1}^N \mathcal{H}_i$ . The product of two creation operators in the full space can be written as

$$\begin{aligned} B(\mu)B(\lambda) &= A_2(\mu)B_1(\mu)A_2(\lambda)B_2(\lambda) + B_2(\mu)D_1(\mu)A_2(\lambda)B_2(\lambda) \\ &\quad A_2(\mu)B_1(\mu)B_2(\lambda)D_1(\lambda) + B_2(\mu)D_1(\mu)B_2(\lambda)D_1(\lambda) \end{aligned}$$

We label the four terms with the following partition of  $\lambda$  and  $\mu$ .  $P_1 = (\{\lambda, \mu\}, \{\})$ ,  $P_2 = (\{\lambda\}, \{\mu\})$ ,  $P_3 = (\{\mu\}, \{\lambda\})$ ,  $P_4 = (\{\}, \{\lambda, \mu\})$ . The first set  $S_1$  contains parameters such that the corresponding B-operator contributes  $A_2B_1$ , the second set  $S_2$  is the set in which B-operator gives  $B_2D_1$ . This notation will be useful when one wants to refer to a term in a product of  $M$  B-opertors.

Now work our these four terms using the commutation relations between A and B (??), B and D (??).

$$P_1 = A_2(\mu)B_1(\mu)A_2(\lambda)B_1(\lambda) = \bar{a}_2(\mu)\bar{a}_2(\lambda)B_1(\mu)B_1(\lambda)$$

$$\begin{aligned} P_2 = B_2(\mu)D_1(\mu)A_2(\lambda)B_1(\lambda) &= f(\mu, \lambda)\bar{a}_2(\lambda)\bar{d}_1(\mu)B_2(\mu)B_1(\lambda) \\ &\quad -g(\mu, \lambda)\bar{a}_2(\lambda)\bar{d}_1(\lambda)B_2(\mu)B_1(\mu) \end{aligned}$$

$$\begin{aligned} P_3 = A_2(\mu)B_1(\mu)B_2(\lambda)D_1(\mu) &= f(\lambda, \mu)\bar{a}_2(\mu)\bar{d}_1(\lambda)B_1(\mu)B_2(\lambda) \\ &\quad -g(\lambda, \mu)\bar{a}_2(\lambda)\bar{d}_1(\mu)B_1(\mu)B_2(\mu) \end{aligned}$$

$$P_4 = B_2(\mu)D_1(\mu)B_2(\lambda)D_1(\lambda) = \bar{d}_1(\mu)\bar{d}_1(\lambda)B_2(\mu)B_2(\lambda)$$

Here  $\bar{a}_2(\lambda) = \prod_{i=M+1}^N a_i(\lambda)$ ,  $\bar{d}_1(\lambda) = \prod_{i=1}^M d_i(\lambda)$ . In  $P_2$  and  $P_3$ , the commutation relation generates two terms, the second of which is *unwanted*. However, due to the fact that  $g(\lambda, \mu) = -g(\mu, \lambda)$ , these unwanted terms cancel each other in the sum, thus we do not need to worry about them. In  $P_2$  and  $P_3$ , the two creation operators act on different regions, therefore, we

can further simply the result using the result of one spin flip

$$\begin{aligned}
P2 &= \sum_{\alpha,\beta} f(\mu, \lambda) \prod_{m>\alpha} a_m(\lambda) b_\alpha(\lambda) \prod_{n<\alpha} d_n(\lambda) \prod_{m'>\beta} a_{m'}(\mu) b_\beta(\mu) \prod_{n'} d_{n'<\beta}(\mu) \sigma_\alpha^- \sigma_\beta^- \\
&\quad \theta(1 \leq \alpha \leq M) \theta(M < \beta \leq N) + C_1 \\
&= \sum_{\alpha,\beta} f(\mu, \lambda) I(\alpha, \lambda) I(\beta, \mu) \sigma_\alpha^- \sigma_\beta^- \theta(1 \leq \alpha \leq M) \theta(M < \beta \leq N) + C_1 \\
P3 &= \sum_{\alpha,\beta} f(\lambda, \mu) I(\alpha, \lambda) I(\beta, \mu) \sigma_\alpha^- \sigma_\beta^- \theta(M < \alpha \leq N) \theta(1 \leq \beta \leq M) - C_1
\end{aligned}$$

Here  $C_1$  represents the unwanted terms which does not matter for the sum. However, in  $P_1$  and  $P_4$ , both creation operators act on the same subregion, which is essentially the same as the original problem. Thus we further divide the M sites into two part. Then  $P_1$  will become a sum of four terms. Two of them have one creation operator in each region and can be simplified as

$$\begin{aligned}
P_{12} &= \sum_{\alpha,\beta} f(\mu, \lambda) I(\alpha, \lambda) I(\beta, \mu) \sigma_\alpha^- \sigma_\beta^- \theta(1 \leq \alpha \leq S) \theta(S < \beta \leq M) + C_2 \\
P_{13} &= \sum_{\alpha,\beta} f(\lambda, \mu) I(\alpha, \lambda) I(\beta, \mu) \sigma_\alpha^- \sigma_\beta^- \theta(S < \alpha \leq M) \theta(1 \leq \beta \leq S) - C_2
\end{aligned}$$

Here  $C_2$  are unwanted terms that will vanish in the sum. The other two terms of  $P_1$  can be further simplified by further division of the space. This division stops when there is only one site in each subregion. The B-operator becomes  $b_m(\lambda) \sigma_m^-$ . Then no two creation operators can act on the same site as  $\sigma_m^- \sigma_m^- = 0$ . The  $P_4$  term will be manipulated in the same way. In the end, summing up all the term we get

$$\begin{aligned}
B(\lambda)B(\mu) &= \sum_{\alpha,\beta} f(\mu, \lambda) I(\alpha, \lambda) I(\beta, \mu) \sigma_\alpha^- \sigma_\beta^- (\theta(1 \leq \alpha \leq M) \theta(M < \beta \leq N) \\
&\quad + \theta(1 \leq \alpha \leq S) \theta(S < \beta \leq m) + \theta(M < \alpha \leq T) \theta(T < \beta \leq N) + \dots) \\
&\quad + \sum_{\alpha,\beta} f(\lambda, \mu) I(\alpha, \lambda) I(\beta, \mu) \sigma_\alpha^- \sigma_\beta^- (\theta(M < \alpha \leq N) \theta(1 \leq \beta \leq M) \\
&\quad + \theta(S < \alpha \leq m) \theta(1 \leq \beta \leq S) + \theta(T < \alpha \leq N) \theta(M < \beta \leq T) + \dots) \\
&= \sum_{\alpha,\beta} (f(\mu, \lambda) \theta(1 \leq \alpha < \beta \leq N) + f(\lambda, \mu) \theta(1 \leq \beta < \alpha \leq N)) I(\alpha, \lambda) I(\beta, \mu) \sigma_\alpha^- \sigma_\beta^- \\
&= \sum_{R=I, P, \mu, \lambda} \sum_{\alpha,\beta} \theta(1 \leq \alpha < \beta \leq N) f(R\mu, R\lambda) I(\alpha, R\lambda) I(\beta, R\mu) \sigma_\alpha^- \sigma_\beta^-
\end{aligned}$$

Therefore, we have derived the expression (??) for system with two excitations.

Now, we want to generalize the result to systems with many spin flips. The procedure is the same, i.e. to successively divide the system into two parts. The division should stop when the number of sites in any subsystem is no more than the number of creation operators acting on

it. This is due to the fact that the product of two  $\sigma^-$  operator acting on the same site vanishes. First, we will divide the N sites in to m sites and N-m sites, like in the case of two excitations. We want to prove that

$$\prod_{i=1}^M B(\mu_i) = \sum_{S_1 \cup S_2 = \{\mu_i\}} \prod_{\mu_\alpha^i \in S_1} \prod_{\mu_\beta^j \in S_2} f(\mu_\beta^j, \mu_\alpha^i) \prod_{\mu_\alpha^i \in S_1} \bar{a}_2(\mu_\alpha^i) \prod_{\mu_\beta^j \in S_2} \bar{d}_1(\mu_\beta^j) \prod_{\mu_\alpha^i \in S_1} B(\mu_\alpha^i) \prod_{\mu_\beta^j \in S_2} B(\mu_\beta^j)$$

As can be seen in the two down spin case, this is true for  $M = 2$ , i.e. all unwanted terms vanish in the sum. We will now prove this for general M. Assume for  $M - 1$  spin flips, only wanted terms are left. Then for  $B(\lambda) \prod_{i=1}^{M-1} B(\mu_i)$ , when we pass  $A_2(\lambda)$  or  $D_1(\lambda)$  in  $B(\lambda)$  through the product of  $B(\mu_i)$ , it may exchange parameter with the B-operator and turn into  $A_2(\gamma)$  or  $D_1(\gamma)$  ( $\gamma \in \{\mu_i\}$ ) multiplied by  $B_1(\lambda)B_2(\lambda)$ . We will show here that unwanted terms characterized by  $\bar{a}_2(\gamma)\bar{d}_1(\gamma)B_1(\lambda)B_2(\lambda)$  cancel with each other.

There are two kinds of partitions resulting in such unwanted terms. ( $\{\gamma, \mu_\alpha^i\}, \{\lambda, \mu_\beta^j\}$ ) and ( $\{\lambda, \mu_\alpha^i\}, \{\gamma, \mu_\beta^j\}$ ). In the first one,  $\lambda \in S_2$ ,  $B(\lambda)$  contributes  $B_2(\lambda)D_1(\lambda)$ , in the second  $B(\lambda)$  contributes  $A_2(\lambda)B_1(\lambda)$ . The above unwanted terms from these two scenarios are

$$\begin{aligned} & B_2(\lambda)D_1(\lambda)f(\mu_\beta^j, \gamma)a_2(\gamma) \prod_{\mu_\alpha^i \in S_1} B_1(\mu_\alpha^i) \prod_{\mu_\beta^j \in S_2} B_2(\mu_\beta^j)B_1(\gamma) \\ \rightarrow & f(\mu_\beta^j, \gamma)\bar{a}_2(\gamma)\bar{d}_1(\gamma)g(\gamma, \lambda)f(\gamma, \mu_\alpha^i) \prod_{\mu_\alpha^i \in S_1} B_1(\mu_\alpha^i) \prod_{\mu_\beta^j \in S_2} B_2(\mu_\beta^j)B_2(\lambda)B_1(\lambda) \\ & A_2(\lambda)B_2(\lambda)f(\gamma, \mu_\alpha^i)d_1(\gamma) \prod_{\mu_\alpha^i \in S_1} B_1(\mu_\alpha^i) \prod_{\mu_\beta^j \in S_2} B_2(\mu_\beta^j)B_2(\gamma) \\ \rightarrow & f(\gamma, \mu_\alpha^i)\bar{a}_2(\gamma)d_1(\gamma)g(\lambda, \gamma)f(\mu_\beta^j, \gamma) \prod_{\mu_\alpha^i \in S_1} B_1(\mu_\alpha^i) \prod_{\mu_\beta^j \in S_2} B_2(\mu_\beta^j)B_1(\lambda)B_2(\lambda) \end{aligned}$$

Here we have dropped the common factor of  $\prod_{\mu_\beta^j} \prod_{\mu_\alpha^i} f(\mu_\beta^j, \mu_\alpha^i) \prod_{\mu_\alpha^i \in S_1} \bar{a}_2(\mu_\alpha^i) \prod_{\mu_\beta^j \in S_2} d_1(\mu_\beta^j)$ . From the above, it is clear that these two terms cancel and no unwanted term characterized by  $\bar{a}_2(\gamma)\bar{d}_1(\gamma)B_1(\lambda)B_2(\lambda)$  exists. Since this  $\gamma$  is chosen arbitrarily, we can conclude that all unwanted terms vanish. Therefore, when we pass all  $A$  and  $D$  operator to the right of the product of B-operator, they become c-numbers without changing its parameter, with a prefactor created by the commutation relation which is the product of  $f(\mu_\beta^j, \mu_\alpha^i)$  for all  $\mu_\alpha^i \in S_1$  and  $\mu_\beta^j \in S_2$ .

In order to obtain (??), iterate the above division procedure until every  $B(\mu)$  acts on a separate region. Like in the two spin flips case, each time  $B(\mu)$  and  $B(\lambda)$  are separated, a factor of  $f(\mu, \lambda)$  or  $f(\lambda, \mu)$  is created, which depends on  $\alpha_\mu < \alpha_\lambda$  or  $\alpha_\mu > \alpha_\lambda$ . Besides this factor, the B-operator acts in the same way as in a single excitation case, i.e.  $B(\mu)$  turns into

$I(\mu, \lambda)\sigma_\alpha^-$ . Therefore, we can write down the final answer as

$$\begin{aligned} \prod_{i=1}^M B(\mu_i) &= \prod_{i < j} (f(\mu_j, \mu_i)\theta(\alpha_j - \alpha_i) + f(\mu_i, \mu_j)\theta(\alpha_i - \alpha_j)) \prod_i I(\mu_i, \alpha_i)\sigma_{\alpha_i}^- \\ &= \prod_{R \in S_M} \prod_{i < j} f(\mu_{R_j}, \mu_{R_i})\theta(\alpha_1 < \dots < \alpha_M) \prod_i I(\mu_{R_i}, \alpha_i)\sigma_{\alpha_i}^- \end{aligned}$$

This agrees with equation (??). For XXZ model, the wavefunction becomes

$$\begin{aligned} \phi(\alpha|\mu)\theta(\alpha_1 < \dots < \alpha_M) &= \sum_R \prod_{i < j} \frac{\sinh(\mu_i - \mu_j + \phi \operatorname{sgn}(\alpha_{R^1_i} - \alpha_{R^1_j}))}{\sinh(\mu_i - \mu_j)} \\ &\quad \prod_j \left( \frac{\sinh(\mu_j - \phi/2)}{\sinh(\mu_j + \phi/2)} \right)^{\alpha_{R^1_j} - 1} \frac{\sinh \phi}{\sinh(\mu_j + \phi/2)} \end{aligned}$$

Multiply the wavefunction by a constant

$$\prod_j \frac{\sinh(\mu_j + \phi/2)}{\sinh \phi} \frac{\sinh(\mu_j + \phi/2)}{\sinh(\mu_j - \phi/2)} \prod_{i < j} \frac{\sinh(\mu_j - \mu_j)}{\sinh(\mu_i - \mu_j - \phi)}$$

we obtain the more commonly seen wavefunction

$$\begin{aligned} &\phi(\alpha|\mu)\theta(\alpha_1 < \dots < \alpha_M) \\ &= \sum_R \prod_{i < j} \frac{\sinh(\mu_i - \mu_j + \phi \operatorname{sgn}(\alpha_{R^1_i} - \alpha_{R^1_j}))}{\sinh(\mu_i - \mu_j - \phi)} \prod_j \left( \frac{\sinh(\mu_j - \phi/2)}{\sinh(\mu_j + \phi/2)} \right)^{\alpha_{R^1_j}} \end{aligned}$$

or

$$\phi(\beta|\mu) = \prod_{i < j} \frac{\sinh(\mu_i - \mu_j + \phi \operatorname{sgn}(\beta_i - \beta_j))}{\sinh(\mu_i - \mu_j - \phi)} \prod_j \left( \frac{\sinh(\mu_j - \phi/2)}{\sinh(\mu_j + \phi/2)} \right)^{\beta_j}$$

The Bethe Equation can be obtained from periodic boundary condition,  $\phi(\alpha|\mu) = \phi(\alpha'|\mu)$ , with  $\alpha = \{\alpha_1, \alpha_2, \dots, \alpha_M\}$  and  $\alpha' = \{\alpha_2, \dots, \alpha_M, \alpha_1 + N\}$ , i.e.

$$\begin{aligned} &\prod_{i < j} \frac{\sinh(\mu_i - \mu_j + \phi \operatorname{sgn}(\alpha_{R^1_i} - \alpha_{R^1_j}))}{\sinh(\mu_i - \mu_j - \phi)} \prod_j \left( \frac{\sinh(\mu_j - \phi/2)}{\sinh(\mu_j + \phi/2)} \right)^{\alpha_{R^1_j}} \\ &= \prod_{i < j} \frac{\sinh(\mu_i - \mu_j + \phi \operatorname{sgn}(\alpha'_{R'^1_i} - \alpha'_{R'^1_j}))}{\sinh(\mu_i - \mu_j - \phi)} \prod_j \left( \frac{\sinh(\mu_j - \phi/2)}{\sinh(\mu_j + \phi/2)} \right)^{\alpha'_{R'^1_j}} \end{aligned}$$

For  $R$  and  $R'$  that satisfy the following relation, many of the terms cancel and we are left with

$$\alpha_{R^1_i} = \begin{cases} \alpha'_{R'^1_i} & i = R2, \dots, RM \\ \alpha'_{R'^1_i} + N & i = R1 \end{cases}$$

$$\prod_{i < j=R1} \frac{\sinh(\mu_i - \mu_{R1} - \phi)}{\sinh(\mu_i - \mu_{R1} + \phi)} \prod_{i=R1 < j} \frac{\sinh(\mu_{R1} - \mu_j + \phi)}{\sinh(\mu_{R1} - \mu_j - \phi)} \prod_j \left( \frac{\sinh(\mu_{R1} - \phi/2)}{\sinh(\mu_{R1} + \phi/2)} \right)^N = 1$$

i.e.

$$\prod_{j \neq R1} \frac{\sinh(\mu_{R1} - \mu_j + \phi)}{\sinh(\mu_{R1} - \mu_j - \phi)} \prod_j \left( \frac{\sinh(\mu_{R1} - \phi/2)}{\sinh(\mu_{R1} + \phi/2)} \right)^N = 1$$

This leads to equation (??)

## 2.3 Nested Bethe Ansatz

Nested Bethe Ansatz solves systems with both spacial and spin degrees of freedom, like Gaudin-Yang model and Hubbard model. It combines the previous two methods, in such a way that the spacial part is derived by the coordinate Bethe Ansatz, while the spin part is solved by the Algebraic Bethe Ansatz. The solution of such problems with only coordinate Bethe Ansatz involves huge matrices whose size increases exponentially with the number of particles. And using Algebraic Bethe Ansatz only can make such problem much more complicated than we have seen before as there are both charge and spinon excitations ([? ]). Therefore, the nested Bethe Ansatz which combines the two methods appears to be very useful for such systems. To illustrate this method, we will solve the Gaudin-Yang model in this section.

### 2.3.1 Gaudin-Yang Model

The Gaudin-Yang model describes a one-dimensional continuous system of Fermi Gas with contact interaction. It is described by the following Hamiltonian

$$H = \sum_{\sigma=\uparrow,\downarrow} \int dx \Psi_{\sigma}^{\dagger}(x) \left( -\frac{\partial^2}{\partial x^2} \right) \Psi_{\sigma}(x) + c \int_x \Psi_{\uparrow}^{\dagger}(x) \Psi_{\downarrow}^{\dagger}(x) \Psi_{\downarrow}(x) \Psi_{\uparrow}(x)$$

where  $\Psi_{\sigma}^{\dagger}(x)$  ( $\Psi_{\sigma}(x)$ ) is the creation(annihilation) operator of a fermion with spin  $\sigma$ . They obey the canonical anticommutation relation  $\{\Psi_{\sigma}^{\dagger}(x), \Psi_{\sigma'}(x')\} = \delta_{\sigma,\sigma'} \delta(x-x')$ .  $c$  is related to the interaction strength. When  $c$  is positive, the particles repel each other when at the same site. Otherwise, the interaction is attraction. Following the same procedure as for the Lieb-Liniger gas, we define an eigenstate with wavefunction  $f_{\sigma}(x)$  as follows, with  $|0\rangle$  being a fock vacuum. Then apply the Hamiltonian to this state, we get the first quantized Hamiltonian

$$|\Psi\rangle = \sum_{\sigma} \int_{\mathbf{x}} f(x, \sigma) \prod_{i=1}^N \Psi_{\sigma_i}^{\dagger}(x_i) |0\rangle$$

$$h = - \sum_i \frac{\partial^2}{\partial x_i^2} + 2c \sum_{ij} \delta(x_i - x_j)$$

The Bethe Ansatz wavefunction of the Gaudin-Yang model can be written as

$$f(x, \sigma) = \sum_{P, Q} e^{i(Pk) \cdot (Qx)} A(Q, P) \theta((Qx)_1 < \dots < (Qx)_N) \quad (2.11)$$

Here  $Pk = (k_{P-1}, \dots, k_{P-N})$  and  $Qx = (x_{Q-1}, \dots, x_{Q-N})$ . Like the Lieb-Liniger solution, the ansatz assumes that the wavefunction is a superposition of plain waves in each ordered regime weighted by prefactor  $A(Q, P)$ . Each plain wave is characterized by the permutations  $P$  and  $Q$ .

Q is related to the ordering of the coordinates and P determines the sequence of ks. Note, the wavefunction is not explicitly dependant on the spin configuration. But any permutation of x may affect the spin as  $f(Qx, \sigma) = (-1)^Q f(x, Q^{-1}\sigma)$  as we are going to use here.

Apply the Schrodinger equation  $hf(x, \sigma) = Ef(x, \sigma)$ , we get two results. First, well within the ordered region, i.e. none of the  $x$ 's are the same, then  $E = \sum_i k_i^2$ . Second, at the boundary of some ordered region, say  $(Qx)_i = (Qx)_j$  ( $Q^{-1}j = Q^{-1}i + 1$ ), we have

$$(i(Pk)_i - i(Pk)_j)(A(Q, P) - A(Q, P_{ij}P) + A(P_{ij}Q, P)) - A(P_{ij}P, P_{ij}Q) + c(A(Q, P) + A(Q, P_{ij}P) + A(P_{ij}Q, P) + A(P_{ij}P, P_{ij}Q)) = 0$$

i.e.

$$i((Pk)_i - (Pk)_j)(A(Q, P) - A(Q, PP_{ij}))(1 - \Pi_{ij}) + c(A(Q, P) + A(Q, PP_{ij}))(1 - \Pi_{ij}) = 0 \quad (2.12)$$

Here we have replaced  $A(P_{ij}Q, P)$  with  $-\Pi_{ij}A(Q, P)$ , where  $\Pi_{ij}$  acts on the spin state and changes spin i and spin j. From the above relation, we obtained the following relation for spin singlet state, projected by  $(1 - \Pi_{ij})/2$ .

$$A(Q, PP_{ij}) = \frac{(Pk)_i - (Pk)_j - ic}{(Pk)_i - (Pk)_j + ic} A(Q, P)$$

For spin triplet state, due to the fermion nature of the problem, the wavefunction vanishes when two coordinate coincides. Therefore, the contact interaction should not play a role and the wavefunction should be simply an antisymmetric function of plain waves, i.e.

$$f(x, \sigma) = \sum_P (-1)^P e^{i(Pk) \cdot x}$$

This means  $A(P_{ij}Q, P_{ij}P) = A(Q, P)$ , i.e.  $A(Q, P_{ij}P) = -\Pi_{ij}A(Q, P) = -A(Q, P)$ . Here, we replaced  $\Pi_{ij}$  with 1 for spin triplet state. To summarize, for  $Q^{-1}j = Q^{-1}i + 1$  we have

$$\begin{aligned} A(Q, P_{ij}P) &= \frac{(Pk)_i - (Pk)_j - ic}{(Pk)_i - (Pk)_j + ic} \frac{1 - \Pi_{ij}}{2} A(Q, P) - \frac{1 - \Pi_{ij}}{2} A(Q, P) \\ &= -\frac{((Pk)_i - (Pk)_j)\Pi_{ij} + ic}{(Pk)_i - (Pk)_j + ic} A(Q, P) \\ &= Y_{ij}((Pk)_i - (Pk)_j)A(Q, P) \end{aligned}$$

$$A(P_{ij}Q, P_{ij}P) = \frac{(Pk)_i - (Pk)_j + ic\Pi_{ij}}{(Pk)_i - (Pk)_j + ic} A(Q, P) = S_{ij}((Pk)_i - (Pk)_j)A(Q, P)$$

Here  $Y_{ij}((Pk)_i - (Pk)_j) = -\Pi_{ij}S_{ij}((Pk)_i - (Pk)_j)$  is called the Yang matrix,  $S_{ij}(k_{Pi} - k_{Pj})$  is the well-studied Scattering matrix (S-matrix). Here the sub-index  $i, j$  are related to the

spin permutation, as we have emphasized before, this permutation is moving *by element* in our convention.

From now on, we will focus on the region with  $Q = \mathbb{1}$ , i.e.  $\theta(x_1 < \dots < x_N)$ . All other regions can be obtained via antisymmetric property of the wavefunction. The S-matrix has an important property, that is it satisfies the Yang-Baxter relation, e.g

$$S_{23}(k_2 - k_3)S_{13}(k_1 - k_3)S_{12}(k_1 - k_2) = S_{12}(k_1 - k_2)S_{13}(k_1 - k_3)S_{23}(k_2 - k_3)$$

Written in the language of the Yang matrix, this relation becomes

$$Y_{12}(k_2 - k_3)Y_{23}(k_1 - k_3)Y_{12}(k_1 - k_2) = Y_{23}(k_1 - k_2)Y_{12}(k_1 - k_3)Y_{23}(k_2 - k_3)$$

If a permutation  $P$  can be written as a product of  $n$  transpositions ( $P^n \dots P^2 P^1$ ), and each transposition  $P^m$  exchanges one pair of adjacent objects  $m_i$  and  $m_j$  ( $m_j = m_i + 1$ ) then we have

$$A(Q, P) = Y_{n_i n_j}(k^n) \dots Y_{1_i 1_j}(k) A(Q, I)$$

Here  $k^n = P^{n-1} \dots P^1 k$  is the set of  $k$ 's after the previous permutations. This completes the coordinate Bethe Ansatz solution of the Gaudin-Yang model. As we have mentioned before, this solution has a problem. As both the Yang matrix and the S-matrix involve permutations on the spin configuration, the solution acts on a  $N!$  dimensional spin space, which is huge for a moderate number of particles. One could wish to find an irreducible representation such that the dimension of  $Y(P)$  could be reduced. Actually, there is such a complete spin basis so that when  $Y(P)$  acts on it, it becomes a c-number. This is the next subject we will talk about.

The construction of this spin basis is closely related to the Algebraic Bethe Ansatz, which constructs spin states using creation operators come from a monodromy matrix. The monodromy matrix is defined as a product of some L-operators expressed in the auxiliary space

$$\mathcal{T}(\mu, k) = L_{an}(\mu - k_n) \dots L_{a1}(\mu - k_1)$$

Both of them need to satisfy the Yang-Baxter relation defined by some R -matrix

$$R_{ab}(\lambda - \mu) \mathcal{T}_a(\lambda, k) \mathcal{T}_b(\mu, k) = \mathcal{T}_b(\mu, k) \mathcal{T}_a(\lambda, k) R_{ab}(\lambda - \mu)$$

$$R_{ab}(\lambda - \mu) L_{ai}(\lambda - k_i) L_{bi}(\mu - k_i) = L_{bi}(\mu, k_i) L_{ai}(\lambda - k_i) R_{ab}(\lambda - \mu)$$

Here, we have shifted the entry of  $L_{ia}$  by  $k_i$ , but as is clear, the Yang-Baxter relation which defines the algebra is unaffected, i.e. if the  $L_{ia}(\lambda)$  and  $L_{ib}(\mu)$  satisfy the relation, so are  $L_{ia}(\lambda - k_i)$  and  $L_{ib}(\mu - k_i)$ . This shift of the entry also makes the  $\mathcal{T}$  operator  $k$  dependant.

We have said that, in general, there is no way one can determine the R-matrix based on the Hamiltonian. But with the coordinate Bethe Ansatz solution, we are equipped with an object which satisfies the Yang-Baxter relation, that is the S-matrix. Therefore, we may simply define the R-matrix and L-operator to be in the form of the S-matrix we obtained, i.e.

$$L_{ai}(\mu - k_i) = -S_{ai}(\mu - k_i) = \frac{\mu - k_i + ic\Pi_{ai}}{\mu - k_i + ic}$$

$$= \begin{pmatrix} \frac{\mu - k_i + ic/2(1 + \sigma_i^z)}{\mu - k_i + ic} & \frac{ic\sigma_i^-}{\mu - k_i + ic} \\ \frac{ic\sigma_i^+}{\mu - k_i + ic} & \frac{\mu - k_i + ic/2(1 - \sigma_i^z)}{\mu - k_i + ic} \end{pmatrix}_a$$

$$R_{ab}(\lambda - \mu) = \begin{pmatrix} \frac{\mu - \lambda + ic}{\mu - \lambda} & 0 & 0 & 0 \\ 0 & 1 & \frac{ic}{\mu - \lambda} & 0 \\ 0 & \frac{ic}{\mu - \lambda} & 1 & 0 \\ 0 & 0 & 0 & \frac{\mu - \lambda + ic}{\mu - \lambda} \end{pmatrix}_{ab}$$

Then the monodromy matrix can be written as follows

$$\mathcal{T}(\mu, k) = S_{an}(\mu - k_n) \dots S_{a1}(\mu - k_1)$$

And the creation operator  $B(\mu, k)$  is just the upright element of the  $2 \times 2$  matrix.

$$B(\mu, k) = \sum_{\alpha=1}^N \prod_{j>\alpha} \frac{\mu - k_j + ic/2(1 + \sigma_j^z)}{\mu - k_j + ic} \frac{ic\sigma_\alpha^-}{\mu - k_\alpha + ic} \prod_{j<\alpha} \frac{\mu - k_j + ic/2(1 - \sigma_j^z)}{\mu - k_j + ic}$$

One interesting property of this B-operator is that when the rapidity is sent to infinity it becomes spin lowering operator [? ? ], i.e.

$$\lim_{\mu \rightarrow \infty} B(\mu, k) = \lim_{\mu \rightarrow \infty} \frac{ic}{\mu} \sum_{\alpha=1}^N \sigma_\alpha^- = \frac{ic}{\mu} S^- \quad (2.13)$$

The advantage of this choice of R-matrix and L-operator is that the Y-operator can pass through  $\mathcal{T}(\mu, k)$  in a simple way as illustrated below. Again,  $k^m = P^{m-1}k^{m-1}$ , i.e.  $\{k^m\}$  is the k set after all previous permutations acting on  $\{k\}$ .

$$\begin{aligned} & Y_{jj+1}(k^m) \mathcal{T}(\mu, k^m) \\ &= P_{jj+1} S_{jj+1}(k_i^m - k_j^m) S_{an}(\mu - k_n^m) \dots S_{a(j+1)}(\mu - k_{j+1}^m) S_{aj}(\mu - k_j^m) \dots S_{a1}(\mu - k_1^m) \\ &= S_{an}(\mu - k_n^m) \dots P_{jj+1} S_{jj+1}(k_j^m - k_{j+1}^m) S_{a(j+1)}(\mu - k_{j+1}^m) S_{aj}(\mu - k_j^m) \dots S_{a1}(\mu - k_1^m) \\ &= S_{an}(\mu - k_n^m) \dots P_{jj+1} S_{aj}(\mu - k_j^m) S_{a(j+1)}(\mu - k_{j+1}^m) S_{jj+1}(k_j^m - k_{j+1}^m) \dots S_{a1}(\mu - k_1^m) \\ &= S_{an}(\mu - k_n^m) \dots S_{a(j+1)}(\mu - k_j^m) S_{aj}(\mu - k_{j+1}^m) P_{jj+1} S_{jj+1}(k_j^m - k_{j+1}^m) \dots S_{a1}(\mu - k_1^m) \\ &= \mathcal{T}(\mu, P_{ij} k^m) Y_{jj+1}(k_j^m - k_{j+1}^m) \\ &= \mathcal{T}(\mu, k^{m+1}) Y_{jj+1}(k^m) \end{aligned}$$

From the above, we can see that

$$A(P)\mathcal{T}(\mu, k) = \mathcal{T}(\mu, Pk)A(P)$$

$$A(P)B(\mu, k) = B(\mu, Pk)A(P)$$

The second relation is obtained by sandwiching the operator between  ${}_a\langle \uparrow |$  and  $|\downarrow\rangle_a$ . Since  $A(P)$  acts on physical space, this projection turns  $\mathcal{T}$  into the B-operator. This relation turns out to be very useful if we choose the spin basis as the products of B-operators acting on vacuum state, i.e.  $\omega(\mu, k) = \prod_i^M B(\mu_i, k)|\uparrow\rangle$ , then

$$A(P)\omega(\mu, k) = A(P) \prod_i^M B(\mu_i, k)|\uparrow\rangle = \prod_i^M B(\mu_i, Pk)A(P)|\uparrow\rangle = (-1)^P \omega(\mu, Pk)$$

In the last line, we have used the fact that  $A(P)|\uparrow\rangle = (-1)^P|\uparrow\rangle$ . With this basis  $\omega(\mu, k)$ , we can describe a state with a new wavefunction with parameter  $k$  and  $\mu$ .

$$\begin{aligned} |\Psi\rangle &= f(k, \mu|x)|x\rangle \otimes |\omega(\mu, k)\rangle \\ &= \sum_P e^{ik_P x_i} A(P)\theta(x_1 < \dots < x_N)|x\rangle \otimes |\omega(\mu, k)\rangle \\ &= \sum_P (-1)^P e^{ik_P x_i} \theta(x_1 < \dots < x_N)|x\rangle \otimes |\omega(\mu, Pk)\rangle \end{aligned}$$

Using the machinery of Algebraic Bethe Ansatz, we can write down the explicit form of  $\omega(\mu, k)$ , i.e.

$$\omega(\mu, k) = \sum_{R \in S_M} \prod_{i < j} f(\mu_{R_j} - \mu_{R_i}) \theta(\alpha_1 < \dots < \alpha_M) \prod_{i=1}^M I(\mu_{R_i}, k, \alpha_i) \sigma_{\alpha_i}^- |\uparrow\rangle$$

with

$$f(\mu_i - \mu_j) = \frac{\mu_i - \mu_j + ic}{\mu_i - \mu_j}$$

$$I(\mu, k, \alpha) = \frac{ic}{\mu - k_\alpha + ic} \prod_{n < \alpha} \frac{\mu - k_n}{\mu - k_n + ic}$$

In summary, we have

$$\begin{aligned} |\mu, k\rangle &= \sum_P (-1)^P e^{i(Pk) \cdot x} \sum_R \prod_{i < j} f(\mu_{R_j} - \mu_{R_i}) \prod_i I(\mu_{R_i}, Pk, \alpha_i) \theta(x_i) \theta(\alpha_i) |x\rangle \otimes |\alpha\rangle \\ &\quad \theta(x_1 < \dots < x_N) \theta(\alpha_1 < \dots < \alpha_M) \end{aligned}$$

Here,  $\theta(x_i) = \theta(x_1 < \dots < x_N)$ ,  $\theta(\alpha_i) = \theta(\alpha_1 < \dots < \alpha_M)$ ,  $|\alpha\rangle = \prod_i^M \sigma_{\alpha_i}^- | \uparrow \rangle$ . The more traditional form is obtained by replacing  $\mu$  by  $\mu - ic/2$  and multiply the state by a normalization constant  $\prod_{i<j} \frac{\mu_i - \mu_j}{\mu_i - \mu_j - ic}$ . This will leads to the following change

$$\begin{aligned} |\mu, k\rangle &= \sum_P e^{i(Pk)\cdot x} \prod_{i<j} \frac{\mu_i - \mu_j}{\mu_i - \mu_j - ic} \prod_i B(\mu_i, Pk) |x\rangle \otimes | \uparrow \rangle \\ &= f(x, \alpha | \mu, k) \theta(x_1 < \dots < x_N) \theta(\alpha_1 < \dots < \alpha_M) \sigma_{\alpha_i}^- |x\rangle \otimes | \uparrow \rangle \end{aligned} \quad (2.14)$$

$$f(x, \alpha | \mu, k) = \sum_P (-1)^P e^{i(Pk)\cdot x} \sum_R \prod_{i<j} \frac{\mu_i - \mu_j + ic \operatorname{Sgn}(\alpha_{R^{-1}i} - \alpha_{R^{-1}j})}{\mu_i - \mu_j - ic} \prod_{i=1}^M I(\mu_i, Pk, \alpha_{R^{-1}i})$$

$$I(\mu, k, \alpha) = \frac{ic}{\mu - k_\alpha + ic/2} \prod_{n<\alpha} \frac{\mu - k_n - ic/2}{\mu - k_n + ic/2}$$

Like in the case of Lieb-Liniger model, permutation on momentums and rapidities does not create new state. This can be easily seen from the first line of (??) since

$$\begin{aligned} |\mu, Pk\rangle &= \sum_{P'} (-1)^{P'} e^{i(P'Pk)\cdot x} \prod_{i<j} \frac{\mu_i - \mu_j}{\mu_i - \mu_j - ic} \prod_i B(\mu_i, P'Pk) |x\rangle \otimes | \uparrow \rangle \\ &= (-1)^P \sum_{P'} e^{i(P'k)\cdot x} \prod_{i<j} \frac{\mu_i - \mu_j}{\mu_i - \mu_j - ic} \prod_i B(\mu_i, P'k) |x\rangle \otimes | \uparrow \rangle \\ &= (-1)^P |\mu, k\rangle \\ |R\mu, k\rangle &= \sum_P (-1)^P e^{i(Pk)\cdot x} \prod_{i<j} \frac{\mu_{Ri} - \mu_{Rj}}{\mu_{Ri} - \mu_{Rj} - ic} \prod_i B(\mu_{Ri}, Pk) |x\rangle \otimes | \uparrow \rangle \\ &= \sum_P (-1)^P e^{i(Pk)\cdot x} \prod_{i<j} \frac{\mu_{Ri} - \mu_{Rj}}{\mu_{Ri} - \mu_{Rj} - ic} \prod_i B(\mu_i, Pk) |x\rangle \otimes | \uparrow \rangle \\ &= S^*(R) |\mu, k\rangle \end{aligned}$$

Here, we have used the fact that  $B(\mu, k)$  commute with each other, thus the permutation on the ordering of the  $B$ -operator does not affect the result. The new phase factor comes from the following relation

$$\prod_{i<j} \frac{\mu_{Ri} - \mu_{Rj}}{\mu_{Ri} - \mu_{Rj} - ic} \Big/ \prod_{i<j} \frac{\mu_i - \mu_j}{\mu_i - \mu_j - ic} = \prod_{\substack{i<j \\ R^{-1}i > R^{-1}j}} \frac{\mu_i - \mu_j - ic}{\mu_i - \mu_j + ic} = S^*(R)$$

Combining the effect of the two kinds of permutation, we obtain the phase factor that relates  $|k, \mu\rangle$  and  $|Pk, R\mu\rangle$ .

$$|Pk, R\mu\rangle = S_{k,\mu}^*(P, R) |k, \mu\rangle$$

$$S_{k,\mu}(P, R) = S(P)S(R) = (-)^P \prod_{\substack{i<j \\ R^{-1}i > R^{-1}j}} \frac{\mu_i - \mu_j + ic}{\mu_i - \mu_j - ic} \quad (2.15)$$

## Bethe Equation

The Bethe Equations which deal with the structure of the solutions, real or string solutions, can be obtained by placing the system under periodic boundary condition. This leads to the following two conditions depending on  $\alpha_1 = 1$  or not.

$$f(x_1, \dots, x_N, \alpha_1, \dots, \alpha_M | \mu, k) = f(x_2, \dots, x_N, x_1 + L, \alpha_1, \dots, \alpha_M | \mu, k)$$

$$f(x_1, \dots, x_N, \alpha_1, \alpha_2, \dots, \alpha_M | \mu, k) = f(x_2, \dots, x_N, x_1 + L, \alpha_2, \dots, \alpha_M, \alpha_1 + M | \mu, k)$$

This leads to

$$e^{ik_{P^{-1}}L} = \prod_{j=1}^M \frac{\mu_j - k_{P^{-1}} - ic/2}{\mu_j - k_{P^{-1}} + ic/2}$$

$$e^{ik_{P^{-1}}L} \prod_{i=R1 < j} \frac{\mu_{R1} - \mu_j + ic}{\mu_{R1} - \mu_j - ic} \prod_{i < j=R1} \frac{\mu_i - \mu_{R1} - ic}{\mu_i - \mu_{R1} + ic} \prod_{i \neq R1} \frac{\mu_i - k_{P^{-1}} + ic/2}{\mu_i - k_{P^{-1}} - ic/2} \prod_{n \neq i} \frac{\mu_{R1} - k_{P^{-1}n} - ic/2}{\mu_{R1} - k_{P^{-1}n} + ic/2} = 1$$

i.e.

$$e^{ik_n L} = \prod_{j=1}^M \frac{k_n - \mu_j + ic/2}{k_n - \mu_j - ic/2} \quad (2.16)$$

$$\prod_{j \neq i} \frac{\mu_i - \mu_j + ic}{\mu_i - \mu_j - ic} = \prod_n \frac{\mu_i - k_n + ic/2}{\mu_i - k_n - ic/2} \quad (2.17)$$

Two patterns can emerge in the  $k$  and  $\mu$  solutions. For the first one,  $\mu_i = k_n + ic/2$  and  $\mu_j = k_n - ic/2$ , with  $k_n$  lying on the real axis. This is for both  $c > 0$  and  $c < 0$ . In the thermodynamic limit with  $N \rightarrow \infty$  and  $M/N < \infty$ , this relaxes to the  $\mu$  strings ( $\mu_i = \bar{\mu} + ic/2(m+1-2i)$ ,  $i = 1, \dots, m$ ) with all  $k$ 's real. This is due to the fact that for  $\mu_i$  with  $i < m/2$ ,  $|\frac{\mu_i - k_n + ic/2}{\mu_i - k_n - ic/2}| > 1$  if  $k_n$  is real. The product of  $n$  such terms blow up in the limit  $n$  goes to infinity. This requires another  $\mu$  lying below it by a distance of  $c$ . Like in the case of attractive Lieb-Liniger gas, if we do not worry about the ambiguity of  $0/0$ , this leads to a string root in the  $\mu$  complex plane. For  $c < 0$ , there is another pattern formed with  $\mu_j$  lying on the real axis, and two  $k$ 's lying above and below  $\mu_j$  by distance  $|c|/2$ , i.e.  $k_m = \mu_j - ic/2$  and  $k_n = \mu_j + ic/2$ . For  $k_m$ , the right hand side of equation (??) vanishes, therefore, it must stay above the real axis to make the left hand side go to zero. This requires that  $c$  being negative, i.e. the interaction being attractive. In the thermodynamic limit, this root pattern can also be relaxed to longer  $k$ -strings with all real  $\mu$ 's. However, this would require a stronger condition that  $M \rightarrow \infty$  also. We use the following graphs to describe the patterns.

Both root patterns correspond to bound states. The first kind with complex  $\mu$  and real  $k$  indicates bound state between down spins. As an example, if  $\mu_1 = \bar{\mu} + ic/2$  and  $\mu_2 = \bar{\mu} - ic/2$

### String Pattern in Roots of Bethe Equations

$$\times \mu_i = k + i|c|/2$$

$$\circ k_n = \mu - ic/2$$



$$\times \mu_j = k - i|c|/2$$

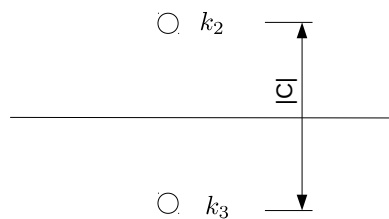
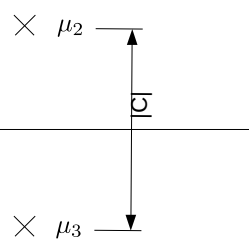
$$\circ k_m = \mu + ic/2$$

(a)  $\mu - k$  string of length 2 for both  $c > 0$  and  $c < 0$

(b)  $k - \mu$  string of length 2 for  $c < 0$

$$\times \mu_1$$

$$\circ k_1$$



(c)  $\mu$  string of length 4 in the limit the total number of particles goes to infinity with  $c > 0$  or  $c < 0$

(d)  $k$  string of length 4 in the limit the number of impurities goes to infinity with  $c < 0$

which forms a 2-string, then the scattering matrix among the spin rapidities enforces  $\alpha_{R^{11}} > \alpha_{R^{12}}$ . Carry out the product of  $J(\mu, k, \alpha)$ , we get

$$\begin{aligned} & J(\mu_1, k, \alpha_{R^{11}})J(\mu_2, k, \alpha_{R^{12}}) \\ &= \frac{ic}{\mu - k_{\alpha_{R^{11}}} + ic/2} \frac{ic}{\mu - k_{\alpha_{R^{12}}} + ic/2} \prod_{\alpha_{R^{12}} < m < \alpha_{R^{11}}} \frac{\bar{\mu} - k_m}{\bar{\mu} - k_m + ic} \prod_{\alpha_{R^{11}} < n} \frac{\bar{\mu} - k_n - ic}{\bar{\mu} - k_n + ic} \end{aligned}$$

Here  $|\frac{\bar{\mu} - k_m}{\bar{\mu} - k_m + ic}| < 1$ . As  $\alpha_{R^{11}} - \alpha_{R^{12}}$  gets greater, the product of  $m$  makes the wavefunction decrease exponentially with this separation. This is why the  $\mu$  string leads to bound states between two down spins. The physical meaning of a  $k$  string is related to a bound state between two electrons. As we have seen how  $k$ -strings leads to bound state in section 1.2, we will not elaborate it here. In the later section on Yudson representation, we will revisit these solution patterns.

## Chapter 3

### Yudson Approach

#### 3.1 Bethe Ansatz as Complete Basis

In the previous section, we have seen how the Bethe Ansatz solves models that are integrable. These solutions are characterized by a set of parameters (momentum, rapidity) which also determine the energy of the states. On one hand, these energies affect the Boltzmann weight of each state, thus determine the thermodynamic properties of the system, like the free energy, pressure, specific heat, etc. On the other hand, the energy also influences the dynamics of a state, as any state, under Hamiltonian  $H$ , evolves with the factor  $e^{-iHt}$ . The Bethe Ansatz has been shown to be quite successful in the first aspect, however, it has not been much exploited in the second due to the following difficulties.

To calculate the time evolution of a given state,  $|\Psi(t)\rangle = e^{-iHt}|\Psi_0\rangle$ , it is convenient to use the basis of eigenstates of the Hamiltonian so as to turn the Hamiltonian operator into a real number, i.e.

$$|\Psi(t)\rangle = \sum_m e^{-iE_m t} |m\rangle \langle m | \Psi_0 \rangle \quad (3.1)$$

For interacting systems that are integrable, these eigenstates are Bethe Ansatz solution which are handy already. However, as we have seen in the previous section, not all states are allowed in a system with a periodic boundary condition. One needs to solve  $O(N)$  coupled equations, only the root of which will be considered as a basis. The number of such solutions increases exponentially with the system size. This makes the summation over a complete basis very hard to implement. The problem becomes even harder for systems with bound states, as one needs to consider complex parameters as well. Another complication comes from the calculation of the overlap. Due to the admittedly unwieldy form of the Bethe solution, each state is composed of a factorially large sum of plain waves with intricate amplitudes corresponding to different orderings of the coordinates. Therefore, each summand evolves  $(N!)^2$  terms. Lastly, even the calculation of simple correlation functions of local physical observables turns out to be quite intimidating.

Recent years have, however, seen much progress in this direction and such process has been implemented numerically in a C++ library called ABACUS(Algebraic Bethe Ansatz-based Computation of Universal Structure factors) [? ]. This algorithm has successfully calculated dynamical correlation function of some important observables [? ? ] as well as nonequilibrium properties [? ? ] in one dimensional spin and atomic system. Following the same principle as discussed above, the implementation consists of three steps. First, Bethe equations are solved to obtain all states satisfying periodic boundary conditions. Then overlap between the initial state and intermediate states as well as further expectation values of observables are calculated from form factors of local operators already exist. Last, the Hilbert space is scanned to include numerically important intermediated states in terms of the form factor. One prominent feature of this algorithm is its extreme accuracy for large number  $N=100 - 1000$  of degrees of freedom. And this precision is well controlled by the sum rule of a complete basis which is energy and momentum independent. However, as pointed out by Caux in [? ], this method has some restrictions. First, it can only treat finite systems as one needs to label the states and have a finite Hilbert space to scan all relevant states. Moreover, the initial state should be close to some bethe states<sup>1</sup> as scanning over multiple eigenstates in the initial state will multiply the numerical cost and is not considered in the implementation. In the end, the numerical nature of the algorithm makes it impossible to obtain closed-form analytical expressions.

### 3.2 Yudson Contour Integral Representation

In this thesis, we are going to talk about an analytical treatment of the aforementioned expansion, which we call Yudson representation or Yudson Approach. This method is proposed by V. Yudson to study the superradiance effect in an infinite system described by the Dicke model in 1988 [? ? ]. The formalism has not gain much attention until recent years when the interest in nonequilibrium process has received a boost from the field of cold atom experiments which allow unprecedentedly finely controlled experiments. So far, the approach has successfully solved the quench dynamics of the Lieb-Liniger model [? ? ] and the XXZ model [? ] on an infinite line, the Lieb-Liniger model with strong interaction on a finite line with periodic boundary condition [? ] as well as hard wall boundary conditions [? ] and Dicke model [? ]. The time evolution of two component fermion gas and boson gas will also be discussed in this thesis.

---

<sup>1</sup>In the original paper [? ], Caux claims that the initial state should be ground state only, which is later loosed to any Bethe states in [? ] as well as the state created by one creation operator from the ground state [? ]

The core of the Yudson approach is a resolution of the identity which takes the form

$$\mathbb{1} = \int_k |k\rangle\langle k|$$

for a non-nested system like single component boson or fermion gas and spin system. And

$$\mathbb{1} = \int_{k,\mu} |k, \mu\rangle\langle k, \mu|$$

for a nested system like two component boson or fermion systems.

Here  $|k\rangle$  and  $|k, \mu\rangle$  represent a general Bethe Ansatz eigenstate and  $|k\rangle$  and  $|k, \mu\rangle$  are called Yudson states. These states refer to the single term in a Bethe Ansatz wavefunction with only identity permutation. For example, in the previous chapter, we have derived the eigenstate of the Lieb-liniger gas as

$$|k\rangle = \int_x \sum_P e^{ik_P x_i} \prod_{\substack{i < j \\ P^{-1}i > P^{-1}j}} \frac{k_i - k_j - ic}{k_i - k_j + ic} \theta(x)|x\rangle$$

with  $\theta(x) \equiv \theta(x_1 < x_2 < \dots < x_N)$ . Then the Yudson state is the simplest term among the  $N!$  terms which is

$$|k\rangle = \int_x e^{ik_i x_i} \theta(x)|x\rangle$$

Therefore, the Bethe Ansatz state can be expressed in terms of the Yudson state as

$$|k\rangle = \sum_P \prod_{\substack{i < j \\ P^{-1}i > P^{-1}j}} \frac{k_i - k_j - ic}{k_i - k_j + ic} |Pk\rangle = \sum_P S_k(P) |Pk\rangle$$

Take the Gaudin Yang model as another example. The Bethe Ansatz solution of the Gaudin Yang model is the following

$$|\mu, k\rangle = \sum_{P,R} \int_x \sum_{\alpha} e^{ik_P x_i} (-1)^P \prod_{i < j} \frac{\mu_i - \mu_j + ic \text{Sgn}(\alpha_{R^{-1}i} - \alpha_{R^{-1}j})}{\mu_i - \mu_j - ic} \prod_{i=1}^M I(\mu_i, Pk, \alpha_{R^{-1}i}) \theta(\alpha) \theta(x) \prod_{i=1}^M \sigma_{\alpha_i}^- |x\rangle \otimes |\uparrow\rangle$$

The Yudson state can be extracted from it as

$$|\mu, k\rangle = \int_x \sum_{\alpha} e^{ik_i x_i} \prod_{i=1}^M I(\mu_i, k, \alpha_i) \theta(\alpha) \theta(x) \prod_{i=1}^M \sigma_{\alpha_i}^- |x\rangle \otimes |\uparrow\rangle$$

Again the Bethe Ansatz state are connected with the Yudson state as

$$|\mu, k\rangle = \sum_{P,R} (-1)^P \prod_{\substack{i < j \\ R^{-1}i > R^{-1}j}} \frac{\mu_i - \mu_j + ic}{\mu_i - \mu_j - ic} |R\mu, Pk\rangle = \sum_{P,R} S_{k,\mu}(P, R) |R\mu, Pk\rangle$$

Compared with the one we have used in equation ??, i.e.  $\mathbb{1} = \sum_m |m\rangle\langle m|$ , Yudson representation seems different due to the new state. However, as we are going to show, the two resolutions are closely related by the following relation

$$\sum_m |m\rangle\langle m| = \sum_m |m\rangle\langle m|\theta(m)$$

Here, we have abused the notation  $\theta(m)$  which becomes ill defined for complex parameters. Its appearance only indicates that the summation is over all distinct states where the ordering of the  $m$ 's is irrelevant and each set of  $m$ 's should be included once.

Recall that Bethe Ansatz states with permuted momentum (and rapidity) are related by the scattering matrix, see page ??,??

$$|Pk\rangle = S_k^*(P)|k\rangle$$

$$|R\mu, Pk\rangle = S_{k,\mu}^*(P, R)|\mu, k\rangle$$

therefore

$$\begin{aligned} \sum_k |k\rangle\langle k|\theta(k) &= \sum_k \sum_P |k\rangle\langle Pk|S_k^*(P)\theta(k) \\ &= \sum_k \sum_P |Pk\rangle\langle Pk|\theta(k) \\ &= \sum_k |k\rangle\langle k| \sum_P \theta(P^{-1}k) \\ &= \sum_k |k\rangle\langle k| \end{aligned}$$

Similarly, one can show

$$\sum_{k,\mu} |\mu, k\rangle\langle \mu, k|\theta(k)\theta(\mu) = \sum_{k,\mu} |\mu, k\rangle\langle \mu, k|$$

The relation between the Yudson representation and the more traditional resolution of identity is to shed some light on the approach. However, that is not the whole story. Instead of taking a summation over sets of discrete momentum (and rapidity), Yudson approach uses contour integrals in the complex plane. The choice of the contour is the essence of the representation and one major step is to look for such a contour and prove that the expansion of any state is a faithful one. We are going to illustrate this point by the Lieb-Liniger model and the Gaudin-Yang model. Before we get down to the specifics, let's list the advantages of the approach.

### 3.3 Advantages and Disadvantages

#### Advantages

1. Simplify the calculation of the overlap with the initial state.

2. Obviate the need to solve Bethe Equations
3. Previous results on form factors can be used directly
4. Complex contour includes the contribution from both free states and bound states.
5. Infinite rapidity guarantees that the expansions scans the whole Hilbert space, not only the highest weight states.
6. Complicated norm factor disappear.

Advantage 1 stems from the simple form of a Yudson state. Instead of being a summation over factorially many terms, in Yudson representation, the overlap is one simple term. Advantage 2 is related to the fact that the system is infinite while the Bethe equations originate from the constraint of periodic boundary conditions. Usually, people place the system on a circle so as to make the momentum discrete. This is helpful to label the states and to include a few low energy states. Such boundary condition becomes unnecessary for the dynamics as all states overlapping with the initial state should be included. After all, most system is on a open line. Moreover, the absence of the Bethe equation is important to keep the calculation analytic as the solution to such transcendental equations is hard if not impossible to obtain when the number of particle is large. Advantage 3 does not ascribe to the Yudson representation. But this is a rather helpful property. Since in a strongly correlated system, all degrees of freedom intertwine with each other. The expectation values of simple observables like density and two point correlation involve integration over all irrelevant variables which is a rather daunting task. Luckily, the action of local operators on Bethe Ansatz states has been studied by itself and many results on the form factors have been obtained already [? ]. This simplifies our calculation. Advantage 4 is the most prominent. From the previous chapter we see that in systems with bound states like attractive Lieb-Liniger gas and Gaudin-Yang model, the Hilbert space is spanned by states with complex parameters. Even though the roots are not scattered on the complex plane randomly, the number of string patterns they fall into is still huge. If we define a given state by the number of strings( $M_j$ ) of length  $j$ , then the total number of string configuration is related to the different sequence  $(M_1, M_2, \dots)$  such that  $\sum_j M_j \cdot j = N$  for  $N$  charges. In addition to that, the center of each string can move along the real axis which multiplies the complication of a complete scan. As a miracle, this difficulty can be circumvented by a proper choice of integration contour in the complex plane. Such a contour integration incorporates contributions from both free states and bound states. To separate them apart, one simply shift all contours to the real axis. Using Cauchy's residue theorem, the original integral decomposes into a real integral

and contribution from residues at singularities. The former can be interpreted as free states while the latter corresponds to bound states. Remarkably, all and only bound states whose parameters follow the string pattern will be generated, that is to say that only wanted terms are created. Advantage 5 is an interesting one. As shown in the book [?] (Appendices 3D), every nested Bethe Ansatz state is a highest weight state with respect to the total spin. This means that it will be annihilated by spin raising operator  $S^+$ . Therefore, a complete basis includes not only Bethe Ansatz states  $|\mu, k\rangle$ , but also states with lower expectation value of  $S^z$ , i.e.  $(S^-)^n|\mu, k\rangle$  with  $n = 1, \dots, N - 2M$  for systems with  $N$  particles and  $M$  down spins. Luckily, as we have shown in equation (??), this spin lowering operator is nothing but  $\lim_{\mu \rightarrow \infty} B(\mu, k)$ . Therefore, by integrating from  $-\infty$  to  $+\infty$  for each rapidity, we are assured to probe every eigenstates in the Hilbert space. Advantage 6 is also associated with the infinite size of the system. In finite volume, the norm of an eigenstate is always complicated that consists of determinant whose dimension equals the number of degree of freedom [? ?]. Simply sending the system size  $L$  to infinity does not simplify the situation as the expression does not have a good limit in thermodynamic limit. Nevertheless, this is not a real problem for Yudson Approach. The condition that the intermediate states be normalized, complete and orthogonal is a sufficient condition, instead of being necessary for the following reason. Normally, in a Bethe Ansatz state, the ratio of amplitudes between different sectors is fixed by the scattering matrix, leaving the overall factor indefinite. In Yudson representation, one first set the amplitude  $A(P)$  to be the s-matrix  $s(p)$  together with other factors if necessary (like the  $J$ -function in nested Bethe Ansatz). Then the identity resolution is sandwiched between two coordinate eigenstate,  $|x\rangle = \theta(x_1 < \dots < x_N) \prod_i \Psi^\dagger(x)|0\rangle$ , or  $|x, \alpha\rangle = \theta(x_1 < \dots < x_N) \theta(\alpha_1 < \dots < \alpha_N) \prod_i \sigma_{\alpha_i}^- \prod_j \Psi_j^\dagger(x_j)|0\rangle$ . Then we will always obtain  $\langle y|k\rangle\langle k|x\rangle = C \prod_i \delta(x_i - y_i)$  or  $\langle y, \beta|k\rangle\langle k|x, \alpha\rangle = C \prod_i \delta(x_i - y_i) \delta_{\alpha_i, \beta_i}$ . In the end, we divide the expansion by  $C$  to make it properly normalised. This, in turn, proves the completeness and orthogonality of the Bethe Ansatz state

### Disadvantages

This method, however, suffers from one disadvantage, which relates to multidimensional integrals. For a system with  $N$  degrees of freedom, the expectation value of local observables involves integration over  $2N$  variables. This obstacle prevents us from getting closed form results. To get around this difficulty, one may focus on the long time limit of the results and adopt saddle points approximation for system with nonlinear spectrum. This will bring us another complication. As the propagating rate of different bound states varies, the contribution from

each state separates apart asymptotically. Technically, this means the following. To impose saddle point approximation, one needs to shift the contour to the saddle points which usually lie on the real axis. For systems with bound states, the integral contours spread out in the imaginary direction and there are many singularities in the complex plane. Shifting the contour reduces the original integral into contributions from the stationary phase as well as residues around the poles. The representation, then, loses the compact expression. Unfortunately, this is what we have so far.

In the next part, we are going to illustrate these points by applying the Yudson Approach to the quench dynamics of the Lieb-Linger model and the Gaudin-Yang model with either repulsive or attractive interaction. To be specific, we are going to talk about the choice of integral contour for each model, prove that the representation is a faithful one (central theorem), calculate local observables mostly with saddle point approximation, and show some interesting results obtained.

## Chapter 4

### Quench Dynamics of Lieb-Liniger Gas

In this chapter, we will apply the Yudson Approach to the quench dynamics of Boson Gas in an one dimensional infinitely system. This system is described by the Lieb-Liniger Hamiltonian

$$H = \int_x \partial_x \Psi^\dagger(x) \partial_x \Psi(x) + c \Psi^\dagger(x) \Psi^\dagger(x) \Psi(x) \Psi(x)$$

First, let's list some of the important results we have obtained already.

The Bethe Ansatz eigenstate

$$|k\rangle = \sum_P \int_x e^{ik_{P^1} x_i} \prod_{\substack{i < j \\ P^{-1}i > P^{-1}j}} \frac{k_i - k_j - ic}{k_i - k_j + ic} \theta(x) |x\rangle$$

The Yudson state

$$|k\rangle = \int_x e^{ik_i x_i} \theta(x) |x\rangle$$

The Yudson representation of the identity operator

$$\int_C dk |k\rangle \langle k| = \int_C dk \int dx \int dy e^{ik_i(x_{P^{-1}i} - y_i)} \prod_{\substack{i < j \\ P^{-1}i > P^{-1}j}} \frac{k_i - k_j - ic}{k_i - k_j + ic} \theta(x) \theta(y) |x\rangle \langle y|$$

We claim that for repulsive interaction, the integration contours lie on the real axis while for the attractive case, the contours spread out in the imaginary direction with the separation between adjacent lines greater than  $|c|$ . For any  $i < j$ , the contour of  $k_i$  is above that of  $k_j$ . See fig ??.

In the next section, we will show why such contours are chosen. Due to the crucial role of such proof, we call it the central theorem.

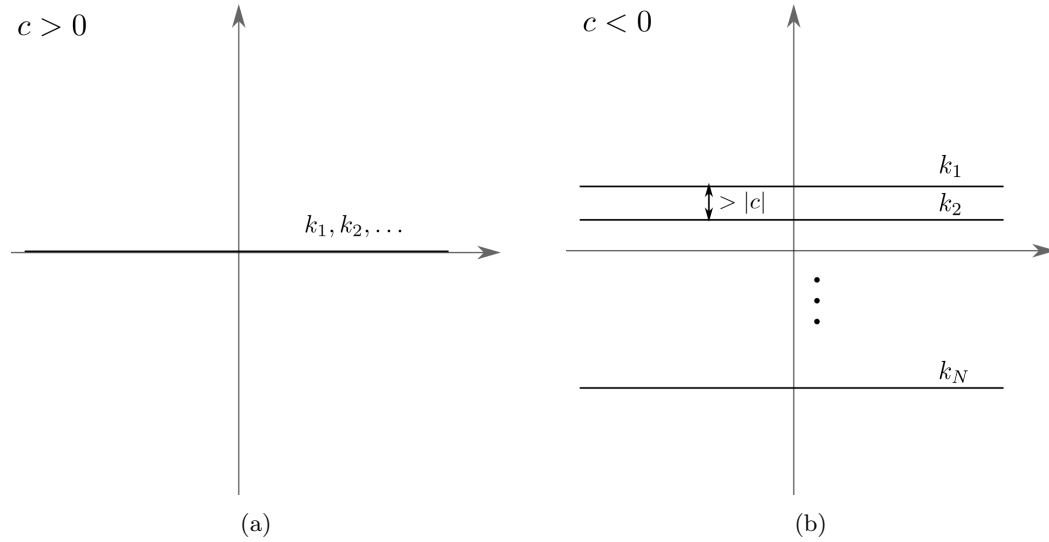


Figure 4.1: Integration contour for the Lieb-Liniger model with attractive or repulsive interaction.

#### 4.1 Central Theorem

One of the most important ingredients of the Yudson approach is a properly chosen contour such that the representation resolves the identity faithfully. In the position space, this means

$$\int_C \langle x|k\rangle \langle k|y\rangle = \prod_i \delta(y_i - x_i)$$

for any ordered set of  $x$  and  $y$ . Without loss of generality, we will always assume  $x_1 < x_2 \dots < x_N$  and  $y_1 < y_2 \dots < y_N$ . We will provide the proof for the case with repulsive and attractive interaction respectively.

### 4.1.1 Repulsive Case

We will begin with the repulsive case as the integral contour is simpler. First, separate the integration into two parts as described in the following

$$\begin{aligned}
I &= \theta(x)\theta(y) \int dk \langle x|k \rangle \langle k|y \rangle \\
&= \theta(x)\theta(y) \int dk \sum_P e^{ik_i(x_{P^{-1}i} - y_i)} \prod_{\substack{i < j \\ P^{-1}i > P^{-1}j}} \frac{k_i - k_j - ic}{k_i - k_j + ic} \\
&= \theta(x)\theta(y) \int dk \sum_P e^{ik_i(x_{P^{-1}i} - y_i)} \\
&\quad + \theta(x)\theta(y) \int dk \sum_P e^{ik_i(x_{P^{-1}i} - y_i)} \sum_{\substack{(m,n) \subseteq \\ \{(i,j) | i < j, P^{-1}i > P^{-1}j\}}} \prod_{m < n} \frac{-2ic}{k_m - k_n + ic} \\
&= I_1 + I_2
\end{aligned}$$

In the fourth line, we transform the fraction  $\frac{k_i - k_j - ic}{k_i - k_j + ic}$  into  $1 - \frac{2ic}{k_i - k_j + ic}$  and extract the contribution of 1 in each factor as  $I_1$  and name the rest as  $I_2$ . In  $I_2$ , the set  $(m, n)$  is a nonempty subset of the original set  $(i, j)$  in the product. Denote  $m_1 < m_2 \dots < m_n$  as the elements in the subset and  $n_i$  as the elements not in the subset. We will show that  $I_2 = 0$ , i.e.

$$\begin{aligned}
I &= I_1 = \theta(x)\theta(y) \sum_P (2\pi)^n \delta(x_{P^{-1}i} - y_i) \\
&= \theta(x)(2\pi)^n \delta(x_i - y_i)
\end{aligned}$$

and

$$\mathbb{1} = \frac{1}{(2\pi)^n} \int dk |k \rangle \langle k|$$

In  $I_2$ , the integration of  $k_{n_i}$  can be carried out trivially, which gives us  $(2\pi)^n \delta(x_{P^{-1}i} - y_i)$ . Thus the core of the central theorem is to prove that the integrations over  $k_{m_i}$ 's vanish. This consists of two steps. First, we will show that  $x_{P^{-1}m} < y_m$  for any  $m$  in the subset. Then it follows that  $x_{P^{-1}m} = y_m$  and this leads to a contradiction with the exist condition of the poles as explained below.

(1) Let's start with the integration over  $k_{m_1}$ . If  $x_{P^{-1}m_1} > y_{m_1}$ , then one can add an additional arc at infinity on the upper half plane because that section gives an exponentially damped contribution. This is due to the Jordan's Lemma which says that

$$\left| \int_{C_R} g(z) e^{iaz} \right| \leq \frac{\pi}{|a|} M_R$$

provided that  $C_R$  lies in the upper half plane for  $a > 0$  and in the lower half plane for  $a < 0$ . Here  $M(R)$  is the maximum value of  $g$  on the arc. For our case,  $M_R = O(\frac{1}{R})$  or  $o(\frac{1}{R})$  determined

by whether there is one or more terms depends on  $k_{m_1}$ . Therefore  $M_R \rightarrow 0$  as  $R \rightarrow \infty$ , so is the integration over the arc.

As  $m_1$  is the smallest in the subset, all of the poles lie below the integration line, see fig.??(a). Therefore, the integration over the closed contour vanishes as it does not encircle any pole. As the integration over the semicircle at infinity is zero, the original integral also vanishes. This means  $x_{P^{-1}m_1} \leq y_{m_1}$ .

If  $x_{P^{-1}m_2} > y_{m_2}$ , then one can close the contour in the upper half plane. There is only one pole at  $k_{m_1} + ic$  which requires  $P^{-1}m_1 > P^{-1}m_2$ . However, as  $x$ 's and  $y$ 's are ordered and  $m_1 < m_2$ , together with the fact that  $x_{P^{-1}m_2} > y_{m_2}$ ,  $x_{P^{-1}m_1} < y_{m_1}$ , this implies that  $P^{-1}m_1 < P^{-1}m_2$ . Therefore, the pole does not exist. This leads to  $x_{P^{-1}m_2} < y_{m_2}$ .

Such argument can be carried out for any  $k_{m_i}$ . If  $x_{P^{-1}m_i} > y_{m_i}$ , then the integration equals the residues in the upper half plane. However, the condition of the poles contradicts with the statement  $x_{P^{-1}i} > y_{m_i}$  and  $x_{P^{-1}m_j} < y_{m_j}$  for any  $i > j$ . Thus, it is proved that  $x_{P^{-1}m_i} \leq y_{m_i}$ .

If  $x_{P^{-1}m_n} < y_{m_n}$ , then the contour of  $k_{m_n}$  can be closed in the lower half plane where the integrand is analytic. Thus, the integration vanishes unless  $x_{P^{-1}m_n} = y_{m_n}$ .

If  $x_{P^{-1}m_{n-1}} < y_{m_{n-1}}$ , then one can close the contour below, encircling the only pole at  $k_{m_n} - ic$ . Combined with the other relations we have, i.e.  $x_{P^{-1}m_n} = y_{m_n}$ ,  $y_{m_n} > y_{m_{n-1}}$ , we get  $x_{P^{-1}m_{n-1}} < x_{P^{-1}m_n}$ , which indicates that  $P^{-1}m_{n-1} < P^{-1}m_n$ . This contradicts with the exist condition of this pole which says  $P^{-1}m_{n-1} > P^{-1}m_n$ . Thus one gets the relation  $x_{P^{-1}m_{n-1}} = y_{m_{n-1}}$ .

Similarly, one can show that  $x_{P^{-1}m_i} = y_{m_i}$  for any  $i$ . On the other hand,  $x_{P^{-1}n_i} = y_{n_i}$ . Thus, we arrive at the conclusion that  $P^{-1} = i$ , i.e.  $P = \mathbb{1}$ . This is inconsistent with the prerequisite for  $I_2$ , which says that there is at least one pair of  $m < n$  such that  $P^{-1}m > P^{-1}n$ . Thus we have shown that  $I_2 = 0$ . This completes the proof of the central theorem for  $c > 0$ .

### 4.1.2 Attractive Case

The integration contours for the attractive case spread out in the imaginary direction. However, the pole position relative to the integration line is the same as the repulsive case. For example, the pole of  $k_1$  due to the S-matrix  $S(P_{12})$  is at  $k_2 + i|c|$ . However, as the integration contour of  $k_2$  is below that of  $k_1$  and the distance is more than  $|c|$ , thus this pole is below the integration line of  $k_1$ . For a general pole structure, see fig ?? . As a result, all arguments there can be carried over. We will not repeat it. Note that this provides us with a guideline for guessing the contour. Usually, the contours simply lie on the real axis if the system does not have bound states. If

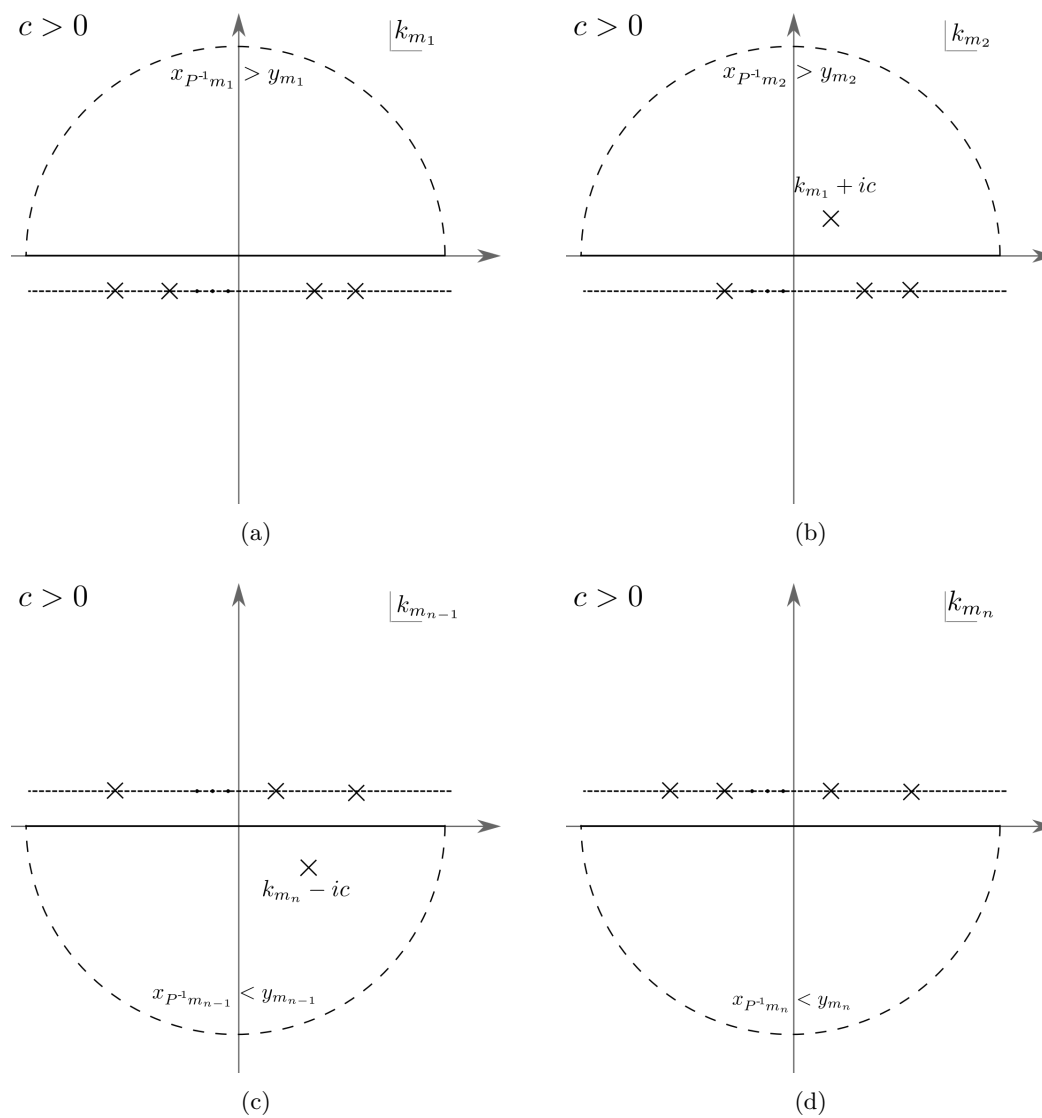


Figure 4.2: Pole positions for various  $k$  integrations in the repulsive case. Integrated variables are marked on the upper-left corner of the graph

one can prove the central theorem with such contours, one may manipulate the contour for the counterpart with attractive interaction such that the relative position between poles and contours remains the same. However, for some model like Gaudin-Yang model, there are bound states for both repulsive and attractive interaction, then one needs to work harder to guess the contour for the repulsive case first, then for the attractive case.

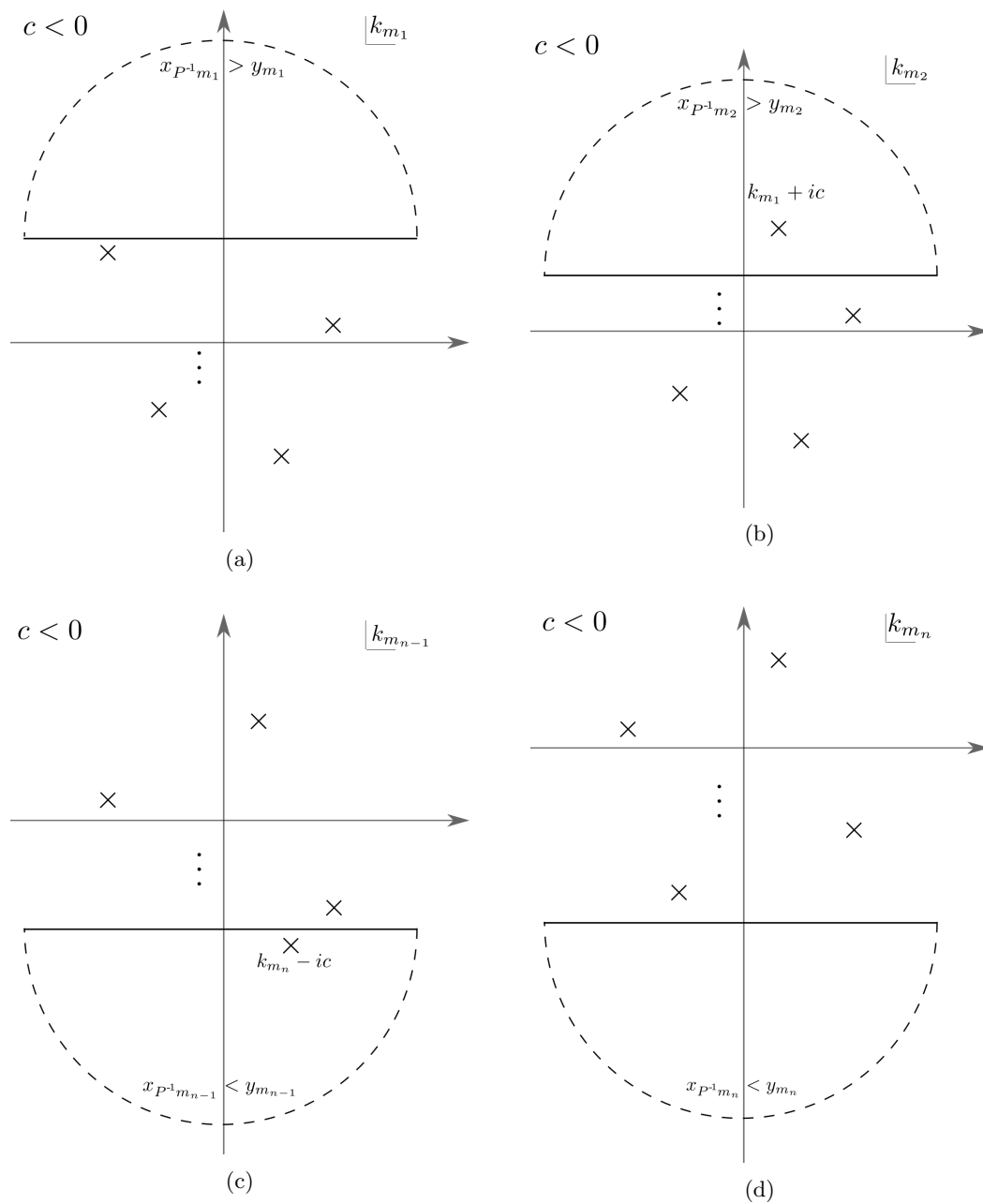


Figure 4.3: Pole positions for various  $k$  integrations in the attractive case. Integrated variables are marked on the upper-left corner of the graph

## Time Evolution

With the Yudson representation, we can expand any state in terms of eigenstates of the Hamiltonian. This makes the time evolution very easy to calculate. In this section, we will study the time evolved state at a later time. We will begin with the two-particle case. This is the simplest situation and the only one where a closed form of the wavefunction can be obtained. For systems with any number of particles, the integration over the momentums can not be carried out explicitly. As a compromise, we will study the behaviour in the long time limit using the saddle point approximation.

### 4.2 Two particle Dynamics

In this part, we will study the system with only two particles. First, we will investigate the evolution of the following initial state

$$|\phi_0\rangle = \frac{1}{\sqrt{\pi\sigma^2}} \int_{x_1, x_2} e^{-\frac{(x_1-x_{10})^2}{2\sigma^2} - \frac{(x_2-x_{20})^2}{2\sigma^2}} \Psi^\dagger(x_1) \Psi^\dagger(x_2) |0\rangle$$

which describes two wavepackets centered at  $x_{10} < x_{20}$  respectively. Here we assume the packet width  $\sigma$  is much smaller than the distance in between  $x_{20} - x_{10}$ , i.e. the two particles are well separated. Then the overlap between this state with the Yudson state can be calculated as the following

$$\begin{aligned} (k_1, k_2 | \phi_0) &= \frac{1}{\sqrt{\pi\sigma^2}} \int_{x_1, x_2} e^{-\frac{(x_1-x_{10})^2}{2\sigma^2} - \frac{(x_2-x_{20})^2}{2\sigma^2} - ik_1 x_1 - ik_2 x_2} \theta(x_2 - x_1) \\ &\quad e^{-\frac{(x_1-x_{10})^2}{2\sigma^2} - \frac{(x_2-x_{20})^2}{2\sigma^2} - ik_1 x_2 - ik_2 x_1} \theta(x_1 - x_2) \\ &= \frac{1}{\sqrt{\pi\sigma^2}} \int_{x_1, x_2} e^{-\frac{(x_1-x_{10})^2}{2\sigma^2} - \frac{(x_2-x_{20})^2}{2\sigma^2} - ik_1 x_1 - ik_2 x_2} \\ &\quad + \frac{1}{\sqrt{\pi\sigma^2}} \int_{x_1, x_2} e^{-\frac{(x_1-x_{10})^2}{2\sigma^2} - \frac{(x_2-x_{20})^2}{2\sigma^2}} (e^{-ik_2 x_1 - ik_1 x_2} - e^{-ik_1 x_1 - ik_2 x_2}) \theta(x_1 - x_2) \\ &= I_1 + I_2 \end{aligned}$$

We will show that  $I_2$  is of the order of  $e^{-\frac{(x_{20}-x_{10})^2}{4\sigma^2}}$  and we will drop this term.

First we replace the terms in the parenthesis by it upper bound which is 2 and then carry out the integration over  $x_1$ . And we get

$$I_2 < \sqrt{2} \int_{x_2} \operatorname{erfc}\left(\frac{x_2 - x_{10}}{\sqrt{2}\sigma}\right) e^{-\frac{(x_2-x_{20})^2}{2\sigma^2}}$$

Then split the integration into two parts. The first part  $I_2^1$  integrate from  $-\infty$  to  $x_{10}$ , and replace the complimentary error function by its upper bound which is 2. Therefore,

$$I_2^1 < 2\sqrt{2} \int_{-\infty}^{x_{10}} dx_1 e^{-\frac{(x_2-x_{20})^2}{2\sigma^2}} = 2\sigma\sqrt{\pi} \operatorname{erfc}\left(\frac{x_{20} - x_{10}}{2\sigma}\right)$$

As

$$\operatorname{erfc}(x) = \frac{e^{-x^2}}{\sqrt{\pi}} \left( \frac{1}{x} + O\left(\frac{1}{x^3}\right) \right)$$

for real and large  $x$ , we have

$$I_2^1 = O\left(\frac{\sigma}{(x_{20} - x_{10})} e^{-\frac{(x_{20} - x_{10})^2}{2\sigma^2}}\right)$$

The second part  $I_2^2$  includes the integration from  $x_{10}$  to infinity. Make use of the fact that

$$\operatorname{erfc}(x) < \frac{\sqrt{\pi}}{2} e^{-x^2} \frac{1}{x+1}$$

and as  $x > 0$ , we further simplify the relation as

$$\operatorname{erfc}(x) < \frac{\sqrt{\pi}}{2} e^{-x^2}$$

Therefore,

$$\begin{aligned} I_2^2 &< \frac{\sqrt{\pi}}{2} \int_{x_1}^{\infty} e^{-\frac{(x_2 - x_{10})^2}{2\sigma^2} - \frac{(x_2 - x_{20})^2}{2\sigma^2}} \\ &< \frac{\sqrt{\pi}}{2} \int_{-\infty}^{\infty} e^{-\frac{(x_2 - x_{10})^2}{2\sigma^2} - \frac{(x_2 - x_{20})^2}{2\sigma^2}} \\ &< \frac{\pi\sigma}{\sqrt{2}} e^{-\frac{(x_{10} - x_{20})^2}{4\sigma^2}} \end{aligned}$$

i.e.

$$I_2^2 = O\left(e^{-\frac{(x_{10} - x_{20})^2}{4\sigma^2}}\right)$$

Thus, we can say

$$I_2 = O\left(e^{-\frac{(x_{10} - x_{20})^2}{4\sigma^2}}\right)$$

Through the estimation, above, one can get a glimpse of the complication a simple  $\theta$ -function brings. Therefore, we will always assume that particles are well separated apart and the tail of the wave packet is negligible so as to ignore the  $\theta$ -function. We will not touch the problem of a condensate in the position basis in this thesis.

To sum up, the overlap between our initial state  $|\phi_0\rangle$  and Yudson state is

$$\begin{aligned} (k_1, k_2 | \phi_0) &= \frac{1}{\sqrt{\pi\sigma^2}} \int_{x_1, x_2} e^{-\left(\frac{(x_1 - x_{10})^2}{2\sigma^2} + \frac{(x_2 - x_{20})^2}{2\sigma^2} - ik_1 x_1 - ik_2 x_2\right)} \\ &= \sqrt{4\pi\sigma^2} e^{-ik_1 x_{10} - ik_2 x_{20} - k_1^2 \sigma^2 / 2 - k_2^2 \sigma^2 / 2} \end{aligned}$$

## Exact Wavefunction

Plug it into the Yudson Representation we get

$$\begin{aligned}
& |\phi(t)\rangle \\
&= \int_C dk e^{-iE_k t} |k_1, k_2\rangle \langle k_1, k_2 | \phi_0\rangle \\
&= \frac{\sqrt{4\pi\sigma^2}}{(2\pi)^2} \int dx \int dy \int_C dk \left( e^{-ik_1^2(t+\sigma^2/2i) - ik_2^2(t+\sigma^2/2i) + ik_1(y_1-x_{10}) + ik_2(y_2-x_{20})} + e^{-ik_1^2(t+\sigma^2/2i)} \right. \\
&\quad \left. e^{-ik_2^2(t+\sigma^2/2i) + ik_1(y_2-x_{10}) + ik_2(y_1-x_{20})} \frac{k_1 - k_2 - ic}{k_1 - k_2 + ic} \right) \theta(y_2 - y_1) |y_1, y_2\rangle \\
&= \frac{\sqrt{4\pi\sigma^2}}{(2\pi)^2} \int dx \int dy \int_C dk \left( e^{-ik_1^2(t+\sigma^2/2i) - ik_2^2(t+\sigma^2/2i) + ik_1(y_1-x_{10}) + ik_2(y_2-x_{20})} \left( \theta(y_2 - y_1) \right. \right. \\
&\quad \left. \left. + \frac{k_1 - k_2 - ic}{k_1 - k_2 + ic} \theta(y_1 - y_2) \right) \right) |y_1, y_2\rangle \\
&= \frac{\sqrt{4\pi\sigma^2}}{(2\pi)^2} \int dx \int dy \int_C dk \left( e^{-ik_1^2(t+\sigma^2/2i) - ik_2^2(t+\sigma^2/2i) + ik_1(y_1-x_{10}) + ik_2(y_2-x_{20})} \left( 1 - \frac{2ic}{k_1 - k_2 + ic} \right. \right. \\
&\quad \left. \left. \theta(y_1 - y_2) \right) \right) |y_1, y_2\rangle \\
&= \int dx \int dy (I_1 + I_2) |y_1, y_2\rangle
\end{aligned}$$

The calculation of the first term is trivial

$$I_1 = \frac{\sqrt{4\pi\sigma^2}}{(2\pi)^2} \frac{\pi}{i(t + \sigma^2/2i)} e^{i \frac{(y_1-x_{10})^2 + (y_2-x_{20})^2}{4(t+\sigma^2/2i)}}$$

To calculate the second term, we transform the fraction into the following integral

$$\frac{1}{k_1 - k_2 + ic} = \frac{1}{i} \int_0^\infty e^{(ik_1 - k_2 + ic)\lambda} d\lambda$$

Note, this transformation is valid for both repulsive and attractive cases as  $\Im(k_1 - k_2 + ic) > 0$  for both situations. (Recall that for attractive case, the contour of  $k_1$  is above that of  $k_2$  by a distance greater than  $|c|$ , this makes  $\Im(k_1) - \Im(k_2) - |c| > 0$ .) Therefore, the expression of the attractive case is the same as that of the repulsive one. With this trick, the second term can be calculated as

$$\begin{aligned}
I_2 &= -2c\theta(y_1 - y_2) \frac{\sqrt{4\pi\sigma^2}}{(2\pi)^2} \int_0^\infty d\lambda \int_C dk e^{-ik_1^2(t+\sigma^2/2i) - ik_2^2(t+\sigma^2/2i) + ik_1(y_1-x_{10}+\lambda) + ik_2(y_2-x_{20}-\lambda)} \\
&\quad e^{-c\lambda} \\
&= -2c\theta(y_1 - y_2) \frac{\sqrt{4\pi\sigma^2}}{(2\pi)^2} \frac{\pi}{i(t + \sigma^2/2i)} \int_0^\infty d\lambda e^{\frac{i\lambda^2}{2(t+\sigma^2/2i)} + \frac{i(y_1-x_{10}-y_2+x_{20}+2ic(t+\sigma^2/2i))\lambda}{2(t+\sigma^2/2i)} + \frac{i(y_1-x_{10})^2}{4(t+\sigma^2/2i)}} \\
&\quad e^{\frac{i(y_2-x_{20})^2}{4(t+\sigma^2/2i)}} \\
&= -c\sqrt{2\pi i(t + \sigma^2/2i)} \theta(y_1 - y_2) \frac{\sqrt{4\pi\sigma^2}}{(2\pi)^2} \frac{\pi}{i(t + \sigma^2/2i)} \operatorname{erfc}(\alpha) e^{\alpha^2}
\end{aligned}$$

where

$$\begin{aligned}\alpha &= \frac{y_1 - x_{10} - y_2 + x_{20} + 2ic(t + \sigma^2/2i)}{2\sqrt{2i(t + \sigma^2)}} \\ &= \frac{(1-i)(y_1 - x_{10} - y_2 + x_{20} + 2ic(t + \sigma^2/2i))}{4\sqrt{(t + \sigma^2/2i)}}\end{aligned}$$

In the first line, we shift the contour of  $k_1$  and  $k_2$  to the real axis for attractive case. This is accredited to the trick we have used which removes the pole at  $k_1 = k_2 - ic$ . In the second line of the  $\alpha$  equation, we take the  $i$  out of the square root. We claim that this will bring us a factor of  $1 - i$  rather than  $i - 1$ . This is a nontrivial assertion as

$$\operatorname{erfc}(-\alpha) = 2 - \operatorname{erfc}(\alpha) \quad (4.1)$$

The extra minus sign will leads to an extra term of the form  $e^{\alpha^2}$  as well as a minus sign in the rest of the contribution. We are going to check the solution by studying its long time limit and show its relevance to the bound states in the attractive case. Before, we go into details, let's summarize the results. Combining the two contributions, the wavefunction at time  $t$  equals the following

$$\begin{aligned}f(y_1, y_2, t) &= \frac{\sigma}{2\sqrt{\pi}i(t + \sigma^2/2i)} e^{\frac{i(y_1 - x_{10})^2 + i(y_2 - x_{20})^2}{4(t + \sigma^2/2i)}} (1 - (1+i)c\theta(y_1 - y_2)\sqrt{(t + \sigma^2/2i)\pi} \\ &\quad \operatorname{erfc}(\alpha)e^{\alpha^2})\end{aligned}$$

$$\text{with } \alpha = \frac{(1-i)(y_1 - x_{10} - y_2 + x_{20} + 2ic(t + \sigma^2/2i))}{4\sqrt{t + \sigma^2/2i}}.$$

### Asymptotic Limit of the Wavefunction

When  $t$  is large, the expression can be simplified using the following asymptotic expansion of the complimentary error function. [?, Eq. 7.12.1].

$$\operatorname{erfc}(z)e^{z^2} \approx \frac{1}{\sqrt{\pi}} \sum_{m=0}^{\infty} (-1)^m \frac{(\frac{1}{2})_m}{z^{2m+1}} \quad |\operatorname{ph}(z)| < \frac{3}{4}\pi$$

Here  $(\frac{1}{2})_m$  is the Pochhammer symbol, defined as  $(x)_n = \frac{\Gamma(x+n)}{\Gamma(x)} = x(x-1)\cdots(x+n-1)$ .

Define

$$\zeta = \frac{y_1 - x_{10} - y_2 + x_{20} + 2ic(t + \sigma^2/2i)}{4\sqrt{t + \sigma^2/2i}}$$

For  $c > 0$ ,  $\zeta$  falls in the first quadrant, being close to the imaginary axis. Then we have

$$|\operatorname{ph}((1-i)\zeta)| \in (0, \frac{\pi}{4})$$

Therefore,

$$\begin{aligned} & \lim_{t \gg 1} f(y_1, y_2, t) \\ &= \frac{\sqrt{4\pi\sigma^2}}{(2\pi)^2} \frac{\pi}{i(t + \sigma^2/2i)} e^{\frac{i(y_1 - x_{10})^2 + i(y_2 - x_{20})^2}{(t + \sigma^2/2i)}} \left( 1 - \frac{4ic(t + \sigma^2/2i)\theta(y_1 - y_2)}{y_1 - x_{10} - y_2 + x_{20} + 2ic(t + \sigma^2/2i)} \right) \end{aligned} \quad (4.2)$$

For  $c < 0$ ,  $\Re[\zeta]$  can be positive or negative (with extreme large interaction strength like in the super Tonks-Girardeau case),  $\zeta$  lies on either side of the imaginary axis in the negative direction.

Thus

$$|\text{ph}((1 - i)\zeta)| \in \left(\frac{\pi}{2}, \pi\right)$$

Together with the relation eq(??), we have

$$\begin{aligned} & \lim_{t \gg 1} f(y_1, y_2, t) \\ &= \frac{\sqrt{4\pi\sigma^2}}{(2\pi)^2} \frac{\pi}{i(t + \sigma^2/2i)} e^{\frac{i(y_1 - x_{10})^2 + i(y_2 - x_{20})^2}{(t + \sigma^2/2i)}} \left( 1 - (1 + i)c\theta(y_1 - y_2)\sqrt{(t + \sigma^2/2i)\pi} \right. \\ & \quad \left. \left( 2e^{-\frac{i(y_1 - x_{10} - y_2 + x_{20} + 2ic(t + \sigma^2/2i)^2}{8(t + \sigma^2/2i)}} - \frac{4\sqrt{t + \sigma^2/2i}}{(1 - i)\sqrt{\pi}(y_1 - x_{10} - y_2 + x_{20} + 2ic(t + \sigma^2/2i))} \right) \right) \end{aligned} \quad (4.3)$$

On the other hand, we can calculate the asymptotic limit of the wavefunction from the very beginning using saddle point approximation.

### Saddle Point Approximation

Saddle point refers to a point in the analytic landscape of the absolute value of the integrand, such that it is a relative minimum along one direction and a relative maximum along another. See Figure ?? . According to the Jensen's theorem, there are no peaks but only saddle points for any function. Therefore, besides the singularities, these points are the most important. To make the saddle point approximation, one first deforms the original path  $C$  to  $C'$  which runs through the saddle points in the direction such that the saddle point is a maximum. Therefore, most of the contribution comes from the vicinity of this point as long as the slope around it is steep enough. For an integral of the form

$$I(s) = \int_C g(z)e^{sf(z)} dz$$

where  $s$  is big, the integral can be approximated by the following expression [? ]

$$I(s) \approx g(z_0)e^{sf(z_0)} \sqrt{\frac{2\pi}{sf''(z_0)}} e^{i\alpha}$$

Here  $\alpha = \pi/2 - \text{ph}(f''(z_0))/2$ . Hence, the original integration becomes the sum of the residues at the pole between the two paths  $C$  and  $C'$  and the saddle point approximated value.

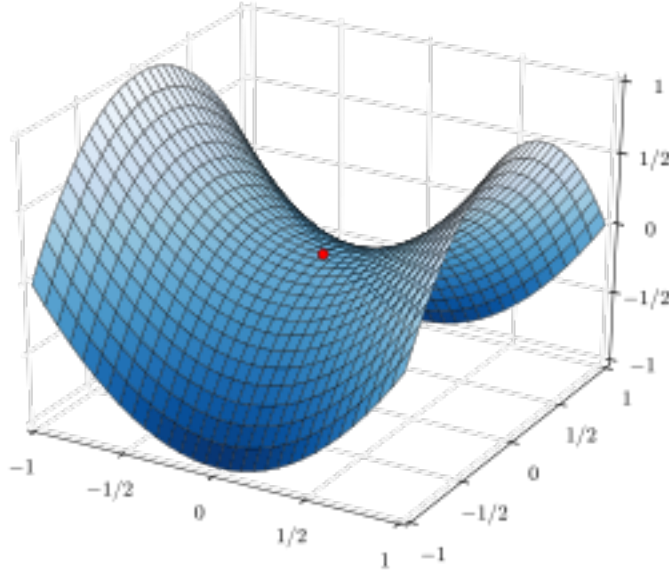


Figure 4.4: Example of a saddle point. Figure from Wikimedia

First, let's apply the method to the wavefunction integration with repulsive interaction. Here the contours of momentum integrations are along the real axis and they run through the saddle points at  $k_1 = (y_1 - x_{10})/2(t + \sigma^2/2i)$  and  $k_2 = (y_2 - x_{20})/2(t + \sigma^2/2i)$ . Thus, we have

$$\begin{aligned}
 f(y_1, y_2, t) &= \frac{\sqrt{4\pi\sigma^2}}{(2\pi)^2} \int dk (e^{-ik_1^2(t+\sigma^2/2i)} - ik_2^2(t+\sigma^2/2i) + ik_1(y_1-x_{10}) + ik_2(y_2-x_{20}) (1 - \frac{2ic}{k_1 - k_2 + ic} \\
 &\quad \theta(y_1 - y_2)) \\
 &\approx \frac{\sqrt{4\pi\sigma^2}}{(2\pi)^2} \frac{\pi}{i(t + \sigma^2/2i)} e^{\frac{i(y_1-x_{10})^2 + i(y_2-x_{20})^2}{4(t+\sigma^2/2i)}} \left(1 - \frac{4ic\theta(y_1 - y_2)t}{y_1 - x_{10} - y_2 + x_{20} + 2ic(t + \sigma^2/2i)}\right)
 \end{aligned} \tag{4.4}$$

However, for the situation with negative interaction, the contours of  $k_1$  lies above the real axis, that of  $k_2$  lies below the axis. In order to perform the saddle point approximation, one needs to deform the contour so that they both lie on the real axis where the singularity exists. This transforms the integral into a sum of two terms. The first is the same as that of the repulsive one. The second term corresponds to the residue at  $k_1 = k_2 - ic$ , and we are free to shift the contour of  $k_2$  such that  $k_1 = k - ic/2$  and  $k_2 = k + ic/2$  for a real  $k$ . Then we carry out the saddle point approximation at  $k = \frac{y_1 - x_{10} + y_2 - x_{20}}{4(t + \sigma^2/2i)}$  and we obtain

$$\begin{aligned}
& f(y_1, y_2, t) \\
&= \frac{\sqrt{4\pi\sigma^2}}{(2\pi)^2} \left( \int dk (e^{-ik_1^2(t+\sigma^2/2i) - ik_2^2(t+\sigma^2/2i) + ik_1(y_1-x_{10}) + ik_2(y_2-x_{20})} \left(1 - \frac{2ic}{k_1 - k_2 + ic}\right) \right. \\
&\quad \theta(y_1 - y_2) - 2ic\theta(y_1 - y_2)(-2\pi i) \int dk e^{-i(k-ic/2)^2 t - i(k+ic/2)^2 t + i(k-ic/2)(y_1-x_{10})} \\
&\quad \left. e^{i(k+ic/2)(y_2-x_{20})} \right) \\
&\approx \frac{\sqrt{4\pi\sigma^2}}{(2\pi)^2} \frac{\pi}{i(t+\sigma^2/2i)} e^{\frac{i(y_1-x_{10})^2 + i(y_2-x_{20})^2}{4(t+\sigma^2/2i)}} \left(1 - \frac{4ic\theta(y_1 - y_2)t}{y_1 - x_{10} - y_2 + x_{20} - 2ic(t+\sigma^2/2i)}\right) \\
&\quad + 2(i-1) \sqrt{\frac{\pi^3}{t+\sigma^2/2i}} c e^{\frac{i(y_1-x_{10})^2 + i(y_2-x_{20})^2}{4(t+\sigma^2/2i)}} e^{-\frac{i(y_1-x_{10}-y_2+x_{20}+2ic(t+\sigma^2/2i))^2}{4(t+\sigma^2/2i)}} \tag{4.5}
\end{aligned}$$

Compare the expressions with the one we get from the asymptotic expansion of the complementary error function, we see that Equation (??),(??) agrees with Equation (??),(??). Thus the choice of the square root of  $i$  is confirmed.

## Observables

Given the wavefunction, density and correlation function can be calculated numerically. Figure ?? shows the density evolution for the initial state with two particles at  $\pm 1$ . Here, we see wave packets diffuse independently, then merge and diffuse coherently. Figure ?? is for system with repulsive interaction  $c = 5$  and Figure ?? is for attraction interaction with  $c = -5$ . However, we do not see much difference between them. Similar result is found when we calculate the density at the origin after the quench. Figure ?? compares the density evolution at  $z = 0$ , we see that the two lines overlap with each other. Figure ?? shows the relative density difference defined as  $\frac{\rho_{\text{repulsive}}(0,t) - \rho_{\text{attractive}}(0,t)}{\rho_{\text{attractive}}(0,t)}$ , and we see that the relative difference is around one percent. Our explanation is that the two wave packets have negligible overlap in the initial state. This remains true at the moment the interaction is turned on. As time goes on, the system probes the states with the same energy. Placing the two particles on top of each other will lower or raising the total energy of the system in attractive or repulsive systems, thus it is suppressed. That is to say that although bound states are preferred energetically in attractive models, their overlaps with the initial state is small. Thus the system will remain in such state for both situations where the two particle's wavefunction are almost orthogonal to each other such that the contact interaction does not affect the density greatly. Therefore, the density for attractive or repulsive particle at any time at any location is well approximated by that of the

free particle, which can be easily calculated from the wavefunction

$$f_{\text{free}}(y_1, y_2, t) = \frac{\sqrt{4\pi\sigma^2}}{(2\pi)^2} \frac{\pi}{i(t + \sigma^2/2i)} e^{\frac{i(y_1 - x_{10})^2 + i(y_2 - x_{20})^2}{4(t + \sigma^2/2i)}}$$

and

$$\rho_{\text{free}}(y, t) = \frac{4\pi\sigma^2}{(2\pi)^4} \frac{\pi^2}{t^2 + \sigma^4/4} \sqrt{\frac{4\pi(t^2 + \sigma^4/4)}{\sigma^2}} \left( e^{-\frac{\sigma^2(y-x_{10})^2}{4(t^2 + \sigma^4/4)}} + e^{-\frac{\sigma^2(y-x_{20})^2}{4(t^2 + \sigma^4/4)}} + 2\sqrt{\frac{2\pi(t^2 + \sigma^4/4)}{\sigma^2}} \Re \left( e^{-\frac{\sigma^2 \left( y - \frac{x_1 + x_2 + 2i(x_{10} - x_{20})t/\sigma^2}{2} \right)^2}{8(t^2 + \sigma^4/4)}} \right) e^{-\frac{(x_{10} - x_{20})^2}{2\sigma^2}} \right)$$

Since we have made the assumption that  $(x_{20} - x_{10}) \gg \sigma$ , we can drop the last term and obtain the simple gaussian dispersion for the density.

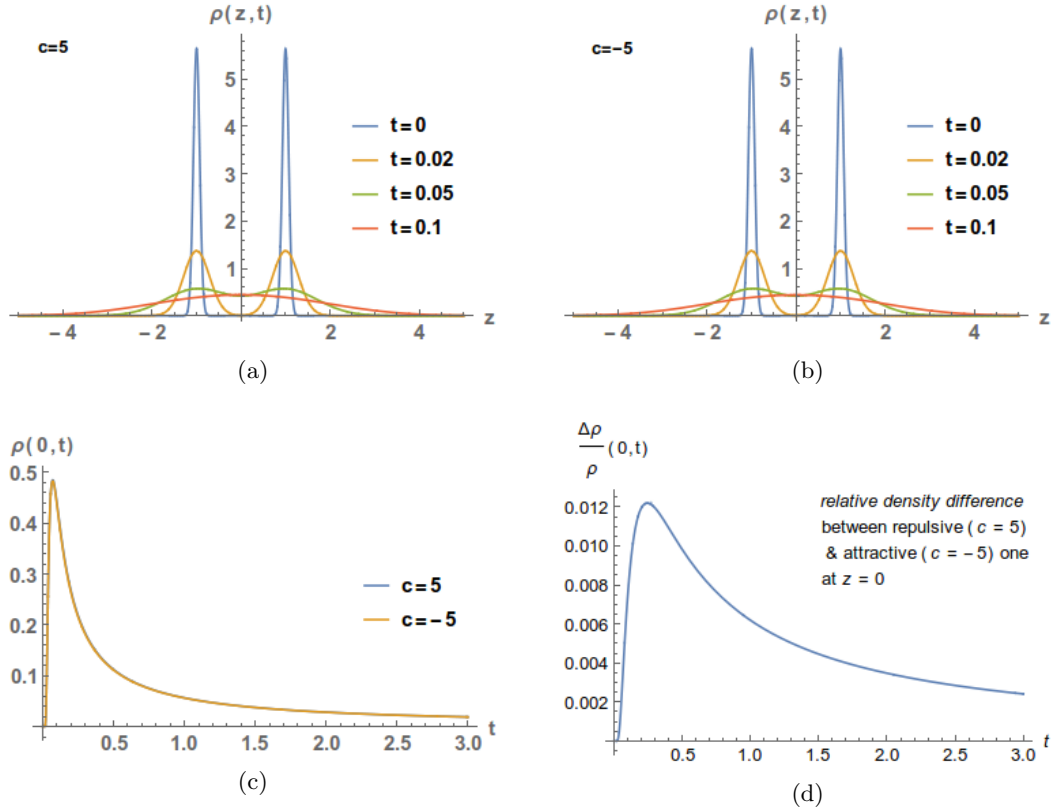


Figure 4.5: Density evolution for systems with two particles. Figure ?? describes repulsive case and Figure ?? describes attractive case. Figure ?? compares the density at the origin between  $c = 5$  and  $c = -5$  cases. Figure ?? shows the relative density difference.

In Figure (??), we compare the evolution of the normalized noise correlation for  $c = 5$ ,  $c = -5$  and  $c = 0$ . Here, the normalized noise correlation is defined as  $C(y_1, y_2, t) = \frac{\langle \rho(y_1)\rho(y_2) \rangle}{\langle \rho(y_1) \rangle \langle \rho(y_2) \rangle} - 1$ . This quantity describes how the density fluctuations at different sites are related to each other, i.e.  $C(y_1, y_2, t) = \frac{\langle (\rho(y_1) - \langle \rho(y_1) \rangle)(\rho(y_2) - \langle \rho(y_2) \rangle) \rangle}{\langle \rho(y_1) \rangle \langle \rho(y_2) \rangle}$ . Note this quantity varies for different normalization of the wavefunction. Here we should impose the constraint that the integration

over the density should be normalized to  $N - 1$ , instead of  $N$  with  $N$  being the total number of particles. Thus, the plots in the figure were obtained by rescaling the density operator by a factor of  $\frac{1}{2}$ . From these plots, we see oscillations in the vicinity of the origin. That's where the correlation begins to develop. Away from zero, we see the correlation stabilizes at 1, which does not mean they are maximally correlated due to interactions. As the correlation is between site  $y$  and  $-y$ , this phenomenon is simply a symmetry effect, since both the initial state and the Hamiltonian has reflection symmetry with respect to the origin. Comparing the four plots, we notice that the correlation first spreads out fast (from  $t = 0.02$  to  $t = 0.1$ ), then slow down (from  $t = 0.1$  to  $t = 0.5$ ), in the end, the speed stabilizes at fermi velocity. Compare the three cases in each plots, we see the oscillation spreads out in a roughly same manner irrespective of the sign of the interaction, though in the repulsive case, the correlation spreads our faster and in the attractive case, it expands slower. In Figure (b),(c),(d), the correlation at zero is clearly suppressed in interacting models than that of the free one. This suppression takes on its strength gradually with time which can be seen from the inset plots which show the detail of the correlation near the origin. In Figure (d), the correlation in the interacting systems is almost  $-1$  at the origin, which indicates that it is almost impossible to have two particles overlap. However, this is not a effect of the repulsive interaction. As the correlation  $C(0, 0, t)$  of a Bethe Ansatz eigenstate of a repulsive Hamiltonian is  $+1$  as we will show later. Instead, this indicates a wide span in the  $k$ -space while it has less fluctuation in the position basis due to the uncertainty principle. For the non-interacting case, the correlation function saturates to the famous Hanbury-Brown Twiss result, i.e  $C(y_1, y_2, t) = \cos(a(y_1, y_2)/t)$  [? ].

In the following part, we will show that, for a Bethe Ansatz eigenstate with no bound state, the magnitude of the correlation at the origin is not related to the sign or magnitude of the interaction. Instead, the slope of it is proportional to  $c$ . While for a state with bound states, the correlation when the two particles overlap goes to infinity with the system size and its magnitude drops exponentially fast with the separation in between.

Let's start with the correlation of a free state  $|k_1, k_2\rangle$  in a finite system of length  $L$ . Here the momentums  $k_1$  and  $k_2$  are real and they satisfy the Bethe equation

$$\begin{aligned} e^{ik_1 L} &= \frac{k_1 - k_2 + ic}{k_1 - k_2 - ic} \\ e^{ik_2 L} &= \frac{k_2 - k_1 + ic}{k_2 - k_1 - ic} \end{aligned}$$

Thus the two-point correlation equals

$$\begin{aligned} \langle \rho(x_1)\rho(x_2) \rangle_{x_1 < x_2} &= |e^{ik_1x_1+ik_2x_2} + \frac{k_1 - k_2 - ic}{k_1 - k_2 + ic} e^{ik_1x_2+ik_2x_1}|^2 \\ &= 2 + e^{i(k_1-k_2)(x_1-x_2)} \frac{k_1 - k_2 + ic}{k_1 - k_2 - ic} + e^{-i(k_1-k_2)(x_1-x_2)} \frac{k_1 - k_2 - ic}{k_1 - k_2 + ic} \end{aligned}$$

In the vicinity of the origin, we have

$$\begin{aligned} \lim_{x_2 \rightarrow x_1 \rightarrow 0} \langle \rho(x_1)\rho(x_2) \rangle &\approx 4 + i(k_1 - k_2)(x_1 - x_2) \left( \frac{k_1 - k_2 + ic}{k_1 - k_2 - ic} - \frac{k_1 - k_2 - ic}{k_1 - k_2 + ic} \right) \\ &\approx 4 - \frac{c(k_1 - k_2)^2(x_1 - x_2)}{(k_1 - k_2)^2 + c^2} \end{aligned}$$

The density can be calculated by integrating out one dummy coordinate, we get

$$\begin{aligned} \langle \rho(x) \rangle &= 2L + \frac{1 - e^{i(k_1-k_2)(-\frac{L}{2}-x_2)}}{i(k_1 - k_2)} \frac{k_1 - k_2 + ic}{k_1 - k_2 - ic} + \frac{e^{i(k_1-k_2)(x-\frac{L}{2})} - 1}{-i(k_1 - k_2)} \frac{k_1 - k_2 + ic}{k_1 - k_2 - ic} \\ &\quad + \frac{1 - e^{-i(k_1-k_2)(-\frac{L}{2}-x)}}{-i(k_1 - k_2)} \frac{k_1 - k_2 - ic}{k_1 - k_2 + ic} + \frac{e^{-i(k_1-k_2)(x-\frac{L}{2})} - 1}{i(k_1 - k_2)} \frac{k_1 - k_2 - ic}{k_1 - k_2 + ic} \\ &= 2L + \frac{1 - e^{i(k_1-k_2)(-\frac{L}{2}-x)}}{i(k_1 - k_2)} e^{ik_1L} + \frac{e^{i(k_1-k_2)(x-\frac{L}{2})} - 1}{-i(k_1 - k_2)} e^{ik_1L} \\ &\quad + \frac{1 - e^{-i(k_1-k_2)(-\frac{L}{2}-x)}}{-i(k_1 - k_2)} e^{ik_2L} + \frac{e^{-i(k_1-k_2)(x-\frac{L}{2})} - 1}{i(k_1 - k_2)} e^{ik_2L} \\ &= 2L + \frac{8c}{(k_1 - k_2)^2 + c^2} \end{aligned}$$

In the second and third line, we made use of the Bethe equation to simplify the expression and we get the density to be uniform as expected. The integration over the density returns  $L(2L + \frac{8c}{(k_1-k_2)^2+c^2})$ . Therefore, we need to renormalize the wavefunction by a factor of  $1/\sqrt{L(2L + \frac{8c}{(k_1-k_2)^2+c^2})}$ . Then we have

$$\langle \rho(x_1)\rho(x_2) \rangle = \frac{4 - \frac{c(k_1-k_2)^2(x_1-x_2)}{(k_1-k_2)^2+c^2}}{2L(L + \frac{4c}{(k_1-k_2)^2+c^2})}$$

and

$$\begin{aligned} C(x_1, x_2, t) &= \frac{\langle \rho(x_1)\rho(x_2) \rangle}{\rho(x_1)\rho(x_2)} - 1 \\ &= \frac{1}{2(L + \frac{4c}{(k_1-k_2)^2+c^2})} \left( 2L - \frac{8c}{(k_1 - k_2)^2 + c^2} - \frac{cL(k_1 - k_2)^2(x_1 - x_2)}{(k_1 - k_2)^2 + c^2} \right) \end{aligned}$$

From this expression, we can understand the behaviour of the normalized noise correlation function of a Bethe Ansatz eigenstate without bound states at the origin. For repulsive case, this quantity is less than one. For attractive case, it is greater than one. Moreover, we see that when the interaction is positive,  $\lim_{x_1 \rightarrow x_2^-} C(x_1, x_2, t) > 1$ , thus we see a dip at the origin, while attractive interaction will bring out a peak.

We can repeat the calculation for a bound state  $|k + ic/2, k - ic/2\rangle$ . This state satisfies the Bethe equation in the limit  $L \rightarrow \infty$ . However, the two-point correlation function and density suffer from divergence problems with  $k_1 - k_2 + ic = 0$ .

$$\langle \rho(x_1)\rho(x_2) \rangle = 2 + \lim_{k_1 \rightarrow k_2 - ic} e^{c|x_2 - x_1|} \frac{k_1 - k_2 + ic}{k_1 - k_2 - ic}$$

$$\langle \rho(x) \rangle = \lim_{k_1 \rightarrow k_2 - ic} \lim_{L \rightarrow \infty} 2L + \frac{8c}{(k_1 - k_2)^2 + c^2}$$

Rescale the wavefunction by a factor of  $\frac{1}{\sqrt{2L(L + \frac{8c}{(k_1 - k_2)^2 + c^2})}}$ , then the normalized noise correlation function becomes

$$C(x_1, x_2) = \lim_{L \rightarrow \infty} \frac{|c|L}{2} e^{-|c||x_1 - x_2|} - 1$$

which diverges with the system size. However, if we ignore the normalization we can tell that, for a bound state, the normalized noise correlation function blows up exponentially when the two particles approach each other.

To sum up, the normalized correlation function when the two particles overlap is greater than one for attractive particles and less than one for repulsive ones in a free state. The correlation decreases exponentially with the separation between the two particles in a bound state. In the vicinity of the origin, the correlation function shows a dip in a repulsive model and displays a peak in an attractive model. In Figure ??, we can see the peak and dip for the orange line and blue line clearly. However, the correlation at the origin is approaching  $-1$  as the system evolves. This indicates that the system spans a lot of eigenstates to avoid overlap between the two particles.

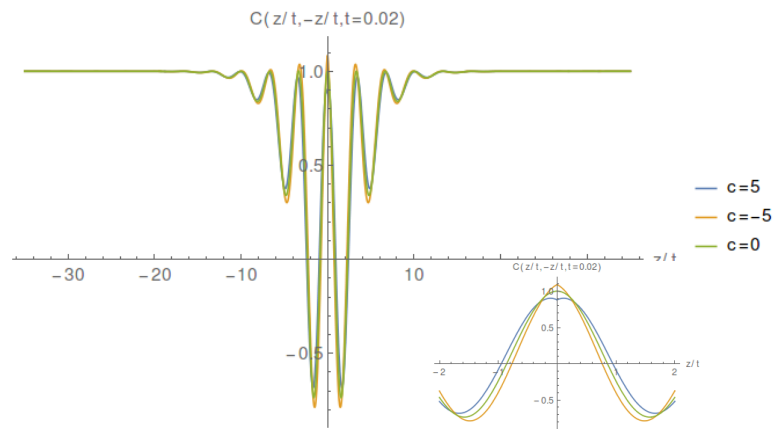
### Colliding Particles

We can also study the case where the two particles are moving towards each other, with speed  $k_0$  and  $-k_0$  respectively. Then the initial state becomes

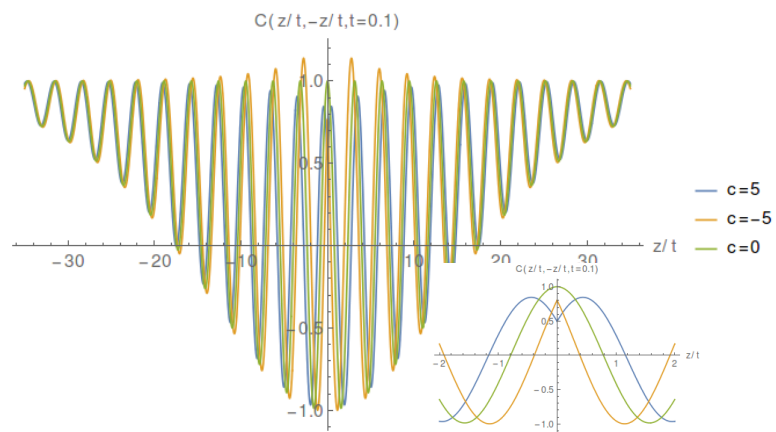
$$|\phi_0(k_0)\rangle = \frac{1}{\sqrt{\pi\sigma^2}} \int_{x_1, x_2} e^{-\frac{(x_1 - x_{10})^2}{2\sigma^2} - \frac{(x_2 - x_{20})^2}{2\sigma^2} + ik_0 x_{10} - ik_0 x_{20}} \Psi^\dagger(x_1) \Psi^\dagger(x_2) |0\rangle$$

This is interesting because the kinetic energy may be transformed into the potential energy. This enables the system to probe states with higher internal energy. (Think of a system with two balls connected with a spring in a classical picture). We suspect that this extra energy will lead to a 'bound' state in the repulsive model. This serves as our motivation of the following study. The procedure is the same as the case with static initial condition. The dropped term in  $(k_1, k_2 | \phi_0(k_0))$  is still of the order of  $O(e^{-\frac{(x_{20} - x_{10})^2}{2\sigma^2}})$ , therefore is negligible. And we get

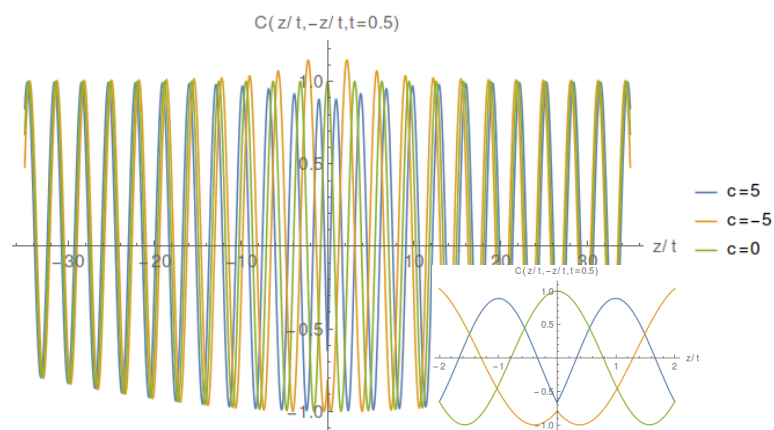
$$(k_1, k_2 | \phi_0(k_0)) = \sqrt{4\pi\sigma^2} e^{-i(k_1 - k_0)x_{10} - i(k_2 + k_0)x_{20} - \frac{(k_1 - k_{10})^2 \sigma^2}{2} - \frac{(k_2 - k_0)^2 \sigma^2}{2}}$$



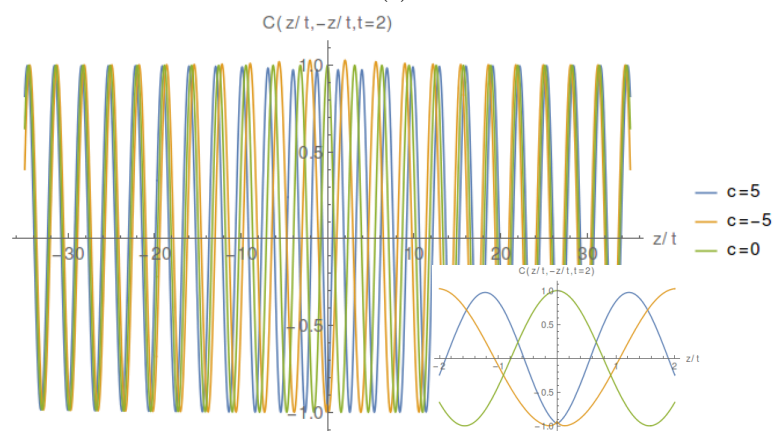
(a)



(b)



(c)



(d)

Figure 4.6: Normalized noise correlation for a two-particle system at  $t = 0.02$ (a),  $0.1$ (b),  $0.5$ (c) and  $2$ (d) respectively. Blue line is for repulsive case. Orange line is for attractive case. Green line depicts the free model.

and the time evolved state becomes

$$|\phi_t\rangle_{k_0} = \frac{\sqrt{4\pi\sigma^2}}{(2\pi)^2} \frac{\pi}{i(t + \sigma^2/2i)} e^{\frac{i(y_1 - x_{10})^2 + i(y_2 - x_{20})^2}{4(t + \sigma^2/2i)} + \frac{k_0\sigma^2(y_1 - y_2)}{2(t + \sigma^2/2i)} + \frac{ik_0(x_{10} - x_{20})t}{t + \sigma^2/2i} - \frac{k_0^2\sigma^2 t^2}{t + \sigma^2/2i}}$$

$$\left(1 - (1 + i)c\theta(y_1 - y_2)\sqrt{\pi(t + \sigma^2/2i)} \operatorname{erfc} \alpha' e^{\alpha'}\right)$$

with

$$\alpha' = \frac{(1 - i)(y_1 - x_{10} - y_2 + x_{20} - 2ik_0\sigma^2 + 2ic(t + \sigma^2/2i))}{4\sqrt{t + \sigma^2}}$$

As is clear from the above expression, the initial momentum modifies  $\alpha$  such that the effective interaction becomes  $c - \frac{k_0\sigma^2}{t + \sigma^2/2i}$ . When  $t$  is small, this reverses the sign of the repulsive interaction, making it more attractive. However, its effect fades away as the time goes on. In terms of the observable, we see that the two particles moves towards each other and merges more quickly, see Figure ???. However, as both attractive and repulsive models have negligible overlaps between the two wavepackets, (correlation function approaches  $-1$  quickly, indicating zero possibility for overlap between the two particles), the wavepackets still evolve as if isolated. However, compare to the static case, the correlation function spreads out slower even though the particle moves towards each other. Since, this is true for the free particles also, we consider this a trivial effect of the initial momentum. The two particles pass each other at  $t = 0.1$  and moves away faster, making the correlation between them built up slower.

This completes our discussion of the two particle situation. In the following, we will study the case with more particles. No exact solution is available, we will focus on the long time limit only.

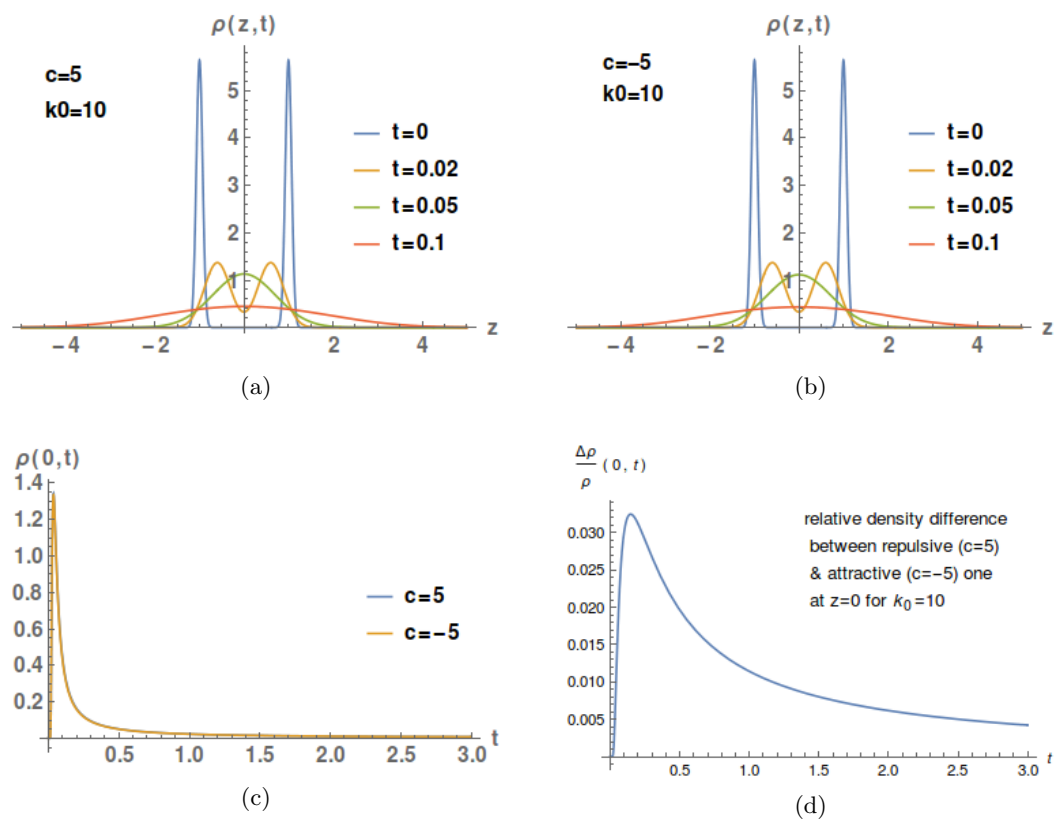


Figure 4.7: Density evolution for two particles moving towards each other. Figure?? is for repulsive case. Figure ?? is for attractive case. Figure ?? compares the density at the origin between  $c = 5$  and  $c = -5$  cases. Figure ?? shows the relative density difference at the origin.

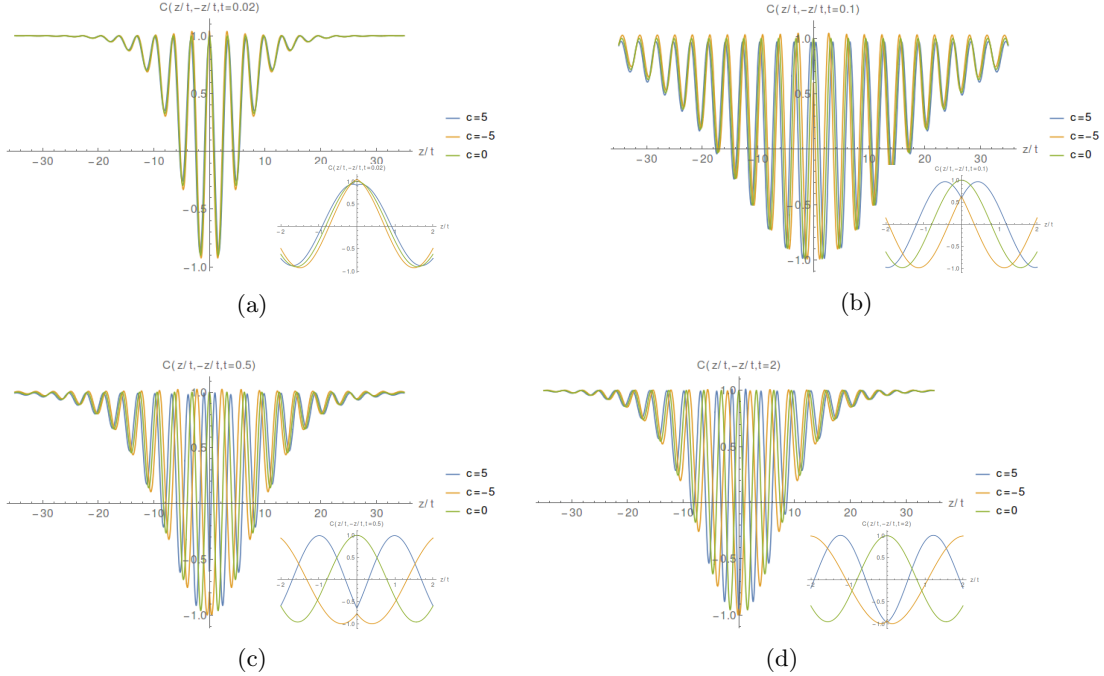


Figure 4.8: Normalized noise correlation for a system with two particles moving towards each other with  $k_0 = \pm 10$ . Various figures show results for different times,  $t = 0.02$ (a),  $0.1$ (b),  $0.5$ (c) and  $2$ (d) respectively. Blue line is for repulsive case. Orange line is for attractive case. Green line works for free model.

### 4.3 Multiparticle Dynamics in Asymptotic Limit

In this section, we will study systems with more than two particles. We will study the time evolution of a static initial state defined by

$$|\phi_0\rangle_N = \frac{1}{(\pi\sigma^2)^{\frac{N}{4}}} \int_x e^{-\sum_{i=1}^N \frac{(x_i - \bar{x}_i)^2}{2\sigma^2}} \prod_{i=1}^N \Psi^\dagger(x_i) |0\rangle$$

which describes  $N$  wave packets localized at  $x_1, x_2, \dots, x_N$  respectively. To simplify the calculation, we will further assume that the particles are evenly spaced, with the separation  $a \gg \sigma$ .

The time evolved state can be written down directly using the Yudson representation

$$|\Psi_t\rangle_N = \frac{1}{(\pi\sigma)^{\frac{N}{4}} (2\pi)^N} \int_x e^{-\sum_i \frac{(x_i - \bar{x}_i)^2}{2\sigma^2}} e^{-i\sum_i k_i^2 t + i\sum_i k_i (y_{P^{-1}i} - x_i)} A_k(P) \theta(y) |y\rangle \quad (4.6)$$

with

$$A_k(P) = \prod_{\substack{i < j \\ P^{-1}i > P^{-1}j}} S_{ij}(k_i - k_j)$$

Like in the two-particle case, we have dropped terms of the order  $O(e^{-\frac{a^2}{2\sigma^2}})$  to avoid complications from the tail of the wave packets. The integration over the  $k$ 's involves integrations over some rational function of the error function, when the number of variables exceeds two. This

integral which is very hard, if possible, to carry out. Thus, we will not try to obtain the explicit expression of the wavefunction. Instead, we will focus on the long time limit directly. This can be done in two ways. In method 1, we will obtain saddle point approximated wavefunction and then calculate observables. As another method, we will use explicit expressions of local observables found in literature and take the long time limit from there. We will talk about difficulties encountered in this method.

### 4.3.1 Wavefunction Approach

Now, we will study the asymptotic behaviour of the wavefunction (??). The saddle point of the integrand are located as  $k_i = \frac{y_{P^{-1}i} - x_i}{2t}$ . For a repulsive systems, these points lie on the integration contour. While for attractive case, whose contour is separated in the imaginary direction, one needs to shift the contour to the real axis and include the contributions from the the poles encountered.

#### Repulsive Case

Thus the wavefunction for  $c > 0$  can be approximated as

$$\begin{aligned}
|\Psi_t\rangle_N &= \frac{1}{(\pi\sigma^2)^{N/4}} \frac{1}{(2\pi)^N} \left(\frac{\pi}{it}\right)^{N/2} \int_{x,y} e^{-\sum_i \frac{(x_i - \bar{x}_i)^2}{2\sigma^2} + i \frac{(y_{P^{-1}i} - x_i)^2}{4t}} A_{k_i = \frac{y_{P^{-1}i} - x_i}{2t}}(P)\theta(y)|y\rangle \\
&\approx \frac{1}{(\pi\sigma^2)^{N/4}} \frac{1}{(2\pi)^N} \left(\frac{\pi}{it}\right)^{N/2} (2t)^N \int_{x,\xi} e^{\sum_i -\frac{(x_i - \bar{x}_i)^2}{2\sigma^2} - it\xi_i^2 - i\xi_{P^{-1}i} x_i} A_{k_i = \xi_{P^{-1}i}}(P)\theta(\xi)|2t\xi\rangle \\
&= \frac{t^{N/2}}{\pi^{3N/4}\sigma^{N/2}i^{N/2}} \int_{x,\xi} e^{\sum_i -\frac{(x_i - \bar{x}_i)^2}{2\sigma^2} - i\xi_i^2 t - i\xi_{P^{-1}i} \bar{x}_i} A_{k_i = \xi_{P^{-1}i}}(P)\theta(\xi)|2t\xi\rangle \quad (4.7)
\end{aligned}$$

In the second line, we have dropped terms of the order  $O(\frac{x_i}{t})$  for large  $t$ . Based on this expression, we can calculate local observables, i.e. density and two-point correlation function. One needs to be careful when carry out the overlap between a bra and ket state. As  $\langle 2t\xi' | 2t\xi \rangle \theta(\xi')\theta(\xi) = \prod_i \delta(2t\xi'_i - 2t\xi_i)\theta(\xi) = \frac{1}{(2t)^N} \prod_i \delta(\xi'_i - \xi_i)\theta(\xi)$ . With this in mind, it's easy to derive the density as

$$\begin{aligned}
\rho(z) &= \frac{1}{2^{N+1}t\pi^{3N/2}\sigma^N} \sum_{P,P'} \int_{x,x',\xi} e^{\sum_i -\frac{(x_i - \bar{x}_i)^2}{2\sigma^2} - \frac{(x'_i - \bar{x}_i)^2}{2\sigma^2} - i\xi_i(x_{P_i} - x'_{P'_i})} A_{k_i = \xi_{P^{-1}i}}^*(P') A_{k_i = \xi_{P_i}}(P) \\
&\quad \sum_i \delta(\xi_i - z/2t)\theta(\xi_i)
\end{aligned}$$

Here

$$\begin{aligned}
A_{k_i=\xi_{P^{1'}i}}^*(P') A_{k_i=\xi_{P^1i}}(P) &= \frac{\prod_{\substack{i<j \\ P^1i>P^1j}} S_{ij}(\xi_{P^1i} - \xi_{P^1j})}{\prod_{\substack{i<j \\ P^{1'}i>P^{1'}j}} S_{ij}(\xi_{P^{1'}i} - \xi_{P^{1'}j})} \\
&= \frac{\prod_{\substack{i<j \\ P^{1'}i>P^{1'}j}} S_{ij}(\xi_i - \xi_j)}{\prod_{\substack{i<j \\ P^1i>P^1j}} S_{ij}(\xi_i - \xi_j)} \\
&= \frac{\prod_{\substack{i<j \\ P^{1'}i>P^{1'}j \\ P^1i<P^1j}} S_{ij}(\xi_i - \xi_j)}{\prod_{\substack{i<j \\ P^1i>P^1j \\ P^{1'}i<P^{1'}j}} S_{ij}(\xi_i - \xi_j)} \\
&= \prod_{\substack{i<j \\ P^{1'}i>P^{1'}j \\ P^1i<P^1j}} S_{ij}(\xi_i - \xi_j) \prod_{\substack{i>j \\ P^1i<P^1j \\ P^{1'}i>P^{1'}j}} S_{ij}(\xi_i - \xi_j) \\
&= \prod_{\substack{P'i>P'j \\ Pi<Pj}} S_{ij}(\xi_i - \xi_j) \\
&= \prod_{\substack{i<j \\ P'P^1i>P'P^1j}} S_{ij}(\xi_{P^1i} - \xi_{P^1j})
\end{aligned}$$

Thus

$$\begin{aligned}
\rho(z) &= \frac{1}{2^{N+1} t \pi^{3N/2} \sigma^N} \sum_{P, P'} \int_{x, x', \xi} e^{\sum_i -\frac{(x_i - \bar{x}_i)^2}{2\sigma^2} - \frac{(x'_i - \bar{x}_i)^2}{2\sigma^2} - i\xi_{P^1i}(x_i - x'_{P^1i})} \prod_{\substack{i<j \\ P'P^1i>P'P^1j}} S_{ij}(\xi_{P^1i} - \xi_{P^1j}) \\
&\quad \sum_i \delta(\xi_i - z/2t) \theta(\xi_i) \\
&= \frac{1}{2^{N+1} t \pi^{3N/2} \sigma^N} \sum_{Q=P'P^1} \int_{x, x', \xi} e^{\sum_i -\frac{(x_i - \bar{x}_i)^2}{2\sigma^2} - \frac{(x'_i - \bar{x}_i)^2}{2\sigma^2} - i\xi_i(x_i - x'_{Qi})} \prod_{\substack{i<j \\ Qi>Qj}} S_{ij}(\xi_i - \xi_j) \\
&\quad \sum_i \delta(\xi_i - z/2t) \sum_P \theta(\xi_{Pi}) \\
&= \frac{1}{2^{N+1} t \pi^{3N/2} \sigma^N} \sum_Q \int_{x, x', \xi} e^{\sum_i -\frac{(x_i - \bar{x}_i)^2}{2\sigma^2} - \frac{(x'_i - \bar{x}_i)^2}{2\sigma^2} - i\xi_i(x_i - x'_{Qi})} \prod_{\substack{i<j \\ Qi>Qj}} \frac{\xi_i - \xi_j - ic}{\xi_i - \xi_j + ic} \\
&\quad \sum_i \delta(\xi_i - z/2t)
\end{aligned}$$

Similarly, one can write down the two point correlation function as

$$\begin{aligned}
\rho_2(z, z') &= \frac{1}{2^{N+2} t^2 \pi^{3N/2} \sigma^N} \sum_Q \int_{x, x', \xi} e^{\sum_i -\frac{(x_i - \bar{x}_i)^2}{2\sigma^2} - \frac{(x'_i - \bar{x}_i)^2}{2\sigma^2} - i\xi_i(x_i - x'_{Qi})} \prod_{\substack{i<j \\ Qi>Qj}} \frac{\xi_i - \xi_j - ic}{\xi_i - \xi_j + ic} \\
&\quad \sum_{i,j} \delta(\xi_i - z/2t) \delta(\xi_j - z'/2t)
\end{aligned}$$

Among the  $N!$  terms corresponding to different permutations, most of the terms are small by the order of  $O(e^{-ca})$  for moderate interaction strength and inter-particle spacing, as we are going to show here.

Let's look at the integration of  $\xi_i$ ,

$$\int dx \int dx' e^{-\frac{(x_i - \bar{x}_i)^2}{2\sigma^2} - \frac{(x'_i - \bar{x}_i)^2}{2\sigma^2}} \int d\xi_i e^{i\xi_i(x'_{Q_i} - x_i)} \prod_{\substack{i < m \\ Q_i > Q_m}} \frac{\xi_i - \xi_m - ic}{\xi_i - \xi_m + ic} \prod_{\substack{i > n \\ Q_i < Q_n}} \frac{\xi_i - \xi_n + ic}{\xi_i - \xi_n - ic}$$

Assume that  $i(j)$  is the smallest(largest) index that get changed by  $Q$ . For  $\xi_i$ , all the poles lie in the lower half plane. Therefore, the integral will vanish if  $x'_{Q_i} > x_i$ . Thus, the integration over  $\xi_i$  contributes a factor of  $\theta(x_i - x'_{Q_i})$ . At the same time, we have  $Q_i > i$ . As we have shown on page ??, this will leads to a term of the order of  $O(e^{-\frac{(x_{Q_i} - x_i)^2}{4\sigma^2}})$ . Thus is negligible. Similarly, the integration over  $\xi_j$  will also yields a small term. For the density, the only term that is not small corresponds to  $Q = \mathbb{1}$ . Therefore, the density becomes

$$\begin{aligned} \rho(z) &= \frac{1}{2^{N+1} t \pi^{3N/2} \sigma^N} \int_{x, x', \xi} e^{\sum_i -\frac{(x_i - \bar{x}_i)^2}{2\sigma^2} - \frac{(x'_i - \bar{x}_i)^2}{2\sigma^2}} \\ &\quad \sum_i \delta(\xi_i - z/2t) \\ &= \frac{\sigma^N}{2t \pi^{N/2}} \int_{\xi} e^{-\sum_i \sigma^2 \xi_i^2} \sum_i \delta(\xi_i - z/2t) \\ &= \frac{\sigma N}{2t \sqrt{\pi}} e^{-\frac{\sigma^2 z^2}{4t^2}} \end{aligned}$$

For the two-point correlation function, when  $Q \neq \mathbb{1}$ , the dominant terms corresponds to the situation when both  $i$  and  $j$  are not integrated over. Then we have

$$\begin{aligned} \rho_2(z, z') &= \frac{1}{2^{N+2} t^2 \pi^{3N/2} \sigma^N} \sum_Q \int_{x, x', \xi} e^{\sum_m -\frac{(x_m - \bar{x}_m)^2}{2\sigma^2} - \frac{(x'_m - \bar{x}_m)^2}{2\sigma^2} - i \sum \xi_m (x_m - x'_{Q_m})} \\ &\quad \prod_{i \leq m < n \leq j} \frac{\xi_m - \xi_n - ic}{\xi_m - \xi_n + ic} \delta(\xi_i - z/2t) \delta(\xi_j - z'/2t) + (z \leftrightarrow z') \end{aligned}$$

For any  $m$  between  $i$  and  $j$ , if  $m \neq Q_m$ , the integration contour of  $\xi_m$  can be closed in the upper half plane or lower half plane depending on the sign of  $x_m - x'_{Q_m}$ . When  $x_m > x'_{Q_m}$ , the integral will pick up some pole in the lower half plane at  $z/2t - inC$  or  $z'/2t - inC$  with  $n$  being some integer. However, this will leads to a factor of  $e^{-nc(x_m - x'_{Q_m})}$  which is of the order  $O(e^{-ac})$ . Same for the case  $x_m < x'_{Q_m}$ . Therefore, when the product of the interparticle spacing and interaction is moderate, we can neglect this term and only keep the case when  $Q$  swap  $i$  and  $j$

only. Therefore, we have

$$\begin{aligned}
& \rho_2(z, z') \\
&= \frac{1}{2^{N+2} t^2 \pi^{3N/2} \sigma^N} \int_{x, x', \xi} e^{\sum_m -\frac{(x_m - \bar{x}_m)^2}{2\sigma^2} - \frac{(x'_m - \bar{x}_m)^2}{2\sigma^2} - \sum_{m \neq i, j} i \xi_m (x_m - x'_m)} \left( 1 + \sum_{i < j} e^{-i \xi_i (x_i - x'_j)} \right. \\
& \quad \left. e^{-i \xi_j (x_j - x'_i)} \prod_{i \leq m \leq j} \frac{\xi_i - \xi_m - ic}{\xi_i - \xi_m + ic} \frac{\xi_m - \xi_j - ic}{\xi_m - \xi_j + ic} \right) \delta(\xi_i - z/2t) \delta(\xi_j - z'/2t) + (z \leftrightarrow z') \\
&= \frac{\sigma^N}{4t^2 \pi^{N/2}} \sum_{i < j} \int_{\xi} e^{-\sum_m \xi_m^2 \sigma^2} \left( 1 + e^{i(\xi_i - \xi_j)(\bar{x}_i - \bar{x}_j)} \prod_{i \leq m \leq j} \frac{\xi_i - \xi_m - ic}{\xi_i - \xi_m + ic} \frac{\xi_m - \xi_j - ic}{\xi_m - \xi_j + ic} \right) \delta(\xi_i - z/2t) \\
& \quad \delta(\xi_j - z'/2t) + (z \leftrightarrow z')
\end{aligned}$$

Now the integration over  $\xi_m$  is disentangled and is easy to carry out.

$$\begin{aligned}
I_{\xi_m} &= \int d\xi_m e^{-\sigma^2 \xi_m^2} \frac{\xi_i - \xi_m - ic}{\xi_i - \xi_m + ic} \frac{\xi_m - \xi_j - ic}{\xi_m - \xi_j + ic} \\
&= \int d\xi_m e^{-\sigma^2 \xi_m^2} \left( 1 + \frac{\xi_i - \xi_j}{\xi_i - \xi_j + 2ic} \left( \frac{2ic}{\xi_m - \xi_i - ic} - \frac{2ic}{\xi_m - \xi_j + ic} \right) \right)
\end{aligned}$$

Using the same trick as the one we have used on page ??, one can bring the fraction into a exponent by introducing an integral over new variable  $\lambda$ . By integrating over  $\xi_m$  first and then  $\lambda$ , one obtain the following result

$$I_{\xi_m} = \frac{\sqrt{\pi}}{\sigma} \left( 1 - 2\sqrt{\pi} \sigma c \frac{\xi_i - \xi_j}{\xi_i - \xi_j + 2ic} (\operatorname{erfc}((i\xi_j + c)\sigma) e^{-(\xi_j - ic)^2 \sigma^2} + \operatorname{erfc}((-i\xi_i + c)\sigma) e^{-(\xi_i + ic)^2 \sigma^2}) \right)$$

Define  $g_{zz'}$  as the terms in the parenthesis, i.e.

$$g_{zz'} = 1 - 2\sqrt{\pi} \sigma c \frac{z_i - z_j}{z_i - z_j + 2itc} (\operatorname{erfc}((iz_j/2t + c)\sigma) e^{-(z_j/2t - ic)^2 \sigma^2} + \operatorname{erfc}((-iz_i/2t + c)\sigma) e^{-(z_i/2t + ic)^2 \sigma^2})$$

Then the two point correlation function can be calculated as

$$\begin{aligned}
\rho_2(z, z') &= \frac{\sigma^2}{4t^2 \pi} e^{-\frac{\sigma^2 z^2}{4t^2} - \frac{\sigma^2 z'^2}{4t^2}} \left( \frac{N(N-1)}{2} + \sum_{i < j} e^{\frac{i(z-z')(\bar{x}_i - \bar{x}_j)}{2t}} \frac{z - z' - 2itc}{z - z' + 2itc} g_{zz'}^{j-i} \right) + (z \leftrightarrow z') \\
& \quad + O(e^{-ca}) \\
&= \frac{\sigma^2}{4t^2 \pi} e^{-\frac{\sigma^2 z^2}{4t^2} - \frac{\sigma^2 z'^2}{4t^2}} \left( \frac{N(N-1)}{2} + \sum_{n=0}^{N-2} (N-1-n) e^{\frac{-i(n+1)a(z-z')}{2t}} \frac{z - z' - 2itc}{z - z' + 2itc} g_{zz'}^n \right) \\
& \quad + (z \leftrightarrow z') + O(e^{-ca}) \\
&= \frac{\sigma^2}{4t^2 \pi} e^{-\frac{\sigma^2 z^2}{4t^2} - \frac{\sigma^2 z'^2}{4t^2}} \left( N(N-1) + 2\Re \left( e^{\frac{-ia(z-z')}{2t}} \frac{N(1 - e^{\frac{-ia(z-z')}{2t}} g_{zz'}) - 1 + e^{\frac{-ia(z-z')N}{2t}} g_{zz'}^N}{(1 - e^{\frac{-ia(z-z')}{2t}} g_{zz'})^2} \right. \right. \\
& \quad \left. \left. \frac{z - z' - 2itc}{z - z' + 2itc} \right) \right) + O(e^{-ca}) \tag{4.8}
\end{aligned}$$

In the second line, we have used the assumption that the particles are evenly spaced with separation  $a$ . In the last line, we simplify the expression by the following relation

$$\sum_{n=0}^{N-2} (N-1-n) q^n = \frac{N(1-q) - 1 + q^N}{(1-q)^2}$$

Expand the term  $e^{-\frac{ia(z-z')}{2t}} g_{zz'}$  around the point  $z = z'$ , we have

$$e^{-\frac{ia(z-z')}{2t}} g_{zz'} = 1 + f_1(z - z') + f_2(z - z')^2$$

Here  $f_1$  and  $2f_2$  are the first and second derivatives at the  $z = z'$  respectively. Plug it into  $\rho_2(z, z')$ , we obtain the leading order of the correlation function as

$$\begin{aligned} \lim_{z \rightarrow z'} \rho_2(z, z') &= \frac{\sigma^2}{4t^2\pi} e^{-\frac{\sigma^2 z^2}{4t^2} - \frac{\sigma^2 z'^2}{4t^2}} (N(N-1) + 2\Re \left( \frac{N(-f_1(z-z') - f_2(z-z')^2) - 1}{f_1^2(z-z')^2} \right. \\ &\quad \left. + \frac{(1 + f_1(z-z') + f_2(z-z')^2)^N}{f_1^2(z-z')^2} \right) \\ &= 0 \end{aligned}$$

Here, we have obtain the same result as the two-particle case, i.e. it is impossible to have two particles on top of each other. We can also calculate the normalized noise correlation function  $C_2(z, z') = \frac{\rho(z, z')}{\rho(z)\rho(z')} - 1$  introduced on page ???. Again, there is some ambiguity about the normalization. Here, we set the normalization such that density be normalized to  $N - 1$ . This is a weird choice and we will explain it now.

If we set the interaction to be zero, then the noise correlation function will only have the first term in the parenthesis of equation ?? and the density will be simply  $\rho(z) = \frac{N\sigma}{2t\sqrt{\pi}} e^{-\frac{\sigma^2 z^2}{4t^2}}$ . If we do not change the normalization, then the noise correlation will becomes  $C_2(z, z') = \frac{N(N-1)}{N^2} - 1 = -\frac{1}{N}$ . Since this quantity describes how fluctuation of density at different sites are correlated with each, it should vanish when the particles do not interaction with each other. Therefore, we need to rescale the density and two point correlation function by a factor of  $\frac{N-1}{N}$  so that  $C_2(z, z')$  vanishes with  $c = 0$ . In this case, the integral over density will yield  $N - 1$ , instead of  $N$ . With this normalization, it's easy to write down the normalized noise correlation function for an interacting system.

$$\begin{aligned} C_2(z, z') &= \frac{2}{N(N-1)} \Re \left( e^{-\frac{ia(z-z')}{2t}} \frac{N(1 - e^{-\frac{ia(z-z')}{2t}} g_{zz'}) - 1 + e^{-\frac{ia(z-z')N}{2t}} g_{zz'}^N}{(1 - e^{-\frac{ia(z-z')}{2t}} g_{zz'})^2} \frac{z - z' - 2itc}{z - z' + 2itc} \right) \\ g_{zz'} &= 1 - 2\sqrt{\pi}\sigma c \frac{z_i - z_j}{z_i - z_j + 2itc} (\operatorname{erfc}((iz_j/2t + c)\sigma) e^{-(z_j/2t - ic)^2 \sigma^2} + \operatorname{erfc}((-iz_i/2t + c)\sigma) \\ &\quad e^{-(z_i/2t + ic)^2 \sigma^2}) \end{aligned}$$

Plot ?? shows the result for  $N = 3$  and  $N = 5$  at large time. Note, the noise function is only a function of  $z/t$  and  $z'/t$ . It has no explicit dependence on the time. In the plot, we see periodic behaviour between  $-1$  and  $1$ . And the overall trend is the same between  $N = 3$  and  $N = 5$ . However, we see "interference fringes" that depends on the number of particles. To be

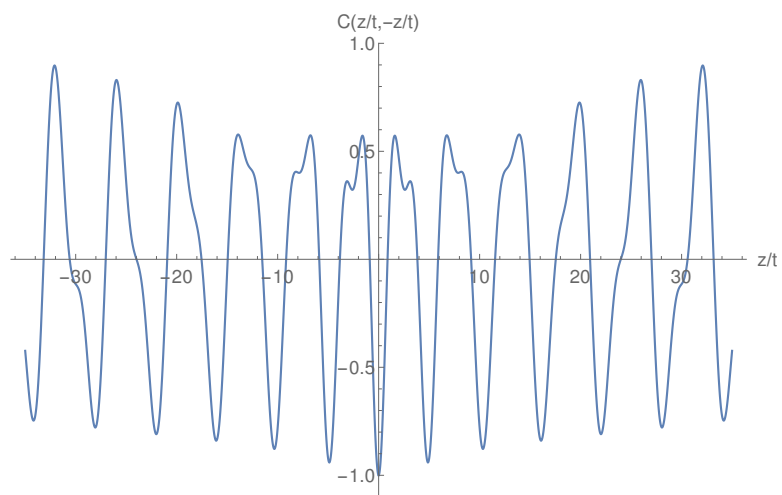
specific, the number of the fringes equals  $N - 1$ . This feature, however, is not an effect of the interaction. As shown in [? ], for a cloud of freely expanding bosonic particle, the normalised noise correlation equals<sup>1</sup>

$$\begin{aligned} C_2^{free}(t) &= 1 + \frac{1}{N^2} \sum_{k,l=1}^N e^{\frac{i(z-z')(k-l)a}{t}} + O\left(\frac{1}{N}\right) \\ &= \frac{N(\cos((z-z')a/t) - 1) + 1 - \cos(N(z-z')a/t)}{N(N-1)(1 - \cos((z-z')a/t))} + O\left(\frac{1}{N}\right) \end{aligned}$$

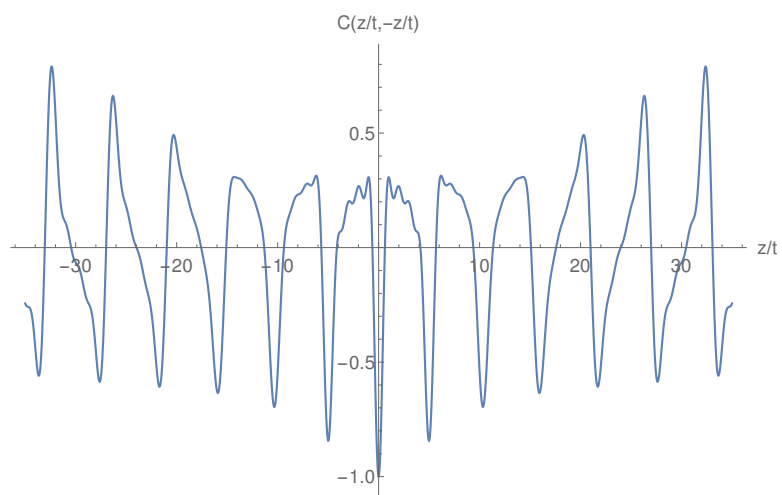
which agrees with our result of  $C_2(z, z')$  after setting  $c$  to be zero. From the above result, we see oscillation in the normalized noise function with frequency  $\frac{2\pi t}{aN}$  and the envelop of its maximum and minimum has a beat frequency of  $\frac{2\pi t}{a}$  as we have seen in the Figure ??.

---

<sup>1</sup>The second line of the expression differs from the result in [? ] by a term of the order  $\frac{1}{N}$



(a)



(b)

Figure 4.9: Normalised noise correlation function in the large time limit. Figure ?? describes a system with 3 particles. Figure ?? describes a 5-particle system.

### Attractive Case

For an attractive Lieb-Liniger model, the integration contours spread out in the imaginary direction. To make the saddle point approximation, whose stationary phase is located at  $k_i = \frac{y_{P^1_i} - x_i}{2t}$ , one needs to shift all contours to the real axis, and pick up pole contributions encountered. As an illustration, we will discuss how to shift an integration contour from the positive imaginary direction to the real axis with a pole in between. Figure ?? shows the original integral we want to carry out. Figure ?? displays a region enclosed by the chosen contour which is analytic everywhere. Therefore, the integration over the closed contour vanishes, i.e.  $\int_{C_1} + \int_{C_2} + \int_{C'_2} + \int_{C_{real}} = 0$ . In the time evolution of the Lieb-Liniger model, integrations over  $C_2$  and  $C'_2$  also vanish due to the factor  $e^{-ik_i^2(t+\sigma^2/2i)} = e^{-ik_i^2 t - \sigma^2 k_i^2/2}$  in the wavefunction for  $|\Re(k_i)| \rightarrow \infty$ . Therefore, the original integration transforms into an integration over the real line and a closed contours encircling the pole. The latter are proportional to the residue at the pole (See Figure ??). As the pole in the Lieb-Liniger model takes the form  $k_i = k_j - ic$ , this corresponds to a 2-string as discussed in page ?? . For a 3-particle system, we again shift all contours to the real axis. Besides the 2-string's, we can also get contributions related to a 3-string. This happens if the integration over  $k_1$  catches the pole at  $k_2 - ic$  while that of  $k_3$  catches the pole at  $k_2 + ic$ . Therefore, after shifting the contours, we will get terms corresponding to all possible string contributions, see Figure ?? . Note, in this figure, we have shifted the integration contour such that the  $k$ 's are symmetric with respect to the real axis. This is essentially the same as shifting all contours to the real axis.

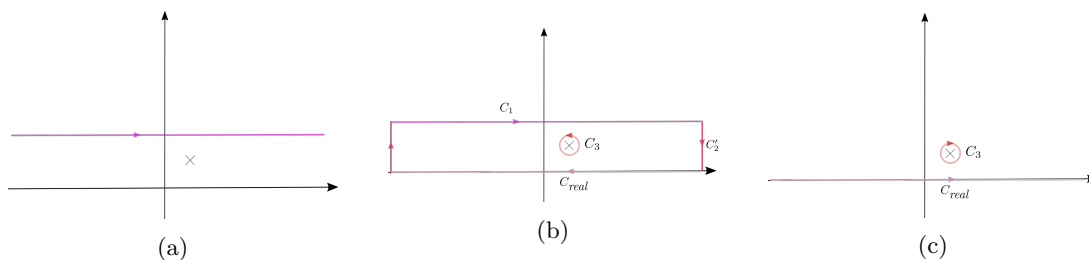


Figure 4.10: Illustration of shifting contours across a pole

Mathematically, the shift of contours described in Figure ?? can be translated into the

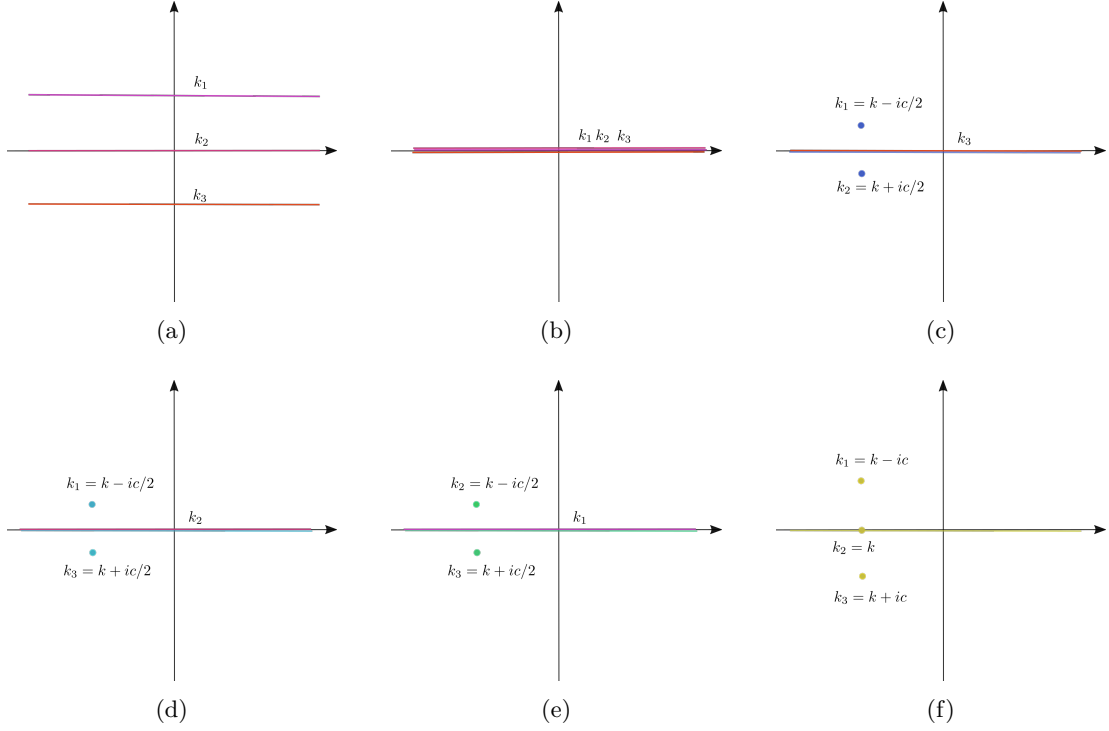


Figure 4.11: Illustration of shifting integration contours in a 3-particle system . Figure ?? represents the original integral. Contours in Figure ?? go through the saddle points. The rest corresponds to pole contributions related to different string configurations.

following relation.

$$\begin{aligned}
& \int_{C_1} dk_1 \int_{C_2} dk_2 \int_{C_3} dk_3 f(k_1, k_2, k_3) \\
&= \int dk_1 \int dk_2 \int dk_3 f(k_1, k_2, k_3) - 2\pi i \int dk_2 \int dk_3 \text{Res}(f(k_1, k_2, k_3), k_1 = k_2 - ic) \\
&- 2\pi i \int dk_2 \int dk_3 \text{Res}(f(k_1, k_2, k_3), k_1 = k_3 - ic) - 2\pi i \int dk_1 \int dk_3 \text{Res}(f(k_1, k_2, k_3), k_2 = k_3 - ic) \\
&+ (2\pi i)^2 \int dk_2 \text{Res}(\text{Res}(f(k_1, k_2, k_3), k_1 = k_2 - ic), k_3 = k_2 + ic) \tag{4.9}
\end{aligned}$$

Now, as all independent variables are integrated along the real axis, we can carry out the saddle point approximation directly. This is easier if we write the wavefunction as

$$\begin{aligned}
& f(k_1, k_2, k_3) \\
&= e^{-i \sum_i k_i^2 t + ik_i(y_i - x_i)} \frac{k_1 - k_2 - ic \text{Sgn}(y_1 - y_2)}{k_1 - k_2 + ic} \frac{k_1 - k_3 - ic \text{Sgn}(y_1 - y_3)}{k_1 - k_3 + ic} \frac{k_2 - k_3 - ic \text{Sgn}(y_2 - y_3)}{k_2 - k_3 + ic}
\end{aligned}$$

Then, we have

$$\begin{aligned}
& \text{Res}(f(k_1, k_2, k_3), k_1 = k_2 - ic) \\
&= e^{-2ik_2^2(t + \sigma^2/2i) + ik_2(y_1 - x_1 + y_2 - x_2 + 2ic(t + \sigma^2/2i)) + ic^2(t + \sigma^2/2i) - c(y_1 - x_1) - ik_3^2(t + \sigma^2/2i) + ik_3(y_3 - x_3)} (-2ic) \\
&\theta(y_1 - y_2) \frac{k_2 - k_3 - 2ic\theta(y_1 - y_3)}{k_2 - k_3} \frac{k_1 - k_3 - ic \text{Sgn}(y_2 - y_3)}{k_2 - k_3 + ic}
\end{aligned}$$

The saddle points are

$$k_2 = \frac{y_1 - x_1 + y_2 - x_2 + 2ic(t + \sigma^2/2i)}{4i(t + \sigma^2/2i)}$$

$$k_3 = \frac{y_3 - x_3}{2i(t + \sigma^2/2i)}$$

Thus, the second term in equation (??) can be approximated as

$$\sqrt{\frac{\pi}{i(t + \sigma^2/2i)}} \sqrt{\frac{\pi}{2\pi(t + \sigma^2/2i)}} (\text{Res}(f(k_1, k_2, k_3), k_1 = k_2 - ic))_{k_2 = \frac{y_1 - x_1 + y_2 - x_2}{4i(t + \sigma^2/2i)} + ic/2, k_3 = \frac{y_3 - x_3}{2i(t + \sigma^2/2i)}}$$

And the original integration becomes

$$\begin{aligned} & \int_{C_1} dk_1 \int_{C_2} dk_2 \int_{C_3} dk_3 f(k_1, k_2, k_3) \\ = & \left( \sqrt{\frac{\pi}{i(t + \sigma^2)}} \right)^3 f(k_1, k_2, k_3)_{k_1 = \frac{y_1 - x_1}{2i(t + \sigma^2/2i)}, k_2 = \frac{y_2 - x_2}{2i(t + \sigma^2/2i)}, k_3 = \frac{y_3 - x_3}{2i(t + \sigma^2)}} \\ & - (2\pi i) \sqrt{\frac{\pi}{i(t + \sigma^2/2i)}} \sqrt{\frac{\pi}{2i(t + \sigma^2/2i)}} \text{Res}(f(k_1, k_2, k_3), k_1 = k_2 - ic)_{k_2 = \frac{y_1 - x_1 + y_2 - x_2}{4i(t + \sigma^2/2i)} + ic/2, k_3 = \frac{y_3 - x_3}{2i(t + \sigma^2/2i)}} \\ & - (2\pi i) \sqrt{\frac{\pi}{i(t + \sigma^2/2i)}} \sqrt{\frac{\pi}{2i(t + \sigma^2/2i)}} \text{Res}(f(k_1, k_2, k_3), k_1 = k_3 - ic)_{k_2 = \frac{y_2 - x_2}{2i(t + \sigma^2/2i)}, k_3 = \frac{y_1 - x_1 + y_3 - x_3}{4i(t + \sigma^2/2i)} + ic/2} \\ & - (2\pi i) \sqrt{\frac{\pi}{i(t + \sigma^2/2i)}} \sqrt{\frac{\pi}{2i(t + \sigma^2/2i)}} \text{Res}(f(k_1, k_2, k_3), k_2 = k_3 - ic)_{k_1 = \frac{y_1 - x_1}{2i(t + \sigma^2/2i)}, k_3 = \frac{y_2 - x_2 + y_3 - x_3}{4i(t + \sigma^2/2i)} + ic/2} \\ & + (2\pi i)^2 \sqrt{\frac{\pi}{3i(t + \sigma^2/2i)}} \text{Res}(\text{Res}(f(k_1, k_2, k_3), k_1 = k_2 - ic), k_2 = k_3 - ic)_{k_3 = \frac{y_1 - x_1 + y_2 - x_2 + y_3 - x_3}{6i(t + \sigma^2/2i)} + ic} \end{aligned}$$

This can be easily implemented in Mathematica, and the results are shown in Figure ??

A major complication in the above calculation of correlation functions of local operators originates from the complicated structure of the Bethe Ansatz wavefunction. One needs to integrate out unmeasured coordinates which are highly entangled. At the same time, evaluating matrix elements of the local operators between Bethe Ansatz eigenstates is a well studied topic itself. People name such quantities as form factor. In the next part, we will try to use the results of form factor for Lieb-Liniger model to avoid the fore-mentioned integration. However, this imposes another complication as we will show.

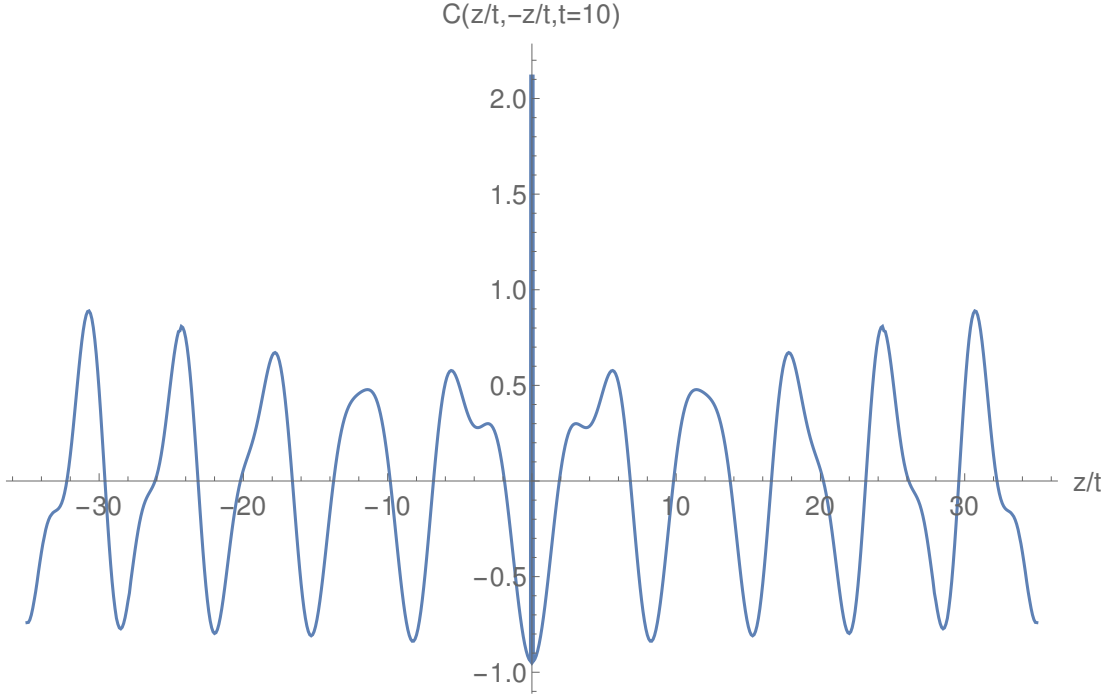


Figure 4.12: Normalised noise correlation function in the large time limit for a system with 3 particles.

### 4.3.2 Form Factor Approach

As we have shown, the time evolved state can be expanded in the basis of Bethe Ansatz states with the amplitude determined by the overlap between the initial state and Yudson states.

$$|\Psi_x(t)\rangle = \frac{1}{(2\pi)^N} \int_k e^{-i \sum_i k_i^2 t} |k\rangle \langle k|x\rangle$$

and local variables are expressed as

$$\langle O(t) \rangle = \frac{1}{(2\pi)^{2N}} \int_{k,p} e^{-i \sum_i (k_i^2 - p_i^2) t} \langle x|p\rangle \langle p|O|k\rangle \langle k|x\rangle$$

Due to the simple form of the Yudson state, the coefficients  $\langle x|p\rangle$  and  $\langle k|x\rangle$  are easier to manipulate than that in a traditional spectral representation. Then the main complication comes from the calculation of the matrix elements between two standard Bethe Ansatz states, i.e. the form factor. This object has been studied a lot in the literature. And the density form factor of the Lieb-Liniger gas is readily available from [?] as the following determinant formulas.

$$\langle p|\rho(y)|k\rangle = \frac{-i}{c} (-1)^{N(N+1)/2} e^{i \sum_i (k_i - p_i) y} \frac{\prod_{o=1}^N \prod_{l=1}^N (k_o - p_l + ic)}{\prod_{o<l} (k_o - k_l + ic)(p_o - p_l - ic)} \det V \quad (4.10)$$

with  $V$  being an  $(N+1) \times (N+1)$  matrix with entries

$$V_{jl} = t(k_j - p_l) + t(p_l - k_j) \prod_{o=1}^N \frac{(p_l - k_o + ic)(p_l - p_o - ic)}{(p_l - k_o - ic)(p_l - p_o + ic)} \quad j, l = 1, \dots, N$$

$$V_{N+1,j} = \prod_{o=1}^N \frac{p_o - p_l + ic}{k_o - p_j + ic} \quad \text{and} \quad V_{j,N+1} = 1 \quad j = 1, \dots, N$$

$$V_{N+1,N+1} = 0$$

and

$$t(u) = \frac{-i}{u(u+ic)}$$

Here, the formulas have been modified according to our choice of normalization. However, this formula suffers from some problems as we will see here.

When  $N = 1$ ,  $\langle p|\rho(y)|k \rangle = 1$ , then the evolution of a wave packet centered at  $\bar{x}$  of width  $\sigma$  becomes

$$\begin{aligned} \rho(y, t) &= \frac{\sqrt{4\pi\sigma^2}}{(2\pi)^2} \int_{k,p} e^{-ik^2(t+\sigma^2/2i)+ip^2(t-\sigma^2/2i)+i(k-p)(y-x)} \\ &= \frac{\sigma}{2\sqrt{\pi}\sqrt{t^2+\sigma^4/4}} e^{-\frac{\sigma^2(y-x)^2}{4(t^2+\sigma^4/4)}} \end{aligned}$$

which is what we expect for a free Gaussian wavepacket.

When  $N = 2$ ,

$$\langle p_1, p_2 | \rho(0) | k_1, k_2 \rangle = \frac{-2c(k_1 + k_2 - p_1 - p_2)^2(k_1 - k_2)(p_1 - p_2)}{(k_1 - p_1)(k_2 - p_1)(k_1 - p_2)(k_2 - p_2)(k_1 - k_2 + ic)(p_1 - p_2 - ic)} \quad (4.11)$$

And the time evolution of two wavepackets initially centered at  $x_1, x_2$  becomes

$$\begin{aligned} \rho(y, t) &= \frac{4\pi\sigma^2}{(2\pi)^4} \int_{\substack{k_1, k_2 \\ p_1, p_2}} e^{-i(k_1^2+k_2^2)(t+\sigma^2/2i)+i(p_1^2+p_2^2)(t-\sigma^2/2i)+ik_1(y-x_1)+ik_2(y-x_2)-ip_1(y-x_1)} \\ &e^{-ip_2(y-x_2)} \frac{-2c(k_1 + k_2 - p_1 - p_2)^2(k_1 - k_2)(p_1 - p_2)}{(k_1 - p_1)(k_2 - p_1)(k_1 - p_2)(k_2 - p_2)(k_1 - k_2 + ic)(p_1 - p_2 - ic)} \quad (4.12) \end{aligned}$$

We can also calculate the form factor from the two particle wavefunction directly by introducing regulator in  $x$  space as in [? ].

$$|k_1, k_2 \rangle = \int_{x_1, x_2} f_\epsilon(|x|) e^{ik_1 x_1 + ik_2 x_2} (\theta(x_2 - x_1) + \frac{k_1 - k_2 - ic}{k_1 - k_2 + ic} \theta(x_1 - x_2)) |x_1, x_2 \rangle$$

$$\begin{aligned}
\langle p_1, p_2 | \rho(y) | k_1, k_2 \rangle &= \int_x \left( \left( e^{-ip_1 y - ip_2 x} (\theta(x-y) + \frac{p_1 - p_2 + ic}{p_1 - p_2 - ic} \theta(y-x)) + e^{-ip_1 x - ip_2 y} (\theta(y-x) \right. \right. \\
&\quad \left. \left. + \frac{p_1 - p_2 + ic}{p_1 - p_2 - ic} \theta(x-y)) \right) \times \left( e^{ik_1 y + ik_2 x} (\theta(x-y) + \frac{k_1 - k_2 - ic}{k_1 - k_2 + ic} \theta(y-x)) \right. \right. \\
&\quad \left. \left. + e^{ik_1 x + ik_2 y} (\theta(y-x) + \frac{k_1 - k_2 - ic}{k_1 - k_2 + ic} \theta(x-y)) \right) \right) f_\epsilon(|x|) \\
&= \left( e^{i(k_1 - p_1)y} \frac{i}{k_2 - p_2} - e^{i(k_2 - p_2)y} \frac{i}{k_1 - p_1} \right) \left( 1 - \frac{k_1 - k_2 - ic}{k_1 - k_2 + ic} \frac{p_1 - p_2 + ic}{p_1 - p_2 - ic} \right) \\
&\quad + \left( e^{i(k_1 - p_2)y} \frac{i}{k_2 - p_1} - e^{i(k_2 - p_1)y} \frac{i}{k_1 - p_2} \right) \left( \frac{p_1 - p_2 + ic}{p_1 - p_2 - ic} - \frac{k_1 - k_2 - ic}{k_1 - k_2 + ic} \right)
\end{aligned} \tag{4.13}$$

When  $y = 0$ , the expression simplifies into ???. At first, it seems that one cannot generalize the result of  $\rho(0)$  to the density at arbitrary location by multiplying it with a phase factor  $e^{ik_1 y + ik_2 y - ip_1 y - ip_2 y}$ . Instead, we see a mixture of  $e^{i(k_1 - p_1)y}$ ,  $e^{i(k_1 - p_2)y}$ ,  $e^{i(k_2 - p_1)y}$  and  $e^{i(k_2 - p_2)y}$  in the expression of density form factor. However, this is an effect due to the regulator. As the physical space is translationally invariant, measuring the density at position  $y$  is equivalent to shifting all particles by  $-y$ , this leads to the phase factor in ???. The same trick has been used in the paper [?] when using the density form factor ???.

The drawback of the expression (??) is related to the singularity when momentums from the two states approach each other. This pole is called a kinetic pole or annihilation pole. And it exists for systems with any number of particles. This makes the integration intractable. To remove such singularity, one may shift the integration contour slightly. This, however, invalidates the Eq. (??) due to divergence problems in its derivation. For example, when  $\Im(k_1 - p_2) < 0$  or  $\Im(k_1 - p_2) > 0$ , the following integration from  $\langle p_1, p_2 | \rho(y) | k_1, k_2 \rangle$  becomes ill-defined

$$\int_x e^{i(k_1 - p_2)x + i(k_2 - p_1)y} \left( \frac{k_1 - k_2 - ic}{k_1 - k_2 + ic} \theta(x-y) + \frac{p_1 - p_2 + ic}{p_1 - p_2 - ic} \theta(y-x) \right)$$

Therefore, there is no consistent way to shift the contour without bringing in more divergent problems to the density form factor. Thus the result of the density form factor can not be applied to the Yudson approach readily due to the kinetic poles in the form factor. This completes our discussion of this method.

## Chapter 5

### Quench Dynamics of Gaudin-Yang Gas

In this chapter, we will use the Yudson Approach to study the real time dynamics of a system with two species of fermions interacting with contact interaction. The system is described by the Gaudin-Yang Hamiltonian defined as

$$H = \sum_{\sigma=\uparrow,\downarrow} \int dx \Psi_{\sigma}^{\dagger}(x) \left(-\frac{\partial^2}{\partial x^2}\right) \Psi_{\sigma}(x) + c \int_x \Psi_{\uparrow}^{\dagger}(x) \Psi_{\downarrow}^{\dagger}(x) \Psi_{\downarrow}(x) \Psi_{\uparrow}(x)$$

We have talked about the Bethe Ansatz solution of this model in chapter 1. Here is a quick recap of some of the important results which will serve as a basis of the discussion in this chapter.

The Bethe Ansatz eigenstate

$$|\mu, k\rangle = \sum_{P,R} \int_x \sum_{\alpha} (-1)^P e^{ik_{P_i}x_i} \prod_{i<j} S(\mu_i - \mu_j) \prod_{i=1}^M I(\mu_i, Pk, \alpha_{R^{-1}i}) \theta(\alpha) \theta(x) |x, \alpha\rangle$$

with  $S(\mu_i - \mu_j)$  defined as

$$S(\mu_i - \mu_j) = \frac{\mu_i - \mu_j + ic \operatorname{Sgn}(\alpha_{R^{-1}i} - \alpha_{R^{-1}j})}{\mu_i - \mu_j - ic}$$

and  $I(\mu, k, \alpha)$  defined as

$$I(\mu, k, \alpha) = \frac{-ic}{\mu - k_{\alpha} + ic/2} \prod_{n<\alpha} \frac{\mu - k_n - ic/2}{\mu - k_n + ic/2}$$

and  $|x, \alpha\rangle$  defined as

$$|x, \alpha\rangle = \prod_{i=1}^M \sigma_{\alpha_i}^- \prod_{j=1}^N \Psi_{\uparrow}^{\dagger}(x_i) |0\rangle$$

The Yudson state can be extracted from it as

$$|k, \mu\rangle = \int_x \sum_{\alpha} e^{ik_i x_i} \prod_{i=1}^M I(\mu_i, k, \alpha_i) \theta(\alpha) \theta(x) |x, \alpha\rangle$$

The Yudson representation of the identity operator

$$\int_C dk \int_C d\mu |k, \mu\rangle \langle k, \mu| = \sum_{\alpha, \beta} \int dx \int dy \sum_{P,R} (-1)^P e^{i \sum_i k_i (y_{P^{-1}i} - x_i)} \prod_{m<n}^M S(\mu_m - \mu_n) \prod_{m=1}^M J(\mu_m, k, P, \alpha_m, \beta_m) |y, \alpha\rangle \langle x, \beta|$$

with  $J(\mu, k, P, \alpha, \beta)$  defined as

$$\begin{aligned}
J(\mu, k, P, \alpha, \beta) &= I(\mu, Pk, \alpha) I^*(\mu, k, \beta) \\
&= \frac{-ic}{\mu - k_{P\alpha} + ic/2} \prod_{\substack{m < \alpha \\ Pm \geq \beta}} \frac{\mu - k_{Pm} - ic/2}{\mu - k_{Pm} + ic/2} \frac{ic}{\mu - k_\beta - ic/2} \prod_{\substack{n < \beta \\ P^{-1}n \geq \alpha}} \frac{\mu - k_n + ic/2}{\mu - k_n - ic/2}
\end{aligned} \tag{5.1}$$

Here, we have taken into account the cancellation between  $I(\mu, Pk, \alpha)$  and  $I(\mu, k, \beta)$ , i.e. when  $m < \beta$  and  $P^{-1}m < \alpha$ , the factor  $\frac{\mu - k_m - ic/2}{\mu - k_m + ic/2}$  in  $I(\mu, Pk, \alpha)$  cancels the term  $\frac{\mu - k_m + ic/2}{\mu - k_m - ic/2}$  in  $I^*(\mu, k, \beta)$ . However, we have left the possible cancellation related to  $k_{P\alpha}$  and  $k_\beta$  unattended in the above expression. To carry it out, one needs to consider the relation between  $P\alpha$  and  $\beta$ ,  $P^{-1}\beta$  and  $\alpha$  separately.

If  $P\alpha \geq \beta$ , and  $P^{-1}\beta \geq \alpha$ , then

$$J(\mu, k, P, \alpha, \beta) = \frac{-ic}{\mu - k_{P\alpha} + ic/2} \prod_{\substack{m < \alpha \\ Pm > \beta}} \frac{\mu - k_{Pm} - ic/2}{\mu - k_{Pm} + ic/2} \frac{ic}{\mu - k_\beta - ic/2} \prod_{\substack{n < \beta \\ P^{-1}n > \alpha}} \frac{\mu - k_n + ic/2}{\mu - k_n - ic/2}$$

If  $P\alpha < \beta$ , and  $P^{-1}\beta \geq \alpha$ , then

$$J(\mu, k, P, \alpha, \beta) = \prod_{\substack{m < \alpha \\ Pm > \beta}} \frac{\mu - k_{Pm} - ic/2}{\mu - k_{Pm} + ic/2} \frac{-ic}{\mu - k_{P\alpha} - ic/2} \frac{ic}{\mu - k_\beta - ic/2} \prod_{\substack{n < \beta \\ P^{-1}n > \alpha}} \frac{\mu - k_n + ic/2}{\mu - k_n - ic/2}$$

If  $P\alpha \geq \beta$ , and  $P^{-1}\beta < \alpha$ , then

$$J(\mu, k, P, \alpha, \beta) = \frac{-ic}{\mu - k_{P\alpha} + ic/2} \frac{ic}{\mu - k_\beta + ic/2} \prod_{\substack{m < \alpha \\ Pm > \beta}} \frac{\mu - k_{Pm} - ic/2}{\mu - k_{Pm} + ic/2} \prod_{\substack{n < \beta \\ P^{-1}n > \alpha}} \frac{\mu - k_n + ic/2}{\mu - k_n - ic/2}$$

If  $P\alpha < \beta$ , and  $P^{-1}\beta < \alpha$ , then

$$J(\mu, k, P, \alpha, \beta) = \frac{ic}{\mu - k_\beta + ic/2} \prod_{\substack{m < \alpha \\ Pm > \beta}} \frac{\mu - k_{Pm} - ic/2}{\mu - k_{Pm} + ic/2} \frac{-ic}{\mu - k_{P\alpha} - ic/2} \prod_{\substack{n < \beta \\ P^{-1}n > \alpha}} \frac{\mu - k_n + ic/2}{\mu - k_n - ic/2}$$

However, to simplify our expression, we will keep the form of  $J$  as in Equation ???. We will also use abbreviated notation  $J(\mu)$  and keep its dependence on all other elements implicit.

In order for the Yudson Representation to hold true, the contours are chosen as follows. For systems with repulsive interaction, the contours of  $k$ 's are separated in the imaginary direction by a distance greater than  $|c|$ . The contours of  $\mu$ 's overlap with that of some  $k$ 's determined by the initial condition. If, for example, the  $N$  particles initially reside at  $x_1 < \dots < x_N$ , while the  $m$ th and  $n$ th ( $m < n$ ) particles are impurities (spin flips), then  $\mu_1$  are integrated along the path of  $k_m$  and the contour of  $\mu_2$  overlaps with that of  $k_n$ . See Figure ??. If the particles

interact with attractive interaction, the contours of the  $k$ 's remain the same. However, each  $\mu$  is integrated along three lines, two forward and one backward. The backward path runs over that of the  $k$  related to the corresponding down spins. The two forward paths lie above and below the backward contour with a separation greater than  $|c|/2$ . Take the same example as above,  $\mu_1$  is integrated backward along the same line as  $k_m$ , and forward above and below the  $k_m$  contour by a distance greater than  $|c|/2$ . Similarly, the  $\mu_2$  contour consists of three lines centered at the contour of  $k_n$ , the first and last goes forward and the middle one runs backwards. See Plot (??).

In the next section, we will explain such choice of contour and prove the Yudson Central theorem for the Gaudin-Yang model.

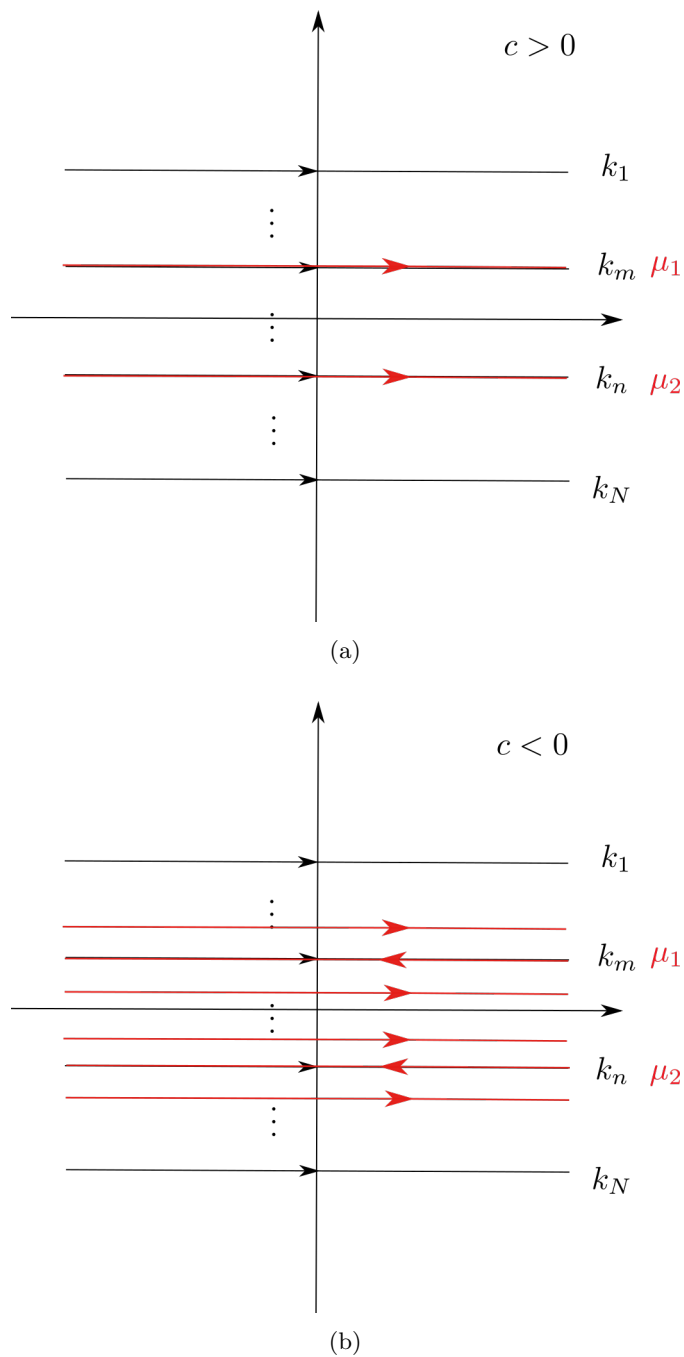


Figure 5.1: Example integration contours in the Yudson representation for a system with  $N - 2$  majority fermions and two impurities. In this example, the  $m$ th and  $n$ th particles are the impurities counting from the left to right. Figure ?? is for repulsive case and Figure ?? is for attractive case.

## 5.1 Central Theorem

In this section, we will prove that the Yudson representation resolves the identity properly with the aforementioned integration contour, i.e.

$$\int_C dk \int_C d\mu \langle y, \alpha | k, \mu \rangle \langle k, \mu | x, \beta \rangle \theta(x) \theta(y) \theta(\alpha) \theta(\beta) = \prod_i \delta(y_i - x_i) \prod_j \delta_{\alpha_j \beta_j}$$

with the abbreviated notation  $\theta(x) = \theta(x_1 < \dots < x_N)$ . We will start with the proof for the one impurity case then generalize to that for multiple spin flips.

### 5.1.1 One Impurity Case

The central theorem of the Yudson representation for Gaudin-Yang model with a single impurity states that

$$\begin{aligned} \text{Const} \int_C dk \int_{C'} d\mu \sum_P (-1)^P e^{i \sum_i k_i (y_{P^{-1}i} - x_i)} \frac{-ic}{\mu - k_{P\alpha} + ic/2} \prod_{\substack{i < \alpha \\ P i \geq \beta}} \frac{\mu - k_{P i} - ic/2}{\mu - k_{P i} + ic/2} \frac{ic}{\mu - k_\beta - ic/2} \\ \prod_{\substack{j < \beta \\ P^{-1} j \geq \alpha}} \frac{\mu - k_j + ic/2}{\mu - k_j - ic/2} \theta(x) \theta(y) \theta(\alpha) \theta(\beta) = \prod_i \delta(y_i - x_i) \prod_j \delta_{\alpha_j \beta_j} \end{aligned}$$

As the integrand is  $O(\frac{1}{\mu^2})$  as  $|\mu| \rightarrow \infty$ , the integration contour can be closed from below or above, either should yield the same result. We choose to close the contour from above. Then, the integral transforms into a sum of contributions from poles enclosed by the contour. For  $c > 0$ , this corresponds to the poles above the integration contour, see Figure ???. For  $c < 0$ , however, the pole at  $\mu = k_\beta + ic/2$  lies below the line of  $k_\beta$ . To capture this pole, a 3-line contour is chosen, see Figure ??. In this way, the  $\mu$  integration transforms into residues at the same set of poles for both  $c >$  and  $c < 0$ . Define  $R(k_o + ic/2)$  as the residue of  $J(\mu)$  at  $\mu = k_o + ic/2$ . Then

$$\int d\mu J(\mu) = 2\pi i \sum_{\substack{o \leq \beta \\ P^{-1} o \geq \alpha}} R(k_o + ic/2)$$

Depending on the relation among the indexes  $o$ ,  $\alpha$  and  $\beta$ , the expression of  $R(k_o + ic/2)$  takes different forms.

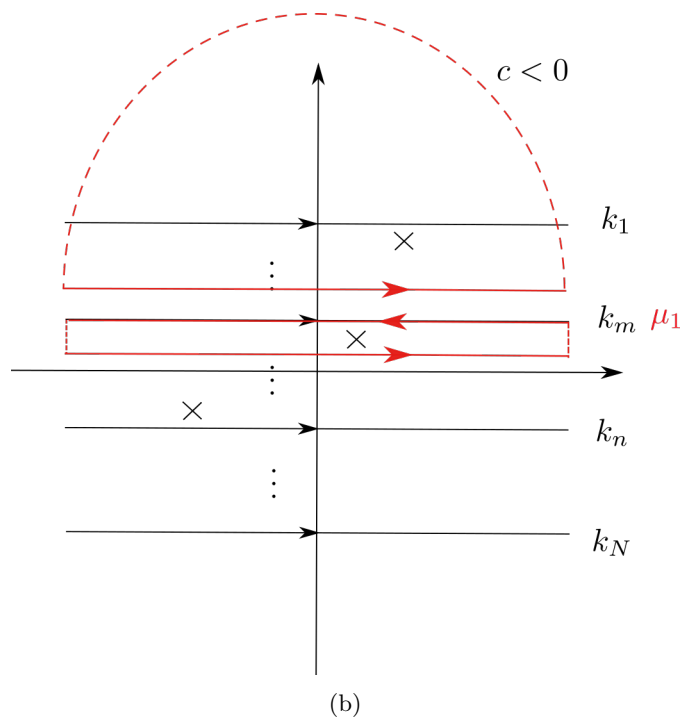
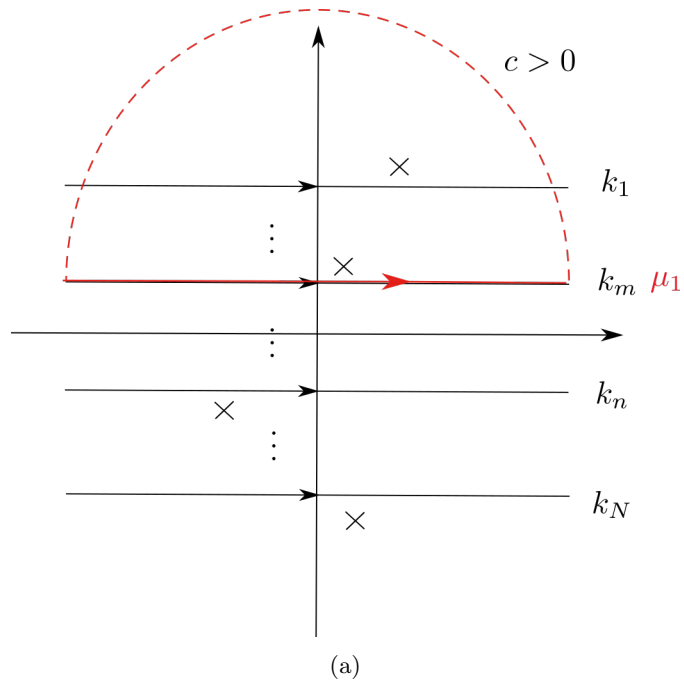


Figure 5.2: Pole structure of the integrand of the  $\mu$  integration. Both plots apply to systems with  $N - 1$  majority fermions and one impurity fermion which is the  $m$ th particle counting from the left. Figure ?? is for systems with repulsive interaction. Figure ?? is for systems with attractive interaction.

If  $o = P\alpha = \beta$ , then

$$\begin{aligned}
R(k_o + ic/2) &= -ic \prod_{m \in S_1} \frac{k_o - k_{Pm}}{k_o - k_{Pm} + ic} \prod_{n \in S_2} \frac{k_o - k_n + ic}{k_o - k_n} \\
&= -ic \prod_{m \in S_1} \left(1 - \frac{ic}{k_o - k_{Pm} + ic}\right) \prod_{n \in S_2} \left(1 + \frac{ic}{k_o - k_n}\right) \\
&= -ic \sum_{\substack{t_1 \in P(S_1) \\ t_2 \in P(S_2)}} \prod_{u \in t_1} \frac{-ic}{k_o - k_{Pu} + ic} \prod_{v \in t_2} \frac{ic}{k_o - k_v}
\end{aligned}$$

If  $o = \beta \neq P\alpha$  and  $P^{-1}\beta > \alpha$ , then

$$\begin{aligned}
R(k_o + ic/2) &= ic \frac{-ic}{k_o - k_{P\alpha} + ic\theta(P\alpha - \beta)} \prod_{m \in S_1} \frac{k_o - k_{Pm}}{k_o - k_{Pm} + ic} \prod_{n \in S_2} \frac{k_o - k_n + ic}{k_o - k_n} \\
&= ic \frac{-ic}{k_o - k_{P\alpha} + ic\theta(P\alpha - \beta)} \sum_{\substack{t_1 \in P(S_1) \\ t_2 \in P(S_2)}} \prod_{u \in t_1} \frac{-ic}{k_o - k_{Pu} + ic} \prod_{v \in t_2} \frac{ic}{k_o - k_v}
\end{aligned}$$

If  $o = P\alpha < \beta$ , then

$$\begin{aligned}
R(k_o + ic/2) &= -ic \sum_{\substack{t_1 \in P(S_1) \\ t_2 \in P(S_2)}} \frac{ic}{k_o - k_\beta + ic\theta(\alpha - P^{-1}\beta)} \prod_{m \in S_1} \frac{k_o - k_{Pm}}{k_o - k_{Pm} + ic} \prod_{n \in S_2} \frac{k_o - k_n + ic}{k_o - k_n} \\
&= ic \frac{-ic}{k_o - k_\beta + ic\theta(\alpha - P^{-1}\beta)} \sum_{\substack{t_1 \in P(S_1) \\ t_2 \in P(S_2)}} \prod_{u \in t_1} \frac{-ic}{k_o - k_{Pu} + ic} \prod_{v \in t_2} \frac{ic}{k_o - k_v}
\end{aligned}$$

If  $o \neq P\alpha \neq \beta$ , then

$$\begin{aligned}
R(k_o + ic/2) &= -ic \frac{-ic}{k_o - k_{P\alpha} + ic\theta(P\alpha - \beta)} \frac{ic}{k_o - k_\beta + ic\theta(\alpha - P^{-1}\beta)} \prod_{m \in S_1} \frac{k_o - k_{Pm}}{k_o - k_{Pm} + ic} \\
&\quad \prod_{n \in S_2} \frac{k_o - k_n + ic}{k_o - k_n} \\
&= -ic \frac{-ic}{k_o - k_{P\alpha} + ic\theta(P\alpha - \beta)} \frac{ic}{k_o - k_\beta + ic\theta(\alpha - P^{-1}\beta)} \sum_{\substack{t_1 \in P(S_1) \\ t_2 \in P(S_2)}} \prod_{u \in t_1} \frac{-ic}{k_o - k_{Pu} + ic} \\
&\quad \prod_{v \in t_2} \frac{ic}{k_o - k_v}
\end{aligned}$$

If  $o \neq P\alpha = \beta$ , then

$$\begin{aligned}
R(k_o + ic/2) &= -ic \frac{-ic}{k_o - k_{P\alpha} + ic} \frac{ic}{k_o - k_\beta} \prod_{m \in S_1} \frac{k_o - k_{Pm}}{k_o - k_{Pm} + ic} \prod_{n \in S_2} \frac{k_o - k_n + ic}{k_o - k_n} \\
&= -ic \frac{-ic}{k_o - k_{P\alpha} + ic} \frac{ic}{k_o - k_\beta} \sum_{\substack{t_1 \in P(S_1) \\ t_2 \in P(S_2)}} \prod_{u \in t_1} \frac{-ic}{k_o - k_{Pu} + ic} \prod_{v \in t_2} \frac{ic}{k_o - k_v}
\end{aligned}$$

Here  $S_1 = \{m | m < \alpha \text{ and } Pm > \beta\}$  and  $S_2 = \{n | n < \beta \text{ and } P^{-1}n > \alpha\}$ .  $P(s)$  is the power set of  $S$  which includes all subset of  $S$  including the empty set. The power set appears after

multiplying each addend respectively. The  $\theta$ -function is the Heaviside step function. It is easier to understand its emergence by looking at the detailed discussion of  $J(\mu)$  on page ???. When  $P\alpha > \beta$ ,  $J(\mu)$  has a factor  $\frac{1}{\mu - k_{P\alpha} + ic/2}$ . When  $P\alpha < \beta$ , this factor is cancelled by another term in  $I^*(\mu, k, \beta)$ , making the factor  $\frac{1}{\mu - k_{P\alpha} - ic/2}$ . Thus, in  $R(k_o + ic/2)$ , we see  $\frac{1}{k_o - k_{P\alpha} + ic}$  when  $P\alpha > \beta$  and  $\frac{1}{k_o - k_{P\alpha}}$  with  $\beta > P\alpha$ .

With  $|k_o| \rightarrow \infty$ , the asymptotic behavior of  $R(k_o + ic/2)$  can be categorized into three cases.

$$R(k_o + ic/2) = \begin{cases} -ic + O(\frac{1}{k_o}) & \text{if } k_o = k_{P\alpha} = k_\beta \\ O(\frac{1}{k_o}) & \text{if } k_o = k_{P\alpha} \neq k_\beta \text{ or } k_o = k_\beta \neq k_{P\alpha} \\ O(\frac{1}{k_o^2}) & \text{In other cases} \end{cases}$$

where the leading term corresponds to the case with both  $t_1$  and  $t_2$  being empty sets. Except for the first term in the first case, all terms vanish as fast or faster than  $1/k_o$  asymptotically. Moreover, if these terms depend on any other  $k_j$ , they also die away as fast as  $1/k_i$ . Therefore, the integral over these explicit variables

$$\int dk_o \prod_j dk_j R(k_o + ic/2) e^{i \sum_i k_i (y_{P^{-1}i} - x_i)}$$

can be transformed into sum of pole residues above or below the integration contour, depending on the relation between elements of  $P\vec{y}$  and  $\vec{x}$ . As we will show in the following, none of these poles contribute to the integral. Denote  $E(k_o)$  as one of the summand of these  $O(\frac{1}{k_o})$  or  $o(\frac{1}{k_o})$  terms, which takes the form

$$E(k_o) = \prod_m \frac{-ic}{k_o - k_m + ic} \prod_n \frac{ic}{k_o - k_n}$$

with  $m$  satisfies the condition  $m \leq \alpha$  and  $Pm \geq \beta$ ,  $n$  satisfies the condition  $n \leq \beta$  and  $P^{-1}n \geq \alpha$ . There are two types of poles in  $E(k_o)$ . One is of the form  $k_o = k_n$ , the other is of the form  $k_o = k_m + ic$ . The former pole is only apparent, but not real. As there is another term in  $E(k_n)$  which cancels its contribution. To be explicit, we have

$$\begin{aligned} \text{Res}(e^{i \sum_i k_{P^i} (y_i - x_{P^i})} \text{Res}(J(\mu), \mu = k_o), k_o = k_n) \\ = - \text{Res}(e^{i \sum_i k_{P^i} (y_i - x_{P^i})} \text{Res}(J(\mu), \mu = k_n), k_n = k_o) \end{aligned}$$

This is what we anticipated. As the nested Bethe Ansatz solution is obtained from the ordinary Bethe Ansatz with matrix operator, see Eq. (??) and (??), it should have the same pole structure as the ordinary one. Thus, we do not need to worry about the first type of pole at  $k_o = k_n$ . The second type of poles ( $k_o = k_m - ic$ ) also exist in the Lieb-Liniger model. These poles form a subset of those in the Lieb-Liniger model, as the requirement for their existence is

stronger ( $n \leq \beta \leq Pm$  and  $P^{-1}n \leq \alpha \leq n$  rather than  $n \leq Pm$  and  $P^{-1}n \leq m$ ). As in the Lieb-Liniger model, these poles do not contribute to the integral due to conflicting conditions. The argument is essentially the same as that of the Lieb-Liniger Gas. Neither does the disappearance of some poles nor the emergence of factors like  $\frac{1}{k_o - k_n}$  affects proof. Thus, we will not repeat that here.

Since none of these poles in  $R(k_o + ic/2)$  contributes to the integral, the integration is essentially the same as an integration of the first term in the first case with  $P\alpha = \beta$ . This will lead to the final result we want, with a properly chosen constant  $\text{Const} = \frac{1}{(2\pi)^{N+1}c}$ , i.e.

$$\begin{aligned} & \frac{1}{(2\pi)^{N+1}c} \theta(x)\theta(y)\theta(\alpha)\theta(\beta) \int_C dk \int_C d\mu \sum_P e^{i \sum_i k_i (y_{P^{-1}i} - x_i)} J(\mu) \\ &= \frac{1}{(2\pi)^N} \theta(x)\theta(y)\theta(\alpha)\theta(\beta) \sum_P \delta_{P\alpha, \beta} \int dk e^{i \sum_i k_i (y_{P^{-1}i} - x_i)} \\ &= \theta(x)\theta(y)\theta(\alpha)\theta(\beta) \sum_P \delta_{P\alpha, \beta} \delta(y_{P^{-1}i} - x_i) \\ &= \theta(x)\theta(y)\theta(\alpha)\theta(\beta) \delta_{\alpha, \beta} \delta(y_i - x_i) \end{aligned}$$

In sum, we have proved the Central theorem of Yudson representation for systems with one impurity which says

$$\frac{1}{(2\pi)^{N+1}c} \int_C dk \int_{C'} d\mu |k, \mu\rangle \langle k, \mu| = \mathbb{1}$$

We will move on to the proof for systems with arbitrary number of impurities.

### 5.1.2 Multi-impurity Case

The Central theorem of the Yudson representation for the Gaudin-Yang model with multiple impurities states that

$$\begin{aligned} \text{Const} \int_C dk \int_{C'} d\mu \sum_P (-1)^P e^{i \sum_i k_i (y_{P^{-1}i} - x_i)} \prod_{m < n}^M \frac{\mu_m - \mu_n + ic \text{Sgn}(\alpha_m - \alpha_n)}{\mu_m - \mu_n - ic} \prod_m^M J(\mu_m) \\ \theta(x)\theta(y)\theta(\alpha)\theta(\beta) = \prod_i^N \delta(x_i - y_i) \prod_m^M \delta_{\alpha_m \beta_m} \end{aligned} \quad (5.2)$$

with abbreviated notations.

$$\begin{aligned} J(\mu_m) &= J(\mu, k, P, \alpha_m, \beta_m) \\ &= \prod_m \frac{-ic}{\mu_m - k_{P\alpha_m} + ic/2} \prod_{\substack{i < \alpha_m \\ P^{-1}i \geq \beta_m}} \frac{\mu_m - k_{Pi} - ic/2}{\mu_m - k_{Pi} + ic/2} \frac{ic}{\mu_m - k_{\beta_m} - ic/2} \prod_{\substack{j < \beta_m \\ P^{-1}j \geq \alpha_m}} \frac{\mu_m - k_j + ic/2}{\mu_m - k_j - ic/2} \end{aligned}$$

and

$$\theta(x) = \theta(x_1 < \dots < x_N)$$

$$\theta(\alpha) = \theta(\alpha_1 < \dots < \alpha_M)$$

In the following section, we will see that the  $\mu$  integrations, as in the previous case, leads to an expression whose poles form a subset of that in the Lieb-Liniger gas. Using similar argument as before, these poles do not contribute to the  $k$  integral. We are left with a constant terms which yields the  $\delta$ -function we are looking for.

First, carry out the integration over  $\mu_1$  by closing the contour from above. As the integrand is  $O(1/\mu_1^2)$ , the integral over the arc vanishes. Since the pole of  $S(\mu_1, \mu_m)$  ( $m > 1$ ) is at  $\mu_1 = \mu_m + ic$ , which is below the  $\mu_1$  contour, see Figure ??, this pole is not included. Thus, the integral becomes sum of residues at the same set of poles as that with  $J(\mu_1)$  alone. In the meanwhile, the factor  $S(\mu_1, \mu_m)$  becomes  $\frac{\mu_m - k_o - ic/2 - ic \text{Sgn}(\alpha_1 - \alpha_m)}{\mu_m - k_o + ic/2}$ . Therefore, we have

$$\int d\mu_1 J(\mu_1) \prod_{m>1} S(\mu_1 - \mu_m) = \sum_o R(k_o + ic/2) \prod_m \frac{\mu_m - k_1 - ic/2 - ic \text{Sgn}(\alpha_1 - \alpha_m)}{\mu_m - k_1 + ic/2}$$

with  $o$  summed over all poles lying above the  $\mu_1$  integral contour.  $R(k_o + ic/2)$  represents the residue of  $J(\mu_1)$  at  $k_o + ic/2$ , and its explicit expression are discussed on page ??.

Then, we can carry out the integration over  $\mu_2$  by closing the contour from above. Among the S-matrices among the  $\mu$ 's, only the pole from  $S(\mu_1 - \mu_2)$  is enclosed, which is located at  $\mu_m = k_o + ic/2$  if  $\alpha_1 > \alpha_2$ . Combined with the condition on  $o$ ,  $\alpha$ 's and  $\beta$ 's, we have  $P^{-1}o \geq \alpha_1 > \alpha_2$  and  $o \leq \beta_1 < \beta_2$ . Thus  $\frac{\mu_2 - k_o + ic/2}{\mu_2 - k_o - ic/2}$  must be a factor of  $J(\mu_2)$ . It cancels the denominator of  $S(k_o + ic/2 - \mu_2)$ . Therefore, the poles above the  $\mu_2$  contour in  $J(\mu_2)S(k_o - \mu_2 + ic/2) \prod_{m>2} S(\mu_2 - \mu_m)$  is the same as that in  $J(\mu_2)$ . Thus, we have

$$\begin{aligned} & \int d\mu_2 J(\mu_2) S(k_o - \mu_2 + ic/2) \prod_{m>2} S(\mu_2 - \mu_m) \\ &= \sum_u R(k_u + ic/2) \frac{k_o - k_u + ic \text{Sgn}(\alpha_1 - \alpha_m)}{k_o - k_u - ic} \prod_{m>2} S(k_u - \mu_m + ic/2) \end{aligned}$$

with  $u \in \{v \leq \beta_2 \text{ and } P^{-1}u \geq \alpha_2\}$ , which form a subset of that of the Lieb-Liniger gas. Note, the apparent pole at  $k_o = k_u + ic$  is not real, as the denominator of  $S(k_o - k_u)$  is canceled by  $R(k_u + ic/2)$ . We have keep the result as here in order to pack the complicated long expression into  $R(k_u + ic/2)$ . One special scenario of the term is when  $u = o$ . Then some poles in  $R(k_o + ic/2)$  overlaps with those in  $R(k_u + ic/2)$ . However, this leads to  $\mu_1 = \mu_2$  which is inhibited by the nested bethe ansatz such that the wavefunction vanishes at overlapping  $\mu$ 's

One can continue the argument for the  $\mu$  integration easily. The integrand always has the same pole structure as  $J(\mu)$  alone in the plane above the contour. What the S-matrix does when it's not identity is changing the numerator from  $\mu - k + ic/2$  to  $\mu - k + i3c/2$ . After the

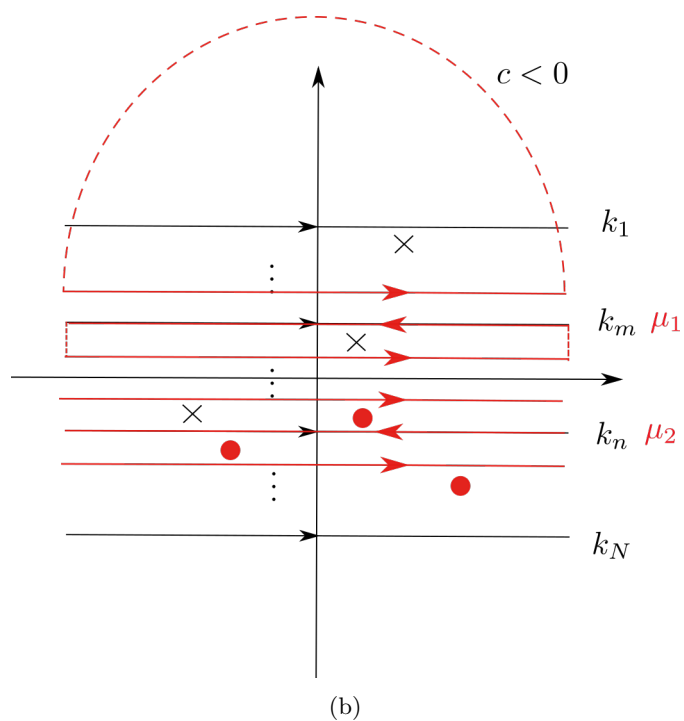
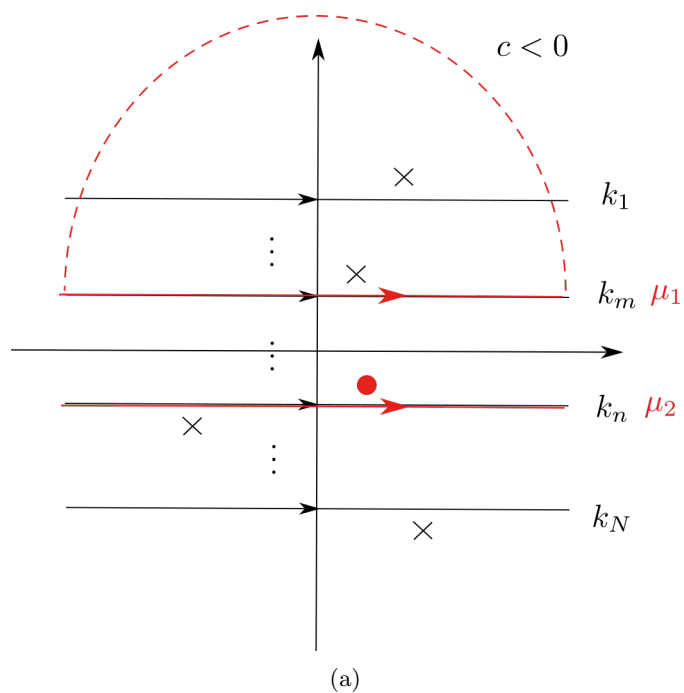


Figure 5.3: Pole structure of the integrand of the  $\mu_1$  integration. Crosses represent poles from  $k$ 's and dots represent pole form  $\mu_2$ . Among the  $N$  fermions, the  $m$ th and  $n$ th are the impurities. Figure ?? is for systems with repulsive interaction. Figure ?? is for systems with attractive interaction.

$\mu$  integration, this changes one of the numerator from  $k_i - k_j + ic$  to  $k_i - k_j + 2ic$ . Thus the poles of the  $k$  integration is unaffected either.

As a result, after all  $\mu$  integrations, the left hand side of equation ?? becomes

$$L = \text{Const} \int_C dk e^{i \sum_i k_i (y_{P^{-1}i} - x_i)} \sum_{\{O_m\}} \prod_{m=1}^M R(k_{O_m} + ic/2) \prod_{m < n} S(k_{O_m} - k_{O_n}) \theta(x) \theta(y) \theta(\alpha) \theta(\beta)$$

with each  $O_m$  satisfies the condition  $O_m \leq \beta_m$  and  $P^{-1}O_m \geq \alpha_m$ . Again, all poles from  $S(k_{O_m} - k_{O_n})$  is artificial. Thus, the pole in this expression is a union of the poles of each  $R(k_{O_m} + ic/2)$ . As the poles of each of them form a subset of that of the Lieb-Liniger gas, so does the whole term. As we have shown for the Lieb-Liniger gas in chapter 3, the existence condition for these Lieb-Liniger type poles always contradicts with the requirement to include them into the contour. Thus, the integration vanishes if the integrand is  $O(1/k_i)$  or  $o(1/k_i)$  for any  $k_i$ . The only exception that contributes to the integral corresponds to the term that is  $O(1)$  for any  $k_i$ . This relates to each  $R(k_{O_m} + ic/2)$  equaling  $-ic$ . This indicates  $P\alpha_m = \beta_m$  for any  $m$ . Then, the integration on the left hand side of Equation ?? becomes

$$\begin{aligned} L &= \text{Const} (2\pi c)^M \int dk \sum_P e^{i \sum_i k_i (y_{P^{-1}i} - x_i)} \prod_{m=1}^M \delta_{P\alpha_m \beta_m} \theta(x) \theta(y) \theta(\alpha) \theta(\beta) \\ &= \text{Const} (2\pi)^{N+M} c^M \sum_P \delta(y_{P^{-1}i} - x_i) \delta_{P\alpha_m \beta_m} \theta(x) \theta(y) \theta(\alpha) \theta(\beta) \\ &= \text{Const} (2\pi)^{N+M} c^M \delta(y_i - x_i) \delta_{\alpha_m \beta_m} \theta(x) \theta(y) \theta(\alpha) \theta(\beta) \end{aligned}$$

This is the expression that we are looking for if the constant is chosen as  $1/(2\pi)^{N+M} c^M$ . Note, in the above discussion, we did not specify the sign of the interaction. As in the case of the single impurity case, the pole structure of the  $\mu$  integration and  $k$  integration is the same thanks to our choice of contour. See Figure ?? for an example with two impurities. Since only the relative position of the poles matters in the argument, the argument applies to either interaction.

This completes our discussion of the central theorem for multiple impurities. We have shown that the identity can be resolved by the following expression, with  $C$  and  $C'$  defined on page ??.

$$\mathbb{1} = \frac{1}{(2\pi)^{N+M} c^M} \int_C dk \int_{C'} d\mu |k, \mu\rangle \langle k, \mu|$$

This serves as a basis to apply the Yudson representation to study the time evolution of systems with two species of fermions. However, before we dive into detailed calculations of states and observables, let's discuss its physical interpretation.

## 5.2 Physical Interpretation in terms of Bound states

In this section, we will recover the string solutions obtained in chapter one. By separating out every string solutions, we will see how the Yudson representation includes them in the contours. Moreover, we will understand why some strings are formed while others will not emerge. We will also observe some larger cluster of roots that are not predicted by the String hypothesis. Then we will discuss the physical nature of these string solutions in terms of bound states. Combined with previous results, we will see how these bound states are formed dynamically in real space.

First of all, let us review the string solutions of the Gaudin-Yang model. As we have shown on page ??, besides being all real, the roots of the Bethe equations may form two types of patterns. They are  $\mu - k$  strings and  $k - \mu$  strings. The  $\mu - k$  string of length  $m$  is composed of  $m$   $\mu$ s and  $m - 1$   $k$ s. And it may exist in systems with either attractive or repulsive interaction. In the second class,  $n$   $k$ s combine with  $n - 1$   $\mu$ s to form a  $k - \mu$  string of length  $n$ . When the total number of fermions and the number of impurities is moderate, the roots only arrange themselves into strings whose length is no longer than two. Otherwise, we will encounter factors of  $\frac{0}{0}$  while solving the Bethe equations.

$$e^{ik_i L} = \prod_m \frac{k_i - \mu_m + ic/2}{k_i - \mu_m - ic/2} \quad (5.3)$$

$$\prod_{n \neq m} \frac{\mu_m - \mu_n + ic}{\mu_m - \mu_n - ic} = \prod_i \frac{\mu_m - k_i + ic/2}{\mu_m - k_i - ic/2} \quad (5.4)$$

To see this, consider a  $\mu - k$  string and a  $k - \mu$  string whose length is at least three, see Figure ???. In  $\mu - k$  string, the imaginary part of  $k$  equals  $(Z + 1/2)c$  with  $Z$  being integers. Then the topmost  $k$ , which we call  $k_i$  must have a positive imaginary part. Thus, the left hand side of equation ?? vanishes with  $L \rightarrow \infty$ . In the meanwhile, we have both  $k_i - \mu_m \pm ic/2 = 0$  and  $k_i - \mu_n \mp ic/2 = 0$  for  $c = \pm|c|$ . This makes both the numerator and denominator vanish. In the second example, the highest  $\mu$  which we call  $\mu_m$  is accompanied by another  $\mu_n = \mu_m + ic$  for  $c < 0$ , this makes the left hand side of equation ?? tend to zero. However, on the other side of the equation, we have both  $\mu_m - k_i - ic/2 = 0$  and  $\mu_m - k_j + ic/2 = 0$ . Thus we are faced with  $0 = \frac{0}{0}$  again. Due to such ambiguity, we have not included any solutions relate to strings longer than two. However, as we will see later, such long string of roots do emerge in systems with attracting interactions.

To separate out the string solutions from the Yudson representation, one first integrates

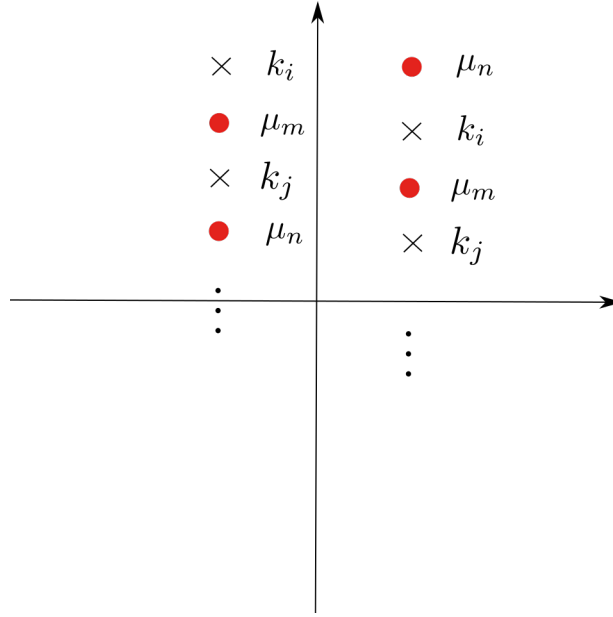


Figure 5.4: Examples of  $k - \mu$  string and  $\mu - k$  string whose length is longer than two.

out the  $\mu$  variables by closing the integration contour from above (or below). Then one shifts the contour of  $k$ 's to the real axis. In this process, if a pole is passed by, the original integral is divided into an integral along the new path and a pole contribution where the integrated variable is fixed by the pole. The latter is related to how the string solutions are formed. In the following, we will elaborate this idea with an example of three majority fermions and two minority fermions with attractive or repulsive interaction respectively. In this example, the initial state is  $|x_1 \uparrow, x_2 \downarrow, x_3 \uparrow, x_4 \downarrow, x_5 \uparrow\rangle$ , with  $x_1 < x_2 < x_3 < x_4 < x_5$ .

First, integrate out  $\mu_1$  and  $\mu_2$  successively by closing their contours from above. As we have shown on page ??, the denominator of the result  $\int \prod_m d\mu_m J(\mu_m) \prod_{m < n} S(\mu_m - \mu_n)$  is the same as that of  $\prod_m \int d\mu_m J(\mu_m)$ . And each  $\int d\mu_m J(\mu_m)$  is a summation over  $2\pi i \text{Res}(J(\mu), \mu = k_i + ic/2)$  for  $i \leq \beta_m$  and  $P^{-1}i \geq \alpha_m$ . The poles of each summand is located at  $k_i - k_j + ic = 0$  for any  $j$  satisfying the condition  $j \geq \beta_m$  and  $P^{-1}j \leq \alpha_m$ . As a result, the poles of  $\int \prod_m d\mu_m J(\mu_m) \prod_{m < n} S(\mu_m - \mu_n)$  are of the form  $k_i - k_j + ic = 0$  with  $i \leq \beta_1 \leq j$  and  $P^{-1}i \geq \alpha_1 \geq P^{-1}j$ , or  $i \leq \beta_2 \leq j$  and  $P^{-1}i \geq \alpha_2 \geq P^{-1}j$ .

For  $c > 0$ , the pole of  $k_i$  at  $k_j - ic$  is located below the  $k_j$  contour. Thus this pole is not encountered if we shift the contours of  $k_i$  and  $k_j$  to the same line. In fact, no pole is caught when one shift all contours to the real axis. For this reason, the only type of string exists, after separating different states apart, is the one with a real  $k_i$  ( $i \leq \beta$  and  $P^{-1}i \geq \alpha$ ) and a complex  $\mu$  at  $k_i + ic/2$ . However, such string depends on how we close the  $\mu$  contours. If we close

both contours from below, we are left with a different string configuration with  $\mu = k_j - ic/2$  for  $j \geq \beta$  and  $P^{-1}j \leq \alpha$ . Physically, it should not matter as how one closes the contour as mathematically it leads to the same result. As we have seen on page ??, the bonds among  $ks$  or among  $\mu s$  are related to bound state. However, the bonds between  $k$  and  $\mu$  do not have any physical effect in real space.

What seems a bit confusing is that the pole of  $\mu_1 = \mu_2 + ic$  does contribute if one close the contour of  $\mu_1$  from below. To understand this, consider the case with  $\alpha_1 = 3$ ,  $\alpha_2 = 2$  and  $P = P_{15}$ . With these conditions, we have

$$\begin{aligned} & S(\mu_1 - \mu_2) \prod_{i=1}^2 J(\mu_i, Pk, \alpha_i) J^*(\mu_i, k, \beta_i) \\ &= \frac{\mu_1 - \mu_2 + ic}{\mu_1 - \mu_2 - ic} \frac{\mu_1 - k_1 + ic/2}{\mu_1 - k_1 - ic/2} \frac{ic}{\mu_1 - k_2 + ic/2} \frac{-ic}{\mu_1 - k_3 + ic/2} \frac{\mu_1 - k_5 - ic/2}{\mu_1 - k_5 + ic/2} \frac{\mu_2 - k_1 + ic/2}{\mu_2 - k_1 - ic/2} \\ & \quad \frac{-ic}{\mu_2 - k_2 - ic/2} \frac{\mu_2 - k_3 + ic/2}{\mu_2 - k_3 - ic/2} \frac{ic}{\mu_2 - k_4 - ic/2} \frac{\mu_2 - k_5 - ic/2}{\mu_2 - k_5 + ic/2} \\ & \equiv I(\mu_1, \mu_2) \end{aligned}$$

The poles of  $\mu_1$  below its integration contour are located at  $k_2 - ic/2$ ,  $k_3 - ic/2$ ,  $k_5 - ic/2$  and  $\mu_2 + ic$ . Thus, the result of the  $\mu_1$  integration consists of the contribution from each of the following terms.

$$\begin{aligned} I_1 &= -2\pi i \text{Res}(I(\mu_1, \mu_2), \mu_1 = k_2 - ic/2) \\ &= 2\pi c \frac{\mu_2 - k_1 + ic/2}{\mu_2 - k_1 - ic/2} \frac{-ic}{\mu_2 - k_2 + 3ic/2} \frac{\mu_2 - k_3 + ic/2}{\mu_2 - k_3 - ic/2} \frac{ic}{\mu_2 - k_4 - ic/2} \frac{\mu_2 - k_5 - ic/2}{\mu_2 - k_5 + ic/2} \\ & \quad \frac{k_2 - k_1}{k_2 - k_1 - ic} \frac{-ic}{k_2 - k_3} \frac{k_2 - k_5 - ic}{k_2 - k_5} \\ I_2 &= -2\pi i \text{Res}(I(\mu_1, \mu_2), \mu_1 = k_3 - ic/2) \\ &= -2\pi c \frac{\mu_2 - k_1 + ic/2}{\mu_2 - k_1 - ic/2} \frac{-ic}{\mu_2 - k_2 - ic/2} \frac{\mu_2 - k_3 + ic/2}{\mu_2 - k_3 + 3ic/2} \frac{ic}{\mu_2 - k_4 - ic/2} \frac{\mu_2 - k_5 - ic/2}{\mu_2 - k_5 + ic/2} \\ & \quad \frac{k_3 - k_1}{k_3 - k_1 - ic} \frac{ic}{k_3 - k_2} \frac{k_3 - k_5 - ic}{k_3 - k_5} \\ I_3 &= -2\pi i \text{Res}(I(\mu_1, \mu_2), \mu_1 = k_5 - ic/2) \\ &= -2\pi c \frac{\mu_2 - k_1 + ic/2}{\mu_2 - k_1 - ic/2} \frac{-ic}{\mu_2 - k_2 - ic/2} \frac{\mu_2 - k_3 + ic/2}{\mu_2 - k_3 - ic/2} \frac{ic}{\mu_2 - k_4 - ic/2} \frac{\mu_2 - k_5 - ic/2}{\mu_2 - k_5 + ic/2} \\ & \quad \frac{\mu_2 - k_5 - ic/2}{\mu_2 - k_5 + 3ic/2} \frac{k_5 - k_1}{k_5 - k_1 - ic} \frac{ic}{k_5 - k_2} \frac{-ic}{k_5 - k_3} \\ I_4 &= -2\pi i \text{Res}(I(\mu_1, \mu_2), \mu_1 = \mu_2 + ic) \\ &= 4\pi c \frac{\mu_2 - k_1 + 3ic/2}{\mu_2 - k_1 - ic/2} \frac{-ic}{\mu_2 - k_2 - ic/2} \frac{ic}{\mu_2 - k_2 + 3ic/2} \frac{\mu_2 - k_3 + ic/2}{\mu_2 - k_3 - ic/2} \frac{-ic}{\mu_2 - k_3 + 3ic/2} \\ & \quad \frac{ic}{\mu_2 - k_4 - ic/2} \frac{\mu_2 - k_5 - ic/2}{\mu_2 - k_5 + 3ic/2} \end{aligned}$$

If one closes the contour of  $\mu_2$  from below, then both  $I_2$  and  $I_4$  consists of a term related to strings of  $\mu_1 - ic = \mu_2 = k_3 - 3ic/2$ . But the sum of the two terms equals zero. Similarly, the  $k - \mu - \mu$  string involving  $k_5$  in  $I_3$  is cancelled by  $I_4$ . There is no other pole contribution that leads to binds between  $\mu_1$  and  $\mu_2$ . Thus, like closing both contours from above, we do not have  $\mu - \mu - k$  strings. However, if we close the contour from above, then the sum of the four terms consists of four  $\mu - \mu - k$  strings of the form  $\mu_1 = \mu_2 + ic = k_i + 3ic/2$  with  $i = 1, 2, 3, 4$  term. Here the  $k$  lies below the  $\mu$  pairs instead of in the middle of it. These strings are not predicted from the Bethe equation and they do not even exist if we close the  $\mu$  contours differently. What is strange about these solutions is that they lead to a result whose denominator has poles at  $k_i - k_j - 2ic$ . This is a new type of pole compared to the matrix form of the Gaudin-Yang solution. But the fact is, if we sum up the contribution from these three strings, these new poles are canceled by the numerator of the sum. This means, the sum of the  $\mu - \mu - k$  strings is equivalent to a collection of states without strings. This does not sounds right at first sight, as we know the  $\mu - \mu - k$  strings relate to bound states between the two down spins, while the states with no bonds among  $k$ 's or  $\mu$ 's are free states. How could a bound state be decomposed into components of free states. In fact, this is quite common. We know an integration over plane wave yields delta function. The situation is similar here. As the energy does not depend on  $\mu$ 's, the bound states keep a coherence phase with all other states. Thus, it is impossible to tell whether the decrease of the wavefunction as the two impurities separate is due to bound states or simply destructive interference among free states. That is to say, the  $\mu - \mu$  string does not play an important role in real space. As there is no  $k - k$  strings when  $c > 0$ , there is no bound states in such system.

When  $c < 0$ , the relative position of the poles for the  $\mu$  integration is the same as before. We still get poles of the form  $k_i - k_j + ic = 0$  for  $i \leq \beta_m \leq j$  and  $P^{-1}i \geq \alpha_m > P^{-1}j$  with  $m$  running through all  $\mu$  indices. Note, if we close the  $\mu$ 's from different directions, we may have other apparent poles that will disappear after summing over all residue contributions. To avoid such complication, we choose to close all  $\mu$  contours from above. What is different with attractive interaction is the pole distribution for the  $k$  integral. Like in the case of the Lieb-Liniger model, the pole of  $k_i$  at  $k_j - ic$  is between the contours of  $k_i$  and  $k_j$ . Thus the original integral separates out a pole contribution after shifting the contours of  $k_i$  and  $k_j$  to the same line. As the appearance of this pole originates from the residue of the  $\mu$  integrand at  $\mu_m = k_i + ic/2$ , this pole contribution yields bonds among  $k_i$ ,  $\mu_m$  and  $k_j$ . Moreover, all roots of the denominator after taking residue at  $\mu_m = k_i + ic/2$  take the form  $k_n = k_i + ic$ . Here  $n$  runs over all indices such that  $n \geq \beta_m$  and  $P^{-1}n \leq \alpha_m$ . Since no two  $k$ s can take the same value,

each  $\mu$  connect at most two  $k$ 's. However when different  $\mu$ 's relate to a same  $k$ , it will snap two  $k - \mu$  strings together to form a longer string. As shown on page ??, such strings involve ambiguity of  $0/0$  in the Bethe equation and are not included as a string solution. However, they do exist in the time evolution of the system.

As an illustration of the above argument, consider the previous example with  $\alpha_1 = 3$ ,  $\alpha_2 = 2$  and  $P = P_{15}$  for  $c < 0$ . Integrating out the  $\mu$  variables from  $I(\mu_1, \mu_2)$ , we obtain

$$\int d\mu_1 \int d\mu_2 I(\mu_1, \mu_2) = \frac{c^4(k_1 - k_5 + 2ic)(k_1 - k_5)(k_3 - k_5)}{(k_1 - k_2 + ic)(k_1 - k_3 + ic)(k_1 - k_5 + ic)^2(k_2 - k_5 + ic)(k_3 - k_5 + ic)(k_4 - k_5 + ic)}$$

After shifting all contours of  $k$ s to the real line, we get extra terms related to pole contributions which are depicted in the graph below. Here the multiple subindex of the  $k$  means a  $k$  with one of the subscripts as long as it does not coincide with any other  $k$  subscripts in the plot. The plot intends to show the relative position among parameters in each strings or pairs. The real part of them is to be integrated over. Any  $k$ 's that are not shown explicitly are assumed to be integrated along the real line.

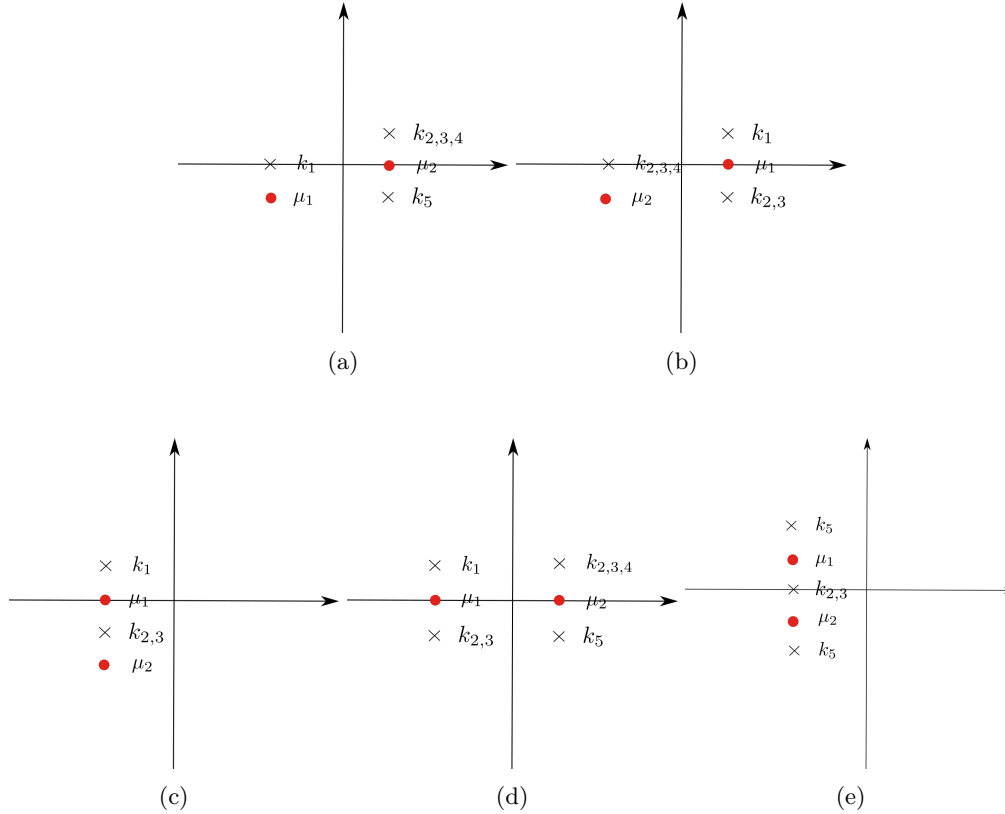


Figure 5.5: String states separated out as a result of closing  $\mu$  contours from above and shifting all  $k$ 's to the real axis. See text for detailed explanation of notations

Figure ??-?? consist of a  $k - \mu$  string and a  $k - \mu$  pair. As discussed on page (??-??), the latter depends on how one closes the integration contour of  $\mu$ 's and has no physical significance. The  $k - \mu$  string describes a bound state among two particles mediated by a spin wave. Figure ?? involve two  $k - \mu$  strings, thus is related to two independent bound states, each intervened by a spin wave. The last plot describes a bound state among three particles which is omitted in the solution of Bethe equations. The necessary condition to form a longer string is the existence of a  $k_i$  such that  $\beta_1 < i < \beta_2$  and  $\alpha_1 > P^{-1}i > \alpha_j$ , which is  $k_2$  and  $k_3$  in this example. This implies that  $\alpha_1 > \alpha_2$ .

In order to interpret these string solutions and the corresponding conditions, we label the particles by their quasimomentum  $ks$ . In the above example, we have  $P = P_{15}$ , thus  $k_1$  couples to  $y_1$  which is the leftmost particle while  $k_5$  couples to  $y_5$  which is the rightmost particle. This happens as a result of the process that particle  $k_5$  swaps with particle  $k_4$  to  $k_1$  successively, then particle  $k_1$  exchanges with  $k_2$  to  $k_4$ . In a nutshell, the permutation in the wavefunction is related to the spacial motion of the particle.  $k_{P_i}$  is the quasimomentum of the  $i$ th particle in the final state.  $P^{-1}i$  is the location of the  $k_i$  particle in that state.

When  $P\alpha = \beta$ , then the spin state of each particle is not changed by the interaction, though the spacial position is different. In this case, the denominator of the  $\mu$  integration consists of both  $\mu - k_\beta - ic/2$  and  $\mu - k_\beta + ic/2$ . Therefore, the function is not analytic no matter how the coutour is closed. Thus the integral does not vanish under any circumstances. This is to say that if the down spin does not transfer to other particles, there is no constraint on the spacial distribution of the particles.

The situation is different if the down spins does move. When  $P\alpha < \beta$ , the down spin transfers to prior particles  $k_{P\alpha}$ . In this case, the denominator consists of factor  $\mu - k_{P\alpha} - ic/2$  and  $\mu - k_\beta - ic/2$ . Both poles are enclosed if the  $\mu$  contour is closed in the upper half plane. Thus the integral will vanish if there is no pole after closing the contour in the other direction. That is to say there must exist a  $k_{P_i}$  such that  $i < \alpha$  and  $Pi \geq \beta$ . This indicates that a particle which is initially the down spin or to the right of it has to move to the left of it in the final state. This makes sense because the particle prior to the impurity can only acquire the spin by passing by a down spin and exchange with it. This may happen in two cases. Either the impurity itself crosses the target particle or the particle after  $\beta$  first passes the impurity and then passes the target particle. Similarly, the particle after the impurity can only obtain the down spin via crossing with the impurity or particles prior to it.

Besides transferring down spins, the interaction can also lead to bound states as we have see above. In order to form a bound state between particle  $i$  and  $j$ , the following condition must be

satisfied  $i \leq \beta \leq j$  and  $P^{-1}i \geq \alpha \geq P^{-1}j$ . Physically, this means one of the following situations. First, one of the up spins may reverse ordering with the down spin to form a bound state with it. Second, the up spin and down spin in the previous case exchange spins while crossing each other. Third, with the up spin particle and the down spin particle crossing each other and binding together, the down spin may be transferred to a particle that lies between them in the final state. Fourth, particle  $i$  and  $j$  that are initially on different side of the down spin each may pass by the impurity to become bound together. Lastly, either particle  $i$  or particle  $j$  in the previous situation may acquire the down spin in the final bound state. See Table 1.

TABLE 1: Mechanism for Bound States Formation

	Initial State	Final State	Bound State Type
$i = \beta < j$ $P^{-1}i = \alpha > P^{-1}j$	$\dots \uparrow \dots \downarrow \dots$ $k_\beta \quad k_j$	$\dots \downarrow \uparrow \dots$ $k_j \quad k_\beta$	Singlet
$i = \beta < j$ $P^{-1}i > \alpha = P^{-1}j$	$\dots \uparrow \dots \downarrow \dots$ $k_\beta \quad k_j$	$\dots \uparrow \downarrow \dots$ $k_j \quad k_\beta$	Singlet
$i = \beta < j$ $P^{-1}i > \alpha > P^{-1}j$	$\dots \uparrow \dots \downarrow \dots$ $k_\beta \quad k_j$	$\dots \uparrow \downarrow \uparrow \dots$ $k_j \quad k_\beta$	Triplet
$i < \beta < j$ $P^{-1}i = \alpha > P^{-1}j$	$\dots \uparrow \dots \downarrow \dots \uparrow \dots$ $k_i \quad k_j$	$\dots \uparrow \downarrow \dots$ $k_j \quad k_i$	Singlet
$i < \beta < j$ $P^{-1}i > \alpha > P^{-1}j$	$\dots \uparrow \dots \downarrow \dots \uparrow \dots$ $k_i \quad k_j$	$\dots \uparrow \downarrow \uparrow \dots$ $k_j \quad k_i$	Triplet

A bound state among more particles can be formed via more spin wave modes. In the example in Figure ??,  $k_1$ ,  $k_2$  and  $k_5$  form a bound state with the help of  $\mu_1$  and  $\mu_2$ . Recall that particle 2 and particle 4 are the down spins and particle arrange themselves in ascending order. In order to form a bound state among particle 1,2 and 5, one needs to reverse the order of particle 1,2,4 and 5. Though particle 4 does not show up in the bound state, the spacial motion of it relative to the particles in the bound state is crucial to the formation of it. Moreover, as particle 4 is sandwiched between particle 2 and particle 5, the wavefunction will also decrease exponentially with the separation between particle 4 and 2 as well as particle 4 and 5. However,

such binds are different to that among  $k_1$ ,  $k_2$  and  $k_5$ . The wavefunction of this bound state consists of the factor  $\exp(ik(y_{P^{1_1}} - x_1 + y_{P^{1_2}} - x_2 + y_{P^{1_5}} - x_5) + c/2(y_{P^{1_1}} - x_1 - y_{P^{1_5}} + x_5)) \exp(ik_4(y_{P^{1_4}} - x_4))$ . Therefore, although particle 4 is bounded with particle 1,2 and 5, it does not move coherently with them and its quasimomentum is different from that of the center of mass of the bound state. Note, such bound state cannot be decomposed into two bound states related to shorter strings, which should take the form  $\exp((ik(y_{P^{1_1}} - x_1 + 2y_{P^{1_2}} - 2x_2 + iy_{P^{1_5}} - x_5) + c/2(y_{P^{1_1}} - x_1 - y_{P^{1_5}} - x_5))$

To sum up, starting from an integral in the complex plane, we have separated out an integral along the real line, i.e. a free state and all string solutions. Some of them are predicted by solving the Bethe equations, which are  $k - \lambda$  strings of length 2. We have also seen  $k - \lambda$  pairs which depend on how one closes the integration contours and do not lead to bound states in real space. Besides, we have noticed that formation of the  $\lambda - k$  strings also depends on the direction to close the  $\lambda$  contour. We have argued that the states related to such string solutions have the same energy as a free states and can be decomposed into the latter. Lastly, we obtain  $k - \lambda$  strings which are longer than 2 which lead to bound states among more particles. Moreover, we have discussed how bound states are formed and the important role of the down spin in such process. In the next section, we will apply the Yudson representation to the calculations of observables.

## Time Evolution

As shown in the previous sections, the Yudson representation provides us with an expansion of a state into components that are eigenstates of the Hamiltonian. Each component evolves with the factor  $e^{-iEt}$  with  $E$  being the eigenenergy of the basis state. Theoretically, this representation solves the time evolution of any initial state. However, due to the complication discussed on page (??-??), we will consider only the case where particles are well separated. If we describe each particle as a Gaussian wavepacket with width  $\sigma$ , the initial state  $|\phi_0\rangle$  can be described as

$$|\phi_0\rangle = |x, \beta\rangle = \frac{1}{(\pi\sigma^2)^{N/4}} e^{-\sum_i^N \frac{(x_i - x_{i0})^2}{2\sigma^2}} \prod_{n=1}^M \sigma_{\beta_n}^- \prod_{i=1}^N \Psi_{\uparrow}^{\dagger}(x_i) |0\rangle$$

with  $x_{(i+1)0} - x_{i0} > 3\sigma$ . In the following calculation, we will exploit such relation and drop terms of order equal or higher than  $O(e^{-\frac{(x_{i0} - x_{j0})^2}{4\sigma^2}})$ . If we neglect those small terms, then the

time evolution of  $|\phi_0\rangle$  can be obtained via the Yudson Representation as

$$|\phi(t)\rangle = \frac{(4\pi\sigma^2)^{\frac{N}{4}}}{(2\pi)^{M+N}c^M} \sum_{\alpha} \int dy \int_C dk \int_{C'} d\mu \sum_P e^{-i\sum_i k_i^2(t+\sigma^2/2i)+ik_i(y_{P^{-1}i}-x_i)} \prod_{m=1}^M I(\mu_m, kP, \alpha_m) I^*(\mu_m, k, \beta_m)\theta(y)\theta(\alpha)|y, \alpha\rangle$$

with

$$I(\mu, k, \alpha) = \frac{-ic}{\mu - k_{\alpha} + ic/2} \prod_{n < \alpha} \frac{\mu - k_n - ic/2}{\mu - k_n + ic/2}$$

Like in the case of Lieb-Liniger model, only the wavefunction of two particle systems has closed form. We have to take asymptotic approximation to study systems with more particles. In the following, we will study systems with two particles and more particles successively.

### 5.3 Two Distinguishable Particle Case

In this section, we will consider the time evolution of a two particle system. In the initial state, the down spin sits to the left of the up spin, i.e.  $\beta = 1$ . Then at  $t > 0$ , the state becomes

$$|\phi(t)\rangle = \int dy_1 dy_2 f_{\uparrow, \downarrow}(y_1, y_2) \Psi_{\uparrow}^{\dagger}(y_1) \Psi_{\downarrow}^{\dagger}(y_2) |0\rangle$$

$$\begin{aligned} & f_{\uparrow, \downarrow}(y_1, y_2) \\ &= \frac{\sqrt{4\pi\sigma^2}}{(2\pi)^2} \int dk_1 dk_2 e^{-ik_1^2(t+\sigma^2/2i) - ik_2^2(t+\sigma^2/2i)} (e^{ik_1(y_2-x_1)+ik_2(y_1-x_2)} (\frac{k_1 - k_2}{k_1 - k_2 + ic} \\ & \quad \theta(y_2 - y_1) + \theta(y_1 - y_2)) - e^{ik_1(y_1-x_1)+ik_2(y_2-x_2)} \frac{ic}{k_1 - k_2 + ic} \theta(y_1 - y_2)) \\ &= \frac{\sigma}{2\sqrt{\pi}i(t+\sigma^2/2i)} (e^{\frac{i(y_2-x_1)^2}{4(t+\sigma^2/2i)} + \frac{i(y_1-x_2)^2}{4(t+\sigma^2/2i)}} (1 \mp \theta(y_2 - y_1)c(1+i)/2\sqrt{\pi(t+\sigma^2/2i)} \operatorname{erfc}(\pm\alpha_1)e^{\alpha_1^2}) \\ & \quad \mp e^{\frac{i(y_1-x_1)^2}{4(t+\sigma^2/2i)} + \frac{i(y_2-x_2)^2}{4(t+\sigma^2/2i)}} \theta(y_1 - y_2)c(1+i)/2\sqrt{\pi(t+\sigma^2/2i)} \operatorname{erfc}(\pm\alpha_2)e^{\alpha_2^2}) \end{aligned}$$

With

$$\alpha_1 = \frac{(1-i)(y_2 - x_1 - y_1 + x_2 + 2ic(t + \sigma^2/2i))}{4\sqrt{t + \sigma^2/2i}}$$

$$\alpha_2 = \frac{(1-i)(y_1 - x_1 - y_2 + x_2 + 2ic(t + \sigma^2/2i))}{4\sqrt{t + \sigma^2/2i}}$$

The  $\pm$  sign results from the ambiguity of pulling out the  $i$  from the square root. Depending on the phase of  $\alpha_{1,2}$ , the signs are chosen as follows

1. When  $c > 0$ ,  $|\operatorname{ph}(\alpha_{1,2})| \in (0, \pi/4)$ . The upper sign is chosen.
2. When  $c < 0$  and  $|c| > 2a/\sigma^2$ ,  $|\operatorname{ph}(\alpha_{1,2})| \in (\frac{1}{4}\pi, \pi)$ . The lower sign is chosen

3. When  $c < 0$  and  $|c| < 2a/\sigma^2$ ,  $\text{ph}(\alpha_{1,2}) \in (\frac{1}{4}\pi, \frac{3}{4}\pi)$ , the upper sign is chosen

The choice is made based on the following properties of the complementary error function, as listed in [?, Eq. 7.12.1]

- (a)  $\text{erfc}(z)e^{z^2}$  diverges in region  $|\text{ph}(z)| \geq \frac{3}{4}\pi$ .
- (b)  $\text{erfc}(z)e^{z^2} \approx \frac{1}{\sqrt{\pi}} \sum_{m=0}^{\infty} (-1)^m \frac{(\frac{1}{2})_m}{z^{2m+1}}$  for  $|\text{ph}(z)| < \frac{3}{4}\pi$
- (c) When  $|\text{ph}(z)| < \frac{\pi}{2}$ , the remainder terms are bounded by the first dropped terms times  $\text{csc}(2\text{ph}(z))$ .
- (d)  $\text{erfc}(z) = 2 - \text{erfc}(-z)$

The first property is enough to fix the sign of the first situations, as the opposite sign makes the function divergent. Property (a) and (d) determines the sign of the second case. To see this, the real part of  $\alpha_{1,2}/(1-i)$  is negative when  $|y_2 - y_1| < |c|\sigma^2/2 - a$ . This means  $|\text{ph}(\alpha_{1,2})| \in (3\pi/4, \pi)$ . To avoid divergence, the lower sign is chosen. At the same time  $\text{erfc}(z) \neq \text{erfc}(-z)$  when  $\Re(z) = 0$ . To make the wavefunction smooth, one need to impose the lower sign for all region of the arguments. For the last scenario, the function behaves well with either sign, and one needs to take into account the rest of the properties. As we have shown, the attractive systems has bound states. These bound states should separate apart with the free state for large time. With our choice, when  $t$  is large,  $|\text{ph}(\alpha_{1,2})| \rightarrow 3\pi/4^-$ . Thus,  $\text{erfc}(\alpha)e^{\alpha^2} \approx 2e^{\alpha^2} - 1/(\sqrt{\pi}\alpha)$ , where the first term corresponds to a bound state with factor  $\exp(-|c|(|y_2 - y_1| + a))$  and the second one is related to a free state which is identical to the repulsive solution. Note, when the attraction is too strong which corresponds to the second category,  $|\text{ph}(\alpha_{1,2})| \rightarrow \pi/4$  when  $t \gg 1$ , thus there is no bound state in the systems.

When  $c = 0$ , the wavefunction simplifies into

$$f_{\uparrow,\downarrow}(y_1, y_2) = \frac{\sigma}{2\sqrt{\pi}i(t + \sigma^2/2i)} e^{\frac{i(y_2 - x_1)^2}{4(t + \sigma^2/2i)} + \frac{i(y_1 - x_2)^2}{4(t + \sigma^2/2i)}}$$

In this case, the density and correlation can be calculated easily.

$$\langle \rho_{\uparrow}(y) \rangle = \frac{\sigma}{2\sqrt{\pi}(t^2 + \sigma^4/4)} e^{-\frac{\sigma^2(y - x_1)^2}{4(t^2 + \sigma^4/4)}} \quad (5.5)$$

$$\langle \rho_{\downarrow}(y) \rangle = \frac{\sigma}{2\sqrt{\pi}(t^2 + \sigma^4/4)} e^{-\frac{\sigma^2(y - x_2)^2}{4(t^2 + \sigma^4/4)}} \quad (5.6)$$

$$\langle \rho_{\uparrow}(y_1)\rho_{\downarrow}(y_2) \rangle = \frac{\sigma^2}{4\pi(t^2 + \sigma^4/4)} e^{-\frac{\sigma^2(y_2 - x_1)^2}{4(t^2 + \sigma^4/4)} - \frac{\sigma^2(y_1 - x_2)^2}{4(t^2 + \sigma^4/4)}}$$

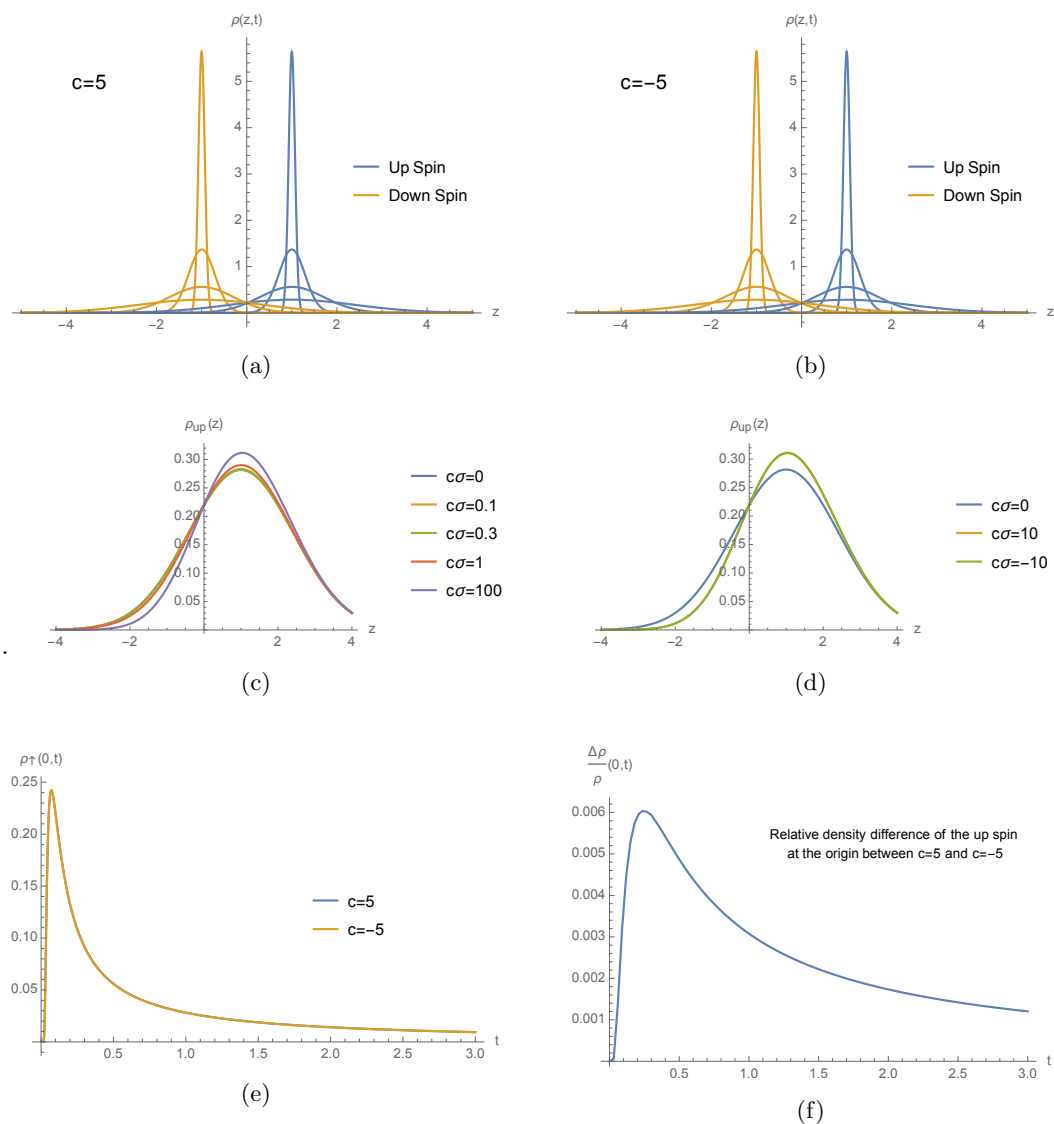


Figure 5.6: Time evolution of density distribution. Figure ?? and ?? shows Time evolution of down spin (yellow) and up spin (blue) at  $t = 0, 0.02, 0.05, 0.1$  for  $c = 5$  and  $c = -5$  respectively. Figure ?? and ?? compare the density of the up spin for different interaction. Figure ?? compares the density of the up spin at the origin between  $c = 5$  and  $c = -5$  cases. Figure ?? shows the relative density difference of the up spin between  $c = 5$  and  $c = -5$  at the origin.

For interacting systems, it is hard to derive the closed form for density and correlation. We will instead resort to numeric method to study these properties. Figure ?? and ?? show the time evolution of the down spin in yellow and the up spin in blue. Figure ?? is for systems with attractive interaction and Figure ?? is for repulsive case. Both particles in these two plots behave as free particles described by equation (??) and (??). This is ascribed to the same reason as in the Lieb-Liniger model, i.e. the particles avoid overlap that leads to energy change. Thus the contact interaction does not affect the behavior of the particles significantly. In Figure ?? and ??, we further compare the density of the up spin at the origin as a function of time for  $c = 5$  and  $c = -5$ . We see that the interaction does not affect this quantity significantly with maximum relative difference being less than 1%. This difference is even less than in the Lieb-Liniger model where the two particles are indistinguishable.

Figure ?? shows the normalized correlation function between the up spin and down spin.  $C(z/t, -z/t, t) = \frac{\langle \rho_{\uparrow}(z/t) \rho_{\downarrow}(-z/t, t) \rangle}{\langle \rho_{\uparrow}(z/t) \rangle \langle \rho_{\downarrow}(-z/t) \rangle} - 1 = \frac{\langle \delta \rho_{\uparrow}(z/t) \delta \rho_{\downarrow}(-z/t) \rangle}{\langle \rho_{\uparrow}(z/t) \rangle \langle \rho_{\downarrow}(-z/t) \rangle}$  On the positive side, the function oscillates as in the Lieb-Liniger model. This corresponds to the case where the up spin remains to the left of the down spins. The oscillation results from the superposition of two terms in the wavefunction, one without particle crossing or spin exchange, one with both of them. The lower envelop is the same as the correlation function on the negative side. It saturates to a curve originating from  $-1$  at  $z = 0$ . The curve depends on the width  $\sigma$  in the initial state. The upper envelop increases with time, meaning a stronger correlation as time goes on. The phase of the function is different for various type of interaction. The changing rates of the phase are also different. Phase of the attractive case evolves faster than that of the repulsive case. On the negative side, the function does not oscillate. This is corresponds to a down spin exchanges position with the up spin. There is only one term in the wavefunction in this scenario, i.e. the particle crosses with each other without spin exchange. This explains the behavior of the function on this side. The correlation at  $z = 0$  shows interesting behavior for different time. When  $t = 0.02$ , the correlation is positive with attractive interaction and is negative with repulsive interaction. However, correlations for both cases approach  $-1$  with greater time. Its explanation is as follows. When  $t$  is close to 0, the wavefunction is close to the initial state we have prepared, a state with some overlap between the particles. Therefore, the interaction determines the correlation between density fluctuation. Then the wavefunction evolves into a state with less overlap between the two particles, which means the correlation function approaches  $-1$ . When time is large enough, the correlation at  $z = 0$  saturated at  $-1$ , where the interaction no longer affects the correlation as there is no contact between the particles.

The behavior in the vicinity of the origin can be understood by studying the correlation of

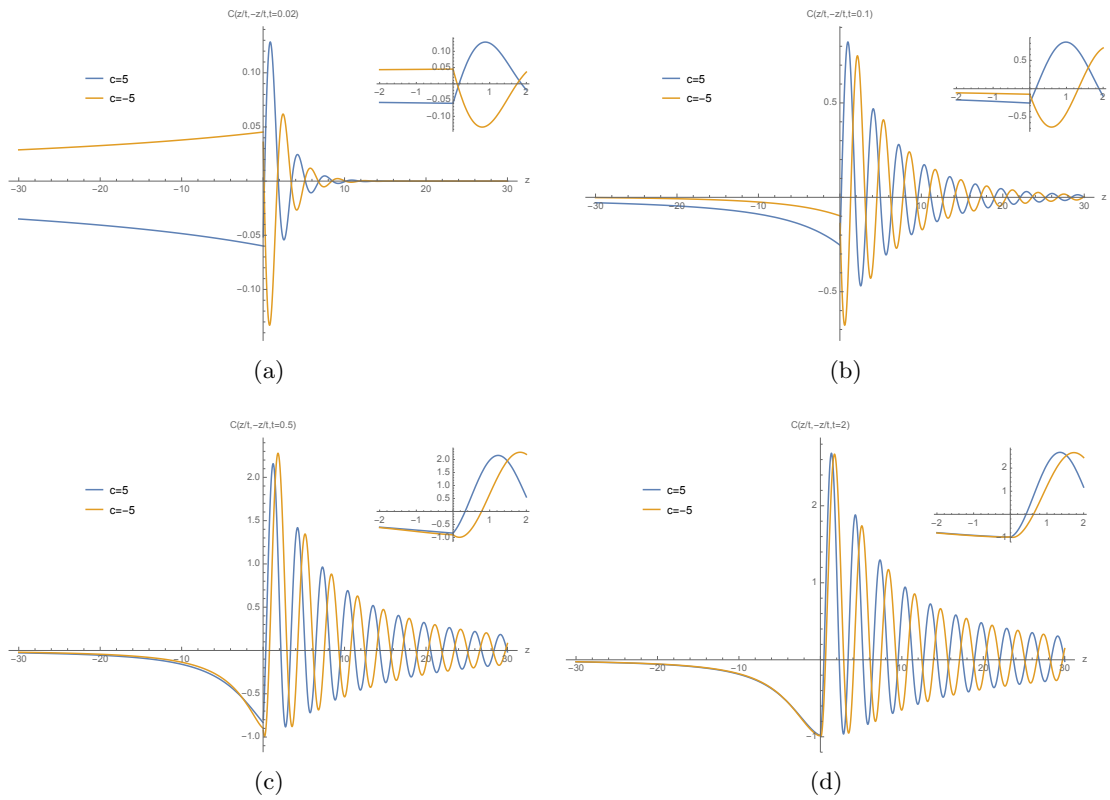


Figure 5.7: Normalized noise correlation for a two-particle system with one up spin and one down spin. The down spin is initially to the left to the up spin. The figure shows the correlation at  $t = 0.02$ (a),  $0.1$ (b),  $0.5$ (c) and  $2$ (d) respectively.

a general Bethe Ansatz eigenstate,  $|k_1, k_2, \mu\rangle$ . For such state, the correlation equals

$$\begin{aligned}
& \langle \rho_\uparrow(x_1) \rho_\downarrow(x_2) \rangle \\
&= \theta(x_1 - x_2) \left| e^{ik_1x_1 + ik_2x_2} \frac{ic}{\mu - k_1 + ic/2} + e^{ik_1x_2 + ik_2x_1} \frac{-ic}{\mu - k_2 + ic/2} \right|^2 + \theta(x_2 - x_1) \\
& \left| e^{ik_1x_1 + ik_2x_2} \frac{-ic}{\mu - k_2 + ic/2} \frac{\mu - k_1 - ic/2}{\mu - k_1 + ic/2} + e^{ik_2x_1 + ik_1x_2} \frac{ic}{\mu - k_1 + ic/2} \frac{\mu - k_2 - ic/2}{\mu - k_2 + ic/2} \right|^2 \\
&= \frac{c^2}{(\mu - k_1)^2 + c^2} + \frac{c^2}{(\mu - k_2)^2 + c^2} - \frac{c^2}{(\mu - k_1 + ic/2)(\mu - k_2 - ic/2)} e^{i(k_1 - k_2)|x_1 - x_2|} \\
& \quad - \frac{c^2}{(\mu - k_1 - ic/2)(\mu - k_2 + ic/2)} e^{-i(k_1 - k_2)|x_2 - x_1|}
\end{aligned} \tag{5.7}$$

Thus, close to the origin, the correlation has the following limit

$$\begin{aligned}
\lim_{x_1 \rightarrow x_2} \langle \rho_\uparrow(x_1) \rho_\downarrow(x_2) \rangle &= \frac{c^2}{(\mu - k_1)^2 + c^2} + \frac{c^2}{(\mu - k_2)^2 + c^2} + \frac{c^3(k_1 - k_2)^2|x_1 - x_2|}{((\mu - k_1)^2 + c^2)((\mu - k_2)^2 + c^2)} \\
& \quad + O((x_1 - x_2)^2)
\end{aligned}$$

From the above expressions, we can see that the correlation goes up on the left side of the origin for  $c > 0$  and goes down for  $c < 0$ . The situation is opposite on the other side. This is true for any state which is not bound state. Thus, the time evolved state, which is a superposition of those states should follow the same trend. This is indeed what we see in plot ??.

The result ?? does not work for bound state  $|k_1 = \mu - ic/2, k_2 = \mu + ic/2, \mu\rangle$ . Using the fact that  $k_1^* = k_2$ ,  $\langle \rho_\uparrow(x_1) \rho_\downarrow(x_2) \rangle$  can be obtained as

$$\begin{aligned}
& \langle \rho_\uparrow(x_1) \rho_\downarrow(x_2) \rangle \\
&= - \frac{c^2}{(\mu - k_1)^2 + c^2/4} - \frac{c^2}{(\mu - k_2)^2 - c^2/4} + \frac{c^2}{(\mu - k_1 - ic/2)(\mu - k_2 + ic/2)} \\
& \quad e^{i(k_1 - k_2)|x_1 - x_2|} + \frac{c^2}{(\mu - k_1 + ic/2)(\mu - k_2 - ic/2)} e^{-i(k_1 - k_2)|x_1 - x_2|}
\end{aligned}$$

Taking the limit  $k_1 = \mu - ic/2$  and  $k_2 = \mu + ic/2$ , this simplifies into

$$\lim_{\substack{k_1 = \mu - ic/2 \\ k_2 = \mu + ic/2}} \langle \rho_\uparrow(x_1) \rho_\downarrow(x_2) \rangle = \lim_{\substack{k_1 = \mu - ic/2 \\ k_2 = \mu + ic/2}} \frac{c^2}{(\mu - k_1 - ic/2)(\mu - k_2 + ic/2)} e^{c|x_1 - x_2|}$$

The density, at the same time, becomes

$$\lim_{\substack{k_1 = \mu - ic/2 \\ k_2 = \mu + ic/2}} \langle \rho_\uparrow(x_1) \rangle = \lim_{\substack{k_1 = \mu - ic/2 \\ k_2 = \mu + ic/2}} \langle \rho_\downarrow(x_1) \rangle = \lim_{\substack{k_1 = \mu - ic/2 \\ k_2 = \mu + ic/2}} \frac{-2c}{(\mu - k_1 - ic/2)(\mu - k_2 + ic/2)}$$

Renormalise the density and noise correlation function such that each density integration over the whole space yields one. Then the normalised noise correlation function becomes

$$\lim_{L \rightarrow \infty} \lim_{\substack{k_1 = \mu - ic/2 \\ k_2 = \mu + ic/2}} \frac{\langle \rho_\uparrow(x_1) \rho_\downarrow(x_2) \rangle}{\langle \rho_\uparrow(x_1) \rangle \langle \rho_\downarrow(x_2) \rangle} = \lim_{L \rightarrow \infty} \frac{L|c|}{2} e^{-|c||x_1 - x_2|}$$

Like in the Lieb-Liniger model, the normalized noise correlation function fades away exponentially with the separation between the two particles. However, the correlation suffer divergence problems. We have not seen character of these bound states in Figure ??, indicating that these states are suppressed and overlap between particles are avoided. This completes our discussion of the two particle case.

We will move on to systems with more particles.

## 5.4 One Impurity in Multi-particle Bath

In this section, we will discuss the time evolution of systems with more particles and one impurity. The wavefunction in this case equals

$$f(y, \alpha, t) = \frac{(4\pi\sigma^2)^{N/4}}{(2\pi)^{N+1}c} \int_C dk \int_{C'} d\mu \sum_P (-1)^P e^{-i\sum_i k_i^2(t+\sigma^2/2i) + i\sum_i k_i(y_{P^{-1}i} - x_i)} I(\mu, Pk, \alpha) I^*(\mu, k, \beta)$$

$$I(\mu, k, \alpha) = \frac{-ic}{\mu - k_\alpha + ic/2} \prod_{n < \alpha} \frac{\mu - k_n - ic/2}{\mu - k_n + ic/2}$$

The  $k$  integrals do not have closed form solution and we will apply the saddle point approximation happened at  $k_i = \frac{y_{P^{-1}i} - x_i}{2t}$  which is further simplified into  $k_i = y_{P^{-1}i}/2t = \xi_{P^{-1}i}$  for large time. Thus, the wavefunction can be written as

$$f(\xi, \alpha, t) = \frac{\sigma^{\frac{N}{2}}}{2^{\frac{N}{2}+1} \pi^{\frac{N}{4}+1} c(it)^{\frac{N}{2}}} \int_\mu e^{\sum_i it\xi_i^2 - \xi_i^2\sigma^2/2 - i\xi_i x_{P_i}} (-1)^P \theta(\xi_1 < \dots < \xi_N) I(\mu, \alpha, \xi) I^*(\mu, \beta, P^{-1}\xi)$$

As we what did for the one impurity cases, the  $\mu$  integration equals the sum over pole contributions, i.e.  $\int_\mu I(\mu, \alpha, \xi) I^*(\mu, \beta, P^{-1}\xi) = 2\pi i \sum_o R(\xi_o + ic/2)$ . Here the  $R(\xi_o + ic/2)$  is the residue term whose expression depends on the relation among  $\alpha$  and  $P^{-1}\beta$ .

If  $o = \alpha = P^{-1}\beta$ , then

$$R(\xi_o + ic/2) = -ic \sum_{\substack{t_1 \in P(S_1) \\ t_2 \in P(S_2)}} \prod_{u \in t_1} \frac{-ic}{\xi_o - \xi_u + ic} \prod_{v \in t_2} \frac{ic}{\xi_o - \xi_{P^{-1}v}}$$

If  $o = P^{-1}\beta \neq \alpha$  and  $P^{-1}\beta > \alpha$  then

$$R(\xi_o + ic/2) = ic \frac{-ic}{\xi_o - \xi_\alpha + ic\theta(P\alpha - \beta)} \sum_{\substack{t_1 \in P(S_1) \\ t_2 \in P(S_2)}} \prod_{u \in t_1} \frac{-ic}{\xi_o - \xi_u + ic} \prod_{v \in t_2} \frac{ic}{\xi_o - \xi_{P^{-1}v}}$$

If  $o = \alpha$  and  $P\alpha < \beta$ , then

$$R(\xi_o + ic/2) = ic \frac{-ic}{\xi_o - \xi_{P^{-1}\beta} + ic\theta(\alpha - P^{-1}\beta)} \sum_{\substack{t_1 \in P(S_1) \\ t_2 \in P(S_2)}} \prod_{u \in t_1} \frac{-ic}{\xi_o - \xi_u + ic} \prod_{v \in t_2} \frac{ic}{\xi_o - \xi_{P^{-1}v}}$$

If  $o \neq \alpha$  and  $P\alpha = \beta$ , then

$$R(\xi_o + ic/2) = ic \frac{-ic}{\xi_o - \xi_\alpha + ic} \frac{ic}{\xi_o - \xi_\alpha} \sum_{\substack{t_1 \in P(S_1) \\ t_2 \in P(S_2)}} \prod_{u \in t_1} \frac{-ic}{\xi_o - \xi_u + ic} \prod_{v \in t_2} \frac{ic}{\xi_o - \xi_{P^{-1}v}}$$

If  $o \neq \alpha$  and  $o \neq P^{-1}\beta$  and  $P\alpha \neq \beta$ , then

$$R(\xi_o + ic/2) = -ic \frac{-ic}{\xi_o - \xi_\alpha + ic\theta(P\alpha - \beta)} \frac{ic}{\xi_o - \xi_{P^{-1}\beta} + ic\theta(\alpha - P^{-1}\beta)} \sum_{\substack{t_1 \in P(S_1) \\ t_2 \in P(S_2)}} \prod_{u \in t_1} \frac{-ic}{\xi_o - \xi_u + ic} \prod_{v \in t_2} \frac{ic}{\xi_o - \xi_{P^{-1}v}}$$

with  $P(S)$  being all subsets of  $S$  and  $S_1 = \{m | m < \alpha \text{ and } Pm > \beta\}$ ,  $S_2 = \{n | n < \beta \text{ and } P^{-1}n > \alpha\}$ . In the following, we will talk about the calculation of density and correlation function. The basis of it is  $|f(\xi, \alpha, t)|^2$  which we will write down explicitly as

$$|f(\xi, \alpha, t)|^2 = \frac{\sigma^N}{2^N \pi^{\frac{N}{2}} t^N c^2} \sum_{P, P'} e^{\sum_i -\sigma^2 \xi_i^2 - i\xi_i(x_{P_i} - x_{P'_i})} (-1)^{P+P'} \theta(\xi_1 < \dots < \xi_N) \sum_{o, e} R(\xi_o + ic/2) R^*(\xi_e - ic/2)$$

In order to obtain observables, one needs to integrate out dummy variables in the above expression. First, we impose the condition that  $x_{P_i} = x_{P'_i}$  if  $\xi_i$  is integrated over without  $\delta$  function. The oscillation related to these terms makes the contribution small by a factor of  $e^{-|c|a}$ . Moreover, the number of terms from  $R(\xi_o + ic/2)R^*(\xi_e - ic/2)$  is as many as  $N^2(N!)^2$ . It becomes difficult to keep track of all of them when the number of particles is large. To make the calculation tractable, we only keep the terms in which  $R(\xi_o + ic/2)R^*(\xi_e - ic/2)$  does not depend on any dummy variables. This leads to approximations in the leading order of  $c\sigma$ . We have checked the contribution of these small terms in a small system ( $N = 3$ ). These dropped terms turn out to be small up to  $(c\sigma)^4$ . In the following calculation, we will exploit these two simplifications.

## Density

The density can be obtained as  $\rho_\downarrow(z) = \int_\xi \sum_\alpha |f(\xi, \alpha, t)|^2 \delta(\xi_\alpha - z/2t)$ . The leading order term comes from  $e = o = \alpha = P^{-1}\beta$  when  $R(\xi_o + ic/2) = -ic$ . All other terms depend on at least

two variables, one of which is a dummy variable. Moreover,  $Pi = P'i$  for any  $i \neq \alpha$  indicates that  $P = P'$ . Thus we have

$$\begin{aligned}\rho_{\downarrow}(x) &= \frac{\sigma^N}{2\pi^{\frac{N}{2}}t} \int_{\xi} \sum_{\alpha, P} e^{-\sum_i \sigma^2 \xi_i^2} \theta(\xi_1 < \dots < \xi_N) \delta(\xi_{\alpha} - z/2t) \delta_{P\alpha, \beta} \\ &= \frac{\sigma^N}{2\pi^{\frac{N}{2}}t} \int_{\zeta} e^{-\sum_i \sigma^2 \zeta_i^2} \delta(\zeta_{\beta} - z/2t) \sum_P \theta(\zeta_{P1} \dots \zeta_{PN}) \\ &= \frac{\sigma}{2\sqrt{\pi t}} e^{-\frac{z^2 \sigma^2}{4t^2}}\end{aligned}$$

In the second line, we replaced  $\xi_i$  by  $\zeta_{Pi}$ . Then we made use of the fact that  $\sum_P \theta(\zeta_{P1} \dots \zeta_{PN}) = 1$  to remove summation over  $P$  and  $\theta$ -function. The result we got is a simple gaussian wavepacket as in the case of the Lieb-Liniger model. That is to say, the down spin diffuses as if isolated. Similarly, we have  $\rho_{\uparrow}(z) = \frac{(N-1)\sigma}{2\sqrt{\pi t}} e^{-\frac{\sigma^2 z^2}{4t^2}}$ .

### Noise Function

To calculate noise function, we first derive the correlation function defined as  $\rho_{\downarrow}(z)\rho_{\uparrow}(z') = \int_{\xi} \sum_{\alpha, i} |f(\xi, \alpha, t)|^2 \delta(\xi_{\alpha} - z/2t) \delta(\xi_i - z'/2t)$ . Again,  $x_{Pj} = x_{P'j}$  is assumed for  $j \neq \alpha$  or  $i$ . Moreover, only terms in  $R(\xi_o + ic/2)R^*(\xi_e - ic/2)$  that do not depend these  $\xi_j$  are included to account for the leading order term when  $\sigma$  is small. These terms are

$$\begin{aligned}R(\xi_o + ic/2) &\rightarrow \\ &-ic\delta_{\alpha, P^{-1}\beta} \left(1 + \frac{-ic}{\xi_{\alpha} - \xi_i + ic} \theta(\alpha - i) \theta(Pi - \beta) + \frac{ic}{\xi_{\alpha} - \xi_i} \theta(\beta - Pi) \theta(i - \alpha) - \frac{-ic}{\xi_i - \xi_{\alpha} + ic} \right. \\ &\frac{ic}{\xi_i - \xi_{\alpha}} \theta(\beta - Pi) \theta(i - \alpha) \left. \right) + ic\delta_{\beta, Pi} \left( \frac{-ic}{\xi_{P^{-1}\beta} - \xi_{\alpha}} \theta(P^{-1}\beta - \alpha) \theta(\beta - P\alpha) + \frac{-ic}{\xi_{P^{-1}\beta} - \xi_{\alpha} + ic} \right. \\ &\theta(P^{-1}\beta - \alpha) \theta(P\alpha - \beta) + \frac{-ic}{\xi_{\alpha} - \xi_{P^{-1}\beta}} \theta(P^{-1}\beta > \alpha) \theta(P\alpha < \beta) + \frac{-ic}{\xi_{\alpha} - \xi_{P^{-1}\beta} + ic} \theta(\alpha - P^{-1}\beta) \\ &\theta(\beta - P\alpha) \left. \right) \\ &= -ic\delta_{P\alpha, \beta} \left(1 + \frac{-ic}{\xi_{\alpha} - \xi_i + ic} \theta(\alpha - i) \theta(Pi - \beta) + \frac{-ic}{\xi_i - \xi_{\alpha} + ic} \theta(\beta - Pi) \theta(i - \alpha) \right) \\ &+ ic\delta_{\beta, Pi} \left( \frac{-ic}{\xi_{P^{-1}\beta} - \xi_{\alpha} + ic} \theta(P^{-1}\beta - \alpha) \theta(P\alpha - \beta) + \frac{-ic}{\xi_{\alpha} - \xi_{P^{-1}\beta} + ic} \theta(\alpha - P^{-1}\beta) \theta(\beta - P\alpha) \right)\end{aligned}$$

Thus, the leading order term in the correlation function equals

$$\begin{aligned}
& \rho_{\downarrow}(z)\rho_{\uparrow}(z') \\
&= \frac{\sigma^N}{4\pi^{N/2}t^2} \int_{\xi} \sum_{P,P'} e^{-\sum_i \sigma^2 \xi_i^2 - i \sum_i \xi_i (x_{P_i} - x_{P'_i})} (-1)^{P+P'} \theta(\xi_1 < \dots < \xi_N) \delta(\xi_{\alpha} - z/2t) \sum_i \delta(\xi_i - z'/2t) \\
& \left| \theta(z - z') \left( \theta(\beta - Pi) \delta_{P\alpha,\beta} + \frac{z - z'}{z - z' + 2ict} \theta(Pi - \beta) \delta_{P\alpha,\beta} + \frac{-2ict}{z - z' + 2ict} \theta(\beta - P\alpha) \delta_{P_i,\beta} \right) \right. \\
& \quad \left( \theta(\beta - P'i) \delta_{P'\alpha,\beta} + \frac{z - z'}{z - z' - 2ict} \theta(P'i - \beta) \delta_{P'\alpha,\beta} + \frac{2ict}{z - z' - 2ict} \theta(\beta - P'\alpha) \delta_{P'_i,\beta} \right) \\
& + \theta(z' - z) \left( \theta(Pi - \beta) \delta_{P\alpha,\beta} + \frac{z - z'}{z' - z + 2ict} \theta(\beta - Pi) \delta_{P\alpha,\beta} + \frac{-2ict}{z' - z + 2ict} \theta(P\alpha - \beta) \delta_{\beta,P_i} \right) \\
& \quad \left. \left( \theta(Pi - \beta) \delta_{P\alpha,\beta} + \frac{z - z'}{z' - z + 2ict} \theta(\beta - Pi) \delta_{P\alpha,\beta} + \frac{2ict}{z' - z + 2ict} \theta(P\alpha - \beta) \delta_{\beta,P_i} \right) \right|^2 \\
&= \frac{\sigma^2}{4\pi t^2} e^{-\frac{\sigma^2(z^2+z'^2)}{4t^2}} \times \\
& \left( \theta(z - z') \left( \left( 1 + \frac{4t^2 c^2}{(z - z')^2 + 4t^2 c^2} \right) (\beta - 1) + (N - \beta) \frac{(z - z')^2}{(z - z')^2 + 4t^2 c^2} - 2\text{Im} \left( \frac{2tc}{z - z' - 2itc} \right) \right. \right. \\
& \quad \left. \frac{e^{-\frac{i(z-z')\alpha}{2t}} - e^{-\frac{i(z-z')\beta\alpha}{2t}}}{1 - e^{-\frac{i(z-z')\alpha}{2t}}} \right) \\
& + \theta(z' - z) \left( \left( 1 + \frac{4t^2 c^2}{(z - z')^2 + 4t^2 c^2} \right) (N - \beta) + (\beta - 1) \frac{(z - z')^2}{(z - z')^2 + 4t^2 c^2} - 2\text{Im} \left( \frac{2tc}{z - z' - 2itc} \right) \right. \\
& \quad \left. \left. \frac{e^{-\frac{i(z-z')\alpha}{2t}} - e^{-\frac{i(z-z')(N-\beta+1)\alpha}{2t}}}{1 - e^{-\frac{i(z-z')\alpha}{2t}}} \right) \right)
\end{aligned}$$

The final expression is obtained by imposing the condition that  $x_{P_j} = x_{P'_j}$  for any  $j \neq \alpha$  or  $i$ . Due to this condition, some terms do not contribute in the final result. As an example, we will consider the term which corresponds to the second term in the first parenthesis multiplied by the last term in the second, i.e.

$$\begin{aligned}
& \frac{\sigma^N}{4\pi^{N/2}t^2} \int_{\xi} \sum_{P,P'} e^{-\sum_i \sigma^2 \xi_i^2 - i \sum_i \xi_i (x_{P_i} - x_{P'_i})} (-1)^{P+P'} \theta(\xi_1 < \dots < \xi_N) \delta(\xi_{\alpha} - z/2t) \sum_i \delta(\xi_i - z'/2t) \\
& \quad \theta(z - z') \frac{-2ict}{z - z' + 2ict} \frac{2ict}{z - z' - 2ict} \theta(Pi - \beta) \delta_{P\alpha,\beta} \theta(\beta - P'\alpha) \delta_{P'_i,\beta}
\end{aligned}$$

As  $P\alpha = P'i = \beta$  and  $Pj = P'j$  for  $j \neq \alpha$  and  $i$ , we have  $Pi = P'\alpha$ . This contradicts with the two heaviside functions. Thus, this term is not included in the result. As a simple check, we can set  $c = 0$ , then we have  $\rho_{\downarrow}(z)\rho_{\uparrow}(z') = e^{-\frac{\sigma^2(z^2+z'^2)}{4t^2}} (N - 1)$  which is what we expect of a non-interacting system. As a last step, we are going to write down the noise function, which equals  $C(z, z', t) = \frac{\langle \rho_{\downarrow}(z)\rho_{\uparrow}(z') \rangle}{(N-1)\langle \rho_{\downarrow}(z) \rangle \langle \rho_{\uparrow}(z') \rangle} - 1$ . Here the prefactor  $1/(N - 1)$  is chosen to make the

noise function zero for non-interaction system. Thus, we have

$$\begin{aligned}
C(z, z', t) = & \frac{1}{N-1} \times \\
& \left( \theta(z-z') \left( \left( 1 + \frac{4t^2 c^2}{(z-z')^2 + 4t^2 c^2} \right) (\beta-1) + (N-\beta) \frac{(z-z')^2}{(z-z')^2 + 4t^2 c^2} - 2\text{Im} \left( \frac{2tc}{z-z'-2itc} \right. \right. \right. \\
& \left. \left. \left. \frac{e^{-i\frac{(z-z')a}{2t}} - e^{-i\frac{(z-z')\beta a}{2t}}}{1 - e^{-i\frac{(z-z')a}{2t}}} \right) \right) \right. \\
& \left. + \theta(z'-z) \left( \left( 1 + \frac{4t^2 c^2}{(z-z')^2 + 4t^2 c^2} \right) (N-\beta) + (\beta-1) \frac{(z-z')^2}{(z-z')^2 + 4t^2 c^2} - 2\text{Im} \left( \frac{2tc}{z-z'-2itc} \right. \right. \right. \\
& \left. \left. \left. \frac{e^{-i\frac{(z-z')a}{2t}} - e^{-i\frac{(z-z')(N-\beta+1)a}{2t}}}{1 - e^{-i\frac{(z-z')a}{2t}}} \right) \right) \right) - 1
\end{aligned}$$

The results for systems with 3 and 10 particles are plotted in Figure ???. In both plots, the second particle is the impurity. In these figures, the noise function hits  $-1$  when  $z = 0$ . This indicates that the up spin and the down spin avoids overlap with each other. In Figure ??, we saw interference fringes on the left side. This is due to the many possible scenarios that the down spin is to the left of the up spin. The period of the fringes is  $2t/(n - \beta + 1)a$ . There is no fringes on the right side. This is because there is only one possibility to have the down spin reside to the right side of the up spin. This corresponds to the case when the impurity exchanges position with the first particle without spin exchange. On the left side, the noise function is mostly positive while on right side, the function is negative. This relates to the fact density fluctuation of the down spin and up spin are positively correlated when the down spin is to the left of the up spin while they become negatively correlated in the other ordering. Such correlation is purely an effect of the interaction. It is easy to check that the normalized noise function vanishes with  $c = 0$ .

This completes our discussion of the time evolution of a system with many fermionic particles and one static fermion impurity. In the next part, we will study the problem of a moving impurity. As we will see, the argument here can be carried over easily to the new situation.

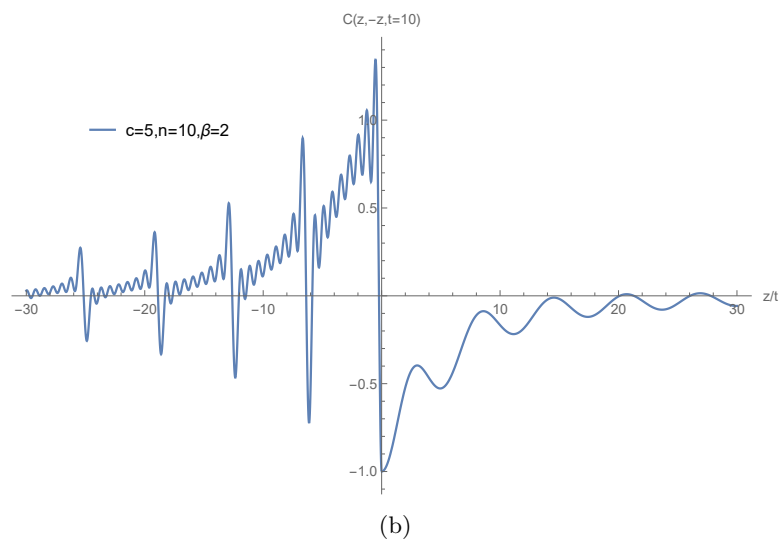
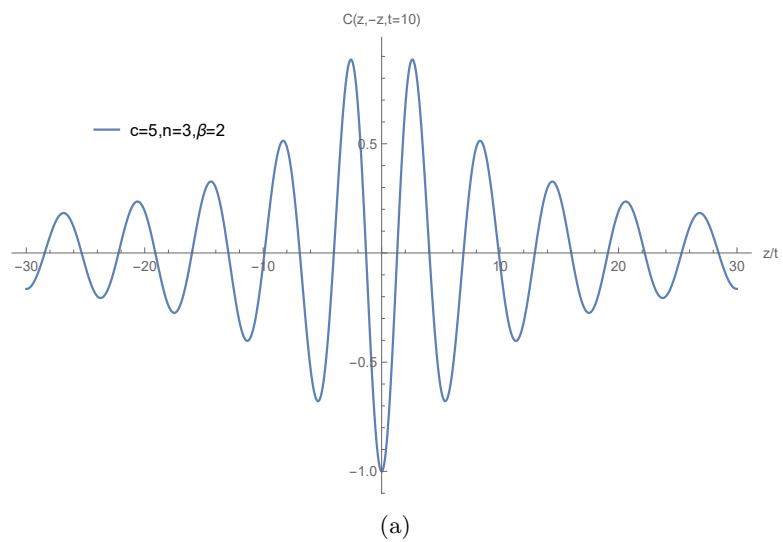


Figure 5.8: The leading order of the noise function with  $\sigma \ll a$  are plotted here. Both figures are for large time  $t = 10$  with the impurity located at the second site. Figure ?? describes a system with 3 particles. Figure ?? is for systems with 10 particles.

## 5.5 Moving Impurity in Multi-particle Bath

In this section, we will deal with the process of shooting an impurity which we will call a down-spin fermion to a bath of host fermions which we will call up-spin fermions. Like in the previous case, each fermion has a Gaussian distribution with width  $\sigma$ . What is different here is that the down spin fermion has a non-zero initial momentum  $k_0$ . Thus, the initial state can be written as

$$|\phi_0\rangle = |x, \beta, k_0\rangle = \frac{1}{(\pi\sigma^2)^{N/4}} e^{-\sum_i^N \frac{(x_i - x_{i0})^2}{2\sigma^2} + ik_0 x_\beta} \prod_{n=1}^M \sigma_\beta^- \prod_{i=1}^N \Psi_\uparrow(x_i)|0\rangle$$

with  $x_{i+1} - x_i > 3\sigma$ . The new phase factor  $e^{ik_0 x_\beta}$  does not affect the proof of the central theorem. As the latter only involves  $k$  and  $\mu$  integration, where the new phase is simply a constant. For the calculation of local observable, we need to integrate over initial position  $x$ s. Here, the extra phase term is equivalent to adding an imaginary part  $i\sigma^2 k_0$  to  $x_0$ , i.e.

$$e^{-\frac{(x-x_0)^2}{2\sigma^2} + ik_0 x} = e^{-\frac{(x-x_0 - ik_0 \sigma^2)^2}{2\sigma^2} + ix_0 k_0 - \frac{k_0^2 \sigma^2}{2}}$$

For the two particle case discussed in section ??, the result is modified as

$$\begin{aligned} & f_{\uparrow, \downarrow}(y_1, y_2) \\ &= \frac{\sigma}{2\sqrt{\pi i}(t + \sigma^2/2i)} \left( e^{\frac{i(y_2 - x_1 - ik_0 \sigma^2)^2}{4(t + \sigma^2/2i)} + \frac{i(y_1 - x_2)^2}{4(t + \sigma^2/2i)} + ik_0 x_1 - \frac{k_0^2 \sigma^2}{2}} (1 - \theta(y_2 - y_1)) c(1+i)/2\sqrt{\pi(t + \sigma^2/2i)} \right. \\ & \quad \text{erfc}(\alpha_1) e^{\alpha_1^2} - e^{\frac{i(y_1 - x_1 - ik_0 \sigma^2)^2}{4(t + \sigma^2/2i)} + \frac{i(y_2 - x_2)^2}{4(t + \sigma^2/2i)} + ik_0 x_1 - \frac{k_0^2 \sigma^2}{2}} \theta(y_1 - y_2) c(1+i)/2\sqrt{\pi(t + \sigma^2/2i)} \text{erfc}(\alpha_2) \\ & \quad \left. e^{\alpha_2^2} \right) \end{aligned}$$

With

$$\begin{aligned} \alpha_1 &= \frac{(1-i)(y_2 - x_1 - y_1 + x_2 - ik_0 \sigma^2 + 2ic(t + \sigma^2/2i))}{4\sqrt{t + \sigma^2/2i}} \\ \alpha_2 &= \frac{(1-i)(y_1 - x_1 - y_2 + x_2 - ik_0 \sigma^2 + 2ic(t + \sigma^2/2i))}{4\sqrt{t + \sigma^2/2i}} \end{aligned}$$

Figure ?? shows the time evolution of the density. We can see clearly that the down spin moves to the right at a constant rate. Like in the static impurity case, we do not see much difference among attractive and repulsive situations. Both of them can be well approximated by the free particle situation whose density equals

$$\begin{aligned} \rho_\uparrow(z, t) &= \frac{\sigma}{2\sqrt{\pi(t^2 + \sigma^4/4)}} e^{-\frac{\sigma^2(z-x_{20})^2}{4(t^2 + \sigma^4/4)}} \\ \rho_\downarrow(z, t) &= \frac{\sigma}{2\sqrt{\pi(t^2 + \sigma^4/4)}} e^{-\frac{\sigma^2(z-x_{10}-2k_0 t)^2}{4(t^2 + \sigma^4/4)}} \end{aligned}$$

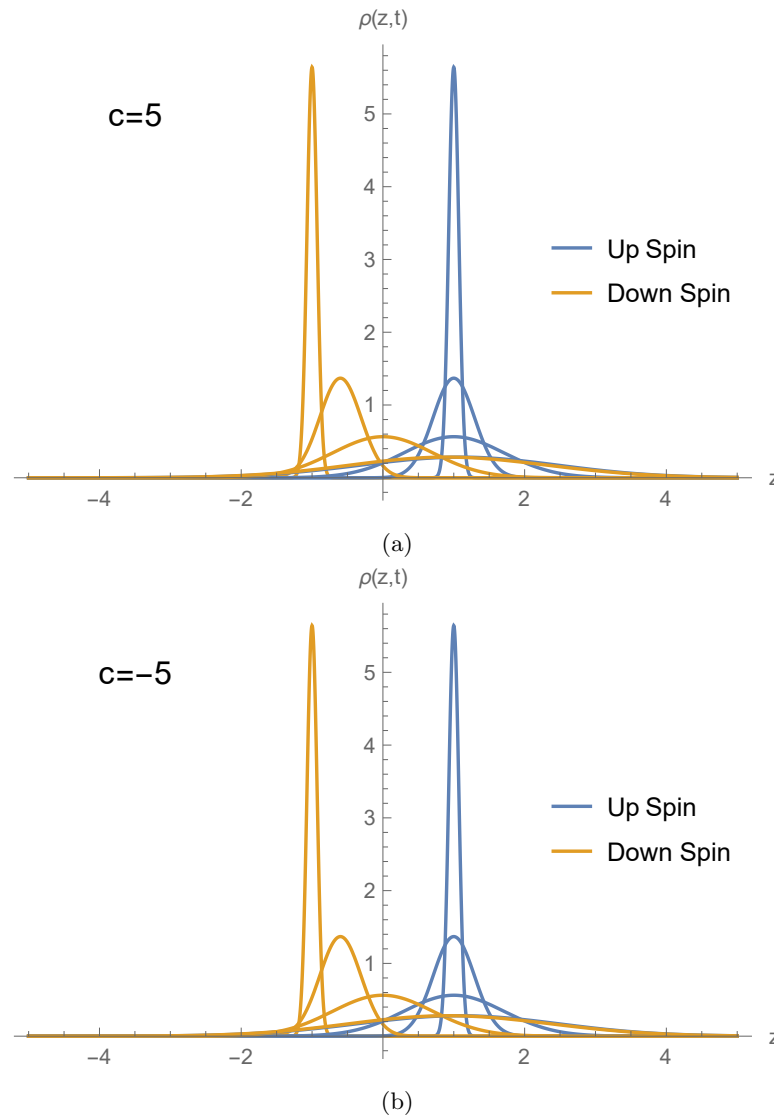


Figure 5.9: Time evolution of the down spin (yellow) and the up spin (blue) at  $t = 0, 0.02, 0.05, 0.1$  for a system with one down spin and one up spin. The down spin moves with  $k_0 = 5$  in the initial state.  $c=5$  is for repulsive case and  $c=-5$  is for attractive case.

In terms of the noise correlation, we are more interested in the behavior when the two particles overlaps. When  $y_1 = y_2$ , we have  $\alpha_1 = \alpha_2$ , thus,

$$f_{\uparrow,\downarrow}(y_1, y_2) = \frac{\sigma}{2\sqrt{\pi}i(t + \sigma^2/2i)} e^{i\frac{(x_1 + ik_0\sigma^2)^2 + x_2^2}{4(t + \sigma^2/2i)} + ik_0x_1 - \frac{k_0^2\sigma^2}{2}} (1 - c(1+i)/2\sqrt{\pi(t + \sigma^2/2i)}) \\ \operatorname{erfc}(\alpha_1)e^{\alpha_1^2}$$

with

$$\alpha_1 = \frac{(1-i)(x_2 - x_1 - ik_0\sigma^2 + 2ic(t + \sigma^2/2i))}{4\sqrt{t + \sigma^2/2i}}$$

Thus when  $t \gg 1$ ,  $\operatorname{erfc}(\alpha_1)e^{\alpha_1^2} = \frac{4}{\sqrt{\pi}(1-i)2ic\sqrt{t + \sigma^2/2i}}$  and  $f_{\uparrow,\downarrow}(0, 0, t) = O(\frac{1}{t})$ . This means that the two particle still avoids overlaps in the moving impurity case.

As to the result about one impurity and many fermions discussed in section ??, they are modified as follows

$$|f(\xi, \alpha, t)|^2 = \frac{\sigma^N}{2^N \pi^{\frac{N}{2}} t^N c^2} \sum_{P, P'} e^{\sum_i -\sigma^2 \xi_i^2 - i\xi_i(x_{P_i} - x_{P'_i}) - k_0\sigma^2(\xi_{P-1_\beta} + \xi_{P'-1_\beta}) - k_0^2\sigma^2} (-1)^{P+P'} \theta(\xi_1 < \dots < \xi_N) \\ \sum_{o,e} R(\xi_o + ic/2) R^*(\xi_e - ic/2)$$

$$\rho_\downarrow(z) = \frac{\sigma^N}{2^N \pi^{N/2} t^N c^2} (2\pi c)^2 \sum_P \int_\xi e^{-\sigma^2 \sum_i \xi_i^2 - 2k_0\sigma^2 \xi_\alpha - k_0^2\sigma^2} \theta(\xi_1 < \dots < \xi_N) \delta(\xi_\alpha - z/2t) \\ = \frac{\sigma}{2\sqrt{\pi}t} e^{-\sigma^2(\frac{z}{2t} - k_0)^2}$$

$$\rho_\downarrow(z) = \frac{\sigma^N}{2^N \pi^{N/2} t^N c^2} (2\pi c)^2 \sum_P \int_\xi e^{-\sigma^2 \sum_i \xi_i^2 - 2k_0\sigma^2 \xi_\alpha - k_0^2\sigma^2} \theta(\xi_1 < \dots < \xi_N) \sum_{j \neq \alpha} \delta(\xi_j - z/2t) \\ = \frac{\sigma}{2\sqrt{\pi}t} e^{-\frac{\sigma^2 z^2}{(2t)^2}}$$

$$\rho_\downarrow(z)\rho_\uparrow(z') \\ = \frac{\sigma^N}{4\pi^{N/2} t^2} \int_\xi \sum_{P, P'} e^{-\sum_i \sigma^2 \xi_i^2 - i\sum_i \xi_i(x_{P_i} - x_{P'_i})} (-1)^{P+P'} \theta(\xi_1 < \dots < \xi_N) \delta(\xi_\alpha - z/2t) \sum_i \delta(\xi_i \\ - z'/2t) e^{-k_0^2\sigma^2} \\ \left( \theta(z - z') \left( e^{\frac{z\sigma^2 k_0}{2t}} \theta(\beta - Pi) \delta_{P\alpha, \beta} + \frac{z - z'}{z - z' + 2ict} e^{\frac{z\sigma^2 k_0}{2t}} \theta(Pi - \beta) \delta_{P\alpha, \beta} + \frac{-2ict}{z - z' + 2ict} \right. \right. \\ \left. \left. e^{\frac{z'\sigma^2 k_0}{2t}} \theta(\beta - P\alpha) \delta_{P_i, \beta} \right) \left( e^{\frac{z\sigma^2 k_0}{2t}} \theta(\beta - P'i) \delta_{P'\alpha, \beta} + \frac{z - z'}{z - z' - 2ict} e^{\frac{z\sigma^2 k_0}{2t}} \theta(P'i - \beta) \delta_{P'\alpha, \beta} \right. \right.$$

$$\begin{aligned}
& + \frac{2ict}{z-z'-2ict} e^{\frac{z'\sigma^2 k_0}{2t}} \theta(\beta - P'\alpha) \delta_{P'i, \beta} \\
& + \theta(z' - z) \left( e^{\frac{z\sigma^2 k_0}{2t}} \theta(Pi - \beta) \delta_{P\alpha, \beta} + \frac{z-z'}{z'-z+2ict} e^{\frac{z\sigma^2 k_0}{2t}} \theta(\beta - Pi) \delta_{P\alpha, \beta} + \frac{-2ict}{z'-z+2ict} \right. \\
& \quad \left. e^{\frac{z'\sigma^2 k_0}{2t}} \theta(P\alpha - \beta) \delta_{\beta, Pi} \right) \left( e^{\frac{z\sigma^2 k_0}{2t}} \theta(Pi - \beta) \delta_{P\alpha, \beta} + \frac{z-z'}{z'-z+2ict} e^{\frac{z\sigma^2 k_0}{2t}} \theta(\beta - Pi) \delta_{P\alpha, \beta} \right. \\
& \quad \left. + \frac{2ict}{z'-z+2ict} e^{\frac{z'\sigma^2 k_0}{2t}} \theta(P\alpha - \beta) \delta_{\beta, Pi} \right)^2 \\
& = \theta(z - z') \frac{\sigma^2}{4\pi t^2} \left| \left( e^{-\frac{\sigma^2(z-2k_0t)^2 + \sigma^2 z'^2}{4t^2}} + \frac{4t^2 c^2}{(z-z')^2 + 4t^2 c^2} e^{-\frac{\sigma^2 z^2 + \sigma^2(z'-2k_0t)^2}{4t^2}} \right) (\beta - 1) + (N - \beta) \right. \\
& \quad \left. \frac{(z-z')^2}{(z-z')^2 + 4t^2 c^2} e^{-\frac{\sigma^2(z-2k_0t)^2 + \sigma^2 z'^2}{4t^2}} - 2\Im \left( \frac{2tc}{z-z'-2ict} \frac{e^{-\frac{i(z-z')a}{2t}} - e^{-i\frac{(z-z')\beta a}{2t}}}{1 - e^{-\frac{i(z-z')a}{2t}}} \right) e^{-\frac{k_0^2 \sigma^2}{2}} \right. \\
& \quad \left. e^{-\frac{\sigma^2(z-k_0t)^2 + \sigma^2(z'-k_0t)^2}{4t^2}} \right. \\
& \quad \left. \theta(z' - z) \frac{\sigma^2}{4\pi t^2} \left( e^{-\frac{\sigma^2(z-2k_0t)^2 + \sigma^2 z'^2}{4t^2}} + \frac{4t^2 c^2}{(z-z')^2 + 4t^2 c^2} e^{-\frac{\sigma^2 z^2 + \sigma^2(z'-2k_0t)^2}{4t^2}} \right) (N - \beta) + (\beta - 1) \right. \\
& \quad \left. \frac{(z-z')^2}{(z-z')^2 + 4t^2 c^2} e^{-\frac{\sigma^2(z-2k_0t)^2 + \sigma^2 z'^2}{4t^2}} - 2\Im \left( \frac{2tc}{z-z'-2ict} \frac{e^{-\frac{i(z-z')a}{2t}} - e^{-i\frac{(z-z')(N-\beta+1)a}{2t}}}{1 - e^{-\frac{i(z-z')a}{2t}}} \right) \right. \\
& \quad \left. e^{-\frac{k_0^2 \sigma^2}{2} - \frac{\sigma^2(z-k_0t)^2 + \sigma^2(z'-k_0t)^2}{4t^2}} \right.
\end{aligned}$$

$$\begin{aligned}
& C(z, z', t) \\
& = \frac{\theta(z-z')}{N-1} \left( 1 + \frac{4t^2 c^2}{(z-z')^2 + 4t^2 c^2} e^{\frac{\sigma^2 k_0(z'-z)}{t}} \right) (\beta - 1) + (N - \beta) \frac{(z-z')^2}{(z-z')^2 + 4t^2 c^2} - 2e^{-\frac{\sigma^2 k_0(z-z')}{2t}} \\
& \quad \Im \left( \frac{2tc}{z-z'-2ict} \frac{e^{-\frac{i(z-z')a}{2t}} - e^{-i\frac{(z-z')\beta a}{2t}}}{1 - e^{-\frac{i(z-z')a}{2t}}} \right) \\
& + \frac{\theta(z-z')}{N-1} \left( 1 + \frac{4t^2 c^2}{(z-z')^2 + 4t^2 c^2} e^{\frac{\sigma^2 k_0(z'-z)}{t}} \right) (N - \beta) + (\beta - 1) \frac{(z-z')^2}{(z-z')^2 + 4t^2 c^2} - 2e^{-\frac{\sigma^2 k_0(z-z')}{2t}} \\
& \quad \Im \left( \frac{2tc}{z-z'-2ict} \frac{e^{-\frac{i(z-z')a}{2t}} - e^{-i\frac{(z-z')(N-\beta+1)a}{2t}}}{1 - e^{-\frac{i(z-z')a}{2t}}} \right) - 1
\end{aligned}$$

Based on these results, we can see that the initial momentum of the impurity does not affect the density distribution a lot. The up spin particles and the impurity still evolve as if isolated in the leading order with  $c\sigma \ll 1$ . The impurity simply passed the bath particle. The extra kinetic energy from the impurity does not lead to more interacting energy in the process. The particle still avoids overlaps that leads to change in the interacting energy. This is confirmed by the calculation of the noise function. As is clear in Figure ??, the noise function equals  $-1$  at the origin. However, the initial momentum does make the left side enhanced and the right side damped.

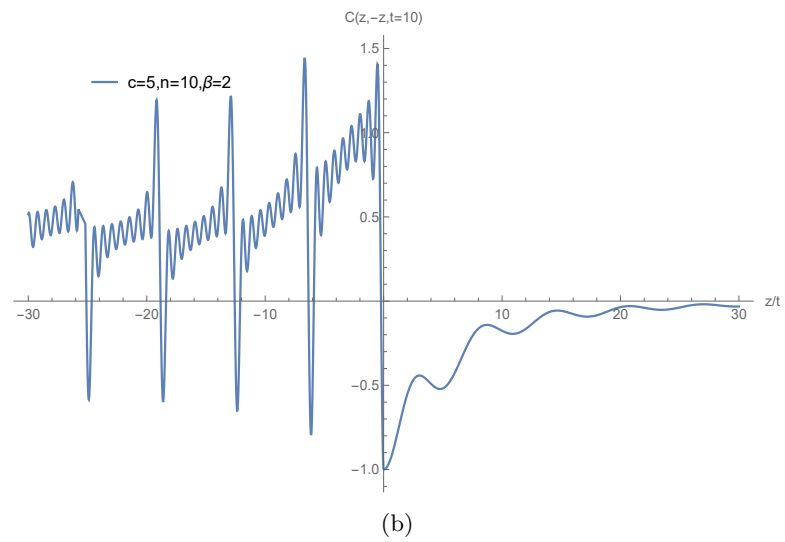
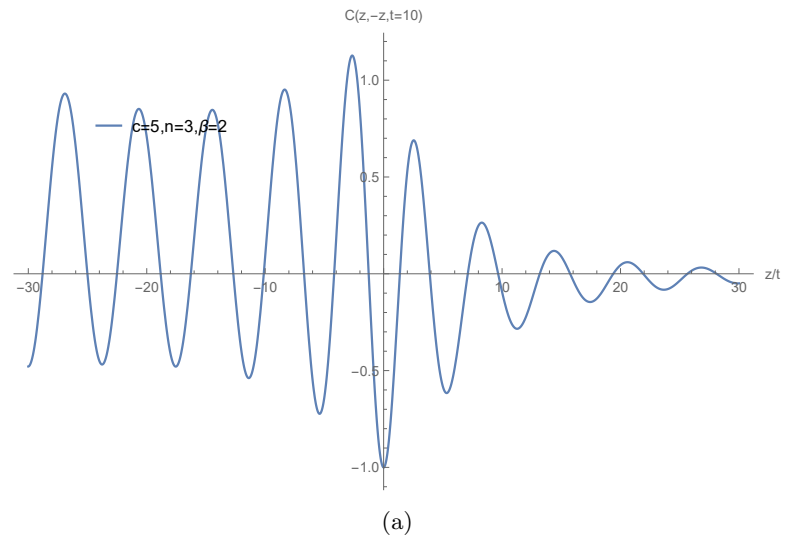


Figure 5.10: Leading order of the noise function with  $\sigma \ll a$ . Both figures are for large time  $t = 10$  with the impurity initially located at the second site and moving with momentum  $k_0 = 5$ . Figure ?? describes a system with 3 particles. Figure ?? is for systems with 10 particles.

## Chapter 6

### Quench Dynamics of Bosonic Gaudin-Yang model

In this section, we will study the quench dynamics of two-component boson particles with contact interaction. This topic has received limited attention in condensed matter literature, as bosonic systems come with an odd number of states relating to different spin components. However, with the ground-breaking progress in ultracold atom, it is amenable to realize such two-component boson gases with different hyperfine states, for review see [? ]. In this part, we will repeat the calculation for the bosonic Gaudin-Yang model and see how the quantum nature of particles affects the result we obtained so far.

#### 6.1 Bethe Ansatz solution

The bosonic Gaudin-Yang model is described by the same Hamiltonian as the fermionic counterpart, except that  $\Psi^\dagger(x)(\Psi(x))$  is a bosonic creation(annihilation) operator satisfying the commutation relation  $[\Psi^\dagger(x), \Psi(y)] = \delta(x - y)$ .

$$H_{GY}^B = \sum_{\sigma=\uparrow,\downarrow} \int dx \Psi_\sigma^\dagger(x) \left( -\frac{\partial^2}{\partial x^2} \right) \Psi_\sigma(x) + c \int_x \Psi_\uparrow^\dagger(x) \Psi_\downarrow^\dagger(x) \Psi_\downarrow(x) \Psi_\uparrow(x)$$

The symmetry property is reflected in the wavefunction. Recall that

$$|\Psi\rangle = \sum_{\sigma} f(x, \sigma) \prod_{i=1}^N \Psi_{\sigma_i}^\dagger(x_i) |0\rangle$$

$$f(x, \sigma) = \sum_{P, Q} e^{i \sum_j (Pk)_j \cdot (Qk)_j} A(Q, P) \theta((Qx)_1 < \dots < (Qx)_N)$$

Then,  $A(P_{ij}Q, P) = \epsilon \Pi_{ij} A(Q, P)$  with  $\Pi_{ij}$  acting on the spin space. Here  $\epsilon = 1(-1)$  for bosons(fermions). Plug it into the schrodinger equation, as derived on page ??

$$(i(Pk)_i - i(Pk)_j)(A(Q, P) - A(Q, P_{ij}P) + A(P_{ij}Q, P)) - A(P_{ij}P, P_{ij}Q) + c(A(Q, P) + A(Q, P_{ij}P) + A(P_{ij}Q, P) + A(P_{ij}P, P_{ij}Q)) = 0$$

one gets

$$A(Q, P_{ij}P) \frac{1 - \epsilon \Pi_{ij}}{2} = \frac{(Pk)_i - (Pk)_j - ic \epsilon P_{ij}}{(Pk)_i - (Pk)_j + ic} \frac{1 - \epsilon \Pi_{ij}}{2}$$

At the same time, the wavefunction should be equal to a plain wave in the other spin configuration  $\frac{1+\epsilon\Pi_{ij}}{2}$ , which means

$$A(P_{ij}Q, P_{ij}P) \frac{1+\epsilon\Pi_{ij}}{2} = A(Q, P) \frac{1+\epsilon\Pi_{ij}}{2}$$

Or equivalently,

$$A(Q, P_{ij}P) \frac{1+\epsilon\Pi_{ij}}{2} = -A(Q, P) \frac{1+\epsilon\Pi_{ij}}{2}$$

Thus, we have

$$A(Q, P_{ij}P) = \frac{(Pk)_i - (Pk)_j \epsilon\Pi_{ij} - ic}{(Pk)_i - (Pk)_j + ic} A(Q, P)$$

Recall this relation defines the Yang matrix  $Y_{ij}((Pk)_i - (Pk)_j)$  from which the scattering matrix  $S_{ij}((Pk)_i, (Pk)_j)$  can be obtained.

$$Y_{ij}((Pk)_i, (Pk)_j) = \frac{(Pk)_i - (Pk)_j \epsilon\Pi_{ij} - ic}{(Pk)_i - (Pk)_j + ic}$$

$$S_{ij}((Pk)_i, (Pk)_j) = \epsilon\Pi_{ij} Y_{ij}((Pk)_i, (Pk)_j) = \frac{(Pk)_i - (Pk)_j - ic\epsilon\Pi_{ij}}{(Pk)_i - (Pk)_j + ic}$$

Using the machinery discussed in chapter (??,??), one can obtain the nested Bethe Ansatz solution. The derivation is quite similar to that of the fermionic counterpart. The only difference results from the fact that

$$Y_{ij}((Pk)_i, (Pk)_j) | \uparrow \rangle = C^B((Pk)_i, (Pk)_j) | \uparrow \rangle$$

$$C^B((Pk)_i, (Pk)_j) = \frac{(Pk)_i - (Pk)_j - ic}{(Pk)_i - (Pk)_j + ic}$$

compared to  $Y_{ij}((Pk)_i, (Pk)_j) | \uparrow \rangle = -| \uparrow \rangle$  in the fermionic situation. Thus, the solution in the nested form in the bosonic systems has the new factor, a product of  $C^B((Pk)_i, (Pk)_j)$ , replacing the  $(-1)^P$  in the fermionic wavefunction, i.e.

$$|\mu, k\rangle = \sum_{\substack{P \in S_N \\ R \in S_M}} \int_x \sum_{\alpha} e^{i \sum_i k_{Pi} y_i} \prod_{P_{ij} \in P} C^B(k_i - k_j) \prod_{m < n} S_R^B(\mu_m - \mu_n) \prod_m I^B(\mu_m, \alpha_m, Pk) \theta(x) \theta(\alpha)$$

$$|x, \alpha\rangle$$

with

$$C^B(k_i - k_j) = \frac{k_i - k_j - ic}{k_i - k_j + ic}$$

$$S^B(\mu_m - \mu_n) = \frac{\mu_m - \mu_n - ic \text{Sgn}(\alpha_{Rm} - \alpha_{Rn})}{\mu_m - \mu_n + ic}$$

$$I^B(\mu, \alpha, k) = \frac{ic}{\mu - k_{\alpha} - ic/2} \prod_{n < \alpha} \frac{\mu - k_n + ic/2}{\mu - k_n - ic/2}$$

With periodic boundary condition, one can obtain the Bethe Ansatz equations

$$e^{ik_i L} = - \prod_{\alpha} \frac{\mu_{\alpha} - k_i + ic/2}{\mu_{\alpha} - k_i - ic/2} \prod_j \frac{k_i - k_j + ic}{k_i - k_j - ic}$$

$$\prod_{\alpha} \frac{\mu_{\beta} - \mu_{\alpha} - ic}{\mu_{\beta} - \mu_{\alpha} + ic} = - \prod_j \frac{\mu_{\beta} - k_j - ic/2}{\mu_{\beta} - k_j + ic/2}$$

These equations determines the root distribution as described by the string hypothesis. So far, there is no systematic discussion of the string structures in this system. But, it should be possible to deduce it by generalizing the conjecture for the fermionic Gaudin-Yang model. On one hand, it should includes the  $\mu$ -string as the consistency equation is the same as the fermimonic case. One the other, one should include  $k$ -string of arbitrary length, due to the same argument for attractive Lieb-Liniger gases. The existance of  $\mu$ - $k$  string of length 2 is now undefined as the new scattering matrix  $C^B$  leads to an extra 0 or  $\infty$ . We will not try to check the validity of this last type of string. Instead, we will move on to the Yudson approach as it will provide a complete list for the string structure.

## 6.2 Yudson Representation

In the previous section, we have derived the nested Bethe Ansatz solution for the bosonic Gaudin-Yang model. In this section, we will written down the Yudson representation based on the solution we had. We will specify the integration contour and discuss the proof of the central theorem.

Given the Bethe Ansatz state, the Yudson state can be obtained easily as

$$|k, \mu\rangle = \sum_P e^{i \sum_i k_i y_i} \prod_m I(\mu_m, \alpha_m, k) \theta(y) \theta(\alpha) |x, \alpha\rangle$$

The Yudson representation in the coordinate basis becomes

$$\int_C dk \int_{C'} d\mu \langle y, \alpha | k, \mu \rangle \langle k, \mu | x, \beta \rangle \theta(x) \theta(y) \theta(\alpha) \theta(\beta)$$

$$= \sum_{P,R} e^{i \sum_i k_i (y_{P^{-1}i} - x_i)} \prod_{P_{ij} \in P} C^B(k_i - k_j) \prod_{m < n}^M S^B(\mu_m - \mu_n) \prod_{m=1}^M I^B(\mu_m, \alpha_m, Pk) I^{B*}(\mu_m, \beta_m, k)$$

$$\theta(x) \theta(y) \theta(\alpha) \theta(\beta)$$

The integral contour for attractive cases is the same as that of fermions for repulsive case, while the coutour for  $c < 0$  duplicates the repulsive situation. To be explicit,  $k_1$  to  $k_N$  are integrated along a horizontal direction. Their contours are separated by a distance greater than  $|c|$ . The line of  $k_1$  stays on the top and that of  $k_N$  lies in the bottom. How  $\mu$ 's are integrated

varies between repulsive and attractive models. For  $c < 0$ ,  $\mu_m$  are integrated forward along the line of  $k_{\beta_m}$ . For  $c > 0$ ,  $\mu_m$  are integrated backward along the contour of  $k_{\beta_m}$  and forward along two lines that lie above and below that of  $k_{\beta_m}$  with a separation greater than  $|c|/2$ .

To explain the choice of such contour, we now discuss how the central theorem can be proved by focusing on the aspects that are unique to the bosonic model.

### 6.3 Central Theorem

As we did for the fermionic case, we start with the single impurity situation. For both  $c > 0$  and  $c < 0$ , the  $\mu$  integral contour can be closed from above. This transforms the integration into pole contributions at  $k_o - ic/2$  for any  $o$  that satisfies the condition  $o \leq \beta$  and  $P^{-1}o \geq \alpha$ . The expressions of the residue here are the same as those in the fermionic case except for the sign in front of  $c$ . Thus, there are two types of poles. The one at  $k_o = k_n$  is only apparent, due to the same reason as before. The other pole, which takes the form  $k_i = k_j - ic$  with  $i < \beta < j$  and  $P^{-1}i > \alpha > P^{-1}j$  is a real one. At the same time, it must be true that  $P_{ij} \in P$ , therefore, the denominator is canceled by the numerator in  $C^B(k_i - k_j)$ , leaving only Lieb-Liniger type of poles defined as  $k_i = k_j + ic$  for  $i < j$  and  $P^{-1}i > P^{-1}j$ . Following the argument in [? ], one can see that these poles do not contribute to the wavefunction integration.

In the presence of multiple  $\mu$ 's, one should carry out the integration over  $\mu_1, \dots, \mu_M$  repeatedly by closing each contour in the upper half plane. Using the same argument as we made on page ??, one can show that the collection of poles lying above the integral contour of  $\mu_m$  is unaffected by the product of scattering matrices among  $\mu$ 's, as long as we do the integration in the aforementioned order. Then each  $\mu_m$  integration results in a collection of poles of the form  $k_i = k_j - ic$  for  $i < \beta_m < j$  and  $i^{-1} > \alpha_m > j^{-1}$ . At the same time,  $\mu_m$  is related to  $k_i$  as  $\mu_m = k_i - ic/2$ . As no two  $\mu$ 's can be identical in the nested Bethe Ansatz, the  $\mu$  integration cannot take the residue at the same point. This guarantees that each pole appears at most once in the denominator. This pole will then be cancelled by the scattering matrices among  $k$ 's. Thus, we still have only Lieb-Liniger type of poles. Further proof of the central theorem in section ?? can be applied directly to here, and one also gets the same normalization constant.

### 6.4 Bound states

In the previous section, we have seen that all poles comes from  $C^B(k_i - k_j)$ . What this indicates is twofold. First, the  $k - \mu$  strings disappear. Secondly,  $k$  strings emerge. That means the formation of bound states no longer depends on the existence of a magnon. This makes sense

as Lieb-linger gases bind together with attractive interaction too. Now, there are three types of strings,  $k - \mu$  pairs,  $k$  strings and composites of these two. A composite may be formed if the  $k$  in the  $k - \mu$  pairs coexists in the  $k$  strings which snaps the two string together. Note, although the  $k - \mu$  string is not a basic type, it may emerge has a composite. For a complete set of basis, one do needs to include all composite configuration as well as the  $k - \mu$  pair and  $k$  strings. This makes the enumeration more complicated. Physically, this is due to the fact that bosonic wavefunction are symmetric, thus particles have more overlap in the highly polarized limit. Therefore, there are more interaction among bosons than fermions.

## 6.5 Time evolution

This section is devoted to the calculation of time evolution in a two-component boson system. With the Yudson representation, the time evolved state can be written down easily as

$$|\Psi^B(t)\rangle = \sum_{P,R} \int_C dk \int_{C'} d\mu e^{-i \sum_i k_i^2 t + i \sum_i k_i (y_{P^{-1}i} - x_i)} \prod_{P_{ij} \in P} C^B(k_i - k_j) \prod_{m < n}^M S^B(\mu_m - \mu_n) \prod_{m=1}^M I^B(\mu_m, \alpha_m, Pk) I^{B*}(\mu_m, \beta_m, k) \theta(x) \theta(y) \theta(\alpha) \theta(\beta) \quad (6.1)$$

Both the initial state and the quench process is the same as before. We will discuss the case with two distinguishable particles by solving the time evolution in terms of the wavefunction explicitly. We will also work in the large time limit and make the saddle point approximation to remove the  $k$  integrations for  $N > 2$ . We want to do a comparison between the quench dynamics between bosonic and fermionic gases. It turns out that the results we have obtained in the previous chapter holds for the bosonic problem as well.

For the two distinguishable particles, i.e  $N = 2$ ,  $M = 1$ , this is easy to understand. Since the statistics only affect the symmetry behaviour among identical particles, thus the time evolved state is exactly the same as the fermionic counterpart.

For  $N > 2$  and  $M = 1$ , however, the bosonic wavefunction developed at a later time is different from the fermionic case, as one can see from equation (??). But the results of the density and noise function with only leading order terms in  $\sigma$  show no difference. To understand it, recall the approximation we have made in the calculation of local observables. To extract the leading order contribution, we put a constraint on the permutation  $P$  such that  $x_{Pm} = x_{P'm}$  for a dummy variable  $y_m$  which is integrated without a  $\delta$ -function. This is due to the fact that

$$\int dy e^{-\sigma^2 y^2 + iy(x_{Pm} - x_{P'm})} O\left(\frac{1}{y + ic}\right) = e^{-\frac{(x_{Pm} - x_{P'm})^2}{\sigma^2}}$$

which is of the order  $O(e^{-|c|a})$ . which we will drop. With this in mind, the leading order terms in the density calculation come from

$$(2\pi i)\delta_{P,P'} \sum_O \mathbf{R}(\xi_{P^{-1}o} - ic/2) = (2\pi c)\delta_{P,P'}\delta_{P\alpha,\beta}$$

The density then becomes

$$\rho_{\uparrow}(z) = \frac{\sigma}{2\sqrt{\pi t}} e^{-\frac{z^2\sigma^2}{4t^2}}$$

$$\rho_{\downarrow}(z) = \frac{(N-1)\sigma}{2\sqrt{\pi t}} e^{-\frac{z^2\sigma^2}{4t^2}}$$

The leading order terms in the noise function calculation result from

$$\mathbf{R}(\xi_{P^{-1}o} - ic/2) \rightarrow ic\delta_{P\alpha,\beta} \left(1 + \frac{ic}{\xi_{\alpha} - \xi_i - ic} \theta(\alpha - i)\theta(Pi - \beta) + \frac{ic}{\xi_i - \xi_{\alpha} - ic} \theta(\beta - Pi)\theta(i - \alpha)\right)$$

$$- ic\delta_{\beta, Pi} \left(\frac{ic}{\xi_{P^{-1}\beta} - \xi_{\alpha} - ic} \theta(P^{-1}\beta - \alpha)\theta(P\alpha - \beta) + \frac{ic}{\xi_{\alpha} - \xi_{P^{-1}\beta} - ic} \theta(\alpha - P^{-1}\beta)\theta(\beta - P\alpha)\right)$$

It is easy to see that the resultant correlation function becomes

$$\rho_{\downarrow}(z)\rho_{\uparrow}(z')$$

$$= \frac{\sigma^N}{4\pi^{N/2}t^2} \int_{\xi} \sum_{P,P'} e^{-\sum_i \sigma^2 \xi_i^2 - i \sum_i \xi_i (x_{P^i} - x_{P'^i})} \frac{\prod_{P_{ij} \in P} S(k_i - k_j)}{\prod_{P_{mn} \in P'} S(k_m - k_n)} \theta(\xi) \delta(\xi_{\alpha} - z/2t) \sum_i \delta(\xi_i - z'/2t)$$

$$\left| \theta(z - z') \left( \theta(\beta - Pi) \delta_{P\alpha,\beta} + \frac{z - z'}{z - z' - 2ict} \theta(Pi - \beta) \delta_{P\alpha,\beta} + \frac{2ict}{z - z' - 2ict} \theta(\beta - P\alpha) \delta_{Pi,\beta} \right) \right.$$

$$\left. + \theta(\beta - P'i) \delta_{P'\alpha,\beta} + \frac{z - z'}{z - z' + 2ict} \theta(P'i - \beta) \delta_{P'\alpha,\beta} + \frac{-2ict}{z - z' + 2ict} \theta(\beta - P'\alpha) \delta_{P'i,\beta} \right)$$

$$+ \theta(z' - z) \left( \theta(Pi - \beta) \delta_{P\alpha,\beta} + \frac{z - z'}{z' - z - 2ict} \theta(\beta - Pi) \delta_{P\alpha,\beta} + \frac{2ict}{z' - z - 2ict} \theta(P\alpha - \beta) \delta_{\beta, Pi} \right)$$

$$\left. \left( \theta(Pi - \beta) \delta_{P\alpha,\beta} + \frac{z - z'}{z' - z - 2ict} \theta(\beta - Pi) \delta_{P\alpha,\beta} + \frac{-2ict}{z' - z + 2ict} \theta(P\alpha - \beta) \delta_{\beta, Pi} \right) \right|^2$$

$$= \frac{\sigma^2}{4\pi t^2} e^{-\frac{\sigma^2(z^2+z'^2)}{4t^2}} \times$$

$$\left( \theta(z - z') \left( \left(1 + \frac{4t^2 c^2}{(z - z')^2 + 4t^2 c^2}\right) (\beta - 1) + (N - \beta) \frac{(z - z')^2}{(z - z')^2 + 4t^2 c^2} - 2\text{Im}\left(\frac{2tc}{z - z' - 2itc}\right) \right. \right.$$

$$\left. \frac{e^{-\frac{i(z-z')\alpha}{2t}} - e^{-\frac{i(z-z')\beta\alpha}{2t}}}{1 - e^{-\frac{i(z-z')\alpha}{2t}}} \right)$$

$$+ \theta(z' - z) \left( \left(1 + \frac{4t^2 c^2}{(z - z')^2 + 4t^2 c^2}\right) (N - \beta) + (\beta - 1) \frac{(z - z')^2}{(z - z')^2 + 4t^2 c^2} - 2\text{Im}\left(\frac{2tc}{z - z' - 2itc}\right) \right.$$

$$\left. \frac{e^{-\frac{i(z-z')\alpha}{2t}} - e^{-\frac{i(z-z')(N-\beta+1)\alpha}{2t}}}{1 - e^{-\frac{i(z-z')\alpha}{2t}}} \right)$$

which is identical to the fermionic equivalent. Like in the fermionic model,  $c(0,0,t) \rightarrow -1$  for large time, indicating that the particles develop a trend to avoid overlap with each other for our chosen initial state. We relate this phenomenon to energy conservation which plays the same role in both systems.

Note, dropping higher order terms in  $\sigma$  decouples the two measured degree of freedom with the rest of the system. Making the multi-particle problem ( $N > 2$ ) equivalent to one with two distinguishable particles. This is not the case for a system with bound states. In these states, one of the measured particle binds together with a third particle. Thus, two of the particles become indistinguishable and statistics plays a big role. We believe that the quench dynamics will be greatly different from the fermionic counterpart if the bound states contribute significantly, i.e. in an attractive system with a lot of overlap in the initial state.

## Chapter 7

### Conclusion and Outlook

#### 7.1 Conclusion

In this thesis, the Yudson approach has been presented as an eigenstate expansion of a general state that are well separated in the coordinate space. Among the many advantages listed in chapter 3, the most prominent one relates to compacting all contributing states into a contour integral. And the contour integration by itself takes care of the weight of each states. Moreover, the Yudson representation includes every states, even those that are not accessible by a Bethe Ansatz solution.<sup>1</sup> This is achieved by integrating the spin rapidities from  $-\infty$  to  $\infty$ .

In general, there is no guideline how to choose a contour, and it varies from model to model [? ?]. One needs to take a guess and check if the central theorem holds, like what we did in chapter 4.1 and 5.1. When the contour is determined, the time evolution of the state is solved in principle.

Unlike many approaches designed for integrable models, say the quench action and ABACUS, the Yudson representation does not depend on the String hypothesis. In fact, the Yudson representation with a properly chosen contour can in turn check the validity of the String hypothesis. As shown in chapter 5.2, shifting all contours to the real axis separates free states and various bound states apart. This provides us with a complete basis in the Hilbert space that is greater than long believed.

In chapter 4, 5 and 6, we demonstrate how the Yudson approach can be applied to the quench dynamics of the Lieb-Liniger gas, Gaudin-Yang gas and bosonic Gaudin-Yang gas respectively. In the three cases, we obtained the exact wavefunction for two-particle scenario and asymptotic limit of the wavefunction for many bosons and many fermions(bosons) with one impurity. We observed that, although the noise function near the origin behaves differently for different type of interaction shortly after the quench, they soon approach  $-1$  which means no overlap between any two particles. We claim that the reason is related to the initial state and energy conservation.

---

<sup>1</sup>Recall that Bethe Ansatz eigenstates are highest weight state

The three examples considered here would contribute to the understanding the nonequilibrium dynamics.

## 7.2 Future Work

In this thesis, we have not studied multi-impurity Gaudin-Yang model. Although the scattering among spin waves makes the calculation more complicated, it is solvable with the Yudson approach. It would be interesting to see how the nonequilibrium dynamics be affected by longer string solutions, which are not predicted by the String hypothesis.

Another interesting direction is changing the initial into one with significant overlap. The Yudson representation works well with such initial condition, as long as we split the initial condition into sections with different orderings. Practically, it leads to a series of Heaviside theta function that brings enormous complications to the integration. However, the problem worth all the efforts as it results in greater effect from the bound states and leads to richer physics, as particles are allowed to overlap and the contact interaction plays a more prominent role.

Aside from these, how Yudson approach can be modified for finite size system is an important question, as already discussed in [?] by Garry Goldstein. So far Goldstein-Yudson approach has been applied to quench dynamics of Lieb-Liniger gas in the thermodynamic limit. The application of the Goldstein-Yudson approach to other nonequilibrium problems with integrable Hamiltonian is a intriguing direction.

Moreover, a promising direction would be incorporating form factor into the Yudson approach. With the Yudson approach, time evolution of the local observable equals

$$\langle O(t) \rangle = \int_C d\vec{k} \int_{C'} d\vec{p} \langle \vec{k} | O | \vec{p} \rangle \langle \phi_0 | k \rangle \langle p | \phi_0 \rangle e^{-i(E(\vec{k}) - E(\vec{p}))t}$$

As the structure of the Yudson state is very simple, most of the complication comes from  $\langle \vec{k} | O | \vec{p} \rangle$ , which is called the form factor. This object has been intensely studied [? ? ?], and many results are available. However, these results are either too complicated or suffer from divergence problems when the some parameters in  $|k\rangle$  and  $|p\rangle$  are the same. Moreover, how the form factor results applies to systems with complex parameters are not clear. Such form factors free one from evaluating high dimensional integrals of spatial coordinates, which we have to make approximation about.

Last but not least, it is desirable if one could work out the  $k$  and  $\mu$  integrations without exploiting the saddle point approximation. If one changes the variable to include the imaginary

part of the contour, the Yudson representation is nothing but a real integration. And one no longer needs to include different bound state contribution separately.

## Bibliography

- [1] I. Bloch, J. Dalibard, and W. Zwerger, “Many-body physics with ultracold gases,” *Rev. Mod. Phys.*, vol. 80, pp. 885–964, Jul 2008.
- [2] T. Langen, R. Geiger, and J. Schmiedmayer, “Ultracold atoms out of equilibrium,” 2015.
- [3] C. Becker, P. Soltan-Panahi, J. Kronjäger, S. D örscher, K. Bongs, and K. Sengstock, “Ultracold quantum gases in triangular optical lattices,” *New Journal of Physics*, vol. 12, no. 6, p. 065025, 2010.
- [4] C. Wu and S. D. Sarma, “p x, y-orbital counterpart of graphene: Cold atoms in the honeycomb optical lattice,” *Physical Review B*, vol. 77, no. 23, p. 235107, 2008.
- [5] G.-B. Jo, J. Guzman, C. K. Thomas, P. Hosur, A. Vishwanath, and D. M. Stamper-Kurn, “Ultracold atoms in a tunable optical kagome lattice,” *Physical review letters*, vol. 108, no. 4, p. 045305, 2012.
- [6] E. Haller, M. Gustavsson, M. J. Mark, J. G. Danzl, R. Hart, G. Pupillo, and H.-C. Nä gerl, “Realization of an excited, strongly correlated quantum gas phase,” *Science*, vol. 325, no. 5945, pp. 1224–1227, 2009.
- [7] C. Chin, M. Bartenstein, A. Altmeyer, S. Riedl, S. Jochim, J. H. Denschlag, and R. Grimm, “Observation of the pairing gap in a strongly interacting fermi gas,” *Science*, vol. 305, no. 5687, pp. 1128–1130, 2004.
- [8] M. Greiner, C. A. Regal, and D. S. Jin, “Probing the excitation spectrum of a fermi gas in the bcs-bec crossover regime,” *Physical review letters*, vol. 94, no. 7, p. 070403, 2005.
- [9] H. Moritz, T. Stöferle, K. Günter, M. Köhl, and T. Esslinger, “Confinement induced molecules in a 1d fermi gas,” *Physical review letters*, vol. 94, no. 21, p. 210401, 2005.
- [10] T. Esslinger, “Fermi-hubbard physics with atoms in an optical lattice,” *Annu. Rev. Con-dens. Matter Phys.*, vol. 1, no. 1, pp. 129–152, 2010.

- [11] M. Greiner, O. Mandel, T. Esslinger, T. W. Hänsch, and I. Bloch, “Quantum phase transition from a superfluid to a mott insulator in a gas of ultracold atoms,” *nature*, vol. 415, no. 6867, pp. 39–44, 2002.
- [12] F. Meinert, M. J. Mark, E. Kirilov, K. Lauber, P. Weinmann, A. J. Daley, and H.-C. N ägerl, “Quantum quench in an atomic one-dimensional ising chain,” *Physical review letters*, vol. 111, no. 5, p. 053003, 2013.
- [13] D. Jaksch, C. Bruder, J. I. Cirac, C. W. Gardiner, and P. Zoller, “Cold bosonic atoms in optical lattices,” *Physical Review Letters*, vol. 81, no. 15, p. 3108, 1998.
- [14] S. Inouye, M. Andrews, J. Stenger, H. Miesner, *et al.*, “Observation of feshbach resonances in a bose-einstein condensate,” *Nature*, vol. 392, no. 6672, p. 151, 1998.
- [15] B. Paredes, A. Widera, V. Murg, O. Mandel, *et al.*, “Tonks-girardeau gas of ultracold atoms in an optical lattice,” *Nature*, vol. 429, no. 6989, p. 277, 2004.
- [16] T. Kinoshita, T. Wenger, and D. S. Weiss, “Observation of a one-dimensional tonks-girardeau gas,” *Science*, vol. 305, no. 5687, pp. 1125–1128, 2004.
- [17] Z. Hadzibabic, *Studies of a quantum degenerate fermionic lithium gas*. PhD thesis, Massachusetts Institute of Technology, Department of Physics, 2003.
- [18] G. Lee, “Feshbach resonances in ultracold atoms,” 2013.
- [19] C. Chin, R. Grimm, P. Julienne, and E. Tiesinga, “Feshbach resonances in ultracold gases,” *Rev. Mod. Phys.*, vol. 82, pp. 1225–1286, Apr 2010.
- [20] I. Bloch, J. Dalibard, and S. Nascimbene, “Quantum simulations with ultracold quantum gases,” *Nature Physics*, vol. 8, no. 4, p. 267, 2012.
- [21] D. Moravchik, “Imaging methods of cold atoms,” Master’s thesis, Ben-Gurion University of the Negev, 1 2009.
- [22] M. Greiner, I. Bloch, O. Mandel, T. W. H änsch, and T. Esslinger, “Exploring phase coherence in a 2d lattice of bose-einstein condensates,” *Physical Review Letters*, vol. 87, no. 16, p. 160405, 2001.
- [23] S. Fölling, F. Gerbier, A. Widera, O. Mandel, T. Gericke, and I. Bloch, “Spatial quantum noise interferometry in expanding ultracold atom clouds,” *arXiv preprint cond-mat/0503587*, 2005.

- [24] T. Rom, T. Best, D. Van Oosten, U. Schneider, S. Fölling, B. Paredes, and I. Bloch, “Free fermion antibunching in a degenerate atomic fermi gas released from an optical lattice,” *arXiv preprint cond-mat/0611561*, 2006.
- [25] N. Gemelke, X. Zhang, C.-L. Hung, and C. Chin, “In-situ observation of incompressible mott-insulating domains of ultracold atomic gases,” *arXiv preprint arXiv:0904.1532*, 2009.
- [26] K. D. Nelson, X. Li, and D. S. Weiss, “Imaging single atoms in a three-dimensional array,” *Nature Physics*, vol. 3, no. 8, p. 556, 2007.
- [27] J. F. Sherson, C. Weitenberg, M. Endres, M. Cheneau, I. Bloch, and S. Kuhr, “Single-atom resolved fluorescence imaging of an atomic mott insulator,” *arXiv preprint arXiv:1006.3799*, 2010.
- [28] W. S. Bakr, A. Peng, M. E. Tai, R. Ma, J. Simon, J. I. Gillen, S. Foelling, L. Pollet, and M. Greiner, “Probing the superfluid–to–mott insulator transition at the single-atom level,” *Science*, vol. 329, no. 5991, pp. 547–550, 2010.
- [29] U. Schneider, *Interacting Fermionic Atoms in Optical Lattices Quantum Simulator for Condensed Matter Physics*. PhD thesis, Johannes Gutenberg-Universität Mainz, 2010.
- [30] J. Stenger, S. Inouye, A. P. Chikkatur, D. Stamper-Kurn, D. Pritchard, and W. Ketterle, “Bragg spectroscopy of a bose-einstein condensate,” *Physical Review Letters*, vol. 82, no. 23, p. 4569, 1999.
- [31] P. T. Ernst, S. Götze, J. S. Krauser, K. Pyka, D.-S. Lühmann, D. Pfannkuche, and K. Sengstock, “Probing superfluids in optical lattices by momentum-resolved bragg spectroscopy,” *Nature Physics*, vol. 6, no. 1, p. 56, 2010.
- [32] M. Gustavsson, E. Haller, M. Mark, J. Danzl, G. Rojas-Kopeinig, and H.-C. Nägerl, “Control of interaction-induced dephasing of bloch oscillations,” *Physical review letters*, vol. 100, no. 8, p. 080404, 2008.
- [33] M. Fattori, C. DErrico, G. Roati, M. Zaccanti, M. Jona-Lasinio, M. Modugno, M. Inguscio, and G. Modugno, “Atom interferometry with a weakly interacting bose-einstein condensate,” *Physical review letters*, vol. 100, no. 8, p. 080405, 2008.
- [34] A. Kastberg, W. D. Phillips, S. Rolston, R. Spreuw, and P. Jessen, “Adiabatic cooling of cesium to 700 nk in an optical lattice,” *Physical review letters*, vol. 74, no. 9, p. 1542, 1995.

- [35] R. Jördens, N. Strohmaier, K. Günter, H. Moritz, and T. Esslinger, “A mott insulator of fermionic atoms in an optical lattice,” *arXiv preprint arXiv:0804.4009*, 2008.
- [36] M. Srednicki, “Chaos and quantum thermalization,” *Physical Review E*, vol. 50, no. 2, p. 888, 1994.
- [37] J. M. Deutsch, “Quantum statistical mechanics in a closed system,” *Physical Review A*, vol. 43, no. 4, p. 2046, 1991.
- [38] S. Khlebnikov and M. Kruczenski, “Thermalization of isolated quantum systems,” *arXiv preprint arXiv:1312.4612*, 2013.
- [39] G. Goldstein and N. Andrei, “Strong eigenstate thermalization hypothesis,” *arXiv preprint arXiv:1408.3589*, 2014.
- [40] M. Rigol, V. Dunjko, and M. Olshanii, “Thermalization and its mechanism for generic isolated quantum systems,” *Nature*, vol. 452, no. 7189, pp. 854–858, 2008.
- [41] T. Kinoshita, T. Wenger, and D. S. Weiss, “A quantum newton’s cradle,” *Nature*, vol. 440, no. 7086, pp. 900–903, 2006.
- [42] T. Langen, S. Erne, R. Geiger, B. Rauer, T. Schweigler, M. Kuhnert, W. Rohringer, I. E. Mazets, T. Gasenzer, and J. ö. Schmiedmayer, “Experimental observation of a generalized gibbs ensemble,” *Science*, vol. 348, no. 6231, pp. 207–211, 2015.
- [43] G. Goldstein and N. Andrei, “Equilibration and generalized gibbs ensemble for hard wall boundary conditions,” *Physical Review B*, vol. 92, no. 15, p. 155103, 2015.
- [44] J. Mossel and J.-S. Caux, “Generalized tba and generalized gibbs,” *Journal of Physics A: Mathematical and Theoretical*, vol. 45, no. 25, p. 255001, 2012.
- [45] M. Kollar and M. Eckstein, “Relaxation of a one-dimensional mott insulator after an interaction quench,” *Physical Review A*, vol. 78, no. 1, p. 013626, 2008.
- [46] M. A. Cazalilla, A. Iucci, and M.-C. Chung, “Thermalization and quantum correlations in exactly solvable models,” *Physical Review E*, vol. 85, no. 1, p. 011133, 2012.
- [47] B. Pozsgay, M. Mestyán, M. Werner, M. Kormos, G. Zaránd, and G. Takács, “Correlations after quantum quenches in the x x z spin chain: Failure of the generalized gibbs ensemble,” *Physical review letters*, vol. 113, no. 11, p. 117203, 2014.

- [48] G. Goldstein and N. Andrei, “Failure of the local generalized gibbs ensemble for integrable models with bound states,” *Physical Review A*, vol. 90, no. 4, p. 043625, 2014.
- [49] B. Pozsgay, “Failure of the generalized eigenstate thermalization hypothesis in integrable models with multiple particle species,” *Journal of Statistical Mechanics: Theory and Experiment*, vol. 2014, no. 9, p. P09026, 2014.
- [50] H. Bethe, “Zur theorie der metalle,” *Zeitschrift für Physik*, vol. 71, no. 3-4, pp. 205–226, 1931.
- [51] N. Andrei, K. Furuya, and J. H. Lowenstein, “Solution of the kondo problem,” *Rev. Mod. Phys.*, vol. 55, pp. 331–402, Apr 1983.
- [52] F. H. Essler, H. Frahm, F. Göhmann, A. Klümper, and V. E. Korepin, *The one-dimensional Hubbard model*. Cambridge University Press, 2005.
- [53] E. H. Lieb and W. Liniger, “Exact analysis of an interacting bose gas. i. the general solution and the ground state,” *Physical Review*, vol. 130, no. 4, p. 1605, 1963.
- [54] E. H. Lieb, “Exact analysis of an interacting bose gas. ii. the excitation spectrum,” in *Condensed Matter Physics and Exactly Soluble Models*, pp. 617–625, Springer, 2004.
- [55] M. Gaudin, “Un systeme a une dimension de fermions en interaction,” *Physics Letters A*, vol. 24, no. 1, pp. 55–56, 1967.
- [56] C.-N. Yang, “Some exact results for the many-body problem in one dimension with repulsive delta-function interaction,” *Physical Review Letters*, vol. 19, no. 23, p. 1312, 1967.
- [57] A. Okiji, “Bethe ansatz treatment of the anderson model for a single impurity,” in *Fermi Surface Effects*, pp. 63–97, Springer, 1988.
- [58] L. Faddeev, “How algebraic bethe ansatz works for integrable model,” *arXiv preprint hep-th/9605187*, 1996.
- [59] F. Franchini, “Notes on bethe ansatz techniques,” *International School for Advanced Studies-Trieste, Lecture Notes*, 2011.
- [60] P. Ramos and M. Martins, “Algebraic bethe ansatz approach for the one-dimensional hubbard model,” *arXiv preprint hep-th/9605141*, 1996.
- [61] D. Braak and N. Andrei, “On the spectrum of the xxz-chain at roots of unity,” *Journal of Statistical Physics*, vol. 105, no. 3-4, pp. 677–709, 2001.

- [62] B. Pozsgay, W.-V. van Gerven Oei, and M. Kormos, “On form factors in nested bethe ansatz systems,” *Journal of Physics A: Mathematical and Theoretical*, vol. 45, no. 46, p. 465007, 2012.
- [63] J.-S. Caux, “Correlation functions of integrable models: a description of the abacus algorithm,” *Journal of Mathematical Physics*, vol. 50, no. 9, p. 095214, 2009.
- [64] F. Meinert, M. Panfil, M. J. Mark, K. Lauber, J.-S. Caux, and H.-C. Nägerl, “Probing the excitations of a lieb-liniger gas from weak to strong coupling,” *Physical review letters*, vol. 115, no. 8, p. 085301, 2015.
- [65] A. Klauser, J. Mossel, J.-S. b. Caux, and J. van den Brink, “Spin-exchange dynamical structure factor of the  $s = 1/2$  heisenberg chain,” *Physical review letters*, vol. 106, no. 15, p. 157205, 2011.
- [66] N. J. Robinson, J.-S. Caux, and R. M. Konik, “Motion of a distinguishable impurity in the bose gas: Arrested expansion without a lattice and impurity snaking,” *Physical review letters*, vol. 116, no. 14, p. 145302, 2016.
- [67] N. J. Robinson, J.-S. Caux, and R. M. Konik, “Exact nonequilibrium dynamics of a class of initial states in one-dimensional two-component integrable quantum gases,” *arXiv preprint arXiv:1602.05532*, 2016.
- [68] V. Yudson, “The dynamics of integrable quantum-systems,” *ZHURNAL EKSPERIMENTALNOI I TEORETICHESKOI FIZIKI*, vol. 88, no. 5, pp. 1757–1770, 1985.
- [69] V. Yudson, “Dynamics of the integrable one-dimensional system photons+ two-level atoms,” *Physics Letters A*, vol. 129, no. 1, pp. 17–20, 1988.
- [70] D. Iyer and N. Andrei, “Quench dynamics of the interacting bose gas in one dimension,” *Physical review letters*, vol. 109, no. 11, p. 115304, 2012.
- [71] D. Iyer, H. Guan, and N. Andrei, “Exact formalism for the quench dynamics of integrable models,” *Physical Review A*, vol. 87, no. 5, p. 053628, 2013.
- [72] W. Liu and N. Andrei, “Quench dynamics of the anisotropic heisenberg model,” *Physical review letters*, vol. 112, no. 25, p. 257204, 2014.
- [73] G. Goldstein and N. Andrei, “Equilibration and generalized gge in the lieb liniger gas,” *arXiv preprint arXiv:1309.3471*, 2013.

- [74] G. Goldstein and N. Andrei, “Equilibration and generalized gibbs ensemble for hard wall boundary conditions,” *Physical Review B*, vol. 92, no. 15, p. 155103, 2015.
- [75] C. Rylands and N. Andrei, “Time evolution of superradiance,” *arXiv preprint arXiv:1408.3652*, 2014.
- [76] V. E. Korepin, N. M. Bogoliubov, and A. G. Izergin, *Quantum inverse scattering method and correlation functions*, vol. 3. Cambridge university press, 1997.
- [77] “NIST Digital Library of Mathematical Functions.” <http://dlmf.nist.gov/>, Release 1.0.16 of 2017-09-18, 2017. F. W. J. Olver, A. B. Olde Daalhuis, D. W. Lozier, B. I. Schneider, R. F. Boisvert, C. W. Clark, B. R. Miller and B. V. Saunders, eds.
- [78] H. J. Weber and G. B. Arfken, *Essential Mathematical Methods for Physicists*, ISE. Academic Press, 2003.
- [79] G. Baym, “The physics of hanbury brown–twiss intensity interferometry: from stars to nuclear collisions,” *arXiv preprint nucl-th/9804026*, 1998.
- [80] N. J. Robinson, J.-S. Caux, and R. M. Konik, “Motion of a distinguishable impurity in the bose gas: Arrested expansion without a lattice and impurity snaking,” *Physical review letters*, vol. 116, no. 14, p. 145302, 2016.
- [81] M. Lewenstein, A. Sanpera, V. Ahufinger, B. Damski, A. Sen, and U. Sen, “Ultracold atomic gases in optical lattices: mimicking condensed matter physics and beyond,” *Advances In Physics*, vol. 56, no. 2, pp. 243–379, 2007.
- [82] G. Goldstein and N. Andrei, “Equilibration and generalized gge in the lieb liniger gas,” *arXiv preprint arXiv:1309.3471*, 2013.
- [83] V. E. Korepin, N. M. Bogoliubov, and A. G. Izergin, “Quantum inverse scattering method and correlation functions,” vol. 3, 1997.
- [84] S. Pakuliak, E. Ragoucy, and N. Slavnov, “Form factors of local operators in a one-dimensional two-component bose gas,” *Journal of Physics A: Mathematical and Theoretical*, vol. 48, no. 43, p. 435001, 2015.